



EST 1892

**London
South Bank**
University

Biocementation of an Organic Soil with Electrokinetics

MUHAMMAD UMAIR SAFDAR

<https://orcid.org/0000-0002-1664-6370>

A thesis submitted in partial fulfilment of the requirements of London South Bank
University for the degree of Doctor of Philosophy in Geotechnical Engineering

July 2020

To my beloved Parents

Mian Muhammad Safdar

and

Naseem Safdar

Abstract

This thesis assesses the feasibility of biocementation of a problematic organic foundation soil of many embankments of the East Anglia railway network. Biocementation has recently attracted the interest of the researchers worldwide as an emerging soil stabilisation technique, proposed as environmentally friendlier and more sustainable than other soil stabilisation techniques; however, evidence of its effectiveness as a stabilisation technique for soils other than sands is limited.

In this research indigenous, non-pathogenic and ureolytic bacterial strains were screened and isolated from the *in situ* soil. Four strains (*Bacillus licheniformis*, *Rhodococcus erythropolis*, *Micrococcus luteus*, and *Lysinibacillus fusiformis*) were selected based on their ability to grow at different temperatures, pH, soil moisture content and to precipitate CaCO_3 through urea hydrolysis. For the implementation of the biocementation treatment, laboratory scale models were designed for pressure flow column and electrokinetic injection. The latter method was of particular interest in this study as a potential *in situ* implementation method under existing embankments. After a first series of pressure flow soil column experiments, with all strains, which studied parameters such as bacterial population and cementation reagent concentration and curing time. Following these, the best performing strain (*Bacillus licheniformis*) in terms of Unconfined Compressive Strength (UCS) and CaCO_3 precipitation (in the flow column tests) was used for further testing and the electrokinetic experiments.

Unconfined Compressive Strength (UCS) and oedometer testing results supported by CaCO_3 measurements, NH_4^+ concentration measurements and pH change measurements, as well as microstructural SEM-EDS analysis, proved that biocementation did occur for both implementation methods and for a number of treatment combinations. EK was the most successful implementation method and was proven effective for degrees of saturation of 85-95%. Whilst treatment non-uniformity when bacteria were injected electrokinetically still needs to be addressed, there is promise that EK could be a viable technique for treating foundation soil under existing infrastructure, which is a major challenge for engineers.

ACKNOWLEDGEMENTS

First of all, my deepest gratitude goes to my director of studies, Dr Maria Mavroulidou. Who dedicatedly directed me first through my MSc and then PhD studies and who shared the enthusiasm of almost six years of discovery. Her unwavering guidance, support and especially the passion for Geotechnics has constantly kept me engaged in research.

My appreciation extends to Prof. Mike J. Gunn, my second supervisor. Who has always inspired and helped me in learning advanced technical and statistical tools for the research.

Besides my supervisors, I would like to thank Mr. Gray Christopher. Geotechnical Lab Technician for his continuous support and assistance throughout the course of PhD research.

My thanks also go to:

Prof. Diane Purchase (Middlesex University)

Alejandra Donzalez Baez (Middlesex University)

Manika Choudhury (Middlesex University)

Jyoti Amin (London Southbank University)

As without their assistance this thesis would not have been completed.

I would also like to acknowledge the partial financial contribution of Network Rail Ltd for this project under research contract NR-ANG-00164.

And most importantly, I am extremely appreciative and obliged towards all my family members as their love to me only grows with age, and who kept me going. Ahtasham Aslam (Brother in law), Tayyaba Safdar (Sister), Zubair Safdar (Brother), Muntaha Aslam (Niece). And finally, I express my thank to my beloved wife (Mubeen Javed) for her friendship love and valuable support.

PUBLICATIONS

The following research papers has been written and published during the PhD research, and based on the reviews the concepts, methodology and results are further refined.

- Safdar, M.U., Mavroulidou, M., Gunn, M.J. et al., (2020). Innovative methods of ground improvement for railway embankment Peat Fens foundation soil. *Géotechnique* (online eprint) <https://doi.org/10.1680/jgeot.19.sip.030>
- Safdar, M.U., Mavroulidou, M., Gunn, M.J. et al., (2020). Implementation of biocementation for a partially saturated problematic soil of the UK railway network. E-UNSAT2020 -Unsaturated Horizons 4th European Conference on Unsaturated Soils, Lisbon, Portugal. <https://doi.org/10.1051/e3sconf/202019505006>
- Safdar, M.U., Mavroulidou, M., Gunn, M.J. et al., (2020). Biocementation of an organic soil using indigenous ureolytic bacteria. 6th International Symposium on Green Chemistry, Sustainable Development and Circular Economy (Greenchem6), Thessaloniki, Greece
- Safdar, M.U., Mavroulidou, M., Gunn, M.J. et al., (2019). Innovative methods of ground improvement for two problematic UK railway earthwork materials. 16th International Conference on Environmental Science and Technology, Rhodes, Greece, 4-7 September 2019. CEST2019_00336

CONTENTS

Abstract
Acknowledgements
Publications
Contents
List of Figures
List of Tables
List of symbols

1	INTRODUCTION	1
1.1	Impetus for the research	1
1.2	Background to the Study	2
1.3	Research Aim and Objectives	4
1.4	Original Contribution to Knowledge	5
1.5	Thesis Outline	6
2	LITERATURE REVIEW	8
2.1	Peat/Organics Soils	8
2.1.1	Definitions	8
2.2	Classification of Peat and Organics Soils	10
2.3	Physicochemical and Engineering Properties	15
2.3.1	Organic content and Ignition Loss	15
2.3.2	Water Content and Index Properties	17
2.3.2.1	Atterberg Limits	18
2.3.3	Specific Gravity	21
2.3.4	Gas Content and Bulk Density	23
2.3.5	Shrinkage and Swelling	24
2.3.6	pH or Hydrogen Ion Activity	27
2.3.7	Cation Exchange Capacity (CEC)	28
2.3.8	Permeability of Peats/Organic Soils	29
2.3.8.1	Permeability Under Load	31
2.3.9	Compressibility of Peats/Organic Soils	33

2.3.10	Shear Strength of Peats/Organic Soils	36
2.3.10.1	Effective Stress Parameters	37
2.3.10.2	Undrained Shear Strength	39
2.4	EK Soil Treatment	39
2.4.1	Definitions and Background	39
2.4.2	Electrokinetic Phenomena in Soils	40
2.4.3	Types of Flow Through the Soil	43
2.4.4	Practical Considerations	46
2.5	Biocementation	47
2.5.1	Definitions and Background	47
2.5.2	Microbial Community Structure in Organic Soils	50
2.5.3	Ureolytic Microorganisms used for MICP Treatment	51
2.5.4	MICP Treatment Implementation Methods	52
2.5.4.1	Injection Method	52
2.5.4.2	Surface Percolation Method	53
2.5.4.3	Spraying	54
2.5.4.4	Mixing Method	54
2.6	Electro-Biogrouting	54
2.7	Effect of MICP on Hydromechanical Properties of Soils	55
2.7.1	Hydraulic Properties	55
2.7.2	Mechanical Properties	57
2.8	Factors Affecting the Precipitation of CaCO ₃ Crystals in MICP Treatment	60
2.9	Large Scale Application of MICP-Practical Considerations	63
3	MATERIALS AND METHODS	65
3.1	Introduction	65
3.2	Tested Soil	67
3.2.1	Selection of Representative Material	68

3.3	Isolation and Screening of Bacteria	70
3.4	Microbial Identification and Diagnosis	73
3.4.1	Matrix-Assisted Laser Desorption Ionization-Time of Flight (MALDI-TOF MS)	73
3.4.2	MALDI-TOF Principle and Methodology	74
3.4.3	Sample Preparation for Microbial Identification using MALDI-TOF MS	75
3.4.4	Formic Acid Extraction Method	76
3.4.5	Summary of Microbial Identification and Diagnosis	77
3.4.6	Storage of Bacteria	78
3.5	Pressure Flow column Experimental Setup	79
3.5.1	Sample Preparation for Injection Method	79
3.5.2	Cementation Reagent	82
3.5.3	Bacteria and Growing Conditions	82
3.6	Sample Preparation for Mixing Method	84
3.7	Chemical Analysis	84
3.7.1	Calcium Carbonate (CaCO ₃) Content Determination	84
3.7.2	Urease activity / Ammonium Concentration Determination	85
3.7.2.1	Measurement Procedure in Effluent	85
3.7.2.2	Measurement Procedure in Soil Samples	86
3.7.2.3	Urease Assay Summary	87
3.7.2.4	Urease Activity Calculation from OD670	88
3.8	Geotechnical Property Testing	89
3.8.1	Oedometer Testing	89
3.8.1.1	Sample Preparation Methods and Testing Methodology	89
3.8.2	Soil Water Retention Curve (SWRC) Testing	90
3.8.2.1	Sample Preparation Methods and Testing Methodology	91
3.9	Electrokinetic (EK) Testing Experimental Setup	91
3.9.1	Sample Extractor	93
3.9.2	Electrodes	93

3.9.3	EK Sample Preparation	94
3.9.4	Data Monitoring	95
3.9.5	Electro-Biocementation Method and Assumptions	95
3.9.6	Hydromechanical Properties	99
3.10	Main Experimental Program	100
4	RESULTS AND DISCUSSION OF FLOW COLUMN EXPERIMENTS	104
4.1	Microbiological Analyses	104
4.1.1	Bacterial Growth Rate	105
4.1.2	Urease Activity and Urea Hydrolysis	108
4.2	UCS Results and Chemical Analysis	109
4.2.1	Main Observations	113
4.2.2	Effect of Cementation Reagent Concentration on UCS strength	114
4.2.3	CaCO ₃ Content and UCS Strength	115
4.2.4	Bacterial Concentration	116
4.2.5	Ammonia Concentration	117
4.2.6	Moisture Content and pH	118
4.2.7	Bio-Stimulation Control Samples (PFC3-C4 & PFCC4-C5)	120
4.2.8	Mixing Method set (MX1-MX4)	121
4.3	Stress-Strain Behavior	122
4.4	Distribution of CaCO ₃ Precipitation across Samples	124
4.5	Summary of Changes in UCS Strength of Treated Samples	125
4.6	Effect of MICP Colum Flow Pressure Treatment on Soil Compressibility and Consolidation Characteristics	128
4.6.1	Sample Preparation	128
4.6.2	Coefficient of Compressibility	130
4.6.3	Coefficient of Consolidation and Secondary Compression	131
4.7	SEM-EDS Results	132
4.8	Executive Results Summary of Injection Method Treatment	135

5	RESULTS AND DISCUSSION OF EK-BIOCEMENTATION EXPERIMENTS	137
5.1	UCS Results and Analysis	137
5.1.1	Main Observations	142
5.1.2	Effect of Moisture Content on UCS Strength	144
5.2	Effect of Degree of Saturation (S_r) on the effectiveness of the EK treatment	145
5.3	Stress Strain Behaviour	146
5.4	Summary of UCS Strength Change in Treated Samples	148
5.5	pH Change in the EK treatment	150
5.6	Temperature Variation	152
5.7	Voltage and Electric Current Variation	153
5.8	Effect of EK-Biocementation Treatment on the Soil Compressibility and Consolidation Characteristics	156
5.8.1	Sample Preparation	156
5.8.2	Coefficient of Compressibility	157
5.8.3	Coefficient of Consolidation and Secondary Compression	158
5.9	Soil Water Retention SWRC Analysis	159
5.10	Executive Results Summary of EK-Biocementation Treatment	161
6	Discussion, Conclusions and Recommendations	163
6.1	Results Comparison of Pressure Flow Column and EK-Biocementation Treatment Methods	164
6.2	Advantages and Disadvantages of Pressure Flow Column and EK-Biocementation Treatment Methods	165
6.3	Practical Applicability of Pressure Flow Column and EK-Biocementation Treatment Methods	167
6.4	Discussion on Pressure Flow Column (cementation) Treatment Results	168

6.4.1	Limitations and Relevant Recommendations for the Pressure Flow Column Treatment	170
6.5	Discussion on EK-Biocementation Treatment Results	173
6.5.1	EK-Biocementation Treatment (Limitations and Recommendations)	174
6.6	Conclusions	177
	References	180
	APPENDIX (A)	200
	APPENDIX (B)	202
	APPENDIX (C)	203
	APPENDIX (D)	204
	APPENDIX (E)	205
	APPENDIX (F)	207
	APPENDIX (G)	213

LIST OF FIGURES

2.1	(a) Liquid Limit vs Water Content for different peat morphologies;(b) Ignition Loss by different researchers (Hobbs, 1986).	18
2.2	Effect of humification on water content and liquid limit (peats having organic content between 50-70%, after (Hobbs, 1986)	19
2.3	Liquid Limit after variation vs Ignition Loss for mires, after (Hobbs, 1986).	19
2.4	Atterberg limits variation with organic content (Abdallah, et al., 1999)	20
2.5	Specific Gravity vs organic content (ignition loss) in mires, after (Hobbs, 1986).	22
2.6	Water content vs Specific Gravity in mires, after (Hobbs, 1986).	23
2.7	Variation of Bulk density vs Water content, after (Hobbs, 1986).	24
2.8	Linear shrinkage vs Moisture content of fen peats after (Hobbs, 1986).	25
2.9	The effect of bulk density on drying and re-wetting (Radforth et al., 1996)	26
2.10	pH variation with Organic content % of fen and bog peats, after (Radforth et al., 1996)	28
2.11	Cation Exchange Capacity variation with Organic Content %, after (Radforth et al., 1996)	29
2.12	Vertical permeability vs. void ratio (Hobbs, 1986)	32
2.13	Back-scattered electron (BSE) image of <i>Sphagnum</i> peat shows the open pore structure, after (Rezanezhad, F., 2016)	34
2.14	Compressions in peat vs Effective stress (originally plotted by Landva & La Rochelle, (1983), updated by O'Loughlin, (2007), after (Ferrell, E. R., 2012)	34
2.15	EOP vs Continuous compression approach, (After Ferrell, 2012 and Hobbs, 1986)	36
2.16	Triaxial tests plot of the fibrous peat, after (Farrell & Hebib, 1998)	38
2.17	DDL and ζ of a charged particle, (source: West & Stewart, 1995)	40
2.18	Different CaCO ₃ polymorphs: (a) calcite; (b) vaterite; (c) aragonite (source: Ivanov and Stabnikov, 2017)	49
2.19	Effective bridging formation by CaCO ₃ crystals: (a) conceptual drawing (after Mujah et al., 2017); (b) SEM (Mahawish et al, 2018)	50

	Correlation of sand UCS and CaCO ₃ content after Ivanov and Stabnikov, (2017)	
2.20	(synthesis of results from Whiffin et al. 2007; Al Qabani and Soga, 2013; Stabnikov et al, 2013a and b; Li and Qu 2012).	57
2.21	Different CaCO ₃ distribution mechanisms, (a) Preferential; (b) Uniform (Ivanov and Stabnikov, 2017)	60
2.22	Effect of degree of saturation on MICP treatment (Gowthaman et al., 2019)	62
3.1	Flowchart of research methodology	66
3.2	Distribution of water contents and organic contents for two boreholes	67
3.3	Particle size distribution of retained soil portion (passing 1.18mm sieve)	70
3.4	Comparison of rate of growth of same strain incubated at (left 4°C, right 37°C) after 3 days	72
3.5	Schematic diagram of the MALDI-TOF MS process, after (Patel, 2014)	75
3.6	Pressure flow column for MICP treatment	79
3.7	Typical ammonia standard calibration curve	89
3.8	Electrokinetic stabilisation cell with dimensions (mm)	93
3.9	Sample extractor and electrode arrangement	94
3.10	EK Experimental setup	95
4.1	Rate of Growth of Bacteria cells against time at 37°C	106
4.2	Urease activity of microorganism at different time	109
4.3	UCS Strength Comparison for Flow column (PFC5-PFC24), Control (C1-C5) and Mixing method (MX1-MX4) experiments	110
4.4	CaCO ₃ % along with the resultant Ammonia concentration for Flow column (PFC5-PFC24), Control (C1-C5) and Mixing method (MX1-MX4) experiments	111
4.5	Moisture Content % along with the end test pH for Flow column (PFC5-PFC24), Control (C1-C5) and Mixing method (MX1-MX4) experiments	112
4.6	Effect of the concentration of Bacterial population of <i>Bacillus licheniformis</i> and <i>Lysinibacillus fusiformis</i> (1 x 10 ⁸ cfu/mL and 1 x 10 ⁷ cfu/mL) and reagent (0.75 and 1.0M) on the UCS strength q _u and CaCO ₃ content % of the MICP treated soils.	116
4.7	Variation of ammonia concentration in effluent overtime with <i>Bacillus l.</i>	118
4.8	Variation of mean pH in effluent overtime with <i>Bacillus licheniformis</i> .	119
4.9	Summarised Results for the comparison of injection and mixing methods	121

4.10	Stress-strain behaviour of indicative treated, untreated and control samples	122
4.11	Comparison of overall, stress-strain evolution	123
4.12	CaCO ₃ % Distribution along the treated Samples height	124
4.13	UCS, Strength Change comparison compared to control (PFC2-C3)	127
4.14	Oedometer Test results (Void ratio vs Pressure)	129
4.15	Coefficient of volume compressibility (m_v) vs Pressure	130
4.16	(a) SEM-EDS Picture	133
4.16	(b) SEM-EDS Picture	133
4.16	(c) SEM-EDS Picture	134
5.1	UCS Strength Comparison for EK-Biocementation (EK3-EK14) experiments	138
5.2	CaCO ₃ % along with the resultant Ammonia concentration for EK-Biocementation (EK3-EK14) Experiments	139
5.3	Moisture Content % change at the end of EK-Biocementation (EK3-EK14) experiments	140
5.4	UCS, Strength Change of EK samples compared to respective MICP (PFC2-C3) and (PFC22) experiments	141
5.5	Stress-Strain relationship of EK, PFC treated, and control samples	147
5.6	Different failure behaviour	148
5.7	pH variation in right and left electrolyte chambers over 14 day	150
5.8	pH change variation across the soil specimen at the end of EK treatment	151
5.9	Temperature variation for both right and left chambers over time	152
5.10	Voltage change across soil specimen during 14 days treatment for (EK11)	154
5.11	Electric current (I) and Electric Resistivity (R) variation during EK treatment	155
5.12	Oedometer Test results (Void ratio vs Pressure)	156
5.13	Coefficient of compressibility (m_v) vs Pressure	158
5.14	SWRC results for untreated and treated soils based on chilled-mirror dew point potentiometer	159

LIST OF TABLES

2.1	Classification of peat and organic soils based on the OC% according to Avery (1980):	12
2.2	Identification and description of Organic Soil, data from EN ISO 14688-1:2002	13
2.3	Wet peat classification on the basis of squeeze test and degree of decomposition, data from BS 5930:1999 (BSI, 1999)	13
2.4	Soil classification on the basis of organic content %, data from EN ISO 14688-2:2004	14
2.5	Von Post degree of humification scale, data from ASTM D5715-00	14
2.6	Correction factor C , for different temperatures	16
2.7	Field permeability measurements for fen and bog peats, after Ingram (1983)	30
2.8	Direct (in the diagonal) and coupled (off-diagonal) flow phenomena through porous medium, (after Mitchell, 1993 and Mitchell & Soga, 2005)	44
2.9	Values of (k_e) of different soils, after (Asadi et al., 2013)	45
2.10	Main factors affecting the EK treatment (modified after Mosavat, 2014)	47
2.11	Summary of Up-scaled MICP treatment experiments	63
3.1	Geotechnical and Physicochemical properties of the soil	69
3.2	Formic Acid and (ACN) quantity used for different sizes of colonies	76
3.3	Treatment variables for Pressure Flow Column experiments	82
3.4	Treatment Variables for EK-Biocementation	99
3.5	MICP (Injection method) Experimental Program	101
3.6	MICP (Mixing method) Experimental Program	102
3.7	EK-Biostimulation Experimental Program	103
4.1	Calculated Growth Constants as per Monod microbial kinetic model	107
4.2	Summary of UCS Strength Change	126
4.3	Coefficient of Consolidation, and Coefficient of Secondary Compression for untreated soil under different applied pressures	131

4.4	Coefficient of Consolidation, and Coefficient of Secondary Compression for Pressure flow column treated soil (PFC-18) under different applied pressures	132
5.1	UCS Strength Change Summary for EK Experiments	149
5.2	Coefficient of Consolidation, and Coefficient of Secondary Compression for EK-treated soil (EK11) under different applied pressures	158
6.1	Results Comparison between PFC and EK Treatments	164
6.2	Advantages and Disadvantages of PFC and EK-Biocementation treatments	166

LIST OF SYMBOLS

A	Cross-sectional Area
A_c	Ash Content
C_v	Coefficient of Consolidation
C_a	Coefficient of Secondary Compression
G	Specific Gravity
J_i	Flow rate of Flux
k_v	Coefficient of Permeability
K_o	Coefficient of Earth Pressure
L_{ii}	Conductivity Coefficient for Flow
m_v	Coefficient of Volume compressibility
q_{eo}	Electro-osmotic Fluid Flow rate
s_u	Undrained Shear Strength
w_L	Liquid Limit
c'	Cohesion
Δe	Change in Void Ratio
σ'_c	Pre-consolidation Pressure
σ'_{vf}	Vertical Effective Stress
ϕ'	Angle of Internal Friction
ζ	Zeta Potential
η	Porosity

LIST OF ACRONYMS

ACN	Acetonitrile
B4	B4-Agar Medium
C	Correction Factor
CEC	Cation Exchange Capacity
DC	Direct Current
DDL	Diffused Double Layer
EDS	Energy- dispersive X-ray spectroscopy
EtOH	Absolute Ethanol
EK	Electrokinetics
EKG	Electrokinetic-geosynthetics
EOP	End of Primary Consolidation
H _n	Degree of Humification
M	Molar
MICP	Microbially Induced Calcite Precipitation
MS	Mass Spectrometry
MX	Mixing Set
N	Ignition Loss
NA	Nutrient Agar Medium
NB	Nutrient Broth Medium
OC	Organic Content
OD	Optical Density
PFC	Pressure Flow Column
PMF	Peptide Mass Fingerprint
TOF	Time of Flight
UCS	Unconfined/Uniaxial Compressive Strength
SEM	Scanning Electron Microscopy
TSA	Tryptic soya agar

Chapter 1

INTRODUCTION

1.1 Impetus for the research

To find construction sites with suitable ground conditions is becoming challenging now more than ever, due to the rapidly growing urbanisation. For instance, 84% Europe's population is predicted to live in urban areas by the year 2050 (European Commission, 2010). This would require the development of new infrastructure, which will involve complex engineering with little tolerance for error (e.g. underground nuclear repositories, high-speed trains, high rise buildings, deep basements in urban areas). Such demanding construction in the future will be increasingly carried out over problematic geotechnical conditions (e.g. unstable slopes, loose grounds, contaminated soils etc.), due to the scarcity of the urban space in the densely populated cities.

Moreover, to mitigate increased environmental loading due to climate change and to fulfil the future demands, existing infrastructure facilities would also require to be upgraded. Several infrastructure sectors owing old earthworks (e.g. railway or road embankments and cuttings) suffer from high remediation or maintenance costs to ensure stability and serviceability of these old assets. The UK Department of Transport predicted that up to £34.7bn would be required in a period of five years (from 2019 to 2024) for the stabilisation of railway embankments which were built in the mid-19th century and are not properly designed according to current geotechnical engineering specifications (DoT, 2017). Similarly, for existing highway earthworks a sum of £20 million/year is being spent by asset management teams for slope stability maintenance or remediation (ARUP, 2010). In addition to these, geotechnical related failures such as tilting or settling of buildings, bridges and foundations, major landslides, instability of dams and failure of pipes have recently been observed more frequently and several attempts are also been made to mitigate or avoid such damages (Mosavat, 2014).

Traditional methods for ground improvement (mechanical, chemical, physical stabilisation of soil) have proven to be successful in minimising severe damage but commonly suffer from high costs, environmental side effects, limited life time, and interruption to services, and can be challenging to implement in existing infrastructure. Therefore, the development of innovative, superior and cost-effective ground improvement techniques to mitigate natural and man-made hazards while minimising waste and other environmental impact, is a field of ongoing intensive research effort.

1.2 Background to the Study

The advances in biotechnology and natural sciences have provided new frontiers of knowledge and led to the emergence of the field of bio-geotechnical engineering and of the bio-soils discipline (DeJong et al, 2007; DeJong et al, 2013). In this context, biocementation of soils is an emerging ground improvement technique, inspired by the natural process of biomineralisation, that is, the biological production of minerals through the metabolic processes of several types of plants and microorganisms. As result of this, a natural cement (biocement) is produced that can be used in a controlled way by engineers to stabilise the soil. The technique was proposed as having less carbon foot-print compared to other traditional stabilisation methods such as lime or cement stabilisation, which are linked to high CO₂ emissions. Moreover, due to the non-pathogenic nature and renewability of the microorganisms used the technique it is also suggested as a potentially overall more sustainable soil stabilisation technique (DeJong et al., 2013).

The use of biomineralisation for other in-situ applications such as bioremediation of contaminated soils and water treatment is already well established (Chen et al., 2015; Arias et al., 2017). However, the use of biomineralisation as a soil stabilisation technique has not been explored thoroughly. The most commonly investigated mechanism has been the precipitation of the calcium carbonate to bio-cement loose sands, using ureolytic bacteria such as *Sporosarcina pasteurii*, which was proven to be effective by a number of researchers (e.g. Gao et al., 2018; Montoya & DeJong, 2015; Al Qabany et al., 2012 Whiffin, 2004 amongst many others). However, the use of biocementation on other problematic soils such as organic soil/peat is very little explored in the literature. The open cellular structure of peat, and due to presence of

fibres the heterogeneous permeability across the peat mass makes it a “problematic” material for the injection treatment methods (Canakci et al, 2015). Moreover, researchers (e.g. Lebron & Suarez, 1998; Lin & Singer, 2006), has shown that at very high organic content the presence of soluble organic ligands and other organic matter is attributed to the inhibition mechanism of the precipitation of the CaCO_3 crystals in the peat. Hence, the overall characteristics of peat for instance, very high-water holding capacity, high percentage of organic matter and fibres and generally high compressibility are the major constraints, and have possibly restricted the researchers to implement the innovative methods for its stabilisation. However, in the case of MICP, these impediments can be controlled effectively by adjusting the treatment variables such as injection pressure, and concentration of cementation reagent.

Electrokinetics (EK) is another ground improvement technique that has attracted renewed interest. The basic principle of the EK treatment is to apply a low electric potential gradient (Direct Current) to non-inert electrodes inserted in the soil, which induces a number of complex electrochemical reactions and electrokinetic phenomena, governing the transport of pore water, pore water ions, and charged particles. The technique has been used both in the laboratory (in the vast majority of studies) and also in-situ for soil remediation, where contaminant removal from soil is required, also combined with bioremediation but to a lesser extent, (e.g. Lageman et al, 2007; Harbottle et al, 2009; Gill et al, 2014 and 2016; Barba et al, 2018). Examples of its use combined with chemical stabiliser injection for soil stabilisation are less frequent, especially for in situ applications (e.g. Barker et al, 2004; Lamont-Black et al, 2012) and its use with biocementation in laboratory studies was only recently introduced (e.g. Keykha et al, 2014 and Keykha and Asadi, 2017).

The main advantage of the EK technique is that it is applicable to fine-grained soils such as clayey silts, silty clays and silts and problematic clays like expansive clays, quick clays, dispersive soils, and highly compressible clays. Therefore, the main focus of the researchers has been the treatment of these soil types (Ahmad et al., 2006; Jayasekera, 2008; Liaki et al., 2010; Mosavat, et al., 2012 and many more). The use of EK stabilisation for the soft peat or organic soil is the area that has not been less widely studied.

Peat is an exceptional and unique geomaterial, as it can retain extraordinarily high-water contents. The existence of the organic matter in the soil associates with the higher compressibility and larger creep coefficients, lower specific gravity and usually unsatisfactory strength characteristics. The quantity of the organic matter present in the soil directly and considerably affects the engineering and physico-chemical properties of soil. Network Rail, who are the operators and owners of the railway infrastructure in England, Wales and Scotland are facing a continuous challenge of settlement and degradation of old railway embankments built on soft peat. For instance, in East Anglia there are 55 miles of embankments founded on Peat Fens subject to severe settlements, causing up to £1 m/year delay minute costs for some of the worst sections. It has therefore become imperative to find durable, cost-effective, low-carbon solutions to stabilise this type of soil.

1.3 Research Aim and Objectives

The aim of this experimental laboratory study is to assess the feasibility of biocementation, as a potential method of improving Peat Fens soil of the East Anglia railway network in the UK, using indigenous microorganisms as well as the suitability of electrokinetics for the in-situ implementation of the treatments. The hypothesis is that biocementation would lead to an increase in the strength and stiffness of the soil accompanied by an increase in its calcium carbonate content. The hypothesis will be tested through unconfined compressive strength (UCS) measurement, oedometer testing and will be supported by chemical and microstructural analysis. In addition to this, the effect of the biocementation on the water retention of the biocemented soil will be assessed.

To achieve this aim, the following objectives were set:

- To perform a preliminary analysis of the native soil to understand its composition and basic physicochemical properties and thus anticipate any problems related to the application of the proposed treatment technique.
- To isolate and screen indigenous non-pathogenic ureolytic bacterial strains that could be suitable candidates for biocementation, based on urease activity, calcite precipitation ability (in tube tests) and other favourable characteristics,
- To assess factors, affecting their growth, activity and CaCO₃ precipitation.

- To design suitable systems for the implementation of the treatments in the laboratory, namely a pressure flow column setup (i.e. pressure driven flow through a soil column), allowing for quicker assessment of parameters as well as an electrokinetic system.
- To inoculate soil with the different selected monocultures and perform a parametric study on the impact of several treatment variables such as concentration of bacteria, cementing reagents and treatment duration, based on UCS testing and CaCO₃ content measurements
- To measure unwanted end-products i.e. ammonia from urea hydrolysis, during and at the end of the Microbially Induced Calcite Precipitation (MICP) treatment.
- To perform EK tests with selected treatments and assess the effects of degree of saturation, treatment duration and pH variation during EK on strength and CaCO₃ precipitation.
- To give engineering recommendations based on the findings

1.4 Original Contribution to Knowledge

In the recent years, the use of Microbial Induced Calcite Precipitation (MICP) has gained popularity as a ground improvement technique, however this technique has not been applied to peat/organic soil.

- This research is primarily focused on MICP treatment through two novel techniques namely pressure injection and electrokinetic injection.
- Unlike most other biocementation studies this research focuses on biocementation of a natural soil matrix of approximately 51% of organic content. The efficiency of the treatment has been determined in terms of gain in strength and effects on compressibility of the organic soil.
- The equipment for both treatments has been designed and manufactured for this study. The effective injection systems were developed for inducing bacterial and cementation solutions into the samples.
- As opposed to the vast majority of other works, here indigenous microorganisms were isolated and screened to be used for biocementation of the same soil.

- Biocemented soil properties and behaviour that have been little researched such as soil water retention properties and volumetric change aspects has been studied.
- Another novelty is the electrokinetic injection of the biocementation treatments, as a potentially suitable method for the implementation of treatments under existing embankments, which, to the Author's knowledge has been realised for the first time in a peat soil.

The results of the experimental research presented in this thesis have enhanced the knowledge of MICP treatment, when implemented to improve the properties of the organic soil. In addition, a better understanding of changes in Engineering and Hydromechanical properties induced by the treatments has been made. Significantly this research has presented how using different treatment variables such as, population of bacterial strain, concentration of cementation reagent and treatment and curing durations can affect the achieved improvement in the organic soil properties. The results show that the technique has the potential to be applied effectively for the in-situ applications, not only to ground improvement for the development of new infrastructure but to improve inferior geomaterials under existing structures and foundations.

1.5 Thesis Outline

This thesis consists of six chapters.

Chapter 1 provides the introduction and the general background of the study. The aim and objectives of the research are also given in this chapter.

The literature review in Chapter 2 is divided into three sections. The first section focuses on organic soils and peats, their formation, classification and their physicochemical and engineering properties. The following two sections concern EK and MICP respectively with particular emphasis on recent evolutions regarding the MICP treatment, which is the main focus of this research.

In Chapter 3, the soil characteristics and the research methodology are discussed, including the details of the microbiological study, the implementation setups, with

particular focus on the EK system design along with the soil testing program methodological details.

The presentation and evaluation of the experimental results are given in Chapter 4 and 5 for the pressure flow and EK implementation methods respectively. The hydromechanical testing findings are supported by physicochemical tests and SEM-EDS testing.

Chapter 6 contains an overall discussion on the findings of the present thesis and the advances made during the Author's research, as well as limitations of the presented research. It then gives the general conclusions as well as engineering recommendations and suggestions for future work. Finally, results of batch testing, through results of MALDI testing and relevant dilution schemes, additional SEM-EDS images and some other visual observations are provided in the Appendixes.

CHAPTER 2

LITERATURE REVIEW

The following chapter provides the review of the literature relevant to the Peat/Organic soils in-terms of their classification and Physicochemical and engineering properties. After discussing the soil, the review of literature of the two ground improvement techniques combined in this project, namely microbially induced calcite precipitation and Electrokinetics (EK) is provided. In this research the later method was considered mostly as a technique to implement the biocementation treatments to the soil; therefore, the main focus is biocementation and a detail review of applications of the EK technique *per se* for soil stabilisation is beyond the scope of this work. The literature review will start with some background on the EK technique, so that when subsequently reviewing its application in combination with bacteria, the background physics are clear. Biocementation review will then follow, specifically focusing on the microbially induced calcite precipitation (MICP) process using ureolytic bacteria, as most relevant to the present study; it discusses the role of different microorganisms and reported changes in geotechnical and engineering properties of biocemented soils. Factors affecting the MICP such as temperature and pH, the implementation and field application of the technique, and advantages and limitation of the MICP are also discussed., Eventually some works combining the two methods, EK and biocementation mostly for contaminant remediation will be reviewed; this information was important to identify suitable conditions for bacteria thus avoiding any pitfalls but also identifying any unknowns that would need to be further researched for a successful combination of the processes.

2.1 Peat/Organics Soils

2.1.1 Definitions

Organic and peat soils consist of a broad range of soils with different characteristics and morphologies that control their engineering properties. Proctor and Wheeler (2000) distinguished the morphology in the following groups in their work:

- **Mire:** is a peat forming ecosystem. A system of water, plants and underlying peat, regardless of size, stage of development, nature and origin may be collectively termed as mire.
- **Peat:** remains of dead plants at different decompositions stages deposited in the mire.
- **Peat soils:** are developed in peat deposits. Peat soils have minimum thickness of peat and comprise of high amount of organic matter. Moreover, peat soils need not to contain peat forming plantation.

Mires can be divided into two major groups: *Bog* and *Fen*. Bog can be further subdivided into two types, raised bog (or above fen bog) and blanket bog. The chemistry and the origin of the water supply distinguish between bogs and fens.

Fens generally are alkaline and are mainly fed by flowing water or groundwater sources, though depending upon the quality of groundwater, the fens can be acidic. Fens can have a greater *degree of humification* (i.e. degree of decomposition of plant debris) as compared to bogs due to the enhanced rate of decay in alkaline environment.

Bogs are acidic and are formed in rain-fed or ombrotropic conditions. The organic growth from or on the banks of a lake starts off the raised bog, i.e. fen peat, which grows to embody the lake, at which stage the whole lake landscape is generally denoted as a fen (Hobbs, 1986). Raised bog forms over what was originally a fen bog under suitable conditions (plants rely more on rainwater for growth and nutrients as compared to groundwater); hence a mounded mass (called raised bog) is formed due to the upward growth of organic matter. Thus, the formation of raised bog includes this transitional stage which should be considered in engineering assessments. The presence of the fen peats can be a critical feature for suitable design and construction options as these fen peats usually formed over the very soft and original deposits of the lake bed.

Blanket bogs are formed directly over the organic soils instead of the lake deposits; similar to the raised bogs these also depend on the rainwater as a main source of nutrients. Blanket bogs are typically formed under the temperate and cold regions where the precipitation is higher compared to evaporation. Subterranean channels or

pipes usually develop over time in some types of blanket bogs. In some locations, the leached minerals through these subterranean channels accumulate near to the base of the peat and forms a hardpan layer of minerals which contributes to the local load bearing and strength of the peat (Ferrell, 2012).

The first step in the peat formation is aerobic, which produces the water and gases due to the breakdown of plant matter (decomposition) due to the action of soil microflora i.e. fungi and bacteria and, in non-acidic soils, also earthworms (Hobbs1986). The availability of oxygen decreases drastically due to immersion in water, thus encouraging not only the anaerobic microorganisms with slow and different metabolic activity but also reducing the aerobic microflora. Thus, the partially decomposed plants and vegetation accumulate as peat. The top (normally 100-600 mm thick) and active (consists of undecomposed fibrous plants) layer of peat is called *Acrotelm*, and the lower layer (consists of partially decayed plant matter) is termed as *Catotelm*. The decaying process of the cellulose structure first starts in the leaves due to the higher moisture and crude protein contents, the decomposition process spread subsequently to stems and roots, and eventually an amorphous-granular material of sponge like structure is produced as a result of complete decomposition; it mainly consists of gelatinous organic acid. However, in the UK and Ireland the complete decomposition of the plant debris is rare (Landva 1980a, and Pheeney, 1980).

2.2 Classification of Peat and Organics Soils

The organic matter in soils mainly comes from the plant debris, but the total organic fraction of soil also includes microbial and animal residues in the form of stabilized organic matter, water-soluble organics, microbial biomass and litter (Farrell, 2012). The presence of organic matter in soils, and the composite mixture of organic compounds distinguishes the organic soils from other soils. Thus, for these soils, a number of different classification systems exists. The majority have a botanical basis and are suitable for ecology and agricultural studies, but are too elaborate for engineering applications. Comprehensive engineering classification systems for peat have been developed by von Post (1922), Radforth (1969), Avery (1980), Clymo (1983), in Canada, Landva et al. (1983), Hobbs (1986, 1987) and later by others. It is remarkable that there are very big differences and lack of communication across

classification systems in what peat is and what organic content would qualify a soil as peat.

In any engineering classification system, the identification of key features of peat are: structure and type of peat, the amount of organic matter and mineral particle present and the degree of decomposition (degree of humification), which have a prominent effect on the peat characteristics. In-situ colour description is also very critical and can be carried out by using simple techniques like Munsell chart; on exposure to air, the oxidation process rapidly changes the colour of the organic soils, so colour discretion of recovered samples at a later stage can be difficult (Ferrell, 2012).

Avery (1980), presented a hierarchical system of soil classification in England and Wales and divided soil into 10 classes primarily on the basis of composition of soil material. In the context of composition, the classification system further divided these 10 classes into groups, subgroups and soil type. For the Peat soils the primary consideration has been given to % of organic content (OC%) (Table 2.1). On a sample of peat or organic soil the OC% can readily be measured by “loss-on-ignition” method as per ASTM D 2974-14.

At soil group level, the peat soils are subdivided into two primary groups:

Raw Peat Soils: are formed under semi-natural fen or bog vegetation and on undrained sites where peat is still accumulating. These are characterised by the ripened surface mineral layer or lack of earthy topsoil.

Earthy Peat Soils: are organic soils which contain no or very little recognizable plant remains. These are formed under semi-natural vegetation and in drained peat lands like agricultural lands, predominantly where the upper surface soils are rich in calcium and well aerated.

Table 2.1 Classification of peat and organic soils based on the OC% according to Avery (1980)

Peat Soils	Organic Soils
Loamy Peats: Organic matter < 35% (organic carbon < 20%)	Humose (Organic) mineral soils With mineral fraction > 50% (Organic matter > 10% & organic carbon > 6%) No clay in mineral fraction (Organic matter ≈ 6% & organic carbon ≈ 3.5%)
Sandy Peats: Organic matter ranging in-between 35-50% and sand > 50% (organic carbon equates to 20%)	Peaty Sand: no clay in mineral fraction or; proportional organic carbon content for intermediate clay content (Organic matter > 20% & organic carbon ≈ 12%)
Peats: Organic matter > 50% (measured by loss-on-ignition)	Peaty Loams: Clay > 50% in mineral fraction (Organic matter > 25% & organic carbon ≈ 14.5%)

Further differentiation is based on the proportion and particle size classes (clay, silt, sand and gravels) of the non-organic soil materials, for example peats can be termed as *very stony* if they contain > 35% stones. The organic soils are also classified on the basis of the calcium carbonate % contents, and are divided into three groups, i.e. (a) *Carbonatic* (extremely calcareous): where $\text{CaCO}_3 > 40\%$; (b) *Calcareous*: where CaCO_3 is ranging in-between 1-40%; (c) *Non-calcareous*: where $\text{CaCO}_3 < 1\%$

In the Eurocodes system the standard EN ISO 14688-1:2002 provides the identification and description of the organic soils. EN ISO 14688-1:2002 describes the origin of the organic matter i.e. plant or/and animal and conversion of products of these materials due to decomposition (see table below 2.2). While the principles of classification are given by the standard EN ISO 14688-2:2004.

Table 2.2 Identification and description of Organic Soil, data from EN ISO 14688-1:2002

Material	Description
Fibrous peat	Clear recognizable plant structure, Fibrous structure, retains suitable strength
Pseudo-fibrous peat	No strength of seeming plant structure, semi-recognizable plant structure
Amorphous peat	Mushy consistency, no recognizable plant structure
Gyttja	Organic bottom deposits at the lake bed, may contain inorganic elements, decomposed animal and plant remains
Humose	Vegetation remains, contain living microorganisms and extractions, may contain inorganic elements from topsoil

BS 5930:1999 (BSI, 1999): Code of practice for site investigation, classifies the peat into three categories based on the visual recognizability of plant fibres. The degree of decomposition in peat is assessed by a simple squeeze test.

Table 2.3 Wet peat classification on the basis of squeeze test and degree of decomposition, data from BS 5930:1999 (BSI, 1999)

Classification	Plant Fibres	Decomposition	Squeeze
Fibrous	Easily Recognizable	No	No solids Only water
Pseudo-fibrous	Recognizable	Moderately	Solids < 50% Turbid water
Amorphous	Not recognizable	Complete	Solids > 50% Paste

EN ISO 14688-2:2004 provides a general classification on the basis of organic mass % (see Table 2.3). However, there is no particular explanation about the organic content measurement method, or when an organic soil can specifically be termed as peat or when a clayey peat changes to a peaty clay etc.

Table 2.4 Soil classification on the basis of organic content %, data from EN ISO 14688-2:2004

Classification	Organic content 5 by dry mass of ($\leq 2\text{mm}$)
High organic	> 20
Moderate organic	6-20
Low organic	2-6

For the detailed description of peat, the von Post system is commonly used. ASTM D5715-00 standard incorporates the modified von Post system which measures the H_n (Degree of Humification) on the scale of one to ten, i.e. from H_1 to H_{10} . (See table 2.5). ASTM specifies an ash content < 25%, to classify as soil as peat; this can be equivalent to 75% of organic content.

Table 2.5 Von Post degree of humification scale, data from ASTM D5715-00

Degree of Humification	Plant fibre structure in peat	State of water and residue on squeezing
H1	Fibrous, unaltered, undecomposed	No organic solids but colourless and clear water squeezed out
H2	Fibrous, virtually unaltered	No organic solids but yellowish water squeezed out
H3	Recognizable easily	No organic solids but turbid brown water squeezed out
H4	Recognizable but clearly altered	No organic solids but turbid dark brown water squeezed out
H5	Hard to identify, recognizable but ambiguous	Some organic solids and turbid water squeezed out
H6	Pasty texture but indistinct	Half of the sample and turbid water squeezed out
H7	Mostly amorphous, very few recognizable remains and indistinctly identifiable	Half of the sample and very turbid water squeezed out
H8	Mainly indistinct	Two-third, pasty and thick sample squeezed out
H9	Not recognizable remains	Most of the sample squeezed out but no free water
H10	Totally amorphous	All of the sample squeezed out but no free water

2.3 Physicochemical and Engineering Properties

The quantity of the organic matter present in the soil directly and considerably affects the geotechnical, engineering and physico-chemical properties of soil like, water content and index properties, bulk density and degree of saturation, specific gravity, hydraulic conductivity, cation exchange capacity, compressibility, permeability and strength. Organic matter in the soil generally leads to larger creep coefficients, higher compressibility, lower specific gravity and usually unsatisfactory strength characteristics of peat. Most of these properties are correlated with each other and many of these appear to have a link with mire morphology (Hobbs, 1986, 1987). Hence, simple index properties data with the geotechnical profiles from the site survey should enable the engineers to generally recuperate the mire history at the given location without taxonomy resources.

The fibres present in the peat produce a reinforcing effect which can considerably affect the load bearing capacity of the peats. As this structure is different from other soil types like sands and clays it was suggested that traditional analysis and measurement methods would be inapplicable for peats (Hobbs 1986, O'Kelly 2005). Nevertheless, it was shown that the interrelation between most of index and engineering properties of peat, except from strength is very similar to the normally consolidated clay. However, the general variability of the peat, the magnitude of liquid limit and water content make it an extraordinary material (Farrell, 2012). The relationship between water content and strength of peat is usually is aberrant due to its fibrous nature, so that its strength is unusually high considering the extremely high-water content. Thus, the general correlations between compressibility and strength used for clayey soils do not apply to peat and organic soils (Ferrell, 2012).

A more detailed review of the individual physicochemical and engineering properties of peats is provided in the following sections.

2.3.1 Organic content and Ignition Loss

The organic content is an important index test and determines the purity of the peat. The accumulation of minerals in peats depends on the natural formation mechanism. For instance, peats formed in basins (subject to continuous inflow and runoff) contain a considerable amount of mineral soils, whereas peats formed above the ground

surface are free from such effects and may only receive small amount of atmospheric dust. Peats entirely free of external mineral soils may have the organic content up to 98% and leaving the less than 2% ash content. On the other hand, the organic content as low as 10% can be found in peaty clays and lake mud (Ferrell, 2012).

The organic content is determined by measuring the Loss due to ignition (*N*) of the peat. BS 1377: Pt3:1990 (BSI, 1990) recommends the initially oven dried sample at 50°C to be ignited or burnt off in a muffle furnace at 440°C ± 40°C. BS 1377: Pt3:1990 (BSI, 1990) also provides (Walkley and Black) a chemical titration method which can only be used for soils having low organic content. Conversely ASTM D 2974-20 standard uses the ash content (*D*) instead of organic content. ASTM D 2974-20 uses two temperatures 440°C and 550°C- 750°C of ignition for the ash content measurement (*D*), where $D=1-N$, both the tests use initial dried peat at 105°C. Some researchers have reported that higher temperature up to 900°C is required for the combustion of fresh plant roots (Hobbs, 1986). However, at temperatures higher than 450°C clay particles (present in organic soil) extant lose fixed water, which can cause an error in the ignition loss. Higher temperature and higher mineral content can cause bigger error (Al-Khafaji & Andersland 1981). Hobbs (1987), thus introduces a correction (*C*) for the ignition loss when igniting at temperature more than 450°C, as follows.

$$\text{Organic content \%} = 100 - C(100 - N) \quad (2.1)$$

Where *C* is the correction factor and *N* is the ignition loss.

Table 2.6 summarises the correction factor values for the temperature and duration of combustion given by different researchers.

Table 2.6 Correction factor *C*, for different temperatures

Temperature °C	Burning time (<i>h</i>)	Factor <i>C</i>	Reference
550	3	1.04	Skempton & Petley (1970)
450	5	1.0	Arman (1971)
900	1.5	1.168	Al-Khafaji & Andersland (1981)
400	12	1.014	

2.3.2 Water Content and Index Properties

The ability of the peat to retain high quantity of water is certainly a most important material characteristic enabled by the microscopically thin wall structure of the plant cell tissues. Five meters of fibrous peat may contain only as little of 300 mm of plant matter and can hold up to 4.7 m of water and yet can have a significant shear strength (Hobbs, 1986). Water can be held in large cavities in the form of free water, in narrow cavities as capillary water and it can also be bound osmotically, colloiddally and physically to the particles and fibres (Ferrell & Hebib, 1998). Hayward and Clymo (1983), recognised three continuum categories or stages of water retention in peat:

- 1) Under the suction of less than 10kPa, water retained within the cell structures or Intercellular water.
- 2) Inter-particle water retained in any part of peat or *Sphagnum* by capillary forces and under the suction exceeding of 10kPa.
- 3) Absorbed water retained by the peat under a suction of not more than 20 MPa.

These states of the water and the relative chemistry and physics greatly influence the index and engineering characteristics of the peat. The bulk water contained in the peat is mainly in the state of interparticle and intercellular water. Only water in stage (1) participates in flows under gravity or drainage whereas water in both stage (1) and (2) can be drained by consolidation. However, all the water can be removed by drying the peat at 105°C, hence water content can be determined by oven drying the peat at 105-110°C for 24 hours (Hobbs, 1986; O'Kelly, 2005). However, MacFarlane and Allen (1964) stated that in order to avoid oxidation of the peat and to prevent the combustion of the material it is appropriate to oven dry the peat at comparatively low temperature, ranging between 80°C 85°C.

Degree of humification, morphology and structure of the various vegetation present in the peat are the major factors that controls the total water content as well as the proportion of each state (but both can be affected by drainage). Thus, fen peats tend to have less interparticle and total retained water compared to bog peats (Landva & La Rochelle, 1983). In fen peats, the volume of interparticle water reduces significantly with the presence of mineral soil, as shown below in figure 2.1 (a) by Hobbs (1986). Landva & Pheeney (1980) published a comprehensive experimental study of water states comparison in a sedge and a *Sphagnum* peat from Canada, and reported a

considerable evidence that highly humified (granular-amorphous) peats have less total water content as compare to low humified (fibrous peats). Moreover, in fibrous peats the amount of interparticle water is also less than the intercellular water, but as the plant cellular structure is destroyed with an increase in degree of humification the proportion of interparticle water increases.

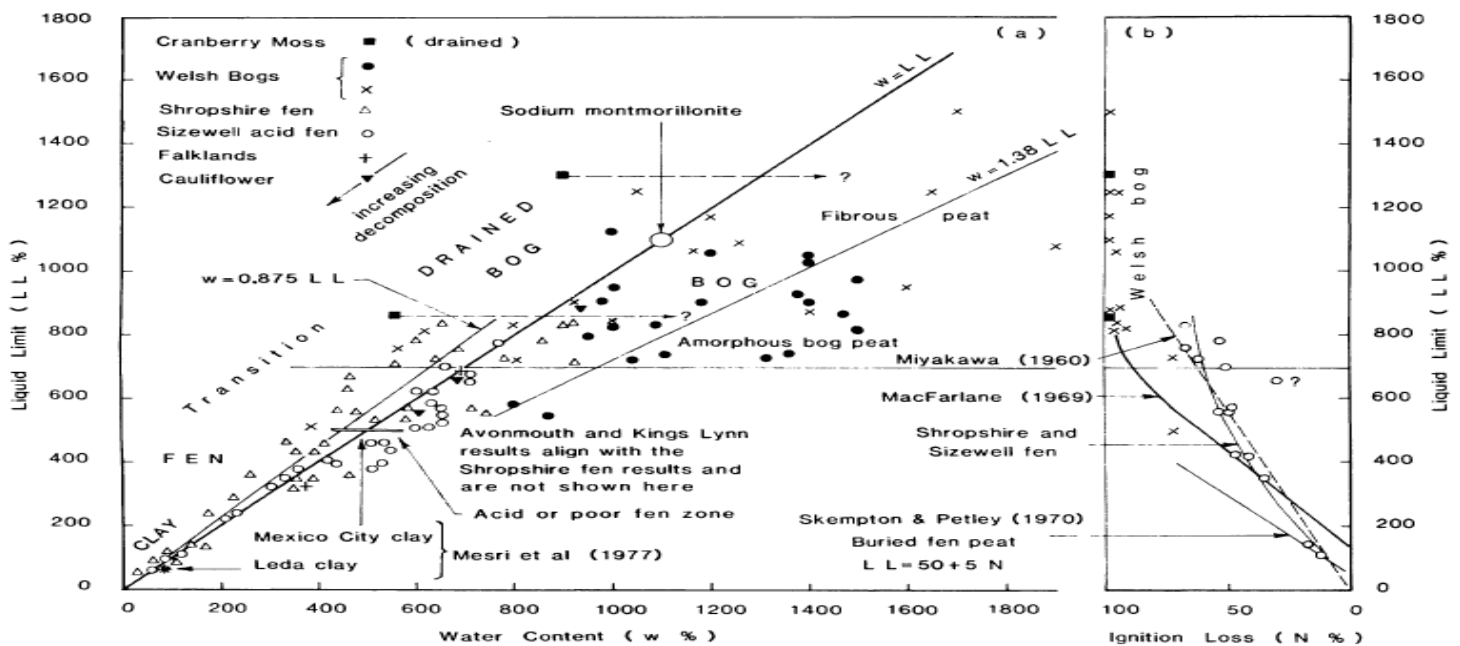


Figure 2.1: (a) Liquid Limit vs Water Content for different peat morphologies;(b) Ignition Loss by different researchers (Hobbs, 1986)

2.3.2.1 Atterberg Limits

The water holding ability of peat directly depends on its organic matter content; negatively charged organic particles may adsorb strongly onto the mineral particle surfaces hence changing the liquid and plastic limits (Mitchell and Soga, 2005). However, the correlation is not simple, as the total water content and the state of the water depends on the degree of humification of the peat. Water content plots against the von Post scale or degree of decomposition (humification) and organic content tend to be very scattered (see figure 2.2). Correlations between organic content or ignition loss and liquid limit were reported by several researchers (Skempton & Petley, 1970; MacFarlane, 1969; Miyakawa, 1960). Hobbs (1986) produced a comparison plot of

these investigations, showing increasing liquid limits with higher organic content for fen and transition peats (see Figure 2.3).

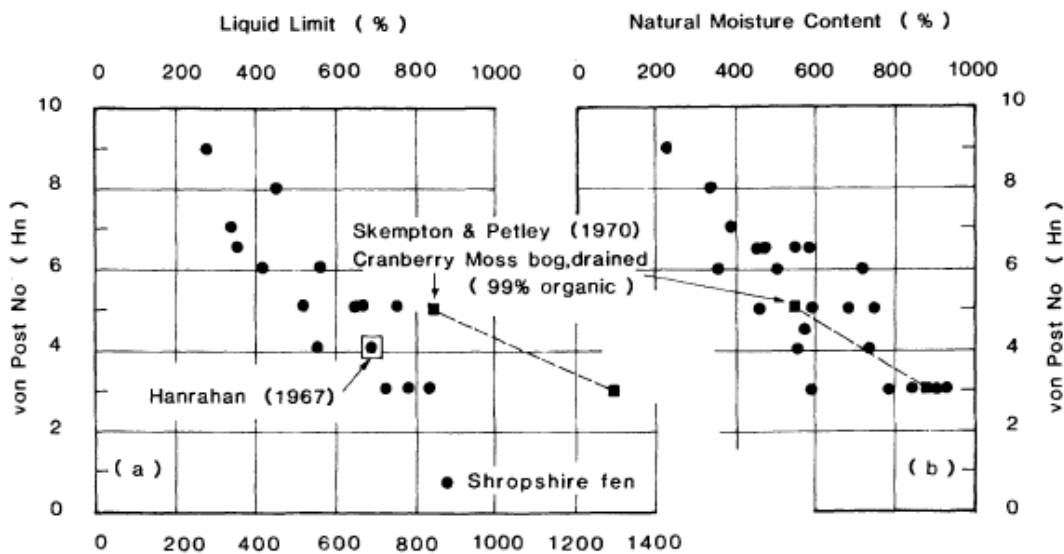


Figure 2.2 Effect of humification on water content and liquid limit (peats having organic content between 50-70%, after (Hobbs, 1986)

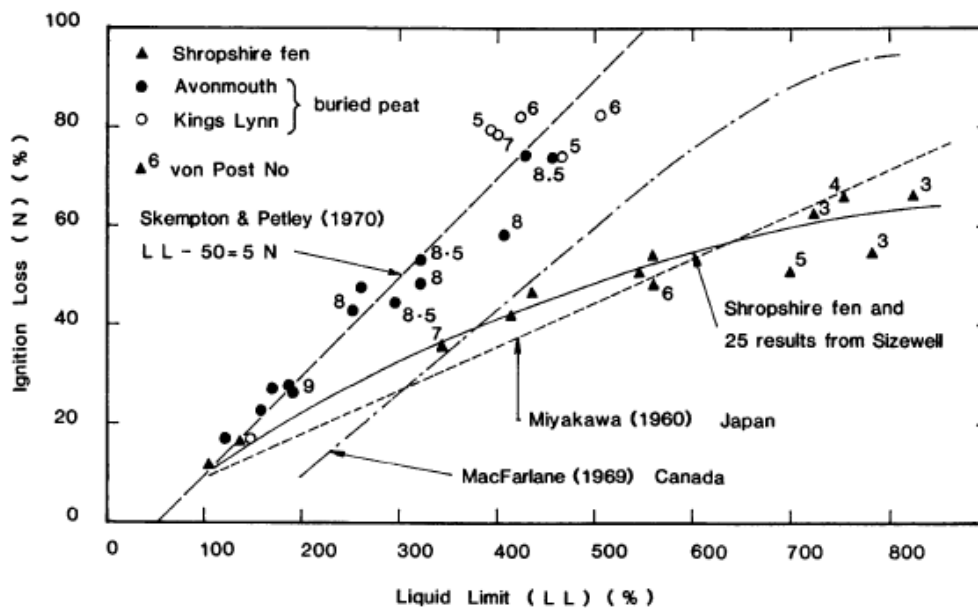


Figure 2.3 Liquid Limit after variation vs Ignition Loss for mires, after (Hobbs, 1986)

The particle aggregation due to the organic materials and the higher water adsorption capacity of organic matter are two opposing characteristics of the peat controlling the Atterberg limits: the tendency of aggregation of soil minerals due to organic matter

decreases the limits, but the higher water adsorption increases the limits. In general peats with higher percentage of organic matter have higher Atterberg limits, as at higher organic contents the capacity to adsorb the water by organic matter exceeds the reduction caused by the soil mineral aggregation (Abdallah, et al., 1999). The trend of Atterberg limits with the organic content % observed by Abdallah, et al., 1999, at different temperatures is given in Figure 2.4, also showing the dependence of Atterberg limits on the drying temperature.

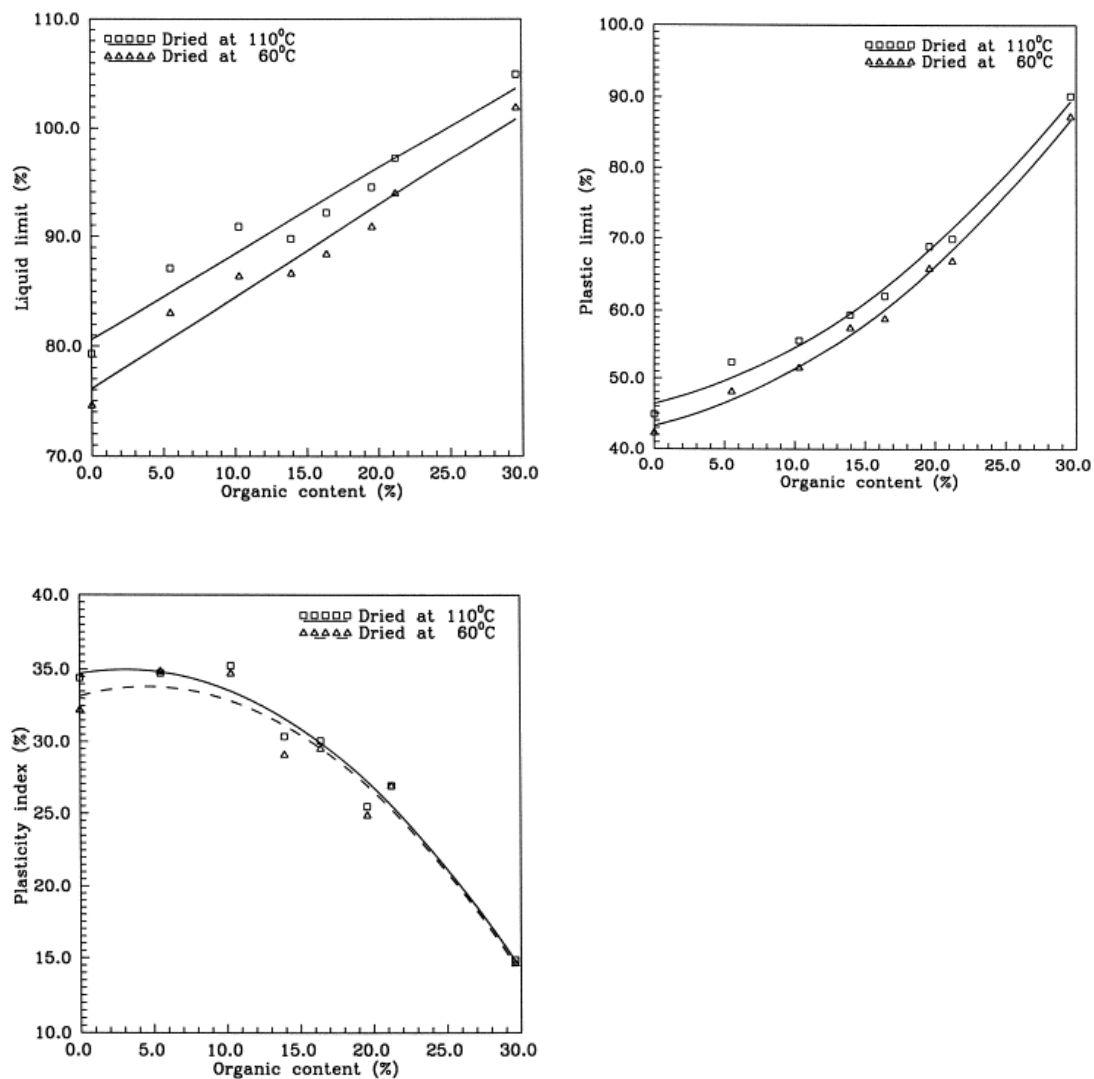


Figure 2.4 Atterberg limits variation with organic content (Abdallah, et al., 1999)

Atterberg limits can thus be a very effective indicator to the degree of humification and peat morphology; generally, the Liquid Limit (w_L) can be determined for peats of

degree of humification greater than H₃ as per von Post scale. Hobbs (1986), observed the decomposition of cauliflower and reported that both water content and liquid limit decreased with degree of humification; natural water content was approximately 0.875w_L and 1.38w_L for fen and bog peat respectively. O'Kelly (2005) also reported that the fen peats (LL 200-600%) usually have lower w_L than the bog peats (LL 800-1500%). The decrease in the liquid limit with increasing decomposition is an evidence of the declining adsorption. Thus, for peats of any plant morphology, the amorphous state would be expected to have lower liquid limit compared to fibrous state. A plot of decreasing water content and liquid limit with increasing humification is shown above in Figure 2.2.

Hobbs (1986) suggested that plastic limit for peats is a useful morphology indicator as this test is possible for fen peats and transitional peats but not for bog peats unless almost completely humified. It should be noted that the preparation of representative samples especially for fibrous peats is very important for index property measurements. Generally, the organic soil/peat structure along with the decomposed material must be broken down to an appropriate size by using a mechanical device (Hobbs, 1986). The chemistry of water has a considerable influence on the liquid limit of the peat hence water from the source should be used while determining the limits (Hanrahan et al., 1967).

2.3.3 Specific Gravity

The literature shows that the specific gravity of the peat is very variable and depend on the proportion of mineral to organic matter. The specific gravity of lignin and cellulose lies in-between 1.4 to 1.5 and hence is the controlling factor in determining the Specific gravity (*G*) of the peat. Specific gravity value as low as 1.1 has been reported by Hobbs, (1986) for some raised bogs due to high organic content while MacFarlane, (1969) has measured the value of *G* up to 2.0 for peaty clays from lake mud due to higher mineral and lower organic content. Theoretically, the loss-on-ignition (*M*) conveniently provides the relationship to calculate the specific gravity, as it provides the proportion of organic matter to the mineral material. Hobbs (1986), plotted the direct results of specific gravity in reference to ignition loss of 5 bogs and fens from Sizewell and Shropshire provided by Skempton & Petley (1970) along with the calculated values (see Figure 2.5). The results show a considerable consistency

as the error in G is up-to 3% and $< 1\%$ for high organic content peats, where organic content is taken equal to the ignition loss; thus, the necessity of direct measurement of G is eliminated. MacFarlane (1969), also observed a linear relationship between G and Ash content (A_c) as:

$$G = (1-A_c)1.5 + 2.7 A_c \quad (2.2)$$

Where, $A_c = 1-0.01N$, Hence $G = 2.7-0.012N$

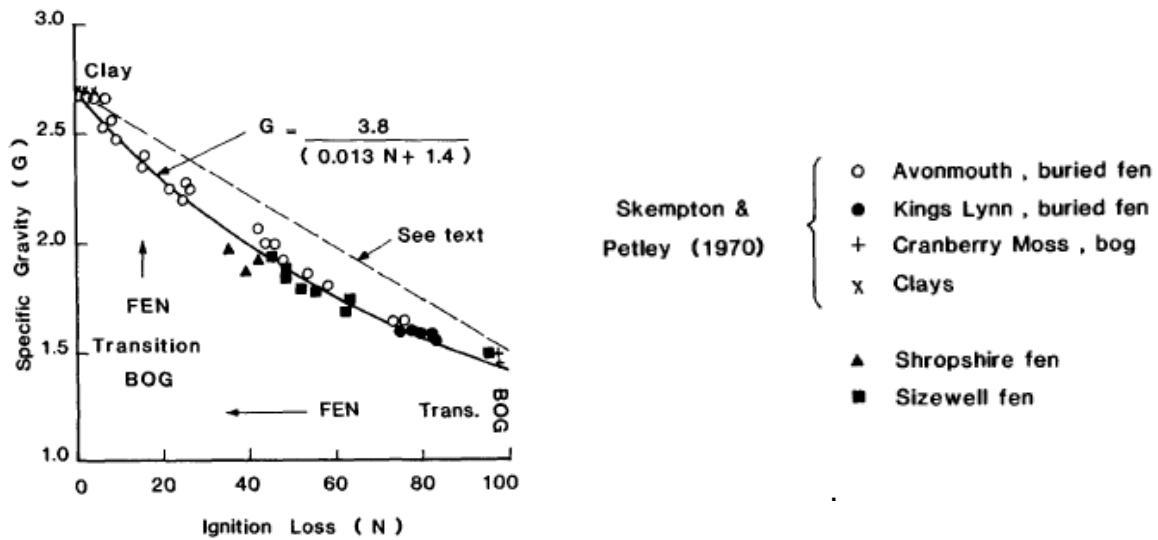


Figure 2.5 Specific Gravity vs organic content (ignition loss) in mires, after (Hobbs, 1986)

Hobbs (1986), plotted water content versus specific gravity for fen and bog peats from the UK and Canada (four different studies) and found a lot of scatter (see Figure 2.6). The Canadian fibrous peats of organic content above 80% and moisture content in excess of 500% had G ranging from 1.4 to 1.7, as observed by MacFarlane (1969). The UK peats had a lower G than the MacFarlane's mean. This shows that fen peats can be distinguished from bog peats by specific gravity in addition to water content.

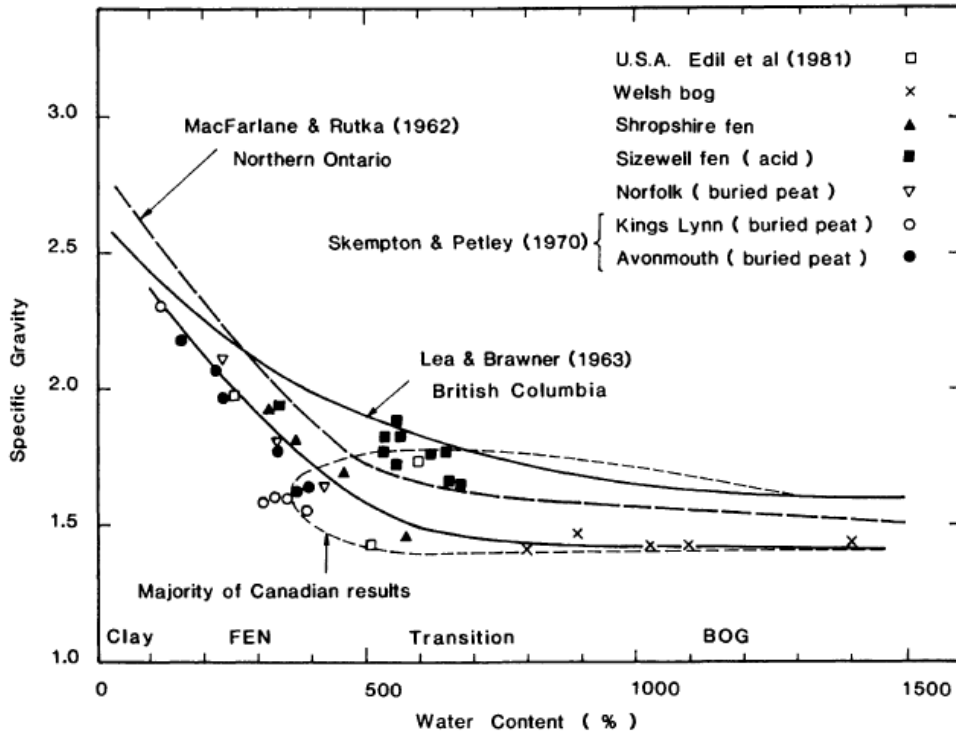


Figure 2.6 Water content vs Specific Gravity in mires, after (Hobbs, 1986)

2.3.4 Gas Content and Bulk Density

The humification process of organic matter in the peats emits various marsh gases and small amount of (CO_2) and (N_2) gases; mires are generally unsaturated due to presence of these gases, whose content changes in time and affects pore pressure, rate of consolidation and permeability (Kellner et al., 2005). The gases in the macrovoids are in free state while the gases in the micro-pores are entrapped. Under normal consolidation, the macro-pores can be reduced easily. Hence, the deformability, and permeability depends on the pore size and nature of the entrapped fluid. Abdallah, et al., (1999) showed that at lower degree of saturation the entrapped gas gets diffused into unsaturated pores of peat and hence decreases the void ratio. Hanrahan (1954), reported gas contents of up to 5% in the Irish *Sphagnum* peat. At this degree of saturation, most of the gas is in free state and considerably affects the pore pressure, rate of consolidation and permeability under loading in the field.

Bulk density for the peat/organic soils is thus variable and low and can be determined by direct measurement of the volume of block or cylindrical method or by liquid displacement method (Farrell & Hebib, 1998). Hobbs (1986), carried out a

comprehensive test and plotted the bulk density measurements of five UK mires. He showed that gas content or degree of saturation is the main factor that controls the bulk density for mires with water contents >600% whereas specific gravity and water content has little effect. In the results the average degree of saturation was reported about 92.5%, hence leaving the gas content of 7.5% of the total volume of the mire (see Figure 2.7). Generally, bogs have lower specific gravity (affecting bulk density) than the fens due the higher organic and fibrous plant content and lower degree of decomposition. The presence of the soil minerals in the base of some bogs can increase its specific gravity but, in any mire, the average bulk density as a whole is typically slightly lower than that of water (Hobbs, 1986).

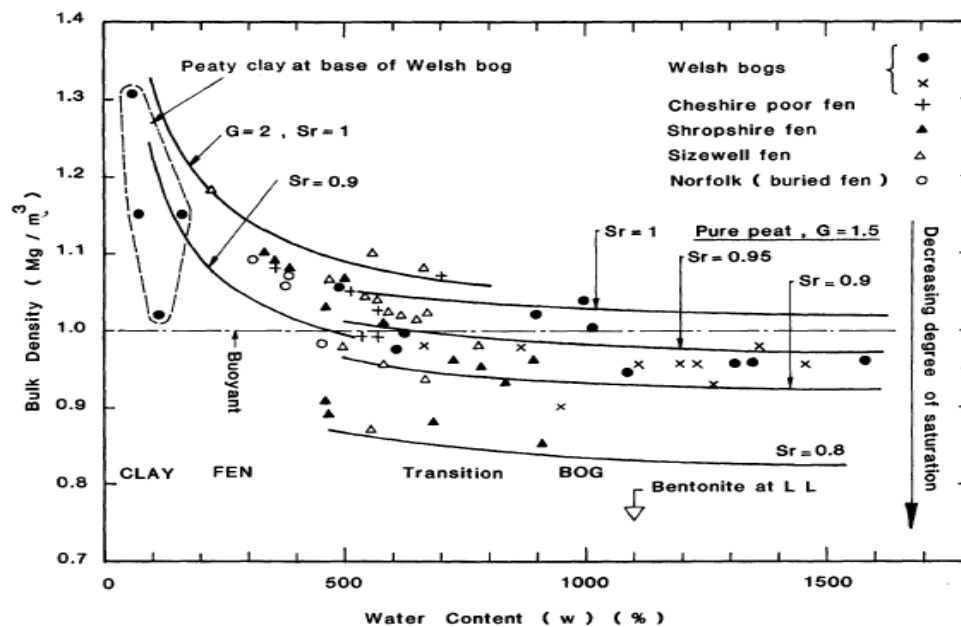


Figure 2.7 Variation of Bulk density vs Water content, after (Hobbs, 1986)

2.3.5 Shrinkage and Swelling

Peats have a high shrinkage potential and a very rapid hardening behaviour upon loss of moisture. Physical ripening of peats produces a permanent material and structure change due to the oxidation process as a result of loss of water, which leads to an irreversible drying. Hence, the re-submergence at any stage cannot recover the lost water in partially dried peats, and the peat/organic soil loses the ability to adsorb the water to the same degree as in virgin state (Michel et al., 2001). This feature has been used in highway and railway engineering, where dried turfs and bales have been used

as a lightweight fill under complete and permanent submergence conditions to avoid any further decomposition (Hobbs, 1986).

In general, despite their low water content the peats having higher degree of humification tends to shrink more as compare to less humified and fibrous peats (Farrell & Hebib, 1998). Lucas (1982), suggested that the nature of the decomposed organic matter affects the shrinkage potential while the amount or mineral content influence the swelling upon re-wetting. Hobbs (1986), produced a plot of linear shrinkage (without re-watering) against the moisture content for slightly humified (H3) and fibrous fen peats. The peats in this study have shown the linear shrinkage in between 35% to 45% in oven drying (see Figure 2.8).

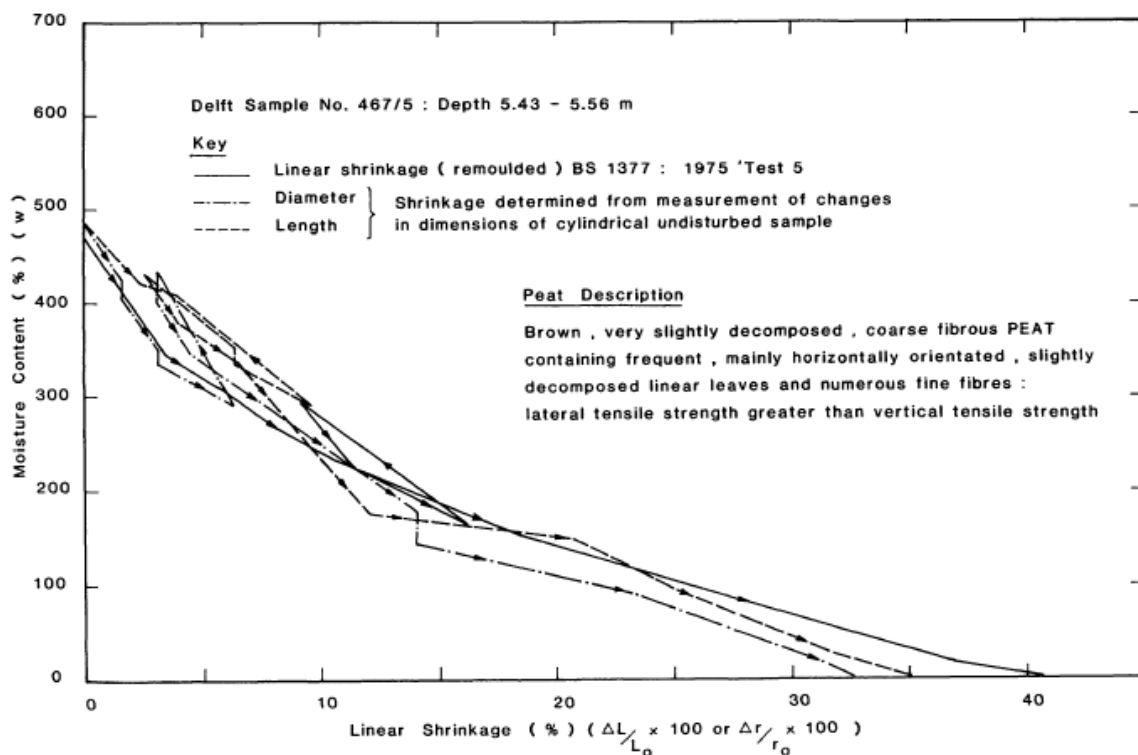


Figure 2.8 Linear shrinkage vs Moisture content of fen peats after (Hobbs, 1986)

Michel et al., (2001), quantified the re-wettability capacity of the peats relative to initial water content and degree of humification. They found that the higher the degree of humification, the higher the shrinkage potential and the more irreversible the re-wettability. The irreversible drying or inability to re-wetting is more prominent in vascular peats (having low bulk density and having large pore spaces) (Hobbs, 1986). Thus, in peats the resistance to re-wetting is related to the bulk density of the soil: a

low bulk density reflects the higher organic content. Radforth et al., (1996), observed the hysteretic response of the peats by drying and then re-wetting the samples having different bulk densities. It was observed that peats of low bulk densities show a higher volume loss on drying and a higher resistance to re-wetting due to higher organic content (see Figure 2.9). Furthermore, in undisturbed samples more shrinkage was reported across the fibres than along them. In fibrous and less humified peats the remoulded samples tends to show a considerably higher linear shrinkage compared to undisturbed samples. However, in highly humified peats the difference is negligible (Farrell, 2012). Note that Dawson, (2006) reported a complete re-wetting of organic soils, having high proportion of mineral contents and high bulk densities $> 4.2 \text{ g/cm}^3$. Organic soils also exhibit the potential to swell on re-wetting, unless they are dried to a threshold value of irreversible drying.

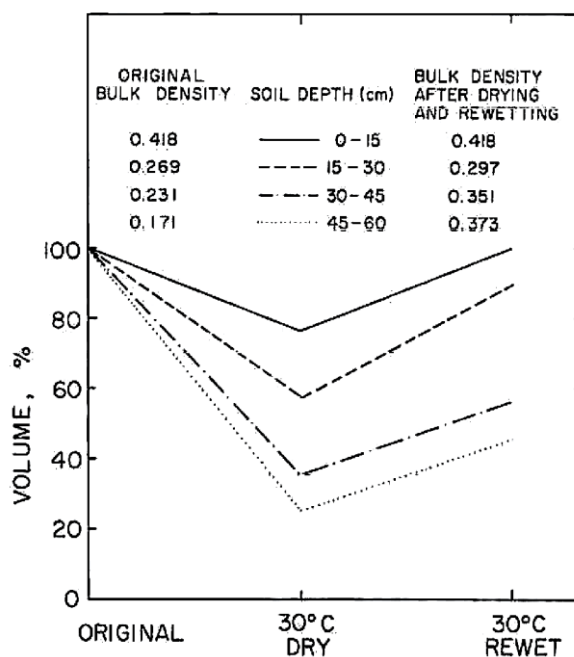


Figure 2.9 The effect of bulk density on drying and re-wetting (Radforth et al., 1996)

Acidic humified peats exhibit higher resistance to re-wetting due to their high lignin content and because of the presence of phenolic hydroxyl and carboxyl groups (Lucas, 1982). The formation of a resinous coating upon drying due to the hydrophobic nature of the peat also prevents the re-adsorption of water (Coulter, 1957). The observation of small changes in low lignin *Sphagnum* peats is consistent with this (Driessen and

Rochimah, 1976). Other findings for the resistance to re-wetting include the accumulation of iron coating around the organic particles and the adsorption of air films (Valat et al., 1991). In the re-wetting process of low moisture or dry soils the transition of adsorbed water from capillary-bound water is of great significance, as the cyclic drying and re-wetting produce more hydrophobic peats. (Valat et al., 1991).

2.3.6 pH or Hydrogen Ion Activity

Chemistry of water and plant or vegetation type are major factors related to the chemical characteristics of the peat. The alkalinity or acidity of the peat water or peat itself is simple and useful indicator of mire morphology, as the base or nutrient deficient water is acidic in nature and is associated with bogs, while characteristically the base and nutrient rich water is alkaline in nature and is associated with fens. The decomposition of the plants and also the metabolic activity in the living plants produce the hydrogen ions, thereby increases the acidity of the peat. Presence of sulphur mobilizing bacteria in the soil is another hypothesized source of acidity in bogs (Hobbs, 1986). Figure 2.10 below, shows the pH transition with the organic content %, observed by Radforth et al., (1996) for several fen and bog peats. In general, the fen peats have a pH > 5, whereas the pH for the majority of bogs range between 3.3 and 4.5; transitional peats have a range of pH from 4.0 to 6.0. For the un-humified peats as the organic content of the soil increases, the pH decreases as represented above in the Figure 2.11. Moreover, the peat water is less acidic compared to the corresponding peat matter. There is always a good correlation between the organic content % and the pH, but local influences like mixing of minerals from flooding may affect it considerably. Hence in view of this situation both organic content and pH should be determined along with other peat parameters to effectively characterize the mire (Radforth et al., 1996; Hobbs, 1986).

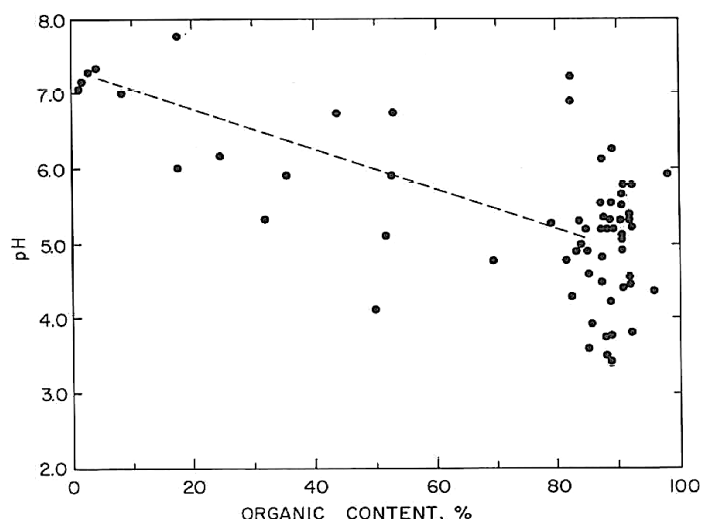


Figure 2.10 pH variation with Organic content % of fen and bog peats, after (Radforth et al., 1996)

The pH of the peat water and the peat soil can easily be measured by colorimetrically or electrometrically by following BS 1377-1990: part 2. Ideally pH of the peat or the peat water should be measured upon extraction in field, otherwise the samples should be transferred to the laboratory in an air tight container to avoid oxidation and tested as soon as possible (Hobbs, 1986).

2.3.7 Cation Exchange Capacity (CEC)

CEC is the ability of the soil to exchange and absorb the cations to the soil particle surface. This, as well as the chemistry of the water conveying the nutrients controls the rigidity and the thickness of the adsorbed water zone around the tissues or soil particles. In general, higher the CEC, the higher the interparticle adherence and the stronger the adsorption complex (Stevenson, 1994). In this respect, peat is not very different from clay, but the magnitude of the CEC of peat tissues is inversely dependent to the mineral concentration in the water supply. In the low organic content soils the metallic cations from the soil minerals like, (*K*), (*Ca*), (*Na*), (*Mg*) saturates the most of the exchange ability. As the organic content increases the percentage and amount of exchangeable hydrogen ions also increases (see Figure 2.11). Due to the humification or drainage as fen converts into bog the saturation of soil minerals decreases, accompanied by a rapid fall in the concentration of exchangeable metallic cations, which promptly increases the concentration of exchangeable hydrogen ions

(Barber, 1981). The CEC of the fen and lake is very similar to illite; whereas bogs have similar CEC to sodium montmorillonite (Radforth et al., 1996).

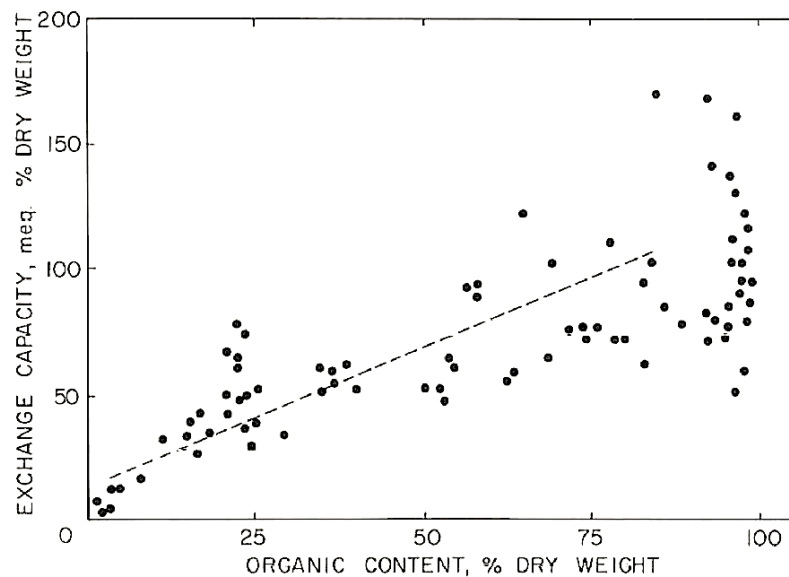


Figure 2.11 Cation Exchange Capacity variation with Organic Content %, after (Radforth et al., 1996)

In partially humified peats pH also affects the CEC as the CEC of the organic matter increases significantly with an increase in pH (Stevenson, 1994). Carboxyl and phenolic-OH are two major chemical groups in the humic substances and controls the hydrogen ion activity in the peats. The carboxyl group lose the proton in the acidic conditions and ionize at a pH as low as 3.0, while the phenolic-OH group is more active in the alkaline conditions and ionize at a pH of 9.0. However, the CEC of the peats cannot increase indefinitely with pH, as hydrolysis reaction at high pH breaks down and dissolves organic matter very rapidly (Tan, 2005).

2.3.8 Permeability of Peats/Organic Soils

As a general rule, the fibrous Acrotel layer is more permeable than the Catotelm layer, which is more decomposed and more compacted. The thickness of the Catotelm depends on the water table level and the depth of the underlying mineral substrate and according to Ingram (1983), its permeability mainly depends on the plant composition; porosity or void ratio and drainable porosity or void ratio; fibre content and degree of humification (inversely related) and bulk density (higher bulk densities imply mineral soil presence or high degree of humification both factors reducing

permeability); and surcharge loading; structure and macrostructure of the peat. The structural variation of fibre arrangement produces a wide diversity in the peat permeability rates. The laboratory tests have shown the permeability in the horizontal direction to be considerably higher than in the vertical direction due to the orientation of fibres (Ingram, 1983) i.e., by the factor of between 3-10 (Mesri, 2007).

The permeability decreases very rapidly along the depth of the mire (Hobbs, 1986). Ingram (1983) measured the permeability by using seepage tubes of the disturbed and slightly humified moss peat in a Scottish raised bog, and recorded high values in the bog Acrotelm, exceeding 10^{-1} m/s, and a declining permeability of 3×10^{-5} to 6×10^{-7} m/s towards the base of the Acrotelm. Large-scale test data by Ingram (1983) are shown in Table 2.7.

Due to the presence of flat gradients and mineral soils fens have lower permeability compared to bogs of high undecomposed organic content. The chemistry of the percolating water also affects the peat permeability as it directly affects the humification and the adsorption complex. Lieszkowski et al., (1977) mentioned a drop in the fen peats permeability with an increase in the pH of the percolating water.

Table 2.7 Field permeability measurements for fen and bog peats, after Ingram (1983)

Peat Description	Von Post Scale	Permeability
Brushwood Peat	H3 to H6	10^{-5} m/s
Sedge peat	H3 to H5	10^{-5} m/s
Sphagnum peat	H3	10^{-5} m/s
Heather peat, Cotton Sedge, Sphagnum peat	H3 to H6	10^{-7} to 10^{-6} m/s
Slightly humified fen peat		5×10^{-3} m/s
Sphagnum peat	H8 to H10	6×10^{-8} m/s
Highly humified blanket peat		6×10^{-10} m/s

The flow in the peats is mainly horizontal, and in the field customarily the local or structural permeability is determined by both constant/negative head and rising head piezometers, the rising head is usually employed at boreholes containing sand packs.

2.3.8.1 Permeability Under Load

Upon compression the permeability of the peat or organic soil changes considerably, depending on type of peat, its degree of humification and most importantly on the macro and microstructure of the peat.

With reference to void ratio the change in permeability can be expressed as:

$$C_k = \frac{\Delta e}{\Delta \log k_v} \quad (2.3)$$

Where, change in void ratio is given by (Δe), and the permeability in the vertical direction is denoted by (k_v).

The variation in peat permeability is considered to be linear on a $\log(e)$ - $\log(k)$ plot by Hanrahan (1954), and provided a relation:

$$k = k_{vo} \left\{ \frac{e}{e_o} \right\}^n \quad (2.4)$$

Where, (k_{vo}) gives the in-situ permeability, and (e_o) gives the in-situ void ratio. Using this relation on the $\log(e)$ - $\log(k)$ plot Hanrahan (1954), has calculated a decrease in the coefficient of permeability (k_v) under the loading of 55 kPa from an initial value of 4×10^{-6} m/s to 2×10^{-8} m/s within first two days, and for the next seven months it decreases further to 8×10^{-11} m/s. Near the surface of the virgin fen peat Hogan et al., (2006), found the value of (k) = 2×10^{-2} m/s, which decreased to 10^{-5} to 10^{-6} m/s at the depth of 2 to 3 m. Similarly, for the fibrous peats Hobbs (1986), reported values of vertical initial coefficient of permeability (k_{vo}) = 4×10^{-6} m/s, $n = 11.03$ and (e_o) = 12. Landva, 1980 reported a permeability decrease by three orders of magnitude for a 50% reduction in void ratio. For fibrous peats, Mesri (2007), has given the change in permeability, $C_k = 0.25e_o$. where (e_o) gives the in-situ void ratio.

The most comprehensive literature on the vertical permeability of the fibrous and undisturbed peat is given by Hobbs, (1986), presenting plots of permeability measurements during the consolidation of 98 series of peat tests by using standard oedometer and 250mm diameter Rowe cell (see Figure 2.12). The hatched section in the figure shows the 8 tests by Lefebvre et al., (1984) from Quebec, 22 tests by

Barden, (1983) of Chat Moss from the Manchester, 18 results by Barden & Vickers, (1975) from a site in Warrington, UK, result on an amorphous peat by Lieszkowski et al., (1977), 2 tests by MacFarlane, (1969) from Japan, 3 results by Casagrande (1966), 2 results set of fibrous bog peat by Hanrahan (1964) and 45 results by Lea & Brawner (1963) on fen peats from Brawner freeway site in British Columbia. It can be seen that permeability values range over three orders of magnitude due to variability in the peat type as well as the different natural void ratios from which the peats were consolidated. In general, taking all the results together, the highly humified and low fibrous peats lie near the lower and the less humified and more fibrous peats lie near the top boundary of the result envelop. Moreover, mires of similar morphologies from different locations may show intense local variation due to different climatic and geographic regions, yet have broadly similar permeability characteristics.

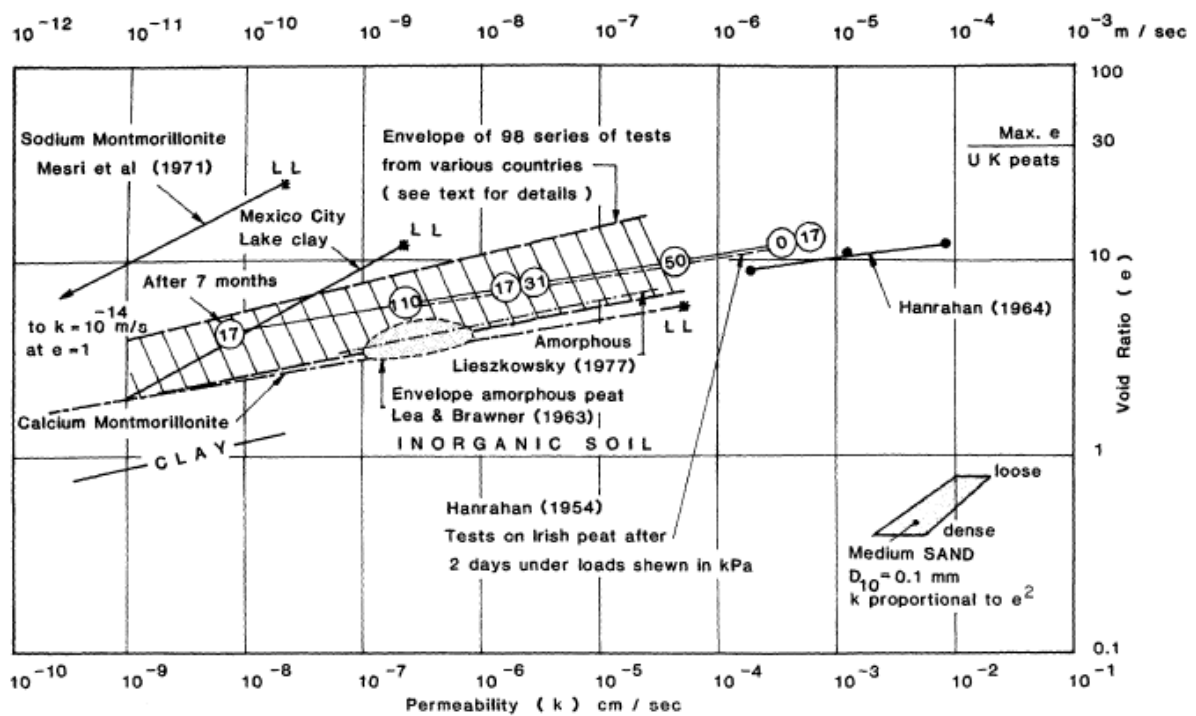


Figure 2.12 Vertical permeability vs. void ratio (Hobbs, 1986)

Hobbs (1986), has provided a correlation of the mean value of this log-log envelop to the Terzaghi & Peck (1948) giving the expression of peat k as:

$$k = 1.4k_{0.85}e^2 \text{ cm/s} \quad (2.5)$$

and:

$$k_{0.85} = (100 \text{ to } 150) D_{10}^2 \text{ cm/s} \quad (2.6)$$

This roughly correlates to loose medium sand in uniform conditions representing the permeability at the void ratio of 0.85. Based on Fig 2.12 the maximum permeability of the peat at a void ratio range of 10 to 20 corresponds to the permeability envelop of the sand. The mean sand porosity is approximately 35% whereas that of the peat at this void ratio lies within the range of 91-95%, but reductions apply due to non-drainable voids in peat. At the other range end of the results, the permeability of the intact clay at 50% porosity corresponds with the compressed peat having porosity range in-between 65-80%. (In clay the water is largely absorbed, therefore no deductions due to porosities due to undrainable voids apply). As it can be seen from the plot the void ratio of sodium montmorillonite clay at its liquid limit (where its permeability is about 10^{-10} m/s) is approximately equal to the upper limit of void ratio of the uncompressed fibrous peat with a permeability of approximately 5×10^{-4} m/s in the range of medium sand permeability. This can be explained by the open structure of the peat and its ability to hold water due to the strong adsorption complex (Hobbs, 1986).

Note that the consolidation results resulting to reduced void ratio due to compression cannot be used to estimate permeability of a peat at its natural void ratio or water content. This is due to the fact that peat compressibility is controlled by the adsorption complex which depends on the void ratio or water content in its natural state and not in the compressed state (Farrell, 2012).

2.3.9 Compressibility of Peats/Organic Soils

Peat is an exceptionally compressible material especially with higher water contents. The cell structure of peat can undergo deformation very easily under the influence of external applied pressure or due to interparticle forces. It distorts under large strains and therefore the compressibility and permeability characteristics change as the peat consolidates. Figure 2.13 shows the open cell structure of a typical peat sample under electron microscope.

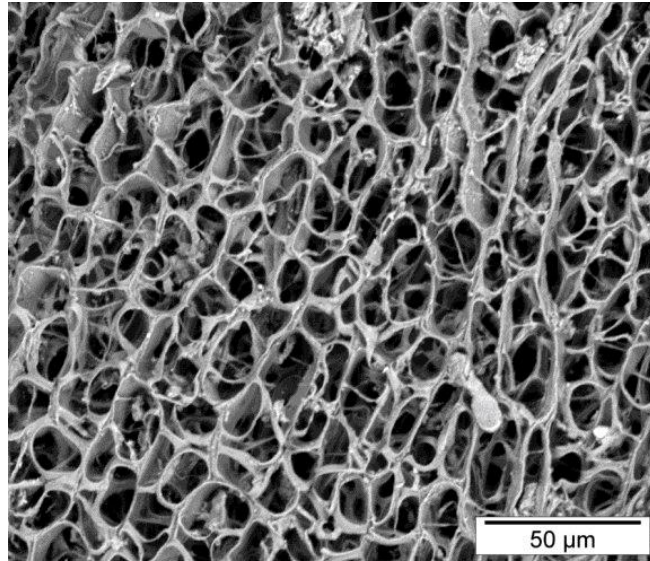


Figure 2.13 Back-scattered electron (BSE) image of *Sphagnum* peat shows the open pore structure, after (Rezanezhad, F., 2016)

The large compressions in peat in terms of vertical strains against the logarithm of the applied effective stress, of many studies as recorded by Landva & La Rochelle, (1983) and O'Loughlin, (2007) are given below in Figure 2.14.

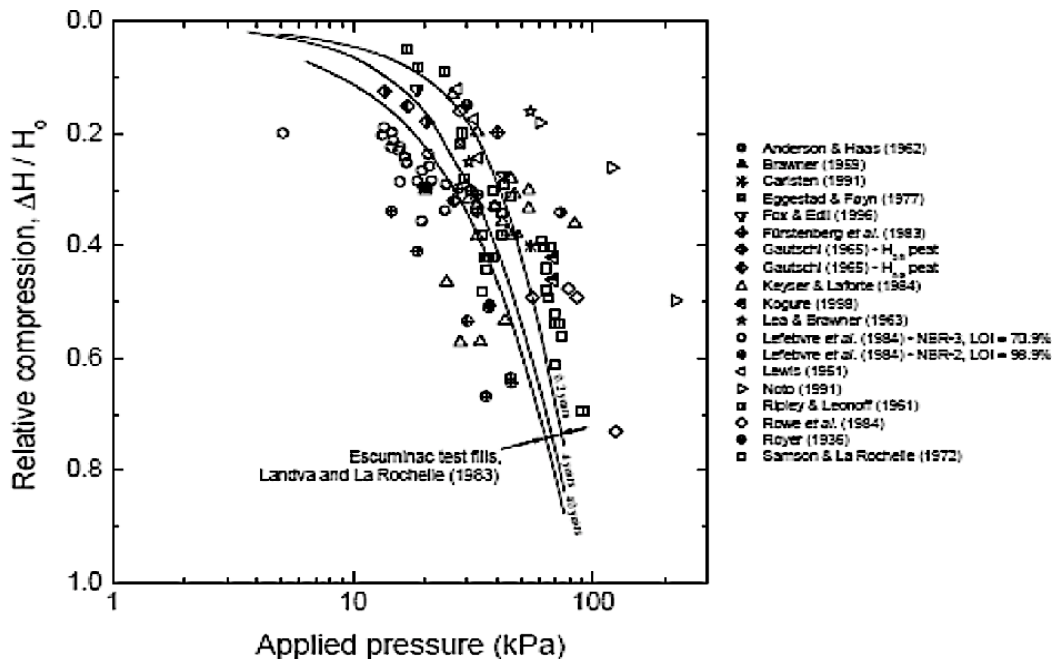


Figure 2.14 Compressions in peat vs Effective stress (originally plotted by Landva & La Rochelle, (1983), updated by O'Loughlin, (2007), after (Ferrell, E. R., 2012)

The results in the above figure indicate that a small increase of about 50 kPa can reduce the thickness of peat stratum by more than 50%. The consolidation of the peat is generally divided into two stages, primary consolidation the hydrodynamic stage, which is mainly controlled by excess pore pressure dissipation and secondary Compression. The latter is a continuous slow creep phase, which can be the predominant phase in the consolidation of peat, accountable for half of the total compression. It is attributed to the water bound to the soil particle or to the connection between the water and soil particles (Farrell, 2012).

Taylor's method and the normal method of semi-log plot was used to determine primary consolidation time in laboratory by Mesri (2007) and Lefebvre et al., (1984) respectively who both found it to be approximately consistent with the end of the dissipation of excessive pore pressure. However, O'Loughlin (2007), argued that the Casagrande's method and to a larger extent the Taylor's method consistently underestimate the primary consolidation time. Hobbs (1986), claimed that the field investigation by using the piezometers is the only way to accurately determine the time of primary consolidation for peats.

The secondary compression has been modelled in two different ways by researchers. Some consider that it starts at the end of the primary consolidation (EOP method). This approach has the advantage to estimate the primary consolidation in a traditional fashion by using an e -log σ'_v plot, but essentially requires some knowledge or assumptions of the yield/pre-consolidation pressure (σ'_c). Due to the small surcharge loading or due to capillary suction forces in the Acrotelm the undisturbed peats were shown to have an obvious yield point (Hobbs, 1986; Mesri, 2007) which can be estimated using Janbu's method (1963) with the e -log σ' curve in the normal Casagrande (1936) construction. Others argue that secondary compression starts already at the primary consolidation stage and continues after completion of this stage (Degago et al., 2011). This necessitates estimation of the secondary compression from the start of the consolidation process. Several settlement models were developed accordingly, of which Den Hann's (1996), abc model (Den Hann, 1996) discussed in detail in Degago et al., (2011) and O'Loughlin & Lehane (2001). Rheological models were also used (e.g. Barden & Poskitt, 1972), but have not been adopted in general design due to large number of variables. In general, the large number of variables and

uncertainties related to the peat makes the implementation of continuous secondary compression approach difficult therefore, except for very large projects, the EOP approach is commonly used (Ferrell, 2012). Figure 2.15, illustrates the comparison of both methods, where H_1 and H_2 are sample heights tested by EOP and continuous approach respectively, and time required to complete primary consolidation is given by t_p .

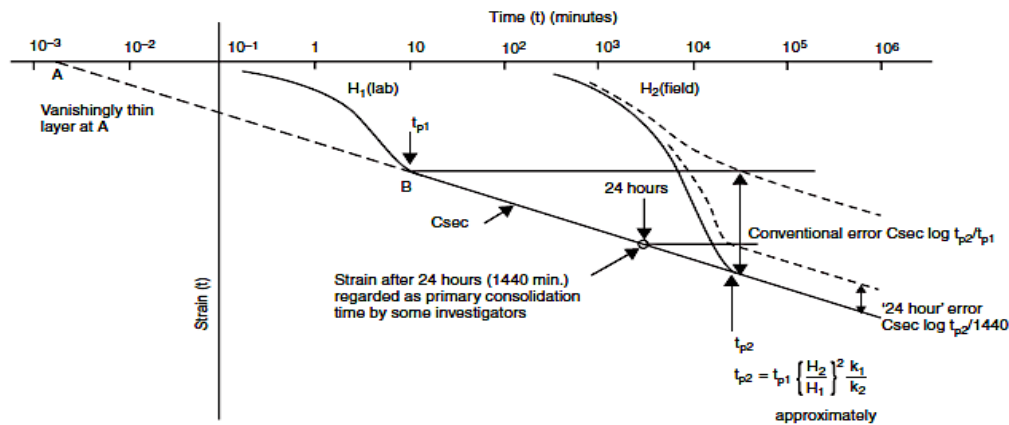


Figure 2.15 EOP vs Continuous compression approach,
(After Ferrell, 2012 and Hobbs, 1986)

2.3.10 Shear Strength of Peats/Organic Soils

In general, traditional methods are used to determine the shear strength of peats, without special consideration given to the high compressibility, gas and fibre content, or to high permeability especially for the fibrous peats, where c' and ϕ' is determined for drained conditions and s_u for the undrained loading. These peculiar characteristics present different challenges in the laboratory tests, for instance, dimensional non-uniformity and necking of samples during the UCS (unconfined/uniaxial compressive strength) or during the consolidation phase of triaxial testing, also the results in the drained triaxial one-dimension behaviour testing cannot be completed up to the 'failure' stage as given by the Mohr Coulomb criteria due to the fibre effects (Farell, 2012). Similarly, in the undrained triaxial testing the pore water pressure quickly rises up to equal the cell pressure due to low Poisson's ratio of the fibres present in peat, which makes the effective lateral stress equal to zero, hence the fibre content can

affect the analysis of effective stress parameters. In the field the fibre content provides difficulties in the determination of the correct field strength as it interrupts the field vane tests, and in general with an increase in size of the vane the recorded s_u decreases (Landva, 1980).

The ring shear tests are most commonly used in practice as these provide a conservative estimate or lower value of ϕ' , and thus eliminate the effects of fibre content (Farrell et al., 1999). For the determination of undrained shear parameters, the direct simple shear tests have gained more attention recently (Boylan et al., 2008).

2.3.10.1 Effective Stress Parameters

The values of the internal friction ϕ' for the peats/organic soils greatly depends on the method of test. For instance, values of ϕ'_{peak} for the fibrous peat has been recorded in the range of 32° to 40° in ring shear test and direct shear tests, while values in the order of 50° to 60° were given for the same material in consolidated undrained triaxial tests (Ferrell, 2012). In the case of undrained triaxial tests, the recorded low lateral effective stresses which essentially are zero at the failure affects the accuracy of the ϕ' . Similarly, due to the continuous compression behaviour of the fibres, generally it is not possible to bring a sample of fibrous peat to failure in a drained triaxial test, this can be compared to the behaviour of a mattress under compression. Moreover, it is also essential to make assumptions considering the effective horizontal stress at failure in the case of direct simple shear tests.

Farrell et al., (1999), has provided an expression to determine the ϕ' , on the basis of finite element analysis of direct shear test.

$$\phi' = \text{Sin}^{-1} \frac{\tau_f}{\sigma'_{vf}} \quad (2.7)$$

Where, τ_f is the shear stress, and σ'_{vf} is the vertical effective stress at failure.

The inherent for the fibrous peat anisotropy in-terms of horizontal and vertical ϕ' has been discussed by Yamaguchi et al., (1985a, 1985b), which gives the recorded value of $\phi' = 51^\circ$ to 55° for vertical samples from the triaxial compression tests as compare to $\phi' = 35^\circ$ in the horizontal samples, the highest value of $\phi' = 62^\circ$ has been reported

in the triaxial vertical extension samples. The higher values in the undrained triaxial tests on the vertical and extension tests are due to the effects of fibre structure and direct shear tests and ring shear tests are considered to be provide inherent ϕ' of the peat elements. Therefore, these higher values should be carefully interpreted and a relevance must be established with actual failure mechanism. Figure 2.16 below shows the results of a series of drained, undrained and extension triaxial compression tests conducted by Farrell & Hebib (1998), on the fibrous peat.

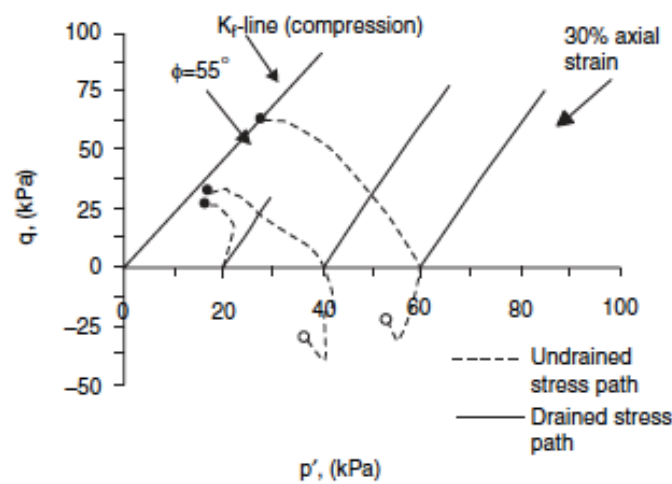


Figure 2.16 Triaxial tests plot of the fibrous peat, after (Farrell & Hebib, 1998)

The results indicate that in compression the $\phi' = 55^\circ$, and is significantly higher than the ϕ' measured in extension, which were $\phi' = 39^\circ$ at the initial consolidation pressure of 40 kPa and $\phi' = 18^\circ$ at 60 kPa. Moreover, for the drained triaxial tests which were conducted at the axial strain of 30% the samples did not extent to the failure line, while the ring shear and direct shear tests recorded $\phi' = 38^\circ$ for the same peat material. For peats having water content in the range of 330 to 850%, Mesri (2007), have measured the values of K_o in between 0.3 to 0.35, which corresponds to the value of ϕ' in the range of 40° to 44° . In a series of laboratory tests Edil and Wang (2000), measured the value of $K_o = 0.33$ for the fibrous peats and $K_o = 0.49$ for the amorphous peats. Hence, for the peats/organic soil which do not have the fibrous structure, the effective stress parameters can be determined by using normal methods. However, very little literature on the possible presence of the gases in the peats and their effect on the effective stress parameters is available.

2.3.10.2 Undrained Shear Strength

Traditional tests, i.e., UCS, triaxial tests, and in-situ CPTu and vanes are used to determine the undrained shear strength (s_u) of the peats or organic soils. Peats have s_u/σ'_{vc} ratios in compression in the range of 0.5-0.6 as opposed to inorganic soils with ratios of approximately 0.3 (where σ'_{vc} stands for the vertical consolidation pressure) (Mesri, 2007). For fibrous peats higher s_u/σ'_{vc} ratios have also been recorded in extension tests. However, for very high-water content peats s_u can be as low as 2 -4 kPa, which equals the accuracy limit of the normal testing apparatus. Fibres can also affect the test results both in the laboratory and in the field.

2.4. EK Soil Treatment

2.4.1. Definitions and Background

Due to the incomplete bonding of the positions available for metal ions and release of protons from hydroxides due to isomorphous substitution, soil particles e.g. clays generally carry a net negative surface charge (Mitchell, 1993). Particle surfaces hold ions of opposite charge to maintain electrical neutrality. The region of the negatively charged particle surface and the attracted positive ions in solution is defined as *diffuse double layer* (DDL) (Mitchell, 1993). The double layer thus consists of a fixed part and a diffuse part, composed of the balancing cations which are held by electrostatic attraction. In organic soils and peats, the DDL is formed around the humus particles in the same pattern as in clay particles (Asadi et al, 2013). The thickness of the DDL decreases with an increase in pore fluid electrolyte concentration and cation valence but increases with an increase in ion size and pH (Alshawabkeh, 2001). The electrical potential generated at the intersection of fixed and the mobile part of the DDL is defined as the *zeta potential* (ζ) and depends on the interfacial chemistry between the solid and liquid phases (Jayasekera, 2008; Pamukcu et al., 1997; West & Stewart, 1995). It is thus a function of mineral type, pH of the porous media, and ionic concentration and species (West & Stewart, 1995). It is usually negative for peats and clayey soils. Amorphous peats have higher zeta potential compared to fibrous peats due to less organic content (Asadi et al., 2013). Figure 2.17 represents the DDL and ζ on a charged particle.

In the EK treatment of peat soils, the thinning or expansion of the DDL around the humus particles is due to the acid-base distribution, changes in the soil surface charges. Cation Exchange Capacity (CEC), and variation in the zeta potential. Increased thickness of DDL produces a dispersed soil structure (of humus particles, in the case of peat); thinning of DDL produces a flocculated structure. These changes affect the engineering characteristics of the soil (Asadi et al., 2013).

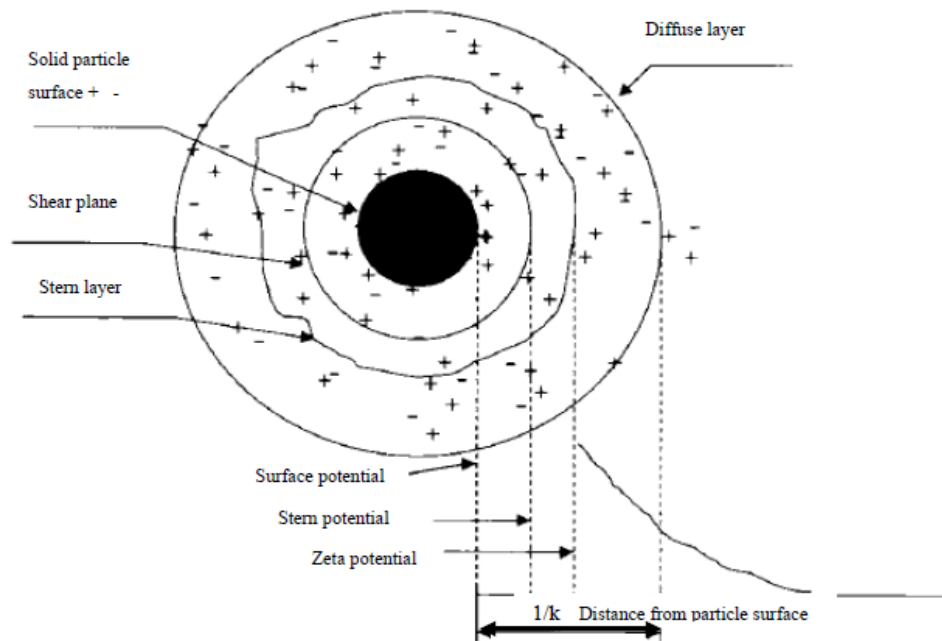


Figure 2.17: DDL and ζ of a charged particle, (source: West & Stewart, 1995)

2.4.2 Electrokinetic Phenomena in Soils

Electrokinetic stabilisation uses a low electric potential or low intensity direct current (DC) to two oppositely charged electrodes, anode (positive) and cathode (negative), to enhance the engineering characteristics of soils (e.g. Asadi et al, 2010 using EK to dewater /stabilise tropical peat; Micic et al, 2001, using EK to strengthen a soft marine clay adjacent to offshore foundations in South Korea, Lamont-Black et al, 2106 and Jones et al, 2014 using EK geosynthetics (EKG) to strengthen embankment slopes made respectively of Weald Clay and London Clay mixed other material such as brick and stone fragments), to dewater and/or remediate/treat: (a) slurries (e.g. Fu et al, 2018 Wenzhou clay slurry dredged from seabed to use as fill for land reclamation; Fourie and Jones, 2010 mine tailings; remediation of mine tailings and a metallurgical

furnace dust with recovery of metals, Peppicelli et al, 2018); (b) sludges (e.g. Lamont-Black et al, 2015 using EKG for the dewatering of nuclear contaminated waste sludge; Glendinning et al, 2008 for in-situ trial dewatering of sewage sludge using EKG; Tang et al, 2018, using biosurfactant-enhanced EK for heavy metal removal from wastewater sludge) and (c) sediments (e.g. Rozas and Castellote, 2012 for dredged harbour sediment remediation and also Masi et al, 2016 and 2017: for the in situ treatment of contaminated harbour sediments). Chemical species, and water molecules migrate according to uncoupled and coupled conduction phenomena induced by the DC thus resulting in a number of hydrological and physicochemical changes in the soil (changes in the DDL, pore fluid chemistry, hydraulic conductivity and the soil fabric, Alshawabkeh, 2001). As in clays, DDL on the humus particles induces and enhances EK phenomena in organic soils, which makes peats and organic soils suitable for EK treatment (Wahab et al., 2018).

Namely, the application of the DC current:

- (a)** initiates *electro-osmosis* i.e. water migration from anode to cathode due to the electric potential difference, a phenomenon first reported by Reuss (1809); once a current applied to the system, excess cations in the DDL start moving towards the cathode together with the surrounding water molecules (Hausmann, 1990). Interaction between flow in the water surrounding the soil particles and flow in the bulk water phase enables the movement of water in the bulk phase, through a drag action. Electro-osmotic flow may eventually stop at some later stages of the EK process due to the overall domination of the acidic front in the soil specimen. Electro-osmosis can play a significant role in the EK stabilisation for low ionic strength of the pore fluid, high water content and the presence of the appropriate mineral. (Alshawabkeh 2001).

- (b)** generates the *electrolysis* of the pore water fluid, as the conversion of electrical energy into chemical potential energy causes oxidation at the anode along with the formation of O₂ and H⁺, and reduction at the cathode and generates H₂ and OH⁻. The acidic front at the anode due to oxidation reaction and alkaline front and the alkaline front at the cathode as a result of reduction reaction, migrate towards each other across the soil mass (Iyer, 2001).

(c) causes *electrophoresis* i.e. transportation of charged particles and solids such as colloids and micelles relative to the stationary liquid; negatively charged particles are transported electrostatically to the anode and positively charged will be attracted towards the cathod;

(d) causes *electro-migration* i.e. ion flow either towards anode or cathode depending on the ion charge. The water molecules layers surrounding the ions can also be dragged along with the ions towards an electrode; thus, the higher the ionic concentration the higher the ionic water flow. Apart from electrical gradient electromigration is driven by concentration, pressure and thermal gradients (Iyer, 2001).

The colloidal particles and charged ions are those present in the soil pore fluid or can be introduced at the electrodes (e.g. ions released from the degradation of electrodes, H^+ and OH^- ions produced during the electrolysis process, ions from chemical stabilising agents introduced at the electrodes). For geotechnical and geo-environmental applications, mass flux due to electrophoresis is usually not as significant as electromigration and electro-osmosis but can play a major role in the decontamination of chemicals adsorbed on the solids (Shenbagavalli & Mahimairaja, 2011). The relative contribution of electromigration and electro-osmosis towards the total transport of chemical species is affected by the soil degree of saturation, pore fluid characteristics and soil fabric.

Together with the above electrokinetic phenomena, a number of geochemical processes occur during the EK process. These can affect either favourably or unfavourably EK transport, which depends on soil-surface chemistry, pH, and equilibrium chemistry of the aqueous system. These geochemical processes are:

(a) *Redox (oxidation-reduction) reactions*, which cause pH to change in the soil; considerable changes in pH leading to highly acidic and alkaline environments can become detrimental for infrastructure and ecosystems, therefore need to be controlled. However, soils have good buffering capacity, therefore changes in soil pH take place slowly (Mosavat, 2014). Soil of low CEC have lower buffering capacity compared to peats such as undecomposed Sphagnum moss, Sphagnum

sedge peat and highly decomposed black peat (Puustjarvi & Robertson, 1975). Thus, the physicochemical composition controls the buffering capacity of soil which ultimately affects the pH dependent electrochemical and geochemical reactions.

(b) *Precipitation and Dissolution* (referring respectively to the extraction of a substance from a solution as a solid and the formation of a solute in a solvent. These processes dependent on the pH of both soil and pore fluid: in low pH environments, precipitates tend to dissolve and form new precipitates. Conversely, in high pH environments, metals precipitate, slowing the EK process due to soil pore clogging (Acar & Alshawabkeh, 1993).

(c) *Sorption and desorption*: The former process referring to attachment of chemical species from the solution onto a solid surface (e.g. particle surface) and includes ion exchange and surface complexation mechanisms; conversely desorption refers to the release of ions from the solid (soil) surface. The electrolysis of the pore fluid during EK, generates hydrogen (H⁺) and hydro-oxide (OH⁻) ions and the migration of these ions changes the soil pH. With an increase in concentration of H⁺ ions cations are desorbed from the surface of soil particles (depending on the soil type). These processes also depend on the existence of carbonates and organic matter in the soil, surface charge density of the soil particles as well as concentration and characteristics of the cationic species (Acar & Alshawabkeh, 1993).

It thus transpires that soil pH, which changes during EK treatment, is crucial to the efficiency of the EK; it is also important for the biocementation process discussed later. Note that decomposition of organic matter due to microorganisms and plant root growth are some natural processes that also affect (increase) the soil pH.

2.4.3 Types of Flow Through the Soil

Flows of fluids, electricity, chemicals and heat flow occur through soils. Each flow rate or flux, J_i , (shown in Table 2.8), is linearly related to its corresponding driving force X_i according to

$$J_i = L_{ii}X_i \quad (2.8)$$

in which L_{ij} is the conductivity coefficient for flow. (Mitchel, 1993)

A summary of conduction occurrences through porous media is given in Table 2.8

Table 2.8: Direct (in the diagonal) and coupled (off-diagonal) flow phenomena through porous medium, (after Mitchell, 1993 and Mitchell & Soga, 2005)

Flow rate (J)	Governing Equation	Conduction phenomenon and Gradient X			
		Hydraulic head	Temperature	Electrical	Chemical concentration
Fluid (q_h)	<i>Darcy's law</i> $q_h = -k_h(\partial h/\partial x)A$	Hydraulic conduction	Thermoosmosis	Electroosmosis	Chemical osmosis
Heat (q_t)	<i>Fourier's law</i> $q_t = -k_t(\partial T/\partial x)A$	Isothermal heat transfer	Thermal conduction	Peltier effect	Dufour effect
Current (I)	<i>Ohm's law</i> $I = -\sigma_e(\partial V/\partial x)A$	Streaming potential	Thermoelectricity (Seebeck effect)	Electric conduction	Diffusion and membrane potentials
Ion (J_D)	<i>Fick's law</i> $J_D = -D(\partial c/\partial x)A$	Streaming potential	Thermal diffusion of electrolyte (Soret effect)	Electrophoresis	Diffusion

Where $(\partial h/\partial x)$, $(\partial V/\partial x)$, $(\partial c/\partial x)$, $(\partial T/\partial x)$ are respectively the hydraulic gradient, thermal gradient, electric potential gradient and chemical gradient and k_h , k_t , σ_e and D the hydraulic conductivity, the thermal conductivity, the electrical conductivity and the diffusion coefficient respectively; A is the cross-sectional area

EK causes all above types of flow in the soil. Note that during the EK process these potential gradients do not remain constant but can vary in space and time.

Conduction of electric current in soils mostly occurs through water in fractures or pore spaces. Thus, electric current mainly passes through bulk pore water, and in some cases, it can also flow through the DDL along the soil particle surface. Geometry of pores and pore space control the hydraulic conductivity and fluid flow in the soil and hence electrical conductivity; good interconnection of pores supports electric conductance. In addition to grain size distribution, porosity, pore geometry and tortuosity, soil and pore fluid composition, degree of saturation, pressure, temperature, salinity also affect electric conductance (Jayasekera, 2008).

In organic soils fiber and organic content and the conductance mechanisms of various fluids, chemicals and electricity through the porous soil medium are the key elements that identify and control the physical and chemical properties of the peats or organic soils. For peats the water conductance is highly related to drainage conditions and depends on the degree of decomposition, type of peat and its bulk density orientation

of fibers and laminations (peat or soil layer) significantly regulate the hydraulic conductivity of the peat which is also considerably affected by macro-pores such as, tillage fractures, structural shrinkage-swelling and continuous voids in soil (Boelter, 1974). In general, herbaceous and decomposed peats have low hydraulic conductivity while the fibrous and undecomposed peats often have moderate values (Lucas, 1982). The hydraulic conductivity values of different peats determined by several researchers was given earlier in section 2.3.8.

Concerning the coupled flows during EK, as shown in Table 2.8, electroosmotic flow adheres to Darcy's law but the electric gradient replaces the hydraulic gradient in the governing equation. The electroosmotic fluid flux q_{eo} per unit area of soil is controlled by the coefficient of electro-osmotic permeability (k_e). Thus, the electro-osmotic fluid flow rate q_{eo} (m^3/sV) under an applied electric gradient $i_e = \frac{\Delta V}{\Delta L}$ in a soil with electroosmotic permeability $k_e(m^2/ V \cdot s)$ is given as:

$$q_{eo} = k_e \left(\frac{\Delta V}{\Delta L} \right) A \quad (2.9)$$

Where ΔV is electrical potential difference, A is cross-sectional area of sample and ΔL is length of soil sample.

Assuming that the soil pore structure is consists of capillary tubes k_e is given as:

$$k_e = \frac{D\zeta}{\eta} n \quad (2.10)$$

Where D is the dielectric constant, n is the porosity, ζ is the zeta potential (V), and η is the viscosity (FT/L^2). Typical values of k_e for different soils are given in Table 2.9.

Table 2.9: Values of (k_e) of different soils, after (Asadi et al., 2013)

Soil Type	k_e ($cm^2/s.V$)
Peat (humified to fibrous)	4.91×10^{-6} to 1.57×10^{-5}
London Clay	5.8×10^{-5}
Clay Silt	5.0×10^{-5}
Kaolin	5.7×10^{-5}
Na-montmorillonite	2.0×10^{-5} to 12×10^{-5}
Boston blue Clay	5.1×10^{-5}

In the unidirectional EK treatment, the water is collected from the anode due to the direction of the electro-osmotic flow, which results in reduction in water content and consolidation in the anode vicinity. Consolidation theory and volume change of a fully saturated soil is based on the quantification of water flow through the soil mass, which, as discussed above, in electroosmosis depends on both the hydraulic conductivity k_h and the electroosmotic permeability k_e . A 1-D governing equation can therefore be derived, see e.g. Esrig and Henkel (1968):

$$\frac{\partial^2 u}{\partial x^2} + \frac{k_e}{k_h} \gamma_w \frac{\partial^2 V}{\partial x^2} = m_v \frac{\partial u}{\partial t} \quad (2.11)$$

Where, x (m) is the horizontal distance from the anode, u the pore water pressure γ_w (kN/m³) the unit weight of water, V the electrical potential and m_v the coefficient of volume compressibility m²/kN).

The ratio of electro-osmotic permeability coefficient to hydraulic conductivity (k_e/k_h) shows the contribution of both electric and hydraulic gradients. As hydraulic conductivities of the coarse-grained soils are relatively high (>10⁻³ cm/s) and due to almost non-existent electro-osmotic flow the (k_e/k_h) ratio is very small and reaches zero. Conversely, in fine-grained soils the (k_e/k_h) ratio is significant due to high (k_e) (>10⁻⁵ cm²/s.V) and low (k_h) (10⁻⁵ cm/s to 10⁻⁷ cm/s).

2.4.4 Practical Considerations

A number of factors affect the effectiveness and efficiency of the EK treatment and need to be considered prior to field implementation. These include soil type, properties and state (e.g. moisture content /saturation), pore fluid pH, as well as the system design factors (e.g. applied voltage, electrode material and spacing, required time etc.) which affect the cost. A summary of primary factors affecting the overall EK process according to Mosavat (2014) is given in Table 2.10.

Table 2.10: Main factors affecting the EK treatment (modified after Mosavat, 2014)

	Affecting Factors	Characteristics
Soil properties and state	Water content	<ul style="list-style-type: none"> Not fully saturated to avoid effects of tortuosity and pore water content, but should be adequate to optimally permit the electro-migration
	Soil type and mineralogy	<ul style="list-style-type: none"> Effective on soils having high cation exchange capacities (CEC), e.g., organic soils, peats, bentonitic and illitic clays, soils not having, soils with moderate plasticity such as silty clays than fine clays and clay soils having 30% or more proportion of the particle size <math> < 2\mu\text{m}</math>. Not effective in soils having high buffering capacity and soils containing high carbonate buffers, e.g., glacial till.
	Electrical conductivity (EC) and pore water pH	<ul style="list-style-type: none"> Effective in soils with high CEC and high pH value ($\text{pH} > 8$).
EK System Design	Electrode type	<ul style="list-style-type: none"> Preferably cheap and inert electrodes (e.g., Electrokinetic geosynthetic, graphite, and "pressed carbon-coated" electrodes). Metal electrodes e.g., iron, steel and copper can be used to introduce metal ions for metal oxide generation.
	Voltage and current	<ul style="list-style-type: none"> Electric voltage and current intensities are in the order of few voltages and amperes per square meter, depending on the electrochemical properties of the soil (e.g., soils with higher EC require higher currents and more charge)
	Cost & treatment time	<ul style="list-style-type: none"> Depend on the depth and type of treatment required, spacing of electrodes, site preparation requirements, type and process designed used, electricity and labour costs, etc. Depend on the rate of chemical transport, electrode spacing and configuration, current and voltage levels

2.5 Biocementation

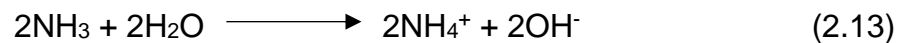
2.5.1. Definitions and Background

As mentioned in the Introduction chapter, *bio-cementation* is a recently developed soil stabilisation technique using the metabolic pathways of microorganisms to produce a cementing agent (usually CaCO_3) that binds the soil particles together, thus improving the engineering properties of soils. It mimics natural processes of biosandstone formation from sand due to microorganism action (see e.g. East cliff in England, Lake Thetis and Pinnacles in Australia, as stated in Mujah et al, 2017).

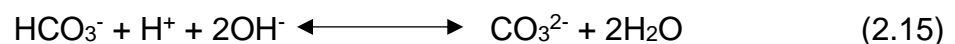
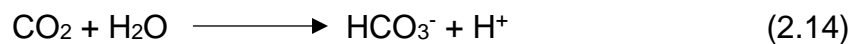
The most widely adopted process to achieve soil bio-cementation is *microbially induced calcite precipitation (MICP)*, in particular through urea hydrolysis, which a rather straight forward and easily controlled process (Al-Thawadi 2013). The conversion efficiency of the chemical species such as urea into CaCO₃ precipitates for this method is up to 90% in the first 24 h of the reaction (Dhami et al., 2013). The precipitation of CaCO₃ by urea hydrolysis is a multi-step chemical reaction (Martinez 2012; Cheng 2012; etc.) The initial urea CO(NH₂)₂ hydrolysis generates the ammonia (NH₃) and carbon dioxide (CO₂) as shown in equation 2.11.



The local increase in pH occurs due to the hydroxyl ions (OH⁻) generated by the conversion of ammonia to ammonium, which leads to the breakdown of bicarbonate to carbonate ions equation 2.12.



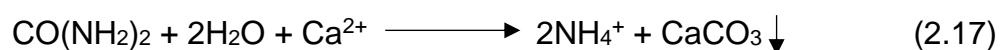
The carbon dioxide quickly reacts with the water and produces bicarbonate (HCO₃⁻), equation 2.13, which further reacts with hydroxyl ions (OH⁻) to generate carbonate ions equation 2.14.



Hence, the precipitation of CaCO₃ occurs in the presence of calcium ions (Ca²⁺).



The overall process of urea hydrolysis and CaCO₃ precipitation is given as:



The crystal formation of the precipitated CaCO₃ occurs in three stages (Ferris et al., 2004).

- 1) The formation of a supersaturated solution.
- 2) Nucleation at the position of critical saturation (the initial site for CaCO_3 formation is usually bacterial nuclei).
- 3) Spontaneous and uniaxial crystal growth on the stable nuclei.

Depending on the supersaturation and attachment conditions different CaCO_3 crystals in morphology (size, shape, type) may develop. The strength of the bio-cemented soil also depends on the CaCO_3 polymorph (aragonite, vaterite, calcite) (Dhami et al. 2013; Ivanov and Stabnikov, 2017 see Fig 2.18); these also depend on the three stages mentioned above the precipitated CaCO_3 may be amorphous (non-crystalline) thus affecting the anticipated soil strength (Al-Thawadi 2013).

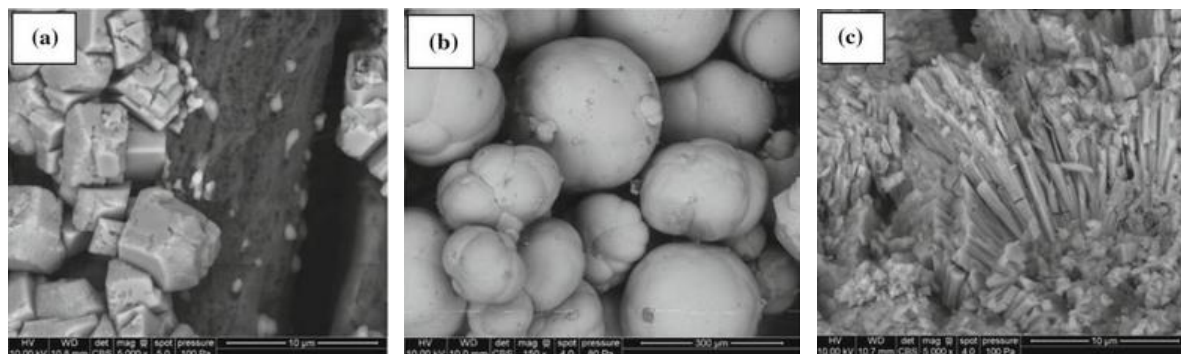


Fig 2.18 Different CaCO_3 polymorphs: (a) calcite; (b) vaterite; (c) aragonite (source: Ivanov and Stabnikov, 2017)

During MICP the precipitated CaCO_3 crystals forming at pore throats (point of contacts) join the soil particles together through an effective bridging (see Fig. 2.19 - note the meniscus shape due to the predominantly concentrated capillary force); bridging was observed by a number of researchers (e.g. DeJong et al., 2010; Cheng et al. 2013; Mahawish et al, 2018 amongst many others).

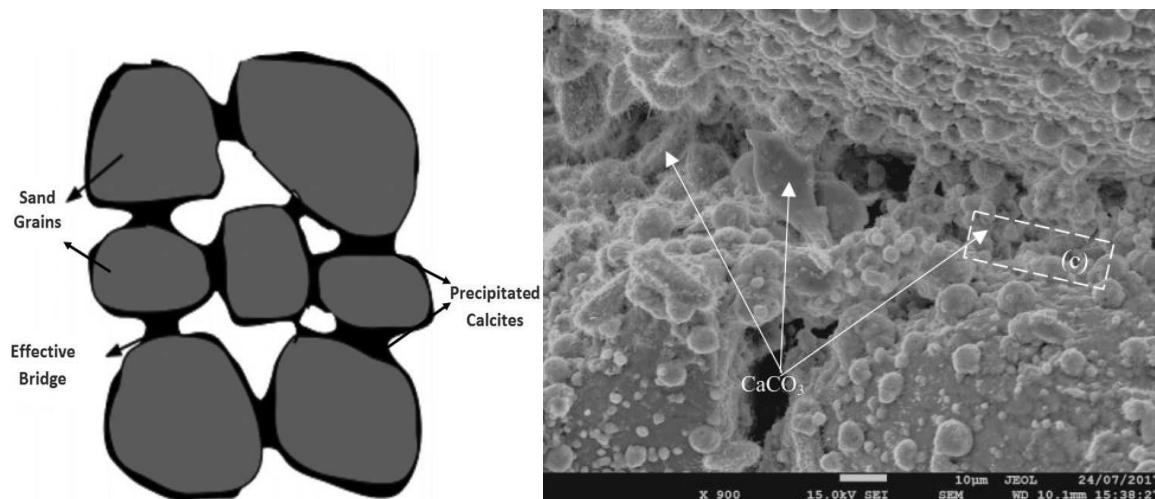


Figure 2.19: Effective bridging formation by CaCO_3 crystals: (a) conceptual drawing (after Mujah et al., 2017); (b) SEM (Mahawish et al, 2018)

Biocementation can be achieved by *bioaugmentation* i.e. the supply of precultured microorganisms into the soil to enhance microorganism populations at a site and/or *biostimulation*, where nutrients are added in the ground to stimulate native microorganism growth. The vast majority of studies used the former process. Biostimulation was applied in a limited amount of studies e.g. in Sato et al, (2016) and Danjo and Kawasaki (2016), who treated respectively peat and created artificial beachrocks against coastal erosion (in laboratory conditions) or in Gomez et al, (2017) who used it in pilot in situ biostimulation to treat sand.

2.5.2 Microbial Community Structure in Organic Soils

The structure and texture of the soil establishes the spatial clustering of microorganisms in the soil and determines the physical habitats of different soil systems (Young & Crawford, 2004). The distribution of microorganisms depends on the spatial location (topsoil vs subsoil) and varies considerably from ordered pattern to completely random pattern (Nunan et al., 2003). The distribution of microbial communities incriminates the mobilization and utilisation of organic carbon and the nature of nutrient within the soil-plant-atmosphere continuum. Depending on the soil composition, the fertile organic soils may comprise 10^4 nematodes, 10^4 protozoa, 10^{12} bacteria and 25km of fungi. However, these microbial populations can only cover the 6-10% surface area of the soil's total surface area (Young & Crawford, 2004).

The sphingolipids and the plasmalogens are two uncommon classes of phospholipid that are only found in the obligate anaerobic bacteria and distinguish these from aerobic and facultative anaerobic bacteria. The Gram staining technique is the most common method of classifying bacterial microbes, which classifies the bacteria into two general categories depending on the capability of the bacterial cell wall to hold the dye during a solvent treatment:

- *Gram positive* bacteria have thicker cell walls; they contain higher peptidoglycan, lower lipid content and stain well. Gram positive bacteria also have the ability to produce spores which enables these to sustain the unfavorable conditions and makes them very effective candidate for the geotechnical applications where phenomena like self-healing and prolonged soil treatment is required. Similar to fungi the gram-positive bacteria absorb nutrients from the extra-organismal environment and are believed to produce exo-enzymes (Prescott et al., 1996).
- *Gram negative* bacteria have thinner cell walls as compared to gram-positive, also have lower lipid content but do not stain well. Due to the retention of digestive enzymes in the periplasm and thinner cell walls the gram-negative bacteria have the ability to adapt better in a wetter environment (Petersen et al., 1997).

2.5.3 Ureolytic Microorganisms used for MICP Treatment

Although other biocementation mechanisms are possible and have been studied to a limited extent (e.g. the use of denitrifying bacteria, van Paassen, 2009; Hamdan et al, 2016), the vast majority of MICP studies used aerobic gram-positive bacteria of high urease activity thus giving a high amount of precipitates in a short time. The by far most widely used bacterium is *Sporosarcina pasteurii* previously known as *Bacillus pasteurii* (Whiffin, 2004; Al Thawadi, 2008; Achal et al, 2015; Dupraz et al, 2009; Al Qabany et al, 2012; Montoya et al, 2013; Wei et al. 2015; Montoya and De Jong, 2015; Gao et al 2018 amongst many others). In addition to its high urease activity (ranging from 4 to 50 mM urea/min for pure ureolytic bacterial cultures, see e.g. Whiffin et al., 2007; Al-Thawadi 2011; Burbank et al., 2012) these bacteria are popular because they exist ubiquitously in the soil and are able to grow at pH above 8.5 and at high concentrations of calcium, which is important for the MICP process (Ivanov and

Stabnikov, 2017). Other physiologically similar bacteria of the genus *Bacillus* such as *Bacillus megaterium* (Duraisamy, 2016) *Bacillus subtilis* (Sharma et al, 2019) and *Bacillus sphaericus* (Cheng et al, 2014; Sharma et al, 2019) were however also used successfully for MICP and were shown to produce calcite precipitation comparable to that of *Sporosarcina pasteurii*. Other species reported for successful MICP via the urea hydrolysis route include *Idiomarina insulisalsae* (Venda Oliveira et al, 2015) and *Sporosarcina ureae* (e.g. Mavroulidou et al, 2011; Botusharova et al, 2020) which is a spore generating species, and hence studied in the latter publication for the potential self-healing of the MICP treatment. Finally, bio-augmentation using indigenous bacteria isolated from the site was also used e.g. *Pararhodobacter sp.* in Danjo and Kawasaki (2016) for artificial beach rock formation to mitigate coastal erosion.

2.5.4 MICP Treatment Implementation Methods

Implementation of bacteria (for the bioaugmentation process), nutrients and cementing solution into the soil matrix is done by *injection*, *surface percolation*, *surface spraying*, or *mixing* methods (Cheng and Cord-Ruwisch, 2014). More rarely (e.g. Keykha et al, 2014b and 2018) researchers also used EK for treatment injection into the soil and called the method *electro-biogrouting*. Here follows a review of these methods.

2.5.4.1 Injection Method

Injection method has been the most widely used and in different ways, including MICP in upscaled tests due to advantages such as controllable injection conditions during the testing such as adjustable pressure, hydraulic gradient, and direction of injection (horizontal and vertical) and applicability to both saturated and unsaturated soils (Mujah et al, 2017).

For the bioaugmentation process, the retention of the injected bacteria into the soil mass is very important for successful MICP and uniformity of treatment. Indeed, the main disadvantage of the method is the potential uneven bacteria distribution, which can result into non-uniform biocementation treatment, i.e. non-uniform CaCO_3 distribution. For instance, in Whiffin et al. (2007), bacteria and cementing reagents were injected in the form of solution from top to bottom 5m long sandy soil column using a

peristaltic pump. It was reported that CaCO_3 precipitated throughout the 5m length of the soil sample, but its distribution was non-uniform along the sample length. It was also found that in order to achieve the compressive strength of 300 kPa a minimum of about 60kg/m^3 of CaCO_3 was precipitated. The non-uniformity in the CaCO_3 precipitation and a considerably high variation in the UCS peak strength was also reported by van Paassen et al., (2010a), in a large-scale experiment where the horizontal injection method was used to biotreat 100 m^3 of soil volume. In spite of non-uniform distribution of the precipitated CaCO_3 . Qian et al., (2010), reported the highest UCS strength of about 2 MPa in a MICP soil treatment by using the injection method in a column experiment. A two-stage injection process is therefore usually recommended whereby bacteria-containing solution is first injected into the soil, then some time is allowed to pass for retention of bacteria onto the soil particles (e.g. Al Qabany et al., 2012, recommended a 24h period), before the injection of cementing solution.

Possible filtration of the injected bacteria through the soil, and the rapid injection of cementation solution which can trigger a quick reaction of bacteria with the cementation reagent can cause localised cementation around the injection points thus pore plugging and uneven CaCO_3 distribution (Cheng & Cord-Ruwisch 2014). To overcome this Harkes et al., (2010), suggested a slower injection rate of bacterial and cementation solutions. Conversely, Whiffin et al. (2007), suggested that in order to allow more solutions to reach the deeper layers of the soil the flow rate of the cementing reagent should be increased.

2.5.4.2 Surface Percolation Method

This technique applies the treatment solution on the soil surface and lets it penetrate under gravity. Due to the free drainage or movement of fluid this method has the main advantage of cost effectiveness as the energy required for solution injection is saved. However, the low permeability and infiltration rate makes it challenging for the fine-grained soils. Depending on the soil type the method is likely to form a surface crust on the soil: for instance, it was found that for the fine sand size $< 0.3\text{mm}$ the cementation reaction was limited up to depth of 1m, while for the coarse sand column the treatment was achieved for the whole 2 m depth with UCS strength ranging between 850 kPa to 2067 kPa (Cheng & Cord-Ruwisch 2014). Reasonably

homogeneous CaCO₃ distribution and strength were however reported due to the self-adjustable preferential flow path in the coarse sand during the treatment.

2.5.4.3 Spraying

Spraying of liquid biocement also creates a layer of specified thickness on top of the soil and is thus suitable for surface applications such as wind erosion control (e.g. Zomorodian et al, 2019) or seepage control by creating an impermeable surface layer, as in Gao et al, (2018) or Ivanov et al (2016) who created an aquaculture pond in desert by sealing of sand through MICP, spraying the sand surface with dead but urease-active bacteria (non-sporogenic *Yaniella sp* strain) and a biocementation solution (in this case ferric hydroxide was precipitated and not CaCO₃).

2.5.4.4 Mixing Method

This method involves mechanically premixing bacteria into soil before introducing the cementation solution. This technique results in lower UCS strengths compared to the injection method (Mujah et al, 2017) but facilitates uniform distribution of bacteria and hence precipitated CaCO₃ (Zhao et al., 2014a). However, mixing involves disturbance to local soil structure and is generally unsuitable for existing infrastructure unless some technique such as deep mixing is used; deep mixing was thought unsuitable due to concerns about bacteria viability under the associated stresses; however recent laboratory work showed promising results for deep mixing using gram-positive bacteria (Duraismy, 2016).

2.6 Electro-Biogrouting

Most recently researchers (Keykha et al., 2014a, b; Keykha 2015; Keykha et al, 2018) coupled the bio-cementation process with EK. In the first three papers, bacteria, urea and calcium ion were all injected into the medium whereas in later papers Keykha et al, (2014) and Keykha et al, (2018) injected electrokinetically into the fine-grained soil externally produced CO₃²⁻ through bacterial action but not the bacteria themselves. The authors explain that during EK ions are moved across the specimen by electromigration from the anode to the cathode; urea (which is non-ionic and solvable), is transported through electro-osmosis from anode to cathode, whereas, bacteria

(which have a negative surface charge) are moved by electrophoresis from the anode to the cathode. The authors found increases in the shear strength of the soil (a high plasticity clay) up to 1080%.

Consideration was given in the literature of possible effects of the electric current on bacteria, such as cell rupture-voltage gradients over 0.4, and indirect effects through soil pH changes, the toxic electrode-effect, and physico-chemical property changes. These can potentially affect the metabolic activity and membrane composition of bacteria. However, bacteria can easily endure environmental stresses and a number of studies indicated that weak DC current does not have negative impact on bacterial viability. For instance, Lear et al., (2004) applying a 3.14 A m^{-2} DC studied the effect of EK on indigenous soil microbial communities. No serious negative effect on the diversity and structure of the bacterial community was found, with some exception of soil close to the anode (with $\text{pH} < 4$ after 27 days of treatment), where an increase in the percentage of Gram-positive species was observed. However, in a later work involving PCB contaminated soil (Lear et al., 2007) reduced microbial counts, respiration and carbon substrate utilisation potential were noted which were explained by the increased toxicity of PCB at lower soil pH. A constant voltage gradient of 0.4 V/cm was recommended in the literature in order to prevent potential direct harm to the bacteria (Mizuno and Hori, 1988). However, Mena et al, (2016), recommended an electric voltage of 1.5 V/cm for the safe optimum microbial activity. Periodic polarity reversal was recommended to prevent high pH gradients that could also be harmful to the bacteria (e.g. Lear et al 2007; Mena et al, 2016).

2.7 Effect of MICP on Hydromechanical Properties of Soils

2.7.1 Hydraulic Properties

In the vast majority of studies, the MICP is utilised in high permeability soils allowing penetration for bacteria and cementing solution to the desired soil depth; Chu et al., (2013a) suggested that a minimum hydraulic conductivity of $1 \times 10^{-4} \text{ m/s}$ must be maintained, to ensure uniform distribution of precipitated CaCO_3 in the treated soil. Biocemented soil samples generally maintain higher permeability compared to soils cemented by traditional cementing materials such as Ordinary Portland Cement (OPC) (Mujah et al, 2017). Literature reports that as long as soil pores between the

soil particles are not completely filled by the CaCO_3 precipitate (see e.g. Figure 2.19) fluid movement is not obstructed, so that for biocemented sands, some studies report values of permeability maintained in the range of 1.0×10^{-6} m/s to 5.0×10^{-3} m/s (e.g. Whiffin et al., 2007; Choi et al., 2016). However, higher permeability reductions are noted as cementing solution concentrations increase due to the filling of pores with precipitates; for instance, Choi et al, 2019 report a decrease by a factor of 100 in the permeability of Ottawa sand between 0% and 4% calcite content. Chu et al, (2014) report that for their range of experiments, the permeability (k) of biocementated sand varied with the precipitated calcium content (C , % w/w) as: $k = (507-403 C)10^{-7}$ m/s. Thus, the use of low concentration solutions was recommended as higher permeability would allow more uniform precipitate distribution (Harkes et al., 2010).

In fact, MICP can also be purposefully used for *bio-clogging* to decrease considerably the hydraulic conductivity of the soil (e.g. for ponds or landfill applications) by filling the soil voids with CaCO_3 and the degree of bio-clogging is a function of the CaCO_3 precipitate content (Chu et al., 2013b). For instance, Hataf & Baharifard (2020) used a strain of *Bacillus sphaericus* for the sealing of soils at landfill sites whereas *Sporosarcina pasteurii* was used to control water leakage in irrigation channels and reservoirs built on sandy soil by the formation of a low-permeability hard crusts layers; these reduced flow rates of biotreated samples by 8, 8 to 379 times depending on treatment method (Gao et al, 2019).

The porosity of the bio-cemented soil generally also decreases with an increase in the degree of cementation; for instance, Tagliaferri et al. (2011) and Qian et al, (2010) reported respectively a reduction of 30% and 25% in porosity after MICP.

There is paucity of information regarding the Soil Water Retention Curve (SWRC) of biocemented soils; an exception to this is a recent paper by Saffari et al, (2019) who used *Bacillus sphaericus* for MICP for both coarse-grained and fine-grained soil samples. SWRC results based on filter paper testing were supported by X-Ray diffraction, and scanning electron microscopy tests. These showed that higher bacterial concentrations produced higher air-entry values in coarse-grained soils but in fine-grained samples an initial increase in the air-entry value was followed by a decrease when the bacterial concentration increased. The authors attributed this to the changes in the soil porous structure and double-layer thickness.

2.7.2 Mechanical Properties

Shear strength increase of biocemented soil is usually reported in the literature in terms of Unconfined Compressive Strength (UCS), as this test is simple and quick and can allow a large number of samples with different treatments to be tested and assessed comparatively. The UCS depends on the soil type and MICP treatment conditions (see e.g. Inagaki et al's, 2011 investigation) therefore reported values vary very widely e.g. ranging from 53 kPa for peat (Sato et al, 2016) to 34 MPa for biocemented sand (Whiffin 2004). Correlations between UCS and the CaCO_3 content are made in the literature, as in the example from Ivanov and Stabnikov (2017), shown in Fig 2.20., based on synthesis of data from the literature on biocemented sands. Similar empirical correlations between the CaCO_3 content and Young's modulus based on the stress-strain curve were also made (e.g. Harkes et al, 2010 and van Paassen et al, 2010).

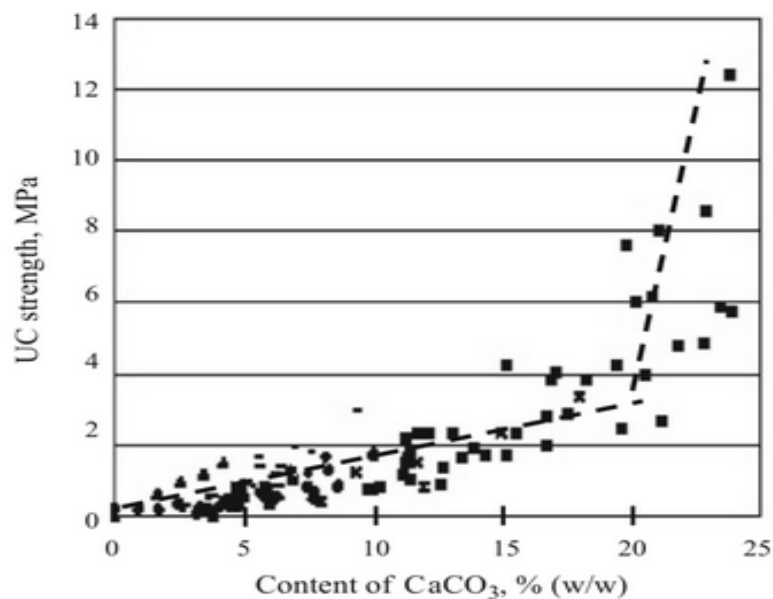


Fig 2.20 Correlation of sand UCS and CaCO_3 content after Ivanov and Stabnikov, (2017) (synthesis of results from Whiffin et al. 2007; Al Qabani and Soga, 2013; Stabnikov et al, 2013a and b; Li and Qu 2012)

There is much fewer data in the literature based on direct shear and triaxial testing. In some of these papers, small strain shear modulus (G_{\max}) was also determined to assess the effect of biocementation; this was done by measuring continuously the

shear wave velocity during the triaxial testing, as an effective monitoring indicator of MICP treatment evolution using bender elements. Measurements of shear wave velocity changes (and henceforth G modulus) are also used in situ (geophysical testing) to monitor the progress of biocementation (e.g. van Paassen et al, 2010a).

Most papers presenting triaxial testing results refer to biocemented sands and report an increase of cohesion of the biocemented soil, and an increase in the angle of friction according to the calcite content. For instance, Choi et al, (2019), performing consolidated undrained triaxial tests, report an increase in the angle of friction from 35.3 (untreated soil) to 37.8 and 39.6 for 2% and 4% calcite content respectively (it is not specified whether these were for peak or constant volume/ultimate conditions); cohesion increased from 0kPa (uncemented sand) to 34.2 and 93 kPa for 2% and 4% calcite content respectively. Montoya and DeJong (2015), performed a series of undrained and drained triaxial tests on sand cemented using *Sporosarcina pasteurii* at various degrees of cementation (light, moderate, heavy i.e. calcite contents of 1.01%, 1.3% and 3.06-5.31%) and reported peak angles of friction ϕ' barely affected in the case of light cementation whereas (compared to the angle of friction of the sand in a loose state) they found increases by 4-6° for the moderate degree of cementation and 8.5-10.7° for the heavily cemented soil; however at critical state the lightly and moderately cemented sand shear strength was similar to that of the untreated loose sand. They also reported a dramatic increase in G_{max} between lightly, moderately and heavily cemented soil i.e. respectively 135 MPa (comparable to the $G_{max}=100$ MPa of the untreated sand in a dense state), 304-634 MPa and 1,815-2,940 MPa; stiffness degradation was also monitored based on the shear wave velocity and for the heavily cemented soil cementation degradation was noted within shear bands only. Similarly, Nafisi et al (2020) performed drained triaxial tests on three types of biocemented silica sands (coarse, medium and fine) at light, moderate, and heavy cementation levels and also used bender elements for shear wave velocity measurements (changing with cementation levels) to monitor biotreatment. The results were interpreted using both linear and nonlinear shear strength envelopes. Again, shear strength was observed to increase as the cementation increased, but the amount of improvement depended on the confining stress and sand type. The authors also determined the secant Young's moduli E_{50} from the stress-strain curves; these increased for all the MICP-treated specimens relative to the respective untreated sands.

Cabalar et al. (2018), found that biological treatment period affected the stiffness of biocemented sand specimens for strain levels up to 1%. This was attributed to the amount of the calcite precipitated which was found to be higher as the period of biological treatment increased. The authors also observed a significant amount of stiffness degradation between 0.001 and 0.1% axial strain. They also concluded that results between biological treatment and treatment with calcite and lime were similar.

A very relevant paper for the present research (Canakci et al, 2015) determined the strength and compressibility of a MICP treated soil of 60% organic content (natural water content 256%, LL =125% and PL not possible to determine) based on direct shear and 1-D oedometer testing respectively. The authors interestingly report only a small increase in cohesion and an increase in the angle of friction by 7-8° for the biocemented samples (which could be a matter of data interpretation); the decrease in the compression index was between 26-35% for the MICP treated samples.

Most studies support the hydromechanical property testing results by microstructural analysis using Scanning Electron Microscopy (SEM) and/or micro-CT scanning to gain insights into the stabilising mechanism of the MICP and the forms and location of the CaCO₃ (e.g. DeJong et al., 2010, Chu et al, 2014; Cabalar et al 2018, Terzis and Laloui, 2019, Nafisi et al, 2020). Thus, a number of studies (e.g. DeJong et al., 2010 or Ivanov and Stabnikov, 2017 amongst others) referred to mechanisms of “preferential” and “uniform” distribution i.e. respectively (a) precipitation of CaCO₃ at the particle-to-particle contacts with crystals effectively contributing towards the soil strength and (b) precipitation of equal thickness of CaCO₃ around the soil grains, which produces a relatively lower bonding between particles (see Fig. 2.21 below).

Based on 3D images of biocemented sands from micro-tomography Dadda (2017) estimated micromechanical properties of sands and their evolution with CaCO₃ content and used these to estimate Coulomb’s cohesion and its evolution with CaCO₃ content. Terzis and Laloui (2019) combined time-lapse video microscopy observations with quantified micro-CT image processing data referring to the number, sizes, orientations and purity of CaCO₃ crystals in different size sands (coarse, medium and fine grained). The authors found that MICP adapts differently depending on the base materials, with crystalline particles growing bigger and more uniformly distributed in medium-grained base materials. They thus concluded that the average mass of bonds

is not enough for a robust estimation of the expected mechanical response, as this must also be associated with the intrinsic properties of the base materials and with quantified characteristics of the bio-improved fabric.

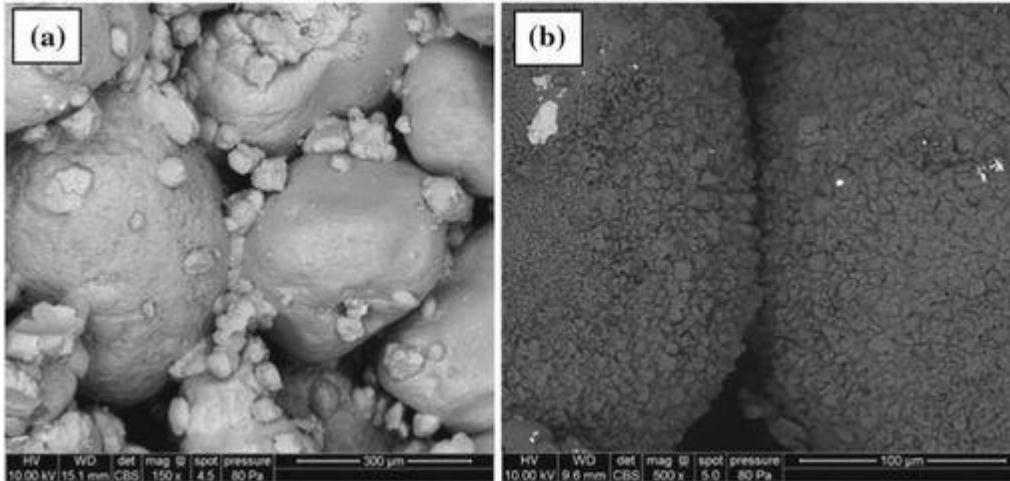


Figure 2.21 Different CaCO_3 distribution mechanisms, (a) Preferential; (b) Uniform (Ivanov and Stabnikov, 2017)

2.8 Factors Affecting the Precipitation of CaCO_3 Crystals in MICP Treatment

The performance of bio-cemented soils is mainly a function of the crystallographic patterns of the precipitated CaCO_3 (size, shape and the distribution pattern). These are affected by bacterial concentration, urease activity, fixation of bacteria, availability of nucleation sites, temperature, pH level, nutrient availability, concentration of cementation solution and degree of saturation, all controlling the success of the MICP treatment (Mortensen et al., 2011; Al Qabany et al, 2012; Keykha et al, 2017). Some of these factors are discussed below:

- (a) *Bacterial cell concentration and urease activity*: An increased urease activity enhances CaCO_3 crystal precipitation which is also linked to the availability of the nucleation sites. The bacteria biomass thus directly relates to the urease activity in the soil and the amount of bacterial cells attached to soil grains. Nucleation of new crystals could however compete and prevail over the process of crystal growth mechanism if abundant nucleation sites (more bacterial cells) are available throughout the MICP process. Also, when abundant nucleation sites are available

in the soil matrix, the produced CO_3^{2-} ions are mainly consumed in the nucleation of new CaCO_3 crystals instead of growth of existing CaCO_3 crystals, leading to the precipitation new, small CaCO_3 crystals, instead of fewer and large crystals. On the other hand, a lower number of bacterial cells inhibits the nucleation and formation of new CaCO_3 crystals in the soil matrix, and facilitates the growth of existing individual crystals. (Mujah et al., 2017).

- (b) Temperature** affects the growth and enzymatic activity of microorganisms, the rate of CaCO_3 production and the shape and size of CaCO_3 crystals. Nemati & Voordouw (2003), showed that the enzymatic activity increased for an increase in temperature from 20°C to 50°C and that *Psychrobacillus sp.*, had a better urease activity at 30°C than at 20°C (Gowthaman et al, 2019). However Cheng et al., (2014b) found that although at 50°C , CaCO_3 crystals formation was approximately three times higher than at 25°C , the strength was about 60% lower due to the small size of CaCO_3 crystals which were uniformly covering the surfaces of the sand grains, whereas at room temperature crystals were larger and mainly deposited at particle-to-particle contact points (see Fig 2.21 above) Conversely Keykha et al (2017) treating a silty clay with *Sporosarcina pasteurii* observed highest UCS strength at a temperature of 40°C Over 60°C Rebata-Landa (2007) saw no CaCO_3 production due to bacteria death.
- (c) The pH** plays a significant role in MICP as CaCO_3 precipitation occurs effectively in the alkaline environment due of (OH^-) ions released during the conversion of ammonia to ammonium (see Equation 2.12, 2.13). For this reason, alkalophilic ureolytic bacteria are used. Cheng et al., (2014), showed that the correlation between the precipitation of CaCO_3 crystals and the soil initial pH is a function of solubility variation of the CaCO_3 crystals caused by different initial pH values. Treating a silty clay with *Sporosarcina pasteurii* Keykha et al, (2017) observed a UCS strength increase as pH increased from pH 5 to 9 for 7 and 14 days of curing thus the highest strength (i.e. 92 kPa) was obtained at pH 9 after 14 days of curing.
- (d) Concentration of cementation solution** directly affects the efficiency of CaCO_3 precipitation and crystal formation. Al Qabany & Soga (2013), used 0.1, 0.25, 0.5 and 1 M urea-calcium chloride solution as the cementing agent and reported more

effective CaCO_3 precipitation solution and higher biocemented sand strength at lower concentrations. Ng et al., (2014), reported similar findings for a biocemented residual soil, as samples treated with 0.5M concentration reagent had higher strength than samples treated with 1M. An explanation offered was that in higher cementation solution concentrations CaCO_3 crystals form randomly in the soil voids due to faster precipitation, while lower cementation solution concentrations give a more homogeneous distribution of CaCO_3 crystals and at the particle contact points also because permeability is less affected, as explained earlier (Mujah, 2017).

(e) Degree of saturation A number of researchers (e.g. Whiffin et al., 2007; van Paassen 2009; Al-Thawadi 2013) claimed that full saturation led to the highest strengths. Gowthaman et al's (2019) findings concur with this (see below Fig 2.22). Conversely, Cheng et al. (2013) found that MICP worked best for lower degrees of saturation, even if CaCO_3 precipitation within the soil matrix was lower. Based on SEM results they claimed that at lower degree of saturation the precipitation of the CaCO_3 crystals occurred at particle-to-particle contacts whereas higher degrees of saturation resulted in ineffective formation of CaCO_3 crystals in pore voids.

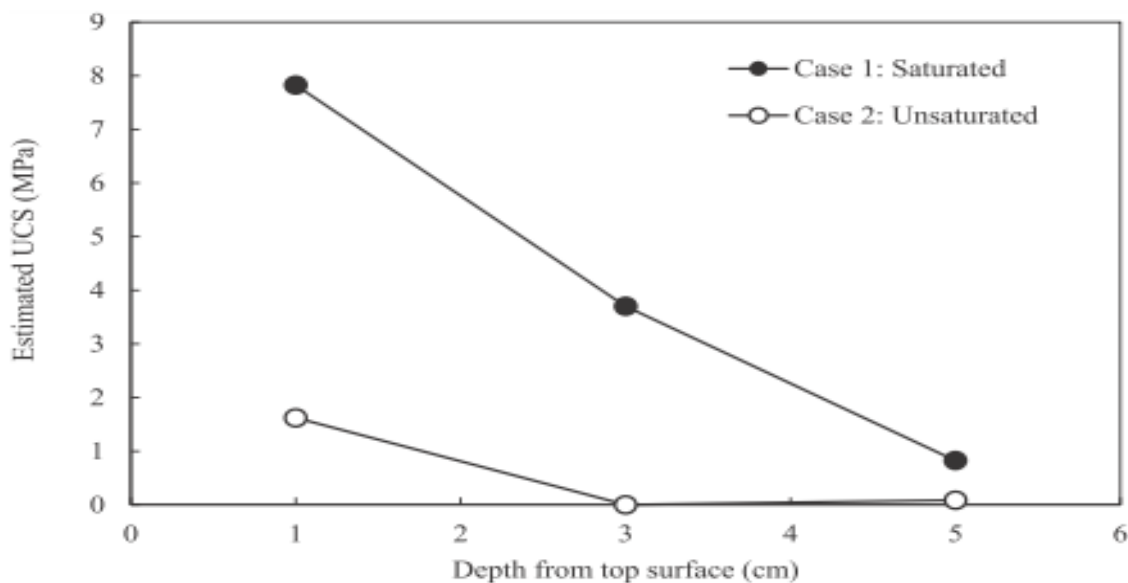


Fig 2.22 Effect of degree of saturation on MICP treatment (Gowthaman et al., 2019)

2.9 Large Scale Application of MICP-Practical Considerations

A relatively limited number of studies performed up-scaled, in particular in-situ trials to verify the effectiveness of bio-cementation for field implementation of MICP. Examples upscaled studies are summarised in Table 2.11 below.

Table 2.11 Summary of Up-scaled MICP treatment experiments

Research Reference	Scale/ material/application	Findings
Van Paassen (2009)	1m ³ to 100 m ³ of sand	Strength of bio-cemented sand significantly increased 43 m ³ (up to 12MPa unconfined compressive strength) but results were not fully satisfactory due to treatment heterogeneity
Van Paassen 2011	Field biogROUT application: cementing gravel for borehole stability plot of 24 by 4 m.	6 injection wells surrounded by 14 extraction wells Preliminary results indicate that the electrical resistivity measurements and the electrical conductivity and ammonium measurements on the extracted liquid are good methods to monitor the flow and transport of the brine solutions
Martinez (2012)	0.5m x 0.5m x 0.15m zone of residual soil	Improved strength of bio-cemented soil Non-homogeneity of precipitate CaCO ₃ along the soil mass
DeJong et al., (2014)	Developed five-spot treatment model to treat sand	Uniform treatment under highly active microbial conditions
Gomez et al., (2015)	Improving the erosion resistance and Surface stabilisation of loose sand deposits for dust control and future re-vegetation	Soil improvement at 28 cm was recorded by using dynamic cone penetration Technique can be further used for large scale treatment by optimising the solution. Modest spatial variability occurred across the sample depth. The low concentration treatment solution provided the best results.
Lee et al., (2019)	3.7m long sand columns to investigate ammonia by-product concentrations	525 L of high pH and high ionic strength solution was injected to the samples for 24 h. The concentration of NH ₄ ⁺ varies from initial values of 100mM-500mM to the final values of 0.3mM-20mM. Approximately 97.9% NH ₄ ⁺ was removed, with no significant effect to the cementation. Higher NH ₄ ⁺ concentration was observed far from the injection wells.
Béguin et al (2019) (BOREAL project)	8 x 4 x 2.25 m laboratory erosion tests on sand and sandy gravels, and interface between coarse and fine layer	MICP shows potential to mitigate mechanical failure of the soil due to seepage (internal erosion or liquefaction) MICP treatment was effective for soils with open porosity, under natural Darcy velocity up to 10 ⁻³ m/s and for contact erosion problems.
Gomez et al., (2019)	MICP by bio-stimulation of native ureolytic bacteria and augmented <i>S. pasteurii</i> in 1.7-m. diameter tank tests plus complementary soil column test (injection)	Similar calcite and engineering properties between approaches Significant differences in ureolysis rates and related precipitation rates Biostimulation showed lower precipitation rates early during the cementation phase allowing calcite precipitation away from injection wells hence better treatment uniformity. Larger and fewer calcite crystals could be observed in biostimulation specimens with a greater number of smaller crystals observed in augmentation specimens

The production of ammonia as a byproduct of the urea hydrolysis is a main barrier for bio-cementation field-scale applications. In addition to its repugnant odour ammonia can harm soil and aquatic ecosystems and can have detrimental effects on health (Keykha et al, 2018; Mujah et al, 2017). Therefore, it is vital to manage, remediate, or remove NH_4^+ by-products (Lee et al, 2019). Several researchers have recommended the repeated flushing to remove it, but there is a danger of the NH_4^+ rich effluent to seep into groundwater (van Paassen et al., 2010; DeJong et al., 2010; Ng et al., 2014). Mujah et al, (2017), also suggest treatment of this effluent before discharge or the use of ammonia as a fertilizer for nearby plants. Keykha et al, (2018) produced an aqueous solution of CO_3^{2-} (i.e., from bacteria) outside of the soil and then used natural zeolite for NH_4^+ removal from this aqueous solution.

Treatment costs are also currently a barrier for the field applications. Most laboratory studies adopted the cultivation of pure ureolytic bacterial strains under sterile conditions to obtain reliably a constant high urease activity and avoid any contamination and related adverse (for the process) effects (Mujah et al, 2017). However, for industrial scale applications the use of pure cultures increases the treatment costs. Biostimulation) of indigenous urease active bacteria was thus used in a relatively limited amount of studies (e.g. Burbank et al., 2012; Gomez et al, 2017 and 2019) as a less costly method and showed promising results. Alternatively, to reduce costs, Terzis and Laloui (2019) proposed the use of lyophilized (freeze-dried, powder) cells instead of vegetative cells. Moreover, Omoregie et al (2020) proposed a scaled-up production of ureolytic bacteria cells under non-sterile conditions using a custom-built reactor for industrial scale MICP application with promising results. To further reduce costs they used technical-grade ingredients for scale-up production of the bacterial cells (carried out from 214 L to 2400 L seed cultures for 90 h). Low grade chemicals to reduce costs were also used by Gowthaman et al (2019) in a feasibility study of Hokkaido expressway slope stabilization through surficial treatment. Reuse of the same cementation solution for up to three more applications was also suggested to reduce costs (Al-Thawadi 2013; Whiffin et al., 2007).

CHAPTER 3

MATERIALS AND METHODOS

3.1 Introduction

This chapter provides the detailed description and analysis of the peat soil, experimental setup and the methods used in the extensive testing of the study. Depending on the nature and type of the experiments, the research was divided into four major experimental programs as follows:

Preliminary testing: it includes the batch testing of all the samples received from the site provided by Network Rail. The details of the samples and the soil selected for the experimental program is given below in section 3.2. The preliminary testing also includes testing to determine the engineering properties of the soil. The summary of these properties is given later in table 3.1. Moreover, the results of the batch testing are given in the Appendix A.

Microbiological study: it involves the, isolation, purification, identification, screening growth, and cultivation of bacterial strains used in the MICP treatment. The isolation and growth of the bacterial strains are done by using carbon rich mediums such as B4 Agar and Nutrient Broth; bacterial identification is done by MALDI Time of flight Mass spectrometry. The bacterial isolation and growing methods are explained below in section 3.3 and the detailed MALDI identification results are provided in Appendix G.

MICP feasibility: this is the major part of the main experimental program. The soil is treated using mixing and flow column tests with treatments implemented under light to medium pressure, where different concentration of cementing reagents and the bacterial strains are employed.

EK and Electro-biocementation experiments: these belong to the second phase of the main experimental program. First the pure system (without any cementing reagent or bacteria) tests are performed to determine the base line for the results and the efficiency of the EK system, followed by the Electro-biocementation method.

The treated samples for both flow column injection and the EK stabilisation were tested for strength, CaCO₃ content and other parameters after suitable curing time. The

results of all the treated samples are explained in Chapter 4 and 5. The complete experimental research methodology process is summarised below in the Figure 3.1.

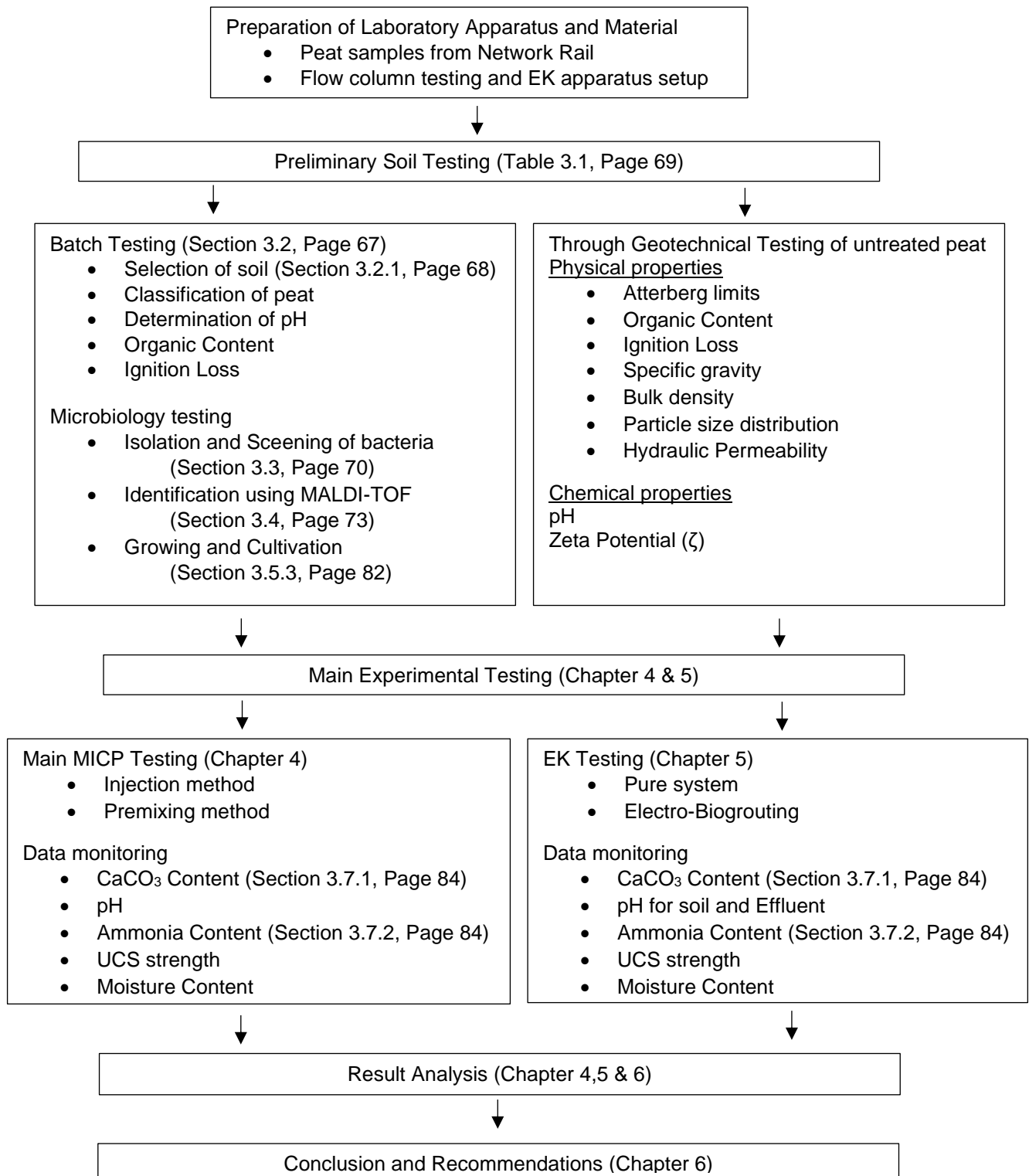


Figure 3.1 Flowchart of research methodology

3.2 Tested Soil

The soil used in this study was provided by the Network Rail; the soil samples were taken from two boreholes more than 50 m apart at a site of the East Anglia railway network route. The boreholes locations are termed as Work Station 01 and Work Station 02 by network rail, and in this thesis, are designated as WS01 and WS02. Each borehole provided an 8m long sample. From visual inspection, the different soil layers varied from pure clay to pure peat and a mixture of both along the depth of the 8m samples. Basic geotechnical laboratory testing was performed to establish the physicochemical characteristics of the soil samples; for this purpose each 8m sample is divided into 16 parts, each 0.5m long. The duplicate samples were tested to establish the geotechnical and physio-chemical characteristics of each layer and as well as for bacterial strain isolation, which makes 32 samples in total. Figure 3.2 shows the distributions of water content and organic content with depth for the two boreholes.

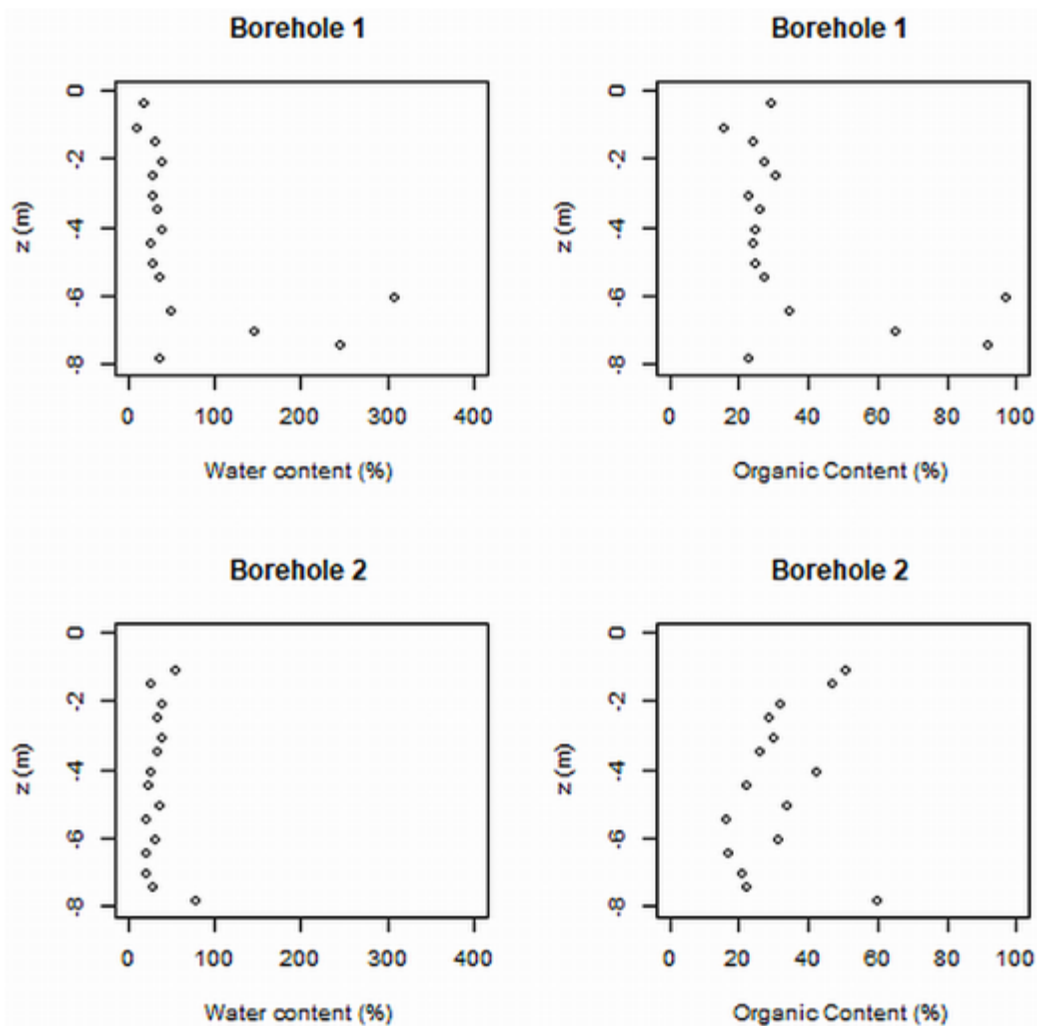


Figure 3.2 Distribution of water contents and organic contents for two boreholes

It can be seen that (apart from three samples taken between depths of 6 and 8m from Borehole 1) organic contents are consistently between 20% and 60% but show considerable variation. The borehole logs record “no water encountered” so a tentative conclusion is that all soil is above the water table and in an unsaturated state. The indication of nearly 100% organic content near the base of Borehole 1 suggests that future site investigations will need to explore greater depths to determine whether there is a significant and extensive layer of softer organic material which could be an important factor in generating settlements under surface loading (as demonstrated by Terzaghi and Peck, 1967). The results of complete batch testing including pH, Moisture contents, Ignition loss, and organic contents are provided in the Appendix A.

3.2.1 Selection of Representative Material

As a large quantity of the material was required to complete this extensive testing and the borehole material was not sufficient enough to fulfil this demand, the material from top (0-2m) layer of the borehole location 2 was selected as the representative material for which bulk excavated material was also available. The selection of the representative material was made on the following additional criteria

- Both the borehole samples were tested thoroughly along the depth (at the interval of 0.5 m and change of material interface) and at both locations soil samples along the depth shows a great consistency in terms of loss on ignition, % of Organic content, pH and Moisture content.
- As primarily this research was on Organic/Peat soil stabilisation, the selected material fulfils the criteria, as it has high ignition loss, and consistent moisture content with the underlying layers, except one. (See table 2 of Appendix A)
- Being the top layer, it provided the abundant and easy access to the required material.

In its as-received state the natural soil was a mixture of mineral and organic fractions of very dark grayish brown colour (10YR 3/2 according to Munsel chart); pocket penetrometer indicated a 76 kPa undrained shear strength. Based on its organic content (>20%), the soil was identified as sandy (sand>50%) amorphous peat (i.e. “of no visible plant structure and mushy consistency”, BS EN ISO 14688-1:2018, BSI, 2018)¹. The samples have a low natural moisture content which is consistent with a humified /decomposed the organic soil. Based on its ash content by dry weight (<

¹It is appropriate to note that the term peat encompasses soils with a very wide variation in composition and properties; the latter are very highly dependent on structure, state and water content. Most of the few academic studies discussing strengths refer to peats with water content of two to ten times higher than that of the soil in the presented study; the latter soil was also partially saturated (degree of saturation $S_r=85\%$) which may have had some effect on its strength.

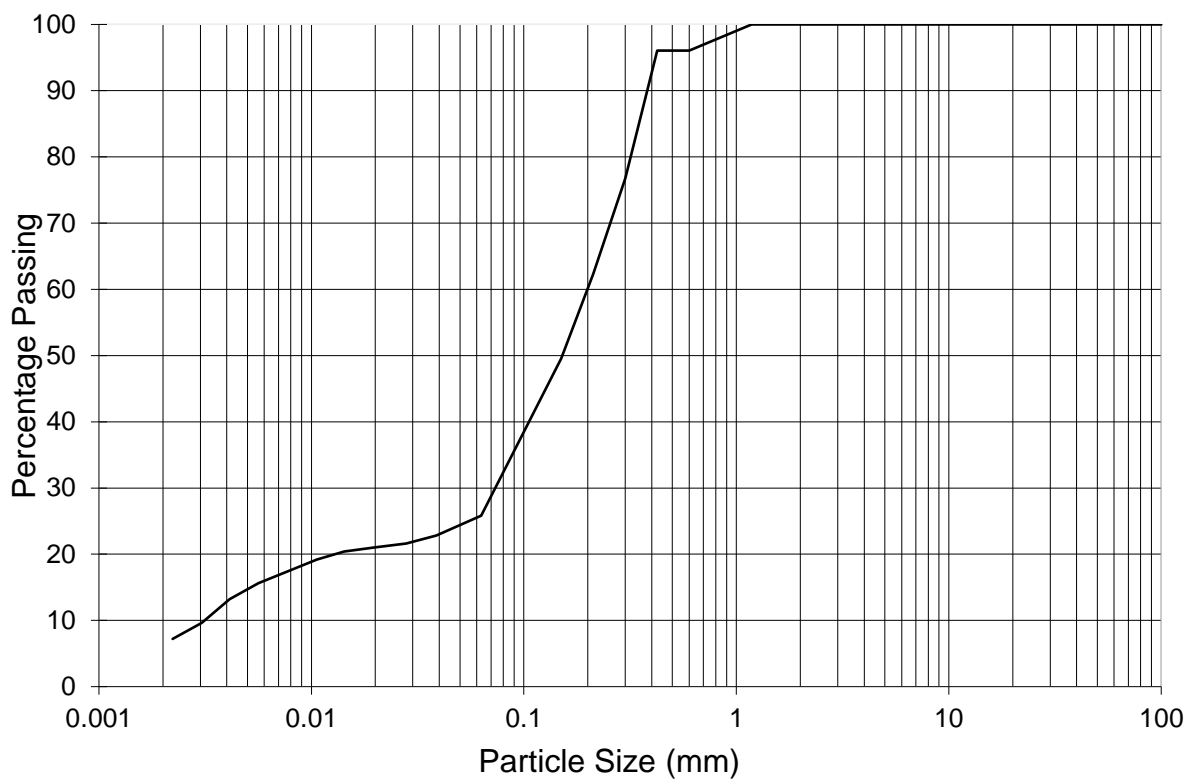
25%) the soil is equally classified as peat (basic sapric peat) according to ASTM D4427-92 (1997). The sample was pulverised and sieved to remove inorganic debris. The plastic limit of the soil could be determined; this is possible for fen peats and transitional peats but not for bog peats unless almost completely humified (Hobbs, 1986). The all possible engineering and chemical characteristics of the soil are determined according to the appropriate British standards and are summarised below in Table 3.1.

Table 3.1 Geotechnical and Physicochemical properties of the soil

* All moisture contents/Atterberg limits were obtained from the wet soil and are expressed on a dry soil mass basis corrected for moisture of the sample

Property	Value	Standard utilised
Natural gravimetric moisture content*	55.5 %	BS 1377-1990: part 2
Organic matter content	50.8 %	ASTM D 2974-14
Loss on Ignition	52.7 %	ASTM D 2974-14
Liquid Limit	101 %	BS 1377-1990: part 2
Plastic Limit	63 %	BS 1377-1990: part 2
Plasticity Index	38 %	BS 1377-1990: part 2
Specific Gravity (G_s)	2.060 g/cm ³ / g/cm ³	BS 1377-1990: part 2
Bulk Density	1.316 g/cm ³	BS 1377-1990: part 2
Dry Density	0.919 g/cm ³	BS 1377-1990: part 4
Particle Density	1.875 g/cm ³	BS 1377-1990: part 2
Hydraulic conductivity	3 x10 ⁻⁹ m/sec	BS EN ISO 22282-5:2012
Void ratio (e)	0.842	BS 1377-1990: part 4
Porosity (η)	0.457	BS 1377-1990: part 5
pH	7.15	BS 1377-1990: part 2
Zeta potential (ζ)	-38.4 mV	ASTM D 4187
Cation Exchange Capacity (CEC)	72 meq/100 g soil	Calculated After Chapman, 1965
Colour Description	10YR 3/2	Munsell Chart

All moisture content and limits mentioned in Table 3.1 are gravimetric moisture contents referring to percent water mass over percent of dry soil mass. In addition to these soil characteristics, the particle size distribution of the soil sample (based on sieving followed by hydrometer testing according to BS 1377:1990) was also performed and the plot is given below in Figure 3.3. The particle size distribution shows that more than 50% of the material is within the size range of the sand particles. Similarly, the combustion test denotes that organic content present in the material is also 52.7%, which indicates that the organic content present in the material is imprecisely of the same size range of that of sand particles.



Clay Fraction	Fine	Medium	Coarse	Fine	Medium	Coarse	Fine	Medium	Coarse	Cobbles
	Silt Fraction			Sand Fraction			Gravel Fraction			

Figure 3.3 Particle size distribution of retained soil portion (passing 1.18mm sieve)

3.3. Isolation and Screening of Bacteria

The first and most important step in several microbiology procedures is the isolation of bacteria from the soil as it practically aims to describe the distribution and composition of microorganisms in the soil. The bacterial isolation is also essential for

further identification of bacterial species and strains and to analyse their function in the soil environment.

The aim for this microbiological testing was to isolate non-pathogenic, indigenous ureolytic bacterial strains capable of producing calcite from the in-situ soil. The main reason for isolating suitable native bacteria is that being indigenous the isolated bacteria would have better chances to survive and perform effectively under same environmental and chemical conditions. For this purpose, 18 soil samples (9 from WS01 and 9 from WS02) were selected out of 32 for the bacteria isolation, with similar pH, Moisture contents and soil specimens having same organic contents to reduce the extensive microbiological laboratory work.

Isolation of bacteria was done by adding and thoroughly mixing 1 g of soil from each soil sample to the conical flasks, containing 99 ml of sterile water. As a very small quantity of the soil can enclose millions of bacteria, the soil-water solution was diluted repeatedly to achieve the final dilution of 10^{-6} . The dilution scheme for the soil-water solution is given in Appendix B. Then the 1mL of the diluted culture solution was plated out on 15mL of molten Tryptic soya agar (TSA) (Oxoid, UK). Total $(18 \times 6) = 108$ plates were inverted and incubated at 25°C for 3-7 days. The number of bacterial colonies from each dilution plate were determined by direct plate counting, and the plates which were unable to grow more than 25 colonies were discarded. Depending on the rate of growth total 140 bacterial colonies were extracted from all dilutions. Bacterial colonies from TSA agar plates were transferred to the individual B4 Agar plates (0.4% yeast extract, 0.5% dextrose, 0.25% calcium acetate and 1.4% agar in solid preparations) for further assessment.

The broaden valuation of the isolated bacteria was done on the basis of growth at different temperatures. The selected 140 bacterial colonies were incubated at 4°C, 10°C, 25°C and 37°C to check their ability to grow at stressed in situ conditions. 98 out of 140 samples showed considerable growth at all temperatures. The further screening of the selected 98 bacterial strains was done on the basis of their ability to form crystals on the solid high carbon media, and most importantly the ability to produce calcite in the soil. For this purpose, the samples were streaked again to the individual B4 Agar plates and incubated at 37°C for one week to form mineral crystals. The B4 agar was selected to check the mineral precipitation of the isolated bacterial

strains. Marvasi et al., (2012), mentioned that the bacterial candidates which develop a good crystalline mineral precipitation on B4 agar media have a far better potential towards CaCO_3 precipitation. Based on these criteria and after one week of incubation 49 out of 98 samples showed good production of crystals as confirmed microscopically; these were selected and passaged twice on B4 plate to obtain purified single colonies.

The 49 purified individual colonies were then transferred to Nutrient Agar (NA) (Oxoid, UK) so that they can be identified further as bacteria cannot form crystals on NA agar and can easily be harvested for further use. The NA is a high nutrient medium (it contains 0.5% peptone, 0.3% beef or yeast extract, 1.5% agar as solidifying agent and 0.5% NaCl).

A pure culture theoretically contains a single bacterial species, and to further test the viability of the selected bacterial strain, the purified samples were again incubated at considerably low temperature from 4°C to 7°C for 7 days. The lower temperature range was selected to match the field conditions and to check the endurance and growth rate of the purified bacterial strains. All the 49 samples showed considerable growth at the lower temperature, but the rate of growth was slower in the first 2-3 days, and increased gradually by the end of the 7 days period. However, the overall growth at lower temperature was one-fourth, and in some cases, one-fifth compared to when the same culture was grown at 25°C (see Figure 3.4).

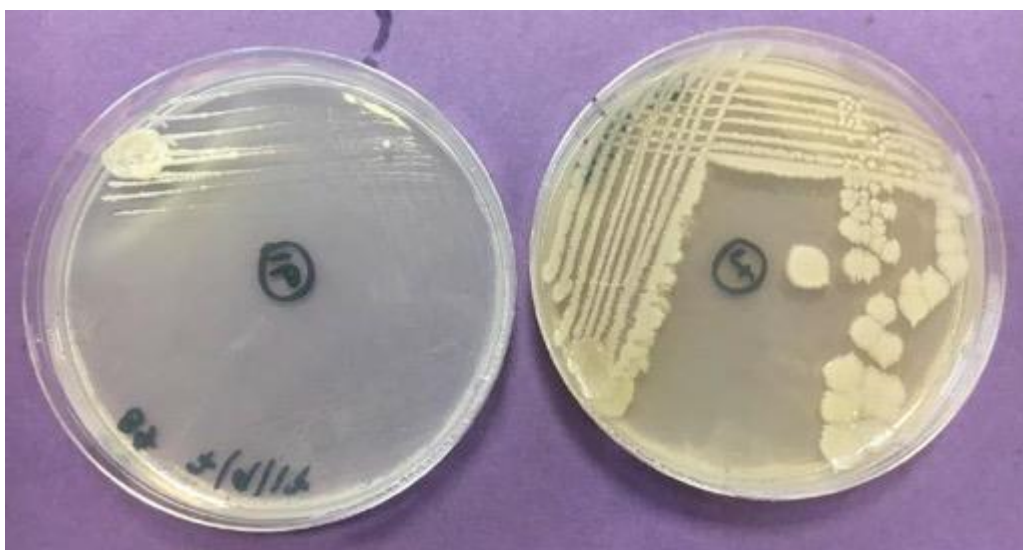


Figure 3.4 Comparison of rate of growth of same strain incubated at (left 4°C , right 37°C) after 3 days

It should be noted that several samples were discarded due to contamination in both isolation and screening stages. However, all the 49 final bacterial strain samples were duplicated in all three purification streaking over B4 media in order to ensure reliability in isolation and screening process.

3.4 Microbial Identification and Diagnosis

Conventionally the identification and classification of the microbial species has been done on the basis of antigenic, metabolic and biochemical characteristics. Commonly the bacteria are identified predominantly on the basis of genomic information such as 16S rRNA and 18S rRNA gene sequencing. These sequences are considered as the “gold standard” as these are present in every prokaryote and allow reestablishment of the global phylogeny (Pace, 1997). Though these DNA fingerprinting techniques such as 16S rRNA are satisfactory in order to assign species or genus to the isolated bacterial strain, however in most cases it is not sufficient for refined bacterial strain typing, e.g. epidemiological studies (O’Leary et al., 2011).

However, recently other quick and reliable methods for the microbial identification such as MALDI-TOF have gained popularity amongst the microbiologists (Singhal et al., 2015). In this study, the identification of the final 49 samples was also performed using Matrix-Assisted Laser Desorption-Ionization Time-of-Flight tandem mass spectrometry (MALDI-TOF/TOF MS) proteomic-based biotyping approach. A very brief introduction of the technique along with the principle and methodology is given below. Moreover, the actual sample preparation method, recipe of the matrix used and the experimental procedure adopted is given in the subsequent section.

3.4.1 Matrix-Assisted Laser Desorption Ionization-Time of Flight (MALDI-TOF MS)

Lately, the MALDI-TOF MS, has surfaced as a very effective method for the identification of microorganisms. The method identifies the microorganisms using either their cell extracts or intact cells. The MALDI-TOF MS is a precise, economical both in-terms of cost and labour, sensitive and rapid technique. Apart from microbial identification the method has gained popularity among the microbiologists for other advanced purposes such as, strain typing, detection of water- and food-borne

pathogens, detection of biological warfare agents, epidemiological studies, detection of blood and urinary tract pathogens, detection of antibiotic resistance and many more (Singhal et al., 2015). However, the identification of the new isolates using MALDI-TOF MS can only be possible if the relevant peptide mass fingerprints of the specific genera, species, subspecies or strains is available in the database, which could be the limitation of the technology (Singhal et al., 2015).

3.4.2 MALDI-TOF Principle and Methodology

The MALDI-TOF uses the analytical technique of the mass spectrometry, where peptides of the target microorganism are transformed into ions by either loss or gain of one or more protons. The singly charged ions are produced by “soft ionization” to avoid substantial loss of sample integrity (Everley et al., 2008). For the identification process, the isolate is coated with the matrix, the matrix is usually an organic compound which absorbs the energy during the ionization process. Upon drying the ionization of the matrix is done by the laser beam for the generation of singly protonated ions. During the MALDI-TOF analysis the mass-to-charge ratio (m/z) of these ions is measured by determining the time of flight (TOF), or the time required for these separated ions to travel to the ion detector through the length of mass analyser tube. On the basis of time of flight, the equipment generates a characteristic Peptide Mass Fingerprint (PMF) spectrum for the microorganism. In the end, the identification is made by comparing the generated PMF with the PMFs available in the database, or by matching the biomarkers masses of the sample with the proteome database. In order to ensure homogeneity and reliability in the results, six different sample spots (replicates) for each sample were laid to generate six combined mass spectra (MSP) per bacterial isolate.

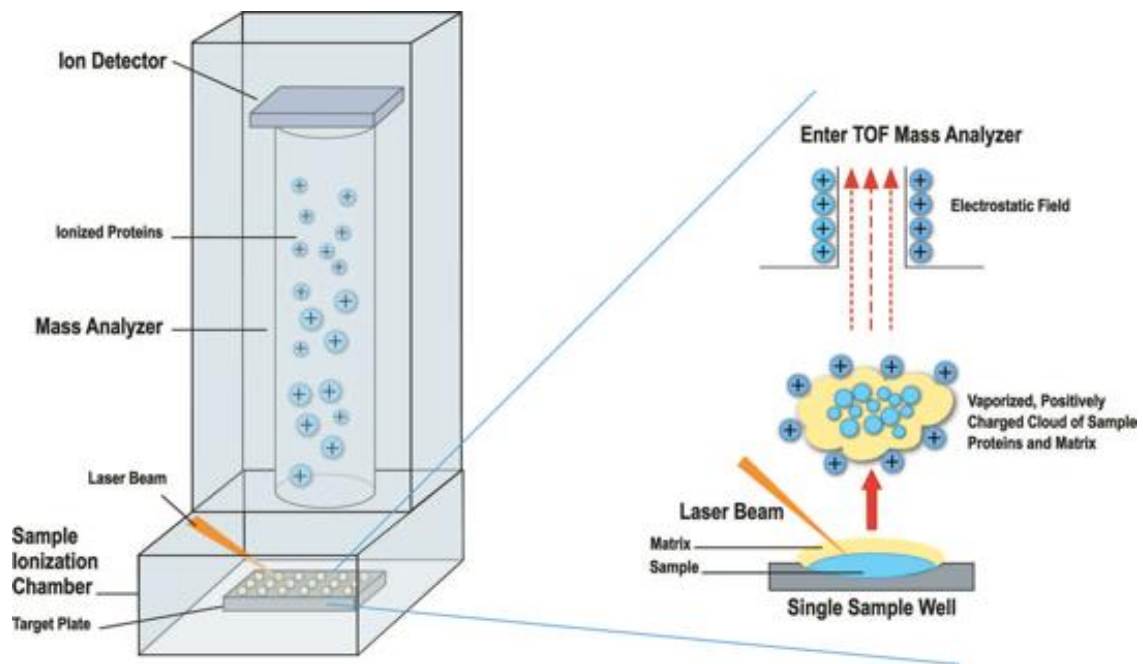


Figure 3.5 Schematic diagram of the MALDI-TOF MS process, after (Patel, 2014)

3.4.3 Sample Preparation for Microbial Identification using MALDI-TOF MS

The selection of sample preparation methods for the microbial identification used in the MALDI-TOF MS, depend on the chemical composition of the cell wall constituents and the source from which the bacteria are isolated. For different groups of microorganisms, the researchers have given several different sample preparation methods. Most of the bacteria can be identified by direct cell profiling also called direct MS profiling, while for identification of other microbes such as fungi, crude cell or whole cell lysates are prepared.

The direct cell profiling method using the “preparatory extraction” technique involves the placing of single bacterial colony onto the sample plate and immediately covering it with matrix solution before putting under laser beam. The utilisation of several chemicals in the “preparatory extraction” has been investigated, but the use of Formic Acid as an extraction agent was described to be most appropriate (Theel et al., 2012; Stevenson et al., 2010b). Therefore, Formic Acid Extraction Method was used here to prepare samples in this study.

3.4.4 Formic Acid Extraction Method

- Individual microbial colony or approximately 5-10 mg of the microbiological substance from the sample was mixed into 300 μ L of deionized water inside an Eppendorf tube, and the solution was mixed thoroughly by appropriate pipetting or vortexing.
- 900 μ L of the absolute ethanol (EtOH) was added and thoroughly mixed with the solution. mixed solution in tubes were then centrifuged for 2 minutes at 13,200 rpm, (limit 13,000 to 15,000), which results accumulation of supernatant. Tubes were again centrifuged, and the residual EtOH was pipetting off and wasted without disturbing the decent pellet produced at the bottom of the Eppendorf tube.
- The pellet was left to dry at room temperature for suitable time (two to three minutes).
- Suitable recommended quantity of the of 70 % formic acid (limit 1 to 80 μ l depending upon the size of colony) was added to the pellet and mixed well by pipetting.
- Equal volume of pure Acetonitrile (ACN) as of formic acid was added to the pellet and mixed carefully. To collect all the material neatly in the pellet, tubes were centrifuged again at maximum speed for 2 minutes. The quantitative scheme of the added formic acid and the (ACN) is given below in the table 3.2.

Table 3.2 Formic Acid and (ACN) quantity used for different sizes of colonies

	10 μ l including loop	1 μ l including loop	Large single colony	Small single colony
Formic acid 70%	> 40-80 μ l	20-40 μ l	10-20 μ l	1-5 μ l
Acetonitrile (ACN)				

- 1 μ L of the supernatant was pipetted out from each Eppendorf tube onto the marked spots of the MALDI target plate, and was allowed to dry out at room temperature. The composition of the supernatant can greatly vary from whole-cell microorganisms to only purified protein.

- The samples spots laid onto the target plate were entirely overlaid with the 1 μ L of HCCA (α -Cyano-4-hydroxycinnamic acid) matrix solution within 1 hour and were allowed to dry again at room temperature. The matrix is necessary to protect the sample molecules from fragmentation by endorsing the process of “soft ionization” which also facilitates the sample desorption into the gas phase.
- Upon drying, the prepared target plate was inserted into the ionization chamber, where an automated sequence irradiates each sample by focusing 337nm ultraviolet nitrogen laser onto the target sample spots. The highwave length laser energy desorbs the matrix molecules and each sample into the gas phase, this process ionized the matrix with a single positive charge which is thereby transferred onto the sample proteins.
- The MALDI Biotyper (Bruker Daltonik) provided the results of the (TOF) of the ionized proteins towards the ion detector in-terms of (m/z) ratio and generated a mass spectrum for each sample.
- The identification of the isolates was automatically done by the computerised comparison of the produced protein “unique fingerprint” or “mass spectrum” with the database provided in the MALDI Biotyper software version 3.0.

3.4.5 Summary of Microbial Identification and Diagnosis

Microbial identification and diagnosis were performed using matrix-assisted laser desorption/ionization time-of-flight/time-of-flight tandem mass spectrometry (MALDI-TOF MS) proteomic-based biotyping approach. The sample preparation and extraction of proteins and peptides of the bacteria were performed according to the Bruker bacterial sample preparation protocol.

Each extracted sample was analysed using a MALDI ground steel target plate. In order to ensure homogeneity and reliability in the results, six different sample spots (replicates) for each sample were laid to generate six combined mass spectra (MSP) per bacterial isolate.

The acquisition and analysis of mass spectra were performed by MALDI-TOF MS. The identification of the isolated bacteria strain through comparison with reference strains and visualization of the mass spectra was performed with MALDI Biotyper software

3.0 (Bruker Daltonik). The detailed MALDI identification results are provided in Appendix G.

3.4.6 Storage of Bacteria

The bacterial strains are the main and living material which were used very extensively in this study. The lengthy nature of the biocementation experimental program required such a viable solution that once the isolated bacterial strains are purified and identified, they can readily be available to use whenever required. It is a significant challenge to store the bacteria over a long period of time. To overcome this issue and to avoid the repetition of the extensive microbiology experimental work, a ready to use system named "Microbank" designed by the pro-lab diagnostics USA was used. Microbank provides small size vials consisting of porous glass beads dipped in the specially formulated cryopreservative. The porous bead surface allows the bacteria to readily adhere onto the glass surface while the cryopreservative keeps the bacteria effective and alive for a long period of time. The formatted couple of porous glass beads and cryopreservative also ensures the uniform distribution of the bacteria cells within the Microbank vials which is essential for rapid and precise regrowth of isolates.

A freshly (overnight) grown culture colonies up-to 3-4 McFarland standard were added into the vial by using sterile loops and using aseptic technique. McFarland Standards are used to rapidly standardise the approximate number of bacteria in a liquid suspension by comparing the turbidity of the test suspension with that of the McFarland Standard. A McFarland standard is a chemical solution of barium chloride and sulfuric acid; the reaction between these two chemicals results in the production of a fine precipitate, barium sulphate. When shaken well, the turbidity of a McFarland standard is visually comparable to a bacterial suspension of known concentration. The 3 and 4 McFarland standards are equivalent to absorbance of 0.582 and 0.669 at 600nm. The Microbank vials containing individual bacterial strains were placed in specially provided Freezer Storage box and were stored at -80°C. The Microbank provided very easy recovery of the frozen bacteria; simply the required number of beads was taken out of the vile using aseptic technique and with sterile loop, and were introduced directly into Nutrient Broth (0.5% peptone, 0.3% beef or yeast extract, 0.1% lab-lemco powder and 0.5% NaCl) (Oxoid, UK) for cultivation.

3.5 Pressure Flow column Experimental Setup

For the implementation of the of the Microbially-Induced Calcite Precipitation (MICP) treatment method for the peat treatment and stabilisation a testing model was designed and manufactured for this study. To facilitate the pressure driven flow through a soil column (referred to herein as “pressure flow column”), a cylindrical mould made of clear transparent Plexiglass and having inner dimension (50mm in diameter, 175mm in length and 8mm thick) was used. The transparent material enabled the continuous monitoring of soil sample under the treatment and also assisted in supervising the uniformity of the cementing reagent flow throughout the treatment period. The experimental setup for the flow column treatment is shown below in figure 3.6. The apparatus consisted of the Plexiglas cylindrical mould a hydraulic pump, a compression frame and an effluent collector.

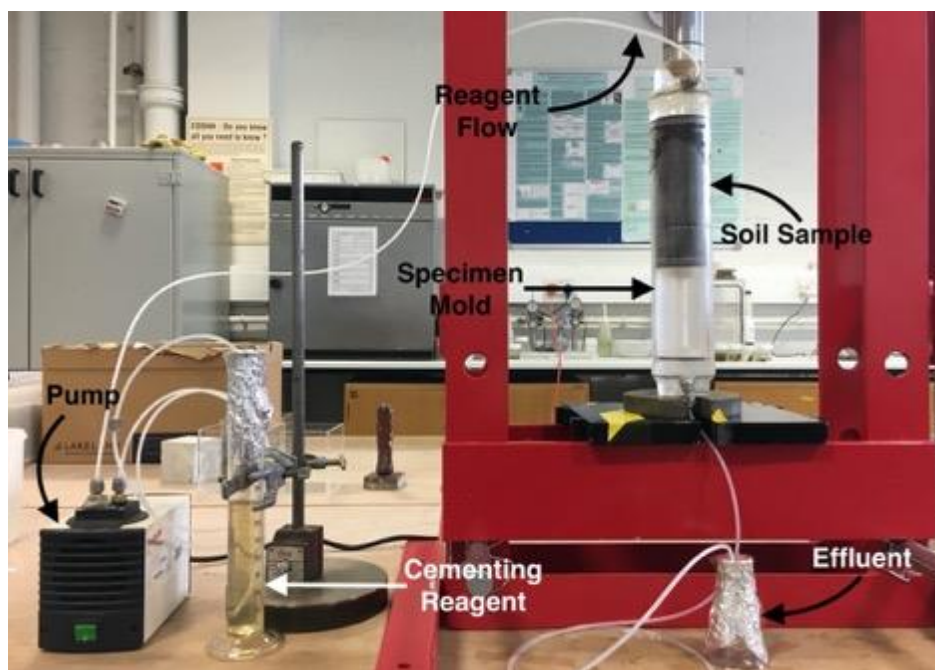


Figure 3.6 Pressure flow column for MICP treatment

3.5.1 Sample Preparation for Injection Method

The sample preparation method for biostimulation and bioaugmentation was different. For the biostimulation no additional bacteria were added into the soil samples, and only a high carbon source (Nutrient Broth) was provided for the natural indigenous bacteria, and in some experiments followed by the cementation reagent. On the other hand, in the case of bioaugmentation the soil samples were supplemented with

selected (isolated from same soil) externally grown bacteria before the injection of cementation reagent. Apart from injection method, the mixing of the bacteria and cementation reagent was also done in one set of bioaugmentation experiment for which the sample preparation method is given below in section 3.6. Only one bacterial strain was added in each individual sample at a time. Moreover, the mixing experimental set (bioaugmentation) was conducted under non-sterile conditions, i.e. the soil was not autoclaved prior to mixing with bacteria and cementation reagent solution, in-order to maintain the soils' original physicochemical characteristics.

A series of control experiments were conducted only using distilled water or solution of Nutrient Broth in-order to test and improve the experimental apparatus, adjust the safe injection pressure and to investigate biocementation feasibility with a simpler method and more likely to supply the bacteria uniformly into the soil. In addition, nutrients and bacteria cells (without cementing reagent) were used as control mix. Once the possible reasons for unsatisfactory MICP results were surmounted and the feasibility of the MICP method was established, the next steps of research such as the implementation of bacteria into the soil and changing the concentration of added bacteria and injected cementation reagent were investigated. All the samples in main Injection method experimental program were triplicated to ensure reliability and consistency in the results. The complete experimental scheme is given later in section 3.10.

The soil specimens provided from site by Network Rail was was dig by the digger, so it was very abrupt in size, diameter ranging from 0.25mm to 370mm, and making it very difficult to use for testing. From site to the lab and prior to testing the soil was kept in air tight bags to avoid oxidation of organic material present in the soil. In order to ensure homogeneity, the soil sample was pulverised with a rubber pestle. As the soil came from a shallow depth it was sieved to remove inorganic debris. Thus, only the portion passing the 1.18 mm sieve was used to prepare all soil specimens for the MICP treatment. The bacteria were cultivated and added in the shape of aqueous solution of Nutrient Broth for the biocementation samples. The hydromechanical testing of the soil indicated that up to 15% increase in moisture by mass of soil did not impacted water retention characteristics and Atterberg limits of the soil. Moreover, in a similar study Ng et al., (2014) also added approximately 18% volume of moisture by

mass of the soil samples. Hence based on these observations the bacterial-broth solution was supplied of a total of 15% by mass of the soil sample and this added % was kept consistent throughout all the samples during the MICP. The bacteria used in the MICP treatment, their selection criteria and growing conditions are discussed below in section 3.5.3.

After thorough mixing, the soil was covered with air tight seal and left for 48-72 hours to attain homogeneity of treatments and mixing throughout the specimen. Standard UCS specimens were then made from the soil sample, by static compaction at a rate of 1mm/min to the original field dry density of 0.919 g/cm³ and were transferred into the Plexiglas mould for treatment. The prepared UCS samples were transferred to the plexiglass mould by using the hydraulic frame without any loading to avoid any further disturbance to the samples. The interior surface of the Plexiglas mould was layered with a non-reactive lubricant for easier specimen extraction after the treatment. The soil sample was sandwiched between the two layers of filter papers and perforated disks, to avoid turbulent inflow and clogging at the inlet and outlet and mounted tightly onto the compression frame.

The mould inlet was connected to the outlet of the pump. The cementing reagent solution was supplied into the specimen mould at a constant flow pressure of 150 kPa by regulating the pressure from the control panel of the pump and at room temperature (22-27°C). Though some researchers such as Ng et al., (2014) mentioned that the variation in reagent solution flow pressure can produce different quantity of the precipitated calcite and the soil strength, to reduce the number of variables the pressure is kept constant for all the MICP experiments. However, there were other treatment variables which are given below in Table 3.3.

The pH of the effluent was monitored by sampling the effluent from the specimen mould at 24-h intervals. Ammonium contents were calculated directly from the treated soil specimens at the end of the curing period, and also from the effluent at 24-h intervals. Similarly, the UCS strength of the treated samples was determined at the end of the curing time period.

3.5.2 Cementation Reagent

In general, the rate and magnitude of the calcite precipitation is controlled by the urea and calcium chloride. Under the influence of urea hydrolysis, the urea is converted into ammonium and carbonate ions (see equations 2.12-2.17) and therefore an increase in the pH is observed due to formation of ammonium ions, the Calcium ions provided by the calcium chloride reacts with the carbonate ions to generate the CaCO₃. It should be noted that the rate of production of ammonium ions is not proportion to the precipitation of CaCO₃, as the precipitation takes more time than the dissolution of urea.

Equimolar concentrations of calcium chloride and urea mixed thoroughly in the 13 g/L of nutrient broth supplement in the shape of aqueous solution was used as the cementation reagent for this study. The equimolar concentration of both urea and calcium chloride was used to maintain the chemical equilibrium during the treatment, as also equimolar concentration of chemicals is employed by several researchers (e.g. Keykha et al., 2018; Ng et al, 2014). The varying concentrations of the cementation reagent employed in the MICP are given above in Table 3.3.

Table 3.3 Treatment variables for Pressure Flow Column experiments

Population of added culture	1x10 ⁷ (cfu/mL)		1x10 ⁸ (cfu/mL)	
Cementing reagent concentration	0.25 (M)	0.5 (M)	0.75 (M)	1.0 (M)
Treatment Duration	3 days		7 days	
Curing Duration	3 days		7 days	

3.5.3 Bacteria and Growing Conditions

Four native bacterial species from different groups of urease-producing microorganisms, *Bacillus licheniformis*, *Rhodococcus erythropolis*, *Micrococcus luteus*, and *Lysinibacillus fusiformis* were used in this study. The bacterial extraction and identification process using MALDI-TOF Mass Spectrometry was explained in section 3.4.

All four selected ureolytic strains are gram positive bacteria, which are abundantly found in the broad range of habitat especially in the majority of soil types. The more

common species of the *Bacillus* have proven to be very effective in their ability to precipitate calcite under different experimental conditions (Cacchio et al., 2003; Lian et al., 2006, etc.). *Bacillus* produce low ammonia as an unwanted end product, as these are large in size (2-5 x 1.2-1.5 μm) and have relatively lower urease enzyme activity compared to other calcite producing bacteria such as *S. pasteurii* (Whiffin 2004; Bachmeier et al., 2002, etc.).

Furthermore, the selection of these four bacterial strains as the urease-producing bacteria in this research is based on following considerations:

- The selected strains especially *Bacillus* and *Lysinibacillus* have the ability to produce the endospores which makes these highly resistant to chemical and physical influences (Nicholson et al., 2000). Due to the spore generation, these strains also have the capability of regeneration, which gives them the potential of being used for the purpose of self-healing of treatment.
- The selected microorganisms have large and elongated rod-shaped cell structures, which allows them to attach firmly to the soil grains and avoid being flushed away by the injection of the cementing reagent (Vary, 1994; Ng et al., 2014).
- All selected strains have the ability to survive and grow at both low and high temperature, and have shown high resistance to other environmental conditions like change in moisture contents in soil and pH (Ng et al., 2014; Dhimi et al., 2017). These characteristics provide enormous advantages to these bacterial strains for in-situ applications of the MICP.

For the hydromechanical property testing, all the test strains were cultivated at pH 7 under aerobic batch conditions in a sterile culture medium of Nutrient Broth (Oxoid, UK) in a shaking incubator at 200 rpm and 37 °C. The strains were grown to an early stationary phase i.e., Optical Density (OD): OD₆₀₀ ranging from 0.5-0.7 ((measured using a Pharmacia LKB Novaspec II spectrophotometer of 325-900 nm Wave length Range); they were then harvested by centrifuging at 8000g for 10 minutes to achieve the final concentration of approximately 1×10^8 cfu/mL (optical density 3.3); a second concentration of 1×10^7 cfu/mL was obtained by dilution with sterile sodium chloride solution (9-g/L NaCl).

3.6 Sample Preparation for Mixing Method

The soil was mixed with each culture medium containing the urease-producing bacteria, having concentration of 1×10^8 cfu/mL. After thorough mixing with bacteria the samples were kept in air tight container for 24 hours to attain homogeneity of the microorganisms through-out the specimen.

Bacterial-broth solution prepared in cementation reagent 15 % by weight of the soil sample (made with equimolar concentrations of urea and calcium chloride prepared in Nutrient Broth) was then added into the soil. The cementation reagent was added and mixed thoroughly in three equal portions i.e., each 24 hours, and the samples were again kept in air tight container for treatment for 7 days (starting from the mixing of microorganisms). After treatment, the standard UCS samples were prepared by static compaction at a rate of 1mm/min to the original field dry density of 0.919 g/cm^3 . The UCS samples were wrapped in the cling film and were tested after 2 days of curing to determine the final strengths of the soil samples.

3.7 Chemical Analysis

At the end of the treatment, the samples were removed from the plexiglass mould and were covered again with air tight seal and left for 48-72 hours to attain homogeneity of treatments and mixing throughout the specimen. For the chemical analysis the pH of the effluent was monitored by sampling the effluent from the specimen mould at 24-h intervals. Ammonium contents were calculated directly from the treated soil specimens at the end of the curing period, and also from the effluent at 24-h intervals. Similarly, the UCS strength of the treated samples was determined at the end of the curing period and was compared with that of the untreated soil. CaCO_3 content was determined from the broken UCS samples to assess further the efficiency of the treatment.

3.7.1 Calcium Carbonate (CaCO_3) Content Determination

The gravimetric analysis method of the acidified samples was used to determine the CaCO_3 content after the MICP treatment. The acid washing method for the determination of the calcite contents has been used by several researchers (Mortensen et al., 2011; Al Qabany, Soga & Santamarina 2012; Ng et al., 2014;). For

this purpose, 20g of oven-dried (at 105° C) soil samples were soaked with 2 M hydrochloric acid (HCl). The acid digestion of the calcite liberates the CO₂ with effervescence. The residue was collected and rinsed several times on a filter paper and again oven dried at 105° C, and the mass loss measured to estimate the calcium carbonate content in the samples as a percentage of the dry sample mass (i.e., 20 g). In order to determine the absolute % of CaCO₃ content in the MICP treated samples produced by the treatment, the CaCO₃ content of the untreated soil (0.018) was subtracted from the acid digestion results. Moreover, it was also assumed that after the MICP treatment, the increase in soil carbonate content is purely due to the CaCO₃ precipitation.

3.7.2 Urease activity / Ammonium Concentration Determination

The urease activity was measured in terms of ammonia production during the MICP, which was been measured for both effluent and for the treated soil.

3.7.2.1 Measurement Procedure in Effluent

(APHA/AWWA/WEF), 2005 (American Public Health Association/American Water Works Association/Water Environment Federation) approved phenate method was been used to determine the ammonium concentration in the effluent.

1. For this purpose, 0.4 mL of phenol solution, 0.4 mL of sodium nitroprusside and 1 mL of oxidizing agent were added and mixed with the 10 mL of the effluent sample in a universal bottle.

Composition of chemical solutions used:

Oxidizing agent: was prepared by mixing 25mL of (5%) sodium hypochlorite into 100 mL of alkaline citrate solution. and:

Alkaline citrate solution: was prepared by dissolving 10 g of sodium hydroxide and 200 g of trisodium citrate into 1L of deionized water.

2. The solution mixed in step 1 was left under low light conditions and at room temperature for 1 hour to achieve the chemical equilibrium.

3. The ammonium concentration was determined by analysing the peak absorbance of the samples at 640 nm, using the ultraviolet-visible spectrophotometer.
4. The standard calibration curves were plotted for each sample and the area under the base peak was calibrated to measure the ammonium concentration (mM) and the values were determined by comparing the several standard solution of NH_4Cl under the same conditions.
5. The urease activity of the bacteria was obtained by dividing the ammonium concentration over the reaction time. As by definition, 1 unit urease activity is the amount of urease which generates 1.0 μmol of ammonium per minute.

The ammonium concentration ranging (0.02-2 mg NH_4^+/l) can be measured accurately with this method. However, the high concentration samples were diluted with distilled water and corrections were made in the end calculations.

3.7.2.2 Measurement Procedure in Soil Samples

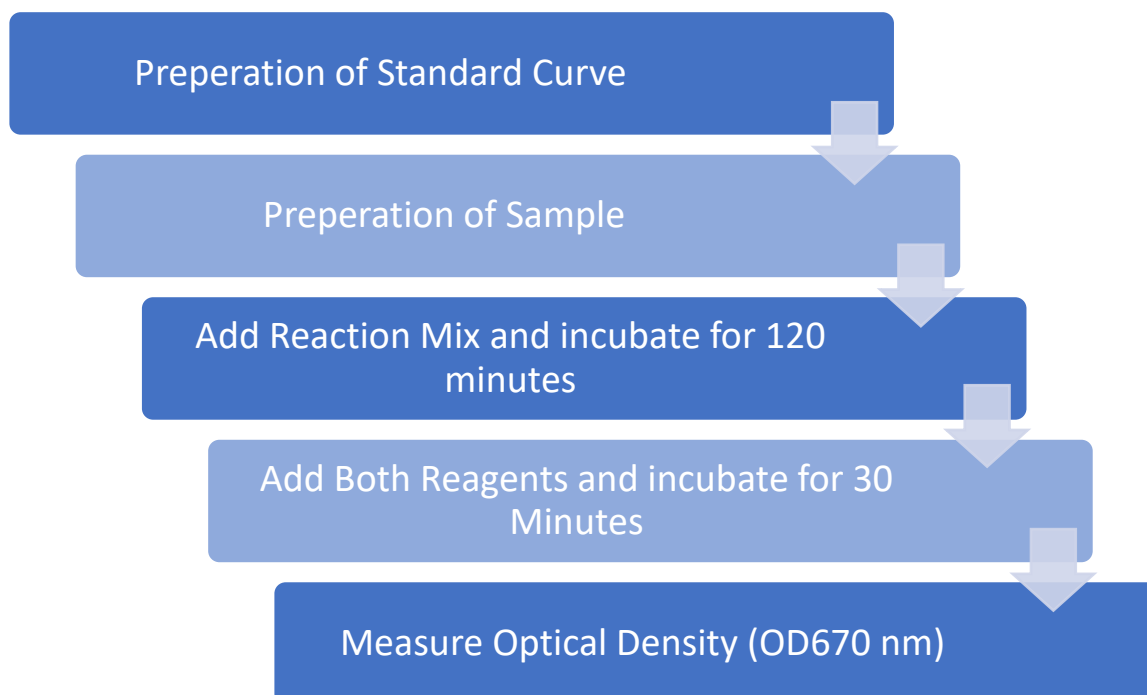
The urease activity and the resulting ammonia concentration in the treated soil was directly measured by using urease Activity Assay kit (Colorimetric; ab204696, Abcam, US) using the following steps:

1. First step in the direct measurement of the Urease activity of the soil is to prepare the standard and prepare the standard calibration curve. It is essential to prepare the standard in order to calibrate the output of the tested samples by using an ultraviolet-visible spectrophotometer or by Colorimetric microplate reader. For this purpose different dilutions of the Ammonium Chloride were prepared by using double distilled H_2O . The Ammonium Chloride dilution scheme is provided in Appendix D. Moreover, the diluted standard solution is unstable and cannot be stored for later use, so a fresh set of standards was prepared for every use. Moreover, each standard dilution was set up to produce duplicate readings (i.e., 2 x 100 μL).
2. Small quantity (0.5g) of the treated soil was homogenized by vigorous stirring in 10mL of 50 mM sodium acetate for two minutes and at controlled pH of 5.
3. 0.2 mL of the solution was pipetted out into a clean tube as soil background control and was centrifuged at 8000 x g for 1 minute. 0.1 mL of the clear supernatant was collected and transferred to a micro vial.

4. Again 0.9 mL of the solution prepared in step 2 was taken in another tube as test sample and was mixed with 0.1 mL of Urea. This test sample was incubated for 2 hours at 37° C and centrifuged at 8000 x g for 1 minute.
5. 0.1 mL of the clear supernatant was collected and transferred to a micro vial, 80 µL of the supplied Reagent 1 was mixed into each micro vial via vortexing with mechanical mixer, followed by 40 µL of the supplied Reagent 2.
6. The solution was again incubated at 37° C for 30 minutes. The output was measured on an ultraviolet-visible spectrophotometer at OD670. At the end of the reaction, strains that produced <30 µm of ammonia were shortlisted.

In the urease activity measurement, all the reagents were prepared and chemicals and materials were equilibrated at room temperature prior to use. All standards to Assay, regarding samples and controls were prepared in duplicate to ensure repeatability. Enzymes and other heat labile components and samples were kept on ice during the Assay preparation. More importantly, the Aseptic technique was adopted to avoid cross contamination, and to prevent formation of foaming or bubbles during mixing or reconstituting of components.

3.7.2.3 Urease Assay Summary



3.7.2.4 Urease Activity Calculation from OD670

- In order to obtain the correct absorbance the mean absorbance value of the blank standard and the OD670 reading of the soil background control was subtracted from the average value of the duplicated readings of each sample.
- The absorbance values for each standard were plotted as a function of total quantity of the ammonium produced by urease against the reaction time. A best fitting curve was plotted through these points. The trendline equation can easily be formulated to crosscheck the results.
- The urease activity of the soil (nmol/mg soil/hour) is calculated as:

$$\text{Soil Urease Activity} = \left(\frac{B}{T \times 5} \right)$$

Where:

B = amount of ammonium (nmol) produced by the sample as per standard curve

T = Reaction time (hour)

5 = soil (mg) used in the assay

Unit Definition

1 Unit Urease activity = amount of Urease which generates 1.0 μmol of ammonia per minute at pH 7 at 37°C.

The NH_4^+ concentration of the treated soil samples was determined from the ammonia calibration curve. The calibration curves and the soil specimens were made by the method described in section 3.7.2.2. The absorbance of the prepared soil specimens was measured at OD 670 and the relevant NH_4^+ concentrations were determined from the calibration curves. A typical ammonia standard calibration curve is given below, however a new standard curve was generated for each assay performed.

The samples which provided OD670 absorbance more than that of highest value in standard curve were diluted with double distilled H_2O and reanalysed. The appropriate dilution factors for such samples were determined by multiplying the concentrations. Moreover, for soil specimen testing several incubation lengths (8-24 hours) were selected to ensure enzyme activity is within the assay range.

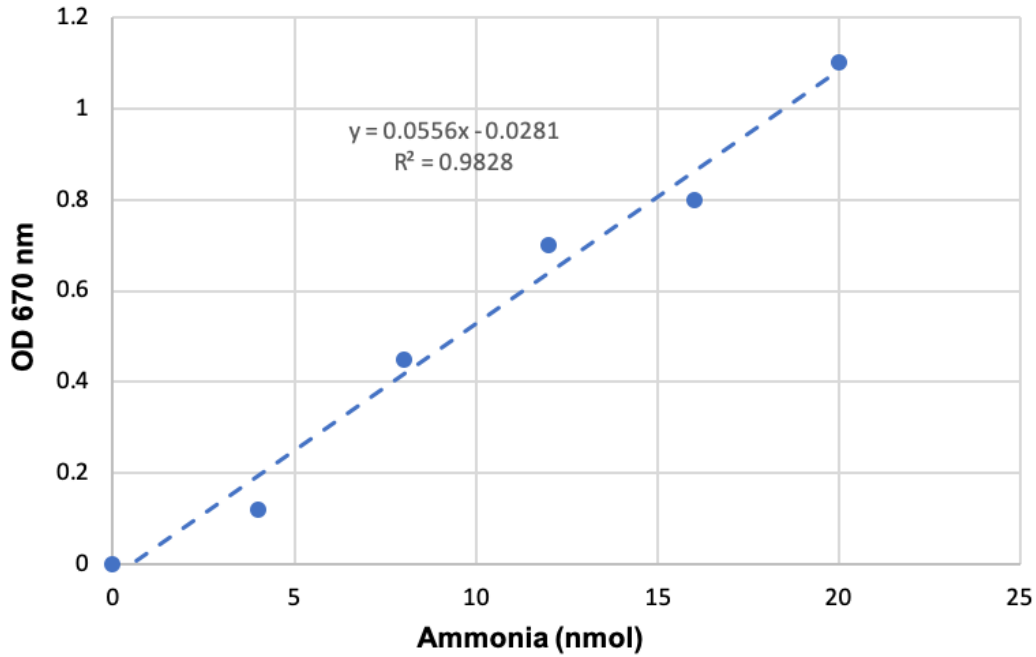


Figure 3.7 Typical ammonia standard calibration curve

3.8 Geotechnical Property Testing

In addition to above explained chemical analysis, Unconfined Compression Tests (UCS) as per ASTM D 2166 for determination of strength improvement, final moisture content and pH of all the MICP treated samples were measured. Moreover, the oedometer tests to determine soil compressibility and consolidation rate changes and soil water retention curve (SWRC) tests were conducted on the best result producing samples. The test results are provided and explained in Chapter 4 and 5.

3.8.1 Oedometer Testing

The conventional oedometer consolidation tests were performed to analyse the compressibility and consolidation behaviour changes in the untreated treated soil samples. The consolidation testing was performed on both Pressure Flow Column and Electrokinetic treated samples. The treated samples were tested in both saturated and unsaturated states and the results are explained in sections 4.6 and 5.8 respectively.

3.8.1.1 Sample Preparation Methods and Testing Methodology

For the untreated soil, the oedometer samples were prepared by statically compacting the soil in the oedometer ring at a rate of 1mm/min to the original field dry density of

0.919 g/cm³. Samples were wrapped in the cling film and were stored for 24 hours before starting the consolidation test.

Because of the respective dimensions of the pressure flow column sample and the oedometer ring, it was not possible to obtain intact samples of the pressure flow column soil. For this reason, the samples from the treated soil was prepared by cutting the soil from the treated UCS size sample, and the oedometer consolidation ring was filled loosely with the chunks of the treated soil and the big visible voids were filled by hand without using any compression frame and excessive pressure to avoid further sample disturbance as much as possible.

The two saturated specimens (one treated and one untreated) were left to swell (free swelling) in the oedometer cell that was filled with water until no further height change was recorded; this was followed by compression at a stepwise increasing applied pressure of 25-400 kPa, which was followed by unloading; conversely the unsaturated treated specimen was subjected to compression and unloading without initial saturation/swelling stage. The consolidation pressure was applied in 5 stages (25, 50,100,200 and 400 kPa), and unloading in two stages (200, and 50 kPa).

The sample for the EK treated soil was prepared by cutting an oedometer specimen directly from the EK treatment box sample. However, the top 2 cm of the soil in the EK cell were not used, to avoid any inconsistencies due small surface cracks formed from the escaping gases. In the case of EK samples again the two saturated specimens (one treated and one untreated) were left to swell (free swelling) in the oedometer cell that was filled with water prior to compression at an applied pressure of 25-800 kPa in 6 stages (25, 50,100,200, 400 and 800 kPa) followed by unloading, in three stages (400, 200 and 50-0 kPa); the unsaturated treated specimen was subjected to compression and unloading without initial saturation/swelling stage.

3.8.2 Soil Water Retention Curve (SWRC) Testing

Soil Water Retention Curve (SWRC) measurements of the untreated soil and indicative treated soils from both pressure flow column and EK-biocementation were performed using WP4C chilled-mirror dew point potentiometer.

3.8.2.1 Sample Preparation Methods and Testing Methodology

For the untreated soil, the SWRC samples were prepared to the required size of 5mm thick and 36mm in diameter. Samples were made by statically compacting the soil at a rate of 1mm/min to the original field dry density of 0.919 g/cm³ and were wrapped in the cling film and were stored for 24 hours before starting the SWRC analysis.

For the Pressure Flow Column and EK Treated soil, the samples were prepared by trimming out the soil to the required size samples from the treated specimens. The trimming technique using small soil spatula was adopted out of several sample extraction techniques as it produced minimum disturbance to the samples. The SWRC measurements of the samples were started at the moisture content % at the end of the treatment, i.e. 55.46%, 64.11% and 69.32% for untreated soil, PFC treated soil and EK treated soil samples respectively. The samples were first wetted up to 75% of moisture content and then were left to dry out. The SWRC measurements were recorded at every 10% increase or drop in moisture contents in the samples and the results are provided in section 5.9.

3.9 Electrokinetic (EK) Testing Experimental Setup

A rectangular EK soil stabilisation cell made of transparent non-conductive and 10 mm Perspex acrylic sheet was designed and manufactured for this study. The design of the purpose built Electrokinetic soil box is based on the original prototype made and used by the author in his MSc. studies but with several improvements. The essential design parameters for the EK soil stabilisation box were:

- A cell capable enough to stabilise the problematic peat with consolidation under its self-weight and uner overburder pressure (not studied in this research), and sufficiently large to treat a specimen volume of up to 5376 cm³.
- The unrestricted migration of water and chemical species from electrolyte compartments to the soil mass and vice versa.
- The elemental rectangular shape for one dimensional ion transport and electro-chemical reactions. The one-dimensional treatment was adopted to minimise the system complexity (in view of future numerical modelling of the test).

- The provision of open rectangular surface enables the easy extraction of gases generated at the electrodes during the EK process and eliminates the soil heaving in the top layer.
- The maintenance of a uniform electric field in the soil sample throughout the treatment, was achieved by providing full face electrodes on both sides of the soil sample (see figure 3.9).

The rectangular shaped boxes have been used by several researchers according to their treatment requirements (e.g. Tajudin, 2012; Jayasekera et al., 2007; Liaki, 2006; Shang et al., 2004; Guy et al., 2004, and many more). However, other researchers have also used different types and shapes of the EK soil stabilisation cell. For the three-dimensional soil treatment, Turer & Genc, (2007) used a circular box, with anode in the middle and several cathodes around the circumference. Similarly, Yeung et al., (1997) modified triaxial apparatus and used it for EK dewatering of compacted clay, but have reported several treatment issues, like non-uniformity of treatment due to smaller and non-inert electrodes and very small quantity of the treated soil.

The nonconductive nature of the Perspex prevents the electric short circuit and thus permits safe working on the cell; the transparent material also enabled the continuous monitoring of soil sample and assisted in monitoring the electrolytes levels during the EK treatment.

The cell consists of three compartments, the main central compartment where the soil sample is placed for treatment has an internal dimensions 210 mm length x 160mm width x 140mm depth after the incorporation of the sample extractor and two small chambers on both sides of the main compartment with internal dimensions of 100mm length x 160mm width x 140mm depth to supply the water, bacterial solution or cementation reagents as electrolytes (see figure 3.8). The partition walls between the main compartment the electrolyte chambers were made perforated by 40% of total wall area in order to ensure uninterrupted movement of chemical ions, bacteria and water across the soil specimen compartment during the EK treatment.

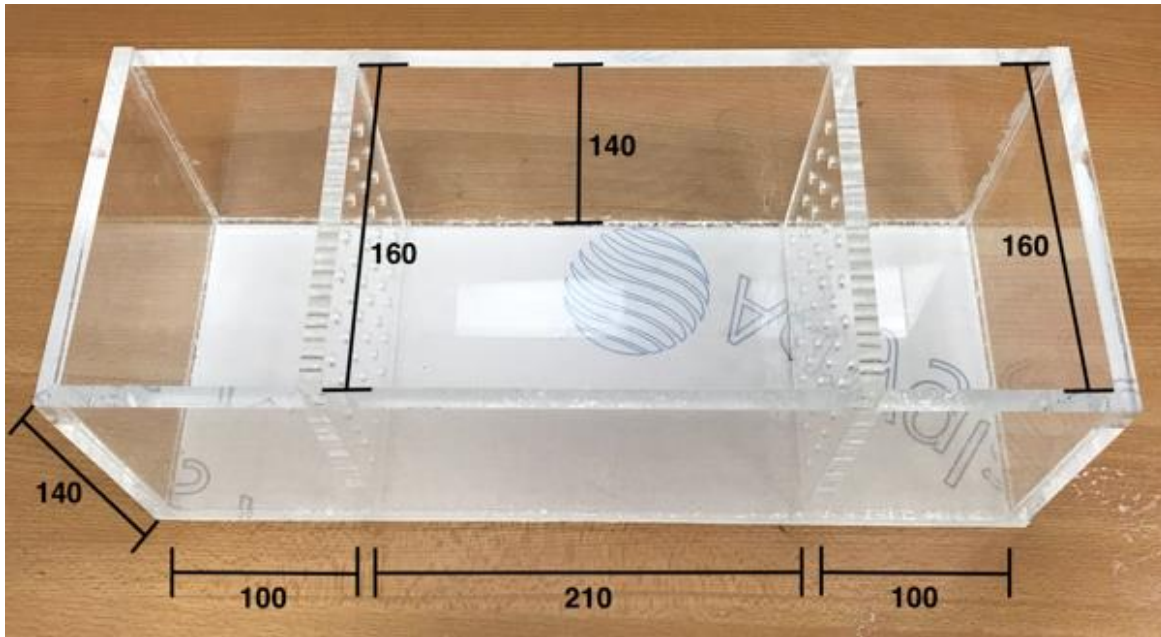


Figure 3.8 Electrokinetic stabilisation cell with dimensions (mm)

3.9.1 Sample Extractor

A purpose-built sample extractor made of the same material was provided as an internal layer to prevent sample disturbance during extraction at the end of the test. The sample extractor facilitated extraction of the whole treated soil block without any disturbance to sample, which made it very easy to conduct further testing such as UCS, oedometer etc. The fitting of the sample extractor inside the soil stabilization compartment does not affect the free migration of chemical species and water across the soil mass as it has only the longitudinal sides and no transverse sides (see figure 3.9).

3.9.2 Electrodes

In the EK soil processing the selection of the electrode material is very vital. There are several factors that should be considered in this context such as: Electric conductivity, chemical reactions, inert and non-inert nature of the material and cost. The metallic conductors such as copper or steel have proven to be effective in enhancing the physicochemical characteristics of the soils (Jayasekera, 2007), but the integration of such electrodes due to formation of acidic and alkaline fronts can induce metallic ions into the soil mass, which can effectively change the chemistry of soil porous media. Therefore, electrodes made of inert and 99% pure graphite sheet (Processed Graphite

Laminate SLS) were used to eliminate electrode corrosion that would introduce secondary reaction products and reduce the effectiveness of the system due to substantial voltage loss at the electrodes.



Figure 3.9 Sample extractor and electrode arrangement

3.9.3 EK Sample Preparation

The soil was compacted hydraulically in 5 equal layers in the sample compartment of the electrokinetic by using a hydraulic compression frame. The target compaction density was the calculated dry density of 0.919 g/cm^3 of in-situ soil. A layer of filter paper was used on both perforated walls to prevent the movement of soil particles into the electrolyte chambers. The electrodes were connected to the power supply and a constant voltage gradient of 0.4V/cm was maintained throughout the tests as recommended in the literature in order to prevent potential harm to the bacteria (Mizuno & Hori, 1988; Hassan et al., 2016). For the same reasons, periodic polarity reversal was applied every 24h. The reversal of polarity is recommended for a better uniformity and effectiveness of the treatment but also to prevent high pH gradients that could also be harmful to the bacteria (Mena et al., 2016).

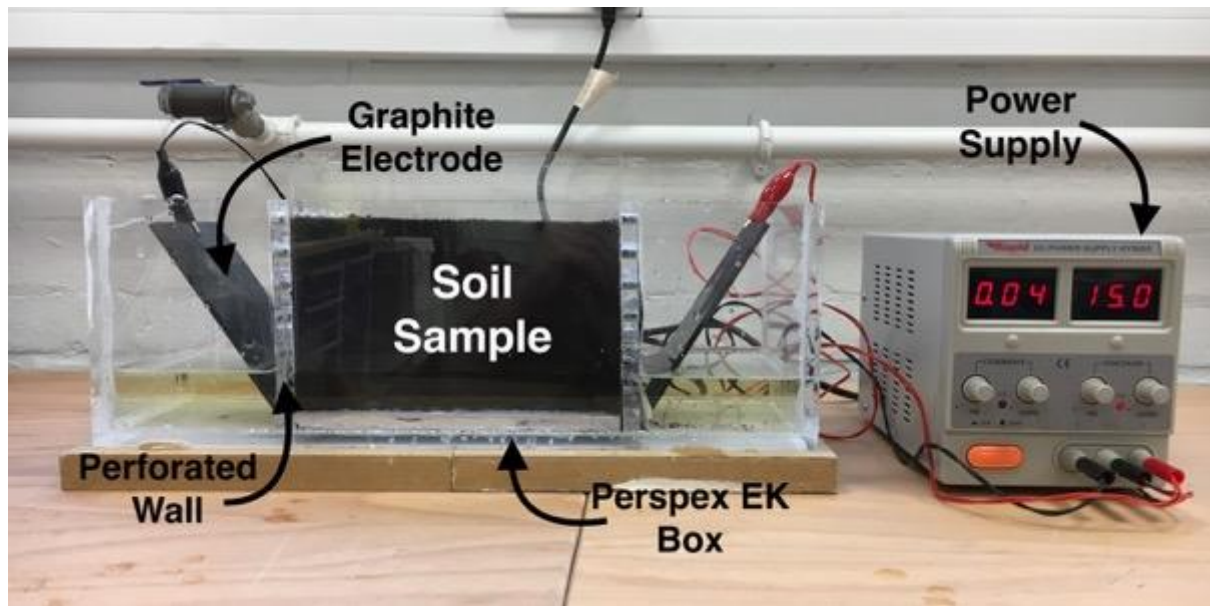


Figure 3.10 EK Experimental setup

3.9.4 Data Monitoring

Several parameters and variables were monitored continuously throughout the EK tests. To ensure that the electric current and passing voltages did not considerably change during treatment, measurements of these quantities were performed at different locations from the electrodes throughout the treatment. pH of the solutions was also monitored inside both electrolyte chambers during the treatment. In addition, temperature was recorded as this can affect bacteria growth. The pH and temperature of the effluents from both electrolyte compartments was determined directly by portable HI-9831-5 pH/EC/TDS/°C meter manufactured by Hanna Instruments. Before every measurement the meter was calibrated for relative humidity by using the calibration salt provided by the manufacturer. However, the pH of soil samples at the end of testing was determined by using BS 1377-1990: part 2. The electric current and voltage was monitored across the soil specimen during the EK treatment by using the portable volt meter. For this purpose, the 210 mm long sample was divided into five equal portions and electric probes were installed at these locations i.e. at 42, 84, 126, 168 and 210 mm from the anode and results are discussed in section 5.7.

3.9.5 Electro-Biocementation Method and Assumptions

The requirement of this part of research, “self-weight stabilisation due to an applied electric potential and bacteria” led to the need of performing preliminary investigatory

tests, before starting the main electrokinetic biocementation testing plan. The preliminary and main tests and their relevant parameters are as follows:

- The control tests starting from the natural moisture content of the soil, where soil was let to dry out due to electroosmosis (without adding any water at the anode compartment); this showed an average of 13.6% change in the volume of the soil.
- Making the simplifying assumption that the soil was saturated, the 13.6% volume change of the soil upon EK was compensated by adding 13.6% at the anode compartment in an attempt to maintain a constant soil volume during EK testing. It is also assumed that 13.6% volume change in experiments with water only would also be equivalent to those where nutrient broth and cementing reagents were supplied and would not impact on soil and its electrokinetic properties.
- This is of practical importance to avoid soil settlement under existing earthworks during EK treatment. The results showed that this water addition had successfully prevented volume change of the soil during EK.
- The addition of 13.6% water increased the original degree of saturation (S_r) of the soil to 82.8%, which was increased further purposely to 85% by calculating and adding some more water. To be precise 14.45% by soil volume was added to obtain the 85% (S_r).
- Therefore, the addition of 15% water (or aqueous solutions, with the water content being reduced approximately up to 14.59 % if the molecular weights of the nutrient broth, urea and calcium chloride are considered) consistent with the pressure flow column tests, was considered acceptable to maintain a relatively constant sample volume during the EK treatment and was adopted for the rest of the tests with bacteria implementation.
- The Electrokinetic treatment was performed on three different degrees of saturation (S_r) 75%, 85% and 95% of the soil samples in order to check the efficiency of the EK system under different saturation conditions and to optimise the treatment variables (see table 3.7 for complete experimental set description). The other degree of saturations were obtained by wetting and drying the 85% saturated soil respectively. Irrespective of degree of saturation

of soil the treatment parameters and procedure were kept same for all the EK treatment experiments.

- The nutrient broth solution and the cementing reagents were supplied all in one homogeneous single solution in all the relevant main EK tests (divided equally in the two electrolyte compartments i.e. 7.5% per dry soil mass per compartment). The Nutrient broth and cementation reagent solution was added in three equal proportions at (starting at day 1, then at day 3 and day 7) of the treatment rather than the continuous supply. The intermediate supply of the solution was provided to control the pH gradient by diluting the solutions in the electrolytes chamber and preventing the solutions to become acidic. As bacterial metabolic activity and the CaCO_3 production require an alkaline environment (Achal et al., 2009), hence the intermediate solution supply more importantly allowed the pH to rise to an optimum range of 7.2 to 7.85 for the *Bacillus licheniformis* to produce CaCO_3 . Which would be difficult to achieve while supplying solution continuously in a combination of 24-h polarity reversal.
- The duration of the EK-Biocementation treatment was two weeks and was fixed for majority (except one set) of the experiments, (i.e. 7 days per electrode polarity). 14 days is a typical field treatment length (e.g. Mena et al., 2016) and was used here to prove the biocementation feasibility.
- The bacterial strain of *Bacillus licheniformis* (population 1×10^8 cfu/mL) and the (0.75 M) concentration of the cementation reagent provided the best results in the flow column treatment (see chapter 4). Hence for the EK- Biocementation treatment the other 4 bacterial strain and the diluted concentration of 1×10^7 cfu/mL was ignored in order to reduce the number of variables and the experimental work.
- The bacteria were added in the EK treatment sample by using both Pre-mixing and electrokinetic injection methods in separate set of experiments.
- In the Pre-mixing method, the bacteria were mixed with the soil before the application of the electrokinetics treatment. After thorough mixing, the bacteria mixed soil was then covered with air tight seal and left for 48-72 hours to attain homogeneity of treatments throughout the sample. However, the nutrients and cementing reagents were transferred under the influence of electric potential. The reason for this was to prove the feasibility of the technique initially having

to consider only the potential effect of the EK on bacteria as an influential factor on the biocementation success, thus eliminating any other complications linked to the bacteria transport and distribution in the sample if supplied electrokinetically.

- In further EK-Biocementation tests the bacteria were also supplied by electrokinetic injection to represent a realistic field implementation of the treatment. For this purpose the bacteria were cultivated directly in the Nutrient Broth solution to the required 1×10^8 cfu/mL concentration which was then homogenized with 1M cementation reagent.
- The concentration of the cementation reagent was also kept constant to 1M for all EK-Biocementation tests. The 1M concentration was selected on the basis of results obtained from the pilot EK experiments. Despite the fact that four different CR concentrations were used in the PFC experiments (see Table 3.3), here in-order to decrease the number of variables and experiments and to complete the experimental program only 1M concentration was used for the EK-Biocementation tests.
- Due to the longer treatment duration and large number of experiments, the EK experiments were not replicated. However, duplicate UCS specimens (50mm diameter and 100 mm height cylinders) from three different locations in the EK treated soil sample were extracted to ensure uniformity and consistency in the results. The duplicate samples were extracted namely from the areas next to the two electrolyte chambers (right and left) and from the middle of the sample (i.e. total 6 UCS specimens for each treatment).
- The EK treatment duration was fixed at 14 days. Before further testing (e.g., strength, pH) the treated soil was then covered with air tight seal and left for 24 hours to attain homogeneity of treatments. The summary of treatment variables is as follows:

Table 3.4 Treatment Variables for EK-Biocementation

Population of added culture	Constant	1x10 ⁸ (cfu/mL)	
Cementing reagent concentration	Constant	1.0 (M)	
Treatment Duration	Constant	14 days	
Bacteria added method	Pre-mixing	Electrokinetic injection	
Degree of Saturation (S _r)	75%	85%	95%
Cementing Reagent reaction time	Constant	14 days	
Curing Duration	Constant	1 day	
Bacteria strain	Constant	<i>Bacillus licheniformis</i>	
Added Reagent + Bacteria in NB	Constant	15% (dry soil mass)	

3.9.6 Hydromechanical Properties

The Unconfined Compression Tests (UCS) were mainly carried out to determine the improvement in the peat soil strength after the EK-Biocementation treatment. Using the sample extractor, the whole treated soil blocks were extracted from the EK stabilisation cell and UCS size specimens were cut. In-order to avoid any impact on the soil structure, the samples were prepared by trimming out the soil to the UCS size samples from the treated block specimen. The trimming technique using small soil spatula was adopted out of several sample extraction techniques as it produced minimum disturbance to the sample. The other techniques for instance the extraction by using the steel and PVC mould produced local punching stresses in the soil around the walls of the moulds, and re-extraction the sample from the mould caused additional disturbance to samples.

The workable open rectangular surface and dimensions of the cell allowed the extraction of duplicate UCS specimens (50mm diameter and 100 mm height cylinders) from three different locations in the soil sample, namely from the areas next to the two electrolyte chambers and from the middle of the sample (i.e. total 6 UCS specimens for each treatment). The extracted UCS specimens were then covered with air tight seal and left for 24 hours before strength testing to attain homogeneity of treatments

or curing. Final moisture content and pH of all the UCS samples were measured. Moreover, oedometer tests to determine soil compressibility and consolidation rate changes and final permeability as well as SWRC testing were conducted on the best result producing samples (see chapter 4 and 5 for results).

3.10 Main Experimental Program

The two main treatment implementation methods used in this study were the light pressure flow column technique and Electrokinetic injection. The experimental program was also divided according to these two techniques. For this purpose, 5 sets of controlled and 22 sets of main pressure flow column experiments have been conducted. Based on the variables explained in table 3.2 these experiments are divided in 6 experimental batches (see below table 3.5).

The second method for the biocementation was by mixing, where both bacterial solution and cementation reagent are added into soil via mixing instead of injection under pressure. In this set all four bacterial strains were mixed individually and the concentration was kept constant to 1×10^8 cfu/mL. the experimental matrix for this technique is given in table 3.6. As this method proved to be unsuccessful it was not pursued after the first set of tests.

The bacterial strain of *Bacillus licheniformis* (population 1×10^8 cfu/mL) and the (0.75 M) concentration of the cementation reagent provided the best results in the MICP treatment (see chapter 4). Hence for the EK- Biocementation treatment the other 3 bacterial strain and the diluted concentration of 1×10^7 cfu/mL were not used in order to reduce the number of variables and the experimental work. Based on this finding and the variables given in table 3.4, 2 sets of control and 4 sets of EK Biocementation tests were conducted. The experimental matrix for this technique is given in Table 3.7.

Table 3.5 MICP (Injection method) experimental program

PFC, Pressure Flow Column; NB, Nutrient Broth; CR, Cementation Reagent (CH₄N₂O + CaCl₂); B, Bacteria

Test ID	Added solutions	Added Strain	Population of added culture (cfu/mL)	CR concentration (M) : (M)	Treatment duration (days)	Curing (days)
Control Samples						
Untreated soil C1	N/A	N/A	N/A	N/A	N/A	N/A
PFC1-C2	Distilled Water	N/A	N/A	N/A	3	7
PFC2-C3	3g/L NB	N/A	N/A	N/A	3	7
PFC3-C4	3g/L NB + CR	N/A (bio-stimulation)	N/A	1:1	3	7
PFC4-C5	3g/L NB + CR	N/A (bio-stimulation)	N/A	1:1	3	1
Batch 1						
PFC5	3g/L NB + B	<i>Bacillus l.</i>	1x10 ⁸	N/A	3	7
PFC6	3g/L NB + B	<i>Rhodococcus e.</i>	1x10 ⁸	N/A	3	7
PFC7	3g/L NB + B	<i>Micrococcus l.</i>	1x10 ⁸	N/A	3	7
PFC8	3g/L NB + B	<i>Lysinibacillus f.</i>	1x10 ⁸	N/A	3	7
Batch 2						
PFC9	3g/L NB + CR	<i>Bacillus l.</i>	1x10 ⁸	1:1	3	7
PFC10	3g/L NB + CR	<i>Rhodococcus e.</i>	1x10 ⁸	1:1	3	7
PFC11	3g/L NB + CR	<i>Micrococcus l.</i>	1x10 ⁸	1:1	3	7
PFC12	3g/L NB + CR	<i>Lysinibacillus f.</i>	1x10 ⁸	1:1	3	7
Batch 3						
PFC13	3g/L NB + CR	<i>Bacillus l.</i>	1x10 ⁷	0.5:0.5	3	7
PFC14	3g/L NB + CR	<i>Rhodococcus e.</i>	1x10 ⁷	0.5:0.5	3	7
PFC15	3g/L NB + CR	<i>Micrococcus l.</i>	1x10 ⁷	0.5:0.5	3	7
PFC16	3g/L NB + CR	<i>Lysinibacillus f.</i>	1x10 ⁷	0.5:0.5	3	7
Batch 4						
PFC17	3g/L NB + CR	<i>Bacillus l.</i>	1x10 ⁸	0.25:0.25	3	1
PFC18	3g/L NB + CR	<i>Bacillus l.</i>	1x10 ⁸	0.75:0.75	3	1
PFC19	3g/L NB + CR	<i>Bacillus l.</i>	1x10 ⁸	1:1	3	1
Batch 5						
PFC20	3g/L NB + CR	<i>Bacillus l.</i>	1x10 ⁷	0.25:0.25	3	1
PFC21	3g/L NB + CR	<i>Bacillus l.</i>	1x10 ⁷	0.75:0.75	3	1
PFC22	3g/L NB + CR	<i>Bacillus l.</i>	1x10 ⁷	1:1	3	1
Batch 6						
PFC23	3g/L NB + CR	<i>Lysinibacillus f.</i>	1x10 ⁸	1:1	3	1
PFC24	3g/L NB + CR	<i>Lysinibacillus f.</i>	1x10 ⁷	1:1	3	1

Table 3.6 MICP (Mixing method) Experimental Program

MX, Mixing Method; NB, Nutrient Broth; CR, Cementation Reagent (CH₄N₂O + CaCl₂)

Test ID	Added solutions	Added Strain	Population of added culture (cfu/mL)	CR concentration (M) : (M)	Treatment duration (days)	Curing (days)
Batch 1						
MX1	3g/L NB	<i>Bacillus l.</i>	1x10 ⁸	1:1	3	2
MX2	3g/L NB	<i>Rhodococcus e.</i>	1x10 ⁸	1:1	3	2
MX3	3g/L NB	<i>Micrococcus l.</i>	1x10 ⁸	1:1	3	2
MX4	3g/L NB	<i>Lysinibacillus f.</i>	1x10 ⁸	1:1	3	2

Table 3.7 EK-Biostimulation Experimental Program

EK, Electrokinetic; NB, Nutrient Broth; CR, Cementation Reagent (CH₄N₂O + CaCl₂)

Test ID	Added solutions	Degree of Saturation (S _r)	Added Strain	Population of added culture (cfu/mL)	CR concentration (M) : (M)	Treatment duration (days)	Curing (days)
Control Samples							
EK1-C1	N/A	N/A	N/A	N/A	N/A	14	1
EK2-C2	Distilled Water	N/A	N/A	N/A	N/A	14	1
Batch 1 (Pure System)							
EK3	Distilled Water	75 %	N/A	N/A	N/A	14	1
EK4	Distilled Water	85 %	N/A	N/A	N/A	14	1
EK5	Distilled Water	95 %	N/A	N/A	N/A	14	1
Batch 2 (Control samples with nutrients)							
EK6	3g/L NB	75 %	N/A	N/A	N/A	14	1
EK7	3g/L NB	85 %	N/A	N/A	N/A	14	1
EK8	3g/L NB	95 %	N/A	N/A	N/A	14	1
Batch 3 (Bio-augmentation with premixed bacteria)							
EK9	3g/L NB + CR	75 %	<i>Bacillus l.</i>	1x10 ⁸	1:1	14	1
EK10	3g/L NB + CR	85 %	<i>Bacillus l.</i>	1x10 ⁸	1:1	14	1
EK11	3g/L NB + CR	95 %	<i>Bacillus l.</i>	1x10 ⁸	1:1	14	1
Batch 4 (Bio-augmentation via Electrokinetic injection)							
EK12	3g/L NB + CR + <i>Bacillus l.</i> (all in one solution)	75 %	Not mixed in the soil sample	1x10 ⁸	1:1	14	1
EK13	3g/L NB + CR + <i>Bacillus l.</i> (all in one solution)	85 %	Not mixed in the soil sample	1x10 ⁸	1:1	14	1
EK14	3g/L NB + CR + <i>Bacillus l.</i> (all in one solution)	95 %	Not mixed in the soil sample	1x10 ⁸	1:1	14	1

Chapter 4

RESULTS AND DISCUSSION OF FLOW COLUMN EXPERIMENTS

This chapter will present and analyse the results of MICP Pressure Flow Column treatments in-terms of Engineering and Hydromechanical properties. These include, Unconfined Compressive strength improvement (UCS) changes in the stress-strain behaviour, CaCO_3 content, Final moisture content % of the treated samples, concentration of Ammonia and change in pH. A thorough discussion on these results and the correlations in-between these are also given with help of several graphical representations. The degree of improvement in the treated soil was also assessed in terms of compressibility behaviour of the treated soil. Moreover, other controlling variables such as population concentration of bacteria and their effect on the strength improvement and CaCO_3 distribution is also discussed.

Before the presentation of the flow column experiments results, the results of the microbiological study are presented first, in the following section.

4.1 Microbiological Analyses

The four best indigenous ureolytic bacterial strain candidates for biocementation were *Bacillus licheniformis*, *Rhodococcus erythropolis*, *Micrococcus luteus*, and *Lysinibacillus fusiformis*, selected on the basis of their ability to grow and survive at low to medium temperatures and pH values of 4.5-10, and their urease enzyme production ability (see section 3.5.3).

According to American Type Culture Collection (ATCC) these four strains were of Biosafety Level (BSL) 1, i.e. not known to consistently cause disease in healthy adults, and of minimal potential hazard to laboratory workers and the environment (based on the U.S. Department of Health and Human Services, CDC/NIH Guidelines, 2007).

First, two different sets of UCS tests were performed on the soil inoculated with the different monocultures, varying the bacteria populations (assessed based on optical density measurements) and cementing agent concentrations (PFC9-16). Subsequently, *Bacillus licheniformis* was selected for further testing based on the

better results produced in the first sets of UCS tests as compared to other bacterial strains (see section 4.2) but also because of the following additional reasons:

- The bacterium is widespread in nature and is found in abundance in natural soils;
- It is motile (using its flagellum) and relatively small (of about 1 μm diameter, against about 2 μm for *B. cereus*, Bisset and Street, 1973) which facilitates its motility through smaller pore throats;
- Its elongated, rod-shaped cell makes it difficult to flush out during pressure or EK injection;
- It is reported to be facultative anaerobic (e.g. Clements et al, 2002), so it can survive in environmental conditions of reduced oxygen supply;
- It is a spore generating bacterium: this feature could be exploited for potential self-healing mechanisms (Petrova-Botusharova, 2017).

4.1.1 Bacterial Growth Rate

For the hydromechanical property testing all strains were cultivated at pH 7 under aerobic batch conditions in a sterile culture medium of Nutrient Broth (Oxoid, UK) in a shaking incubator at 200 rpm and 37°C. The strains were grown to an early stationary phase i.e., Optical Density (OD): OD600 ranging from 0.5-0.7 (measured using a Pharmacia LKB Novaspec II spectrophotometer of 325-900 nm Wave length Range); they were then harvested by centrifuging at 8000g for 10 minutes to achieve the final concentration of approximately 1×10^8 cfu/mL (optical density 3.3); a second concentration of 1×10^7 cfu/mL was obtained by dilution with sterile sodium chloride solution (9-g/L NaCl).

Different bacterial strains took different time periods to reach to the final required optical density of 1×10^8 cfu/mL. For this purpose, the rate of growth for each bacterial strain was recorded against time (see figure 4.1), and then growth controlling factors such as temperature of incubation were adjusted accordingly to quickly and effectively obtain the required growth OD. As it would be difficult to achieve bacterial concentrations higher than 1×10^8 cfu/mL at 37°C within a practical growth time (7-10 days), the maximum concentration for the bacterial growth was fixed at 1×10^8 cfu/mL.

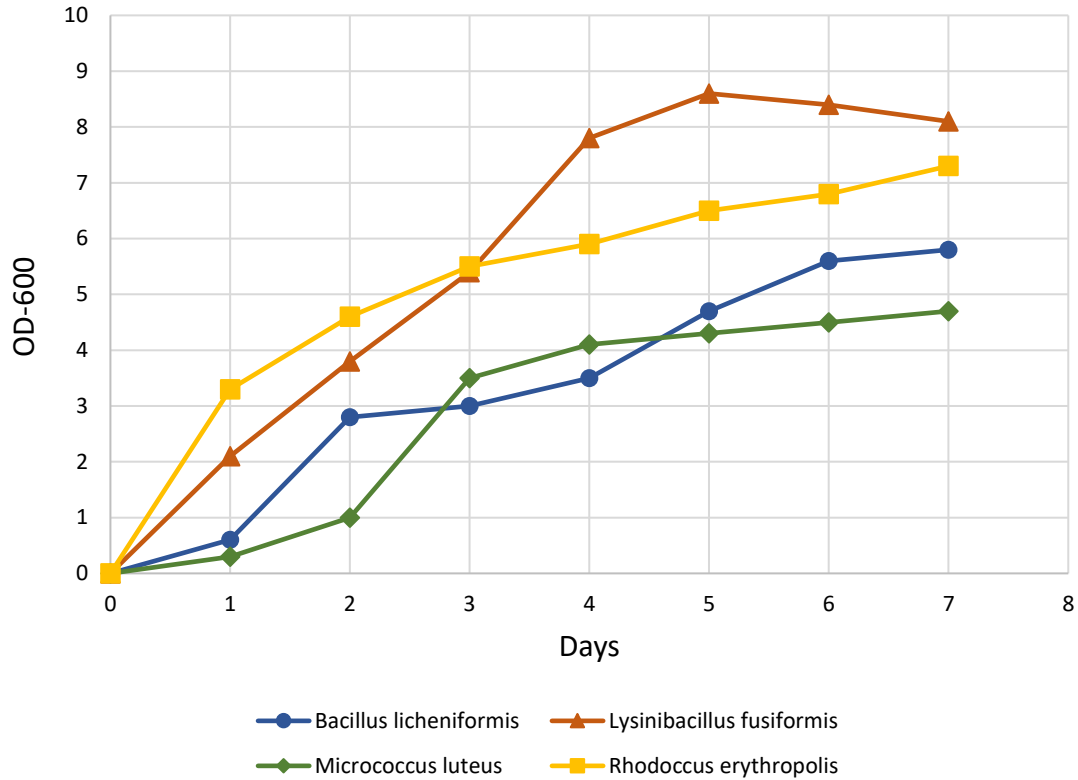


Figure 4.1 Rate of growth of bacteria cells against time at 37°C

Moreover, the growth constants for all the bacterial strains were determined using the Monod microbial kinetic model. The Monod kinetic model describes the specific growth rate (μ) as a function of substrate concentration (S). The "Batch" system with initially a known growth substrate concentration (S) was repeated by varying initial substrate concentration (S) over a wide range of values resulting in observation of individual (μ) values which correspond to each substrate concentration. The arithmetic plots of (μ) vs (S) were generated to exhibit the general growth behaviour and the specific growth rate constants were determined by using the equation 4.1.

$$\mu = \mu_{max} \left(\frac{S}{S+K_s} \right) \quad (4.1)$$

Where, μ_{max} is the maximum specific growth rate observed and K_s is the substrate concentration corresponding to $1/2 \mu_{max}$.

The calculated growth constants of the bacterial strains along with other parameters are given below in table 4.1.

Table 4.1 Calculated Growth Constants as per Monod microbial kinetic model

	μ_{\max} (1/h)	$1/2 \mu_{\max}$ (1/h)	S (g/L)	K_s (g/L)	μ (1/h)
<i>Bacillus licheniformis</i>	0.0043	0.00215	0.50	0.15	0.003308
<i>Micrococcus luteus</i>	0.0038	0.0019	0.52	0.155	0.002927
<i>Rhodococcus erythropolis</i>	0.0085	0.00425	0.55	0.125	0.006926
<i>Lysinibacillus fusiformis</i>	0.0103	0.00515	0.6	0.181	0.007913

The figure 4.1 indicates that the growth rate for each bacterial strain is different. *Lysinibacillus fusiformis* showed the maximum growth after day 5 and the death phase for *Lysinibacillus fusiformis* starts immediately after attaining the maximum growth without going into the stationary phase. The highest growth rate for *Lysinibacillus fusiformis* is also indicated by the calculated (μ) values. *Rhodococcus erythropolis* showed a continuous and constant growth with the (μ) slightly lower as compared to *Lysinibacillus fusiformis*. *Bacillus licheniformis* showed an intermediate stationary phase after first 48 hours however after 96 hours a continuous growth was observed. *Micrococcus luteus* exhibited the least growth against time and also the lowest growth constant (μ), however *Micrococcus luteus* also exhibited the longest stationary phase on the growth curve.

The arithmetic plots of (μ) vs (S) for each bacterial strain are given in Appendix E.

4.1.2 Urease Activity and Urea Hydrolysis

The urease activity of the microorganisms during the incubation period in crude enzyme solution was determined. It was observed that the extracellular enzyme activity of the bacterial strains increased with the increase in incubation time, as rate of urea hydrolysis is a direct function of the bacterial cell population (see figure 4.2). At high cell concentration the bacteria produce more urease per unit volume for the urea hydrolysis (Ng et al., 2012).

- For the *Bacillus licheniformis*, and *Lysinibacillus fusiformis*. the maximum Urease activity was recorded at 72h despite the fact that cell population for both these strains continue to increase well after first 72 hours. However, the urease activity for these strains did not drop after first 72 hours, but was maintained around the maximum value but with some fluctuations.
- In the case of *Micrococcus luteus*. and *Rhodococcus erythropolis*. the urease activity kept on increasing with incubation duration. *Rhodococcus erythropolis*. showed the lowest enzyme activity which also reflects in the lower urea hydrolysis and resultant lower CaCO₃ production (see figure 4.4 and relevant discussion on results).
- In this study, it was assumed that the rate of urea hydrolysis is in proportion to the urease activity, however, the exact determination can be made by measuring the residual (remaining) urea in the enzyme solution; this is an area which can be further investigated.

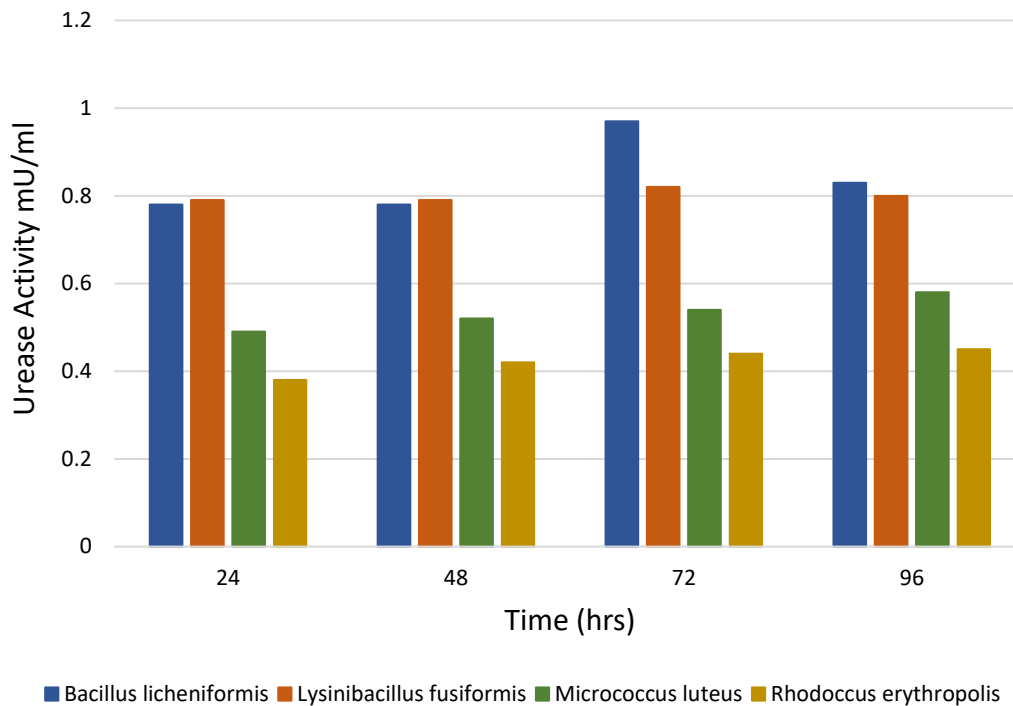


Figure 4.2 Urease activity of microorganism at different time

4.2 UCS Results and Chemical Analysis

A comparative analysis of the UCS results is provided in Figure 4.3, which contains the results of 24 pressure flow column experiment sets (including four control and one untreated control), and four sets of Mixing experiments. Three samples were treated for each individual experimental set; average UCS values (with error bars showing maximum and minimum values) are shown.

To interpret the UCS results, other relevant parameters are also plotted. Figure 4.4 presents the CaCO_3 % along with the resultant ammonia concentration. The CaCO_3 %, based on the acid digestion testing (section 3.7.1) directly correlates to the UCS strength while ammonia concentrations are linked to the process of urea hydrolysis reactions (equations 2.12-2.17), and must be monitored as they are an undesirable reaction product. Water content of the samples at the end of testing and resultant pH is presented in Figure 4.5. The pH evolution is also a function of urea hydrolysis and an indicator of microbial activity and calcite precipitation.

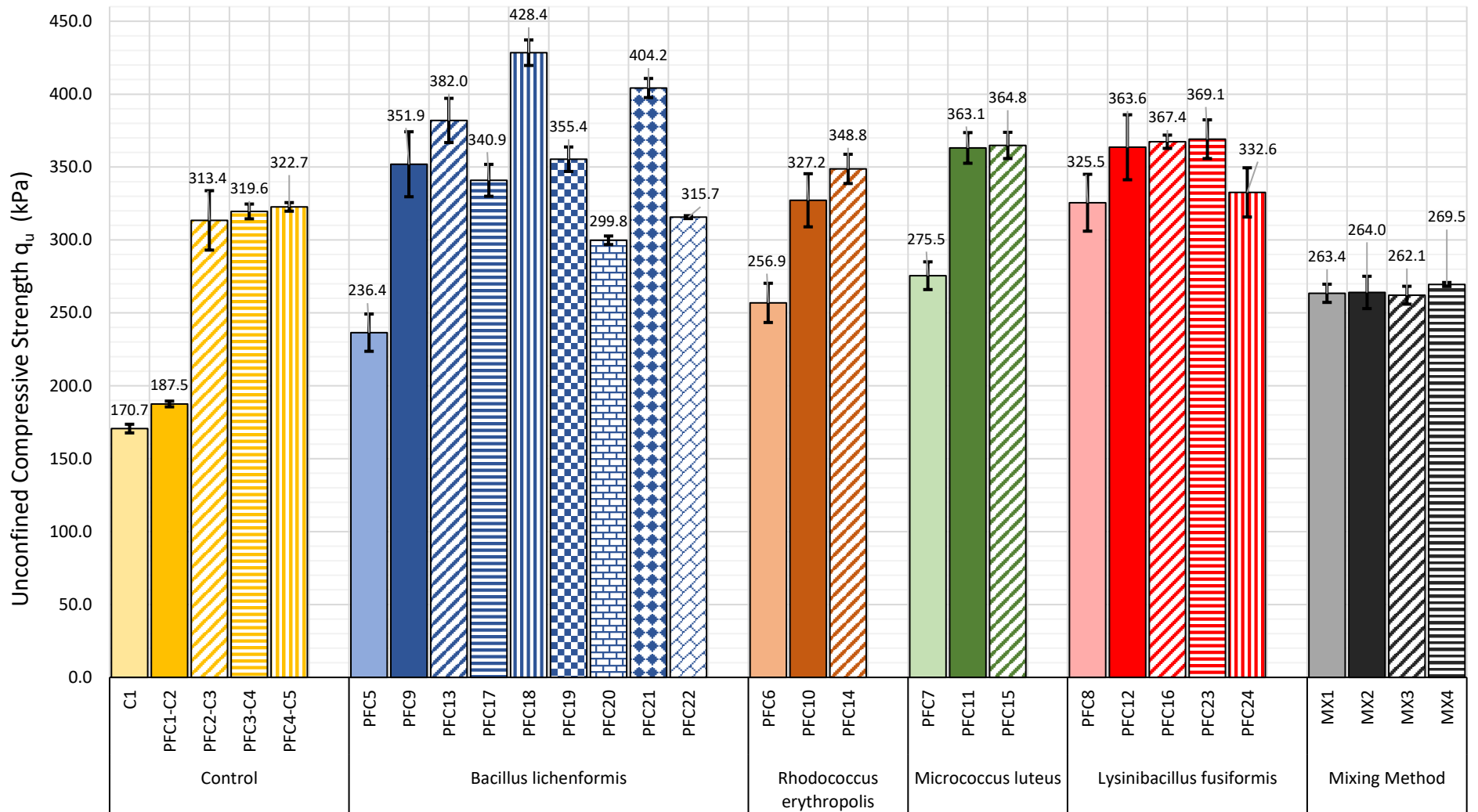
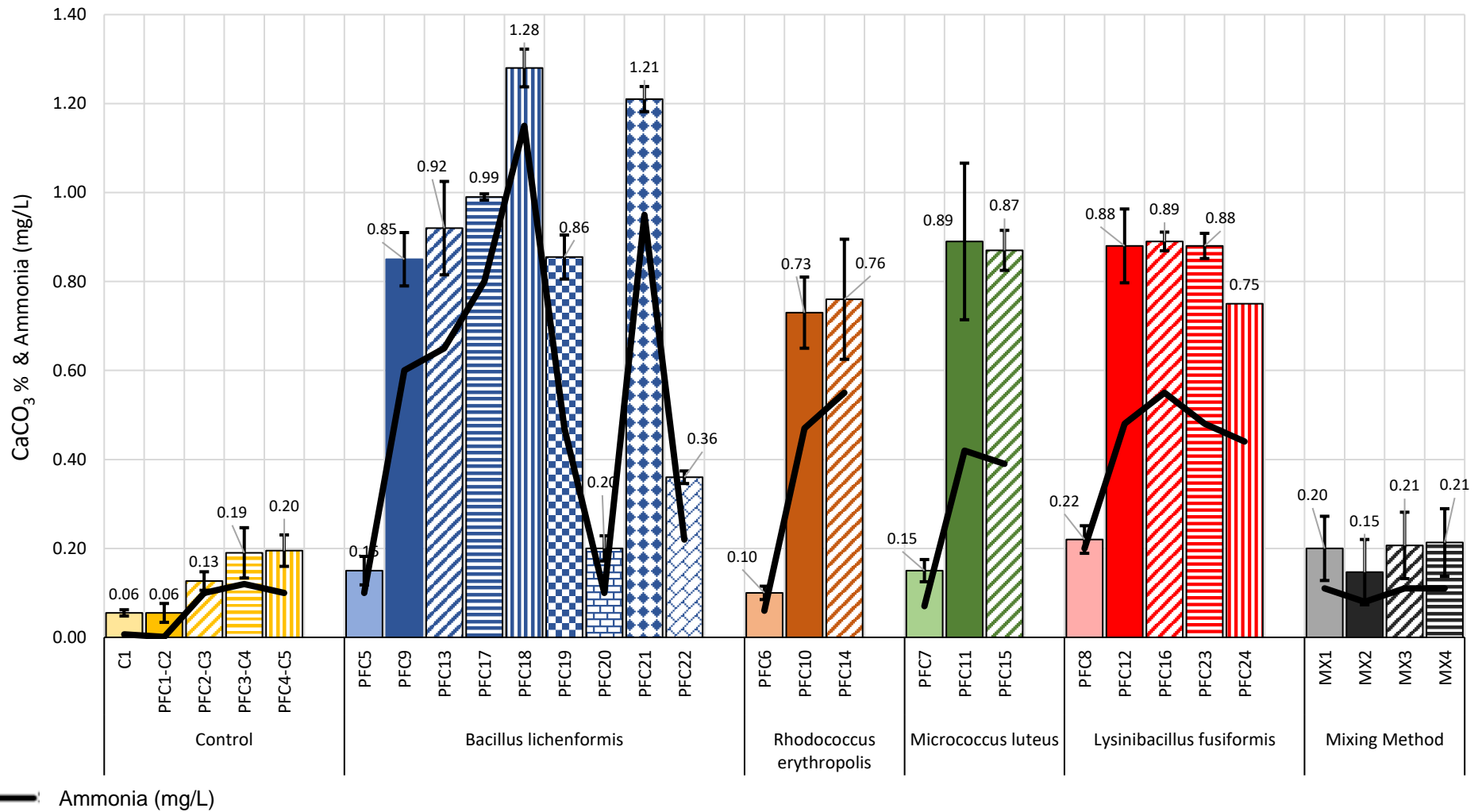


Figure 4.3 UCS strength comparison for Flow Column (PFC5-PFC24), Control (C1-C5) and Mixing method (MX1-MX4) experiments



The NH₄⁺ concentration of the treated soil samples was determined by the method described in sections 3.7.2.2 - 3.7.2.4.

Figure 4.4 CaCO₃ % along with the resultant ammonia concentration for Flow Column (PFC5-PFC24), Control (C1-C5) and Mixing method (MX1-MX4) experiments

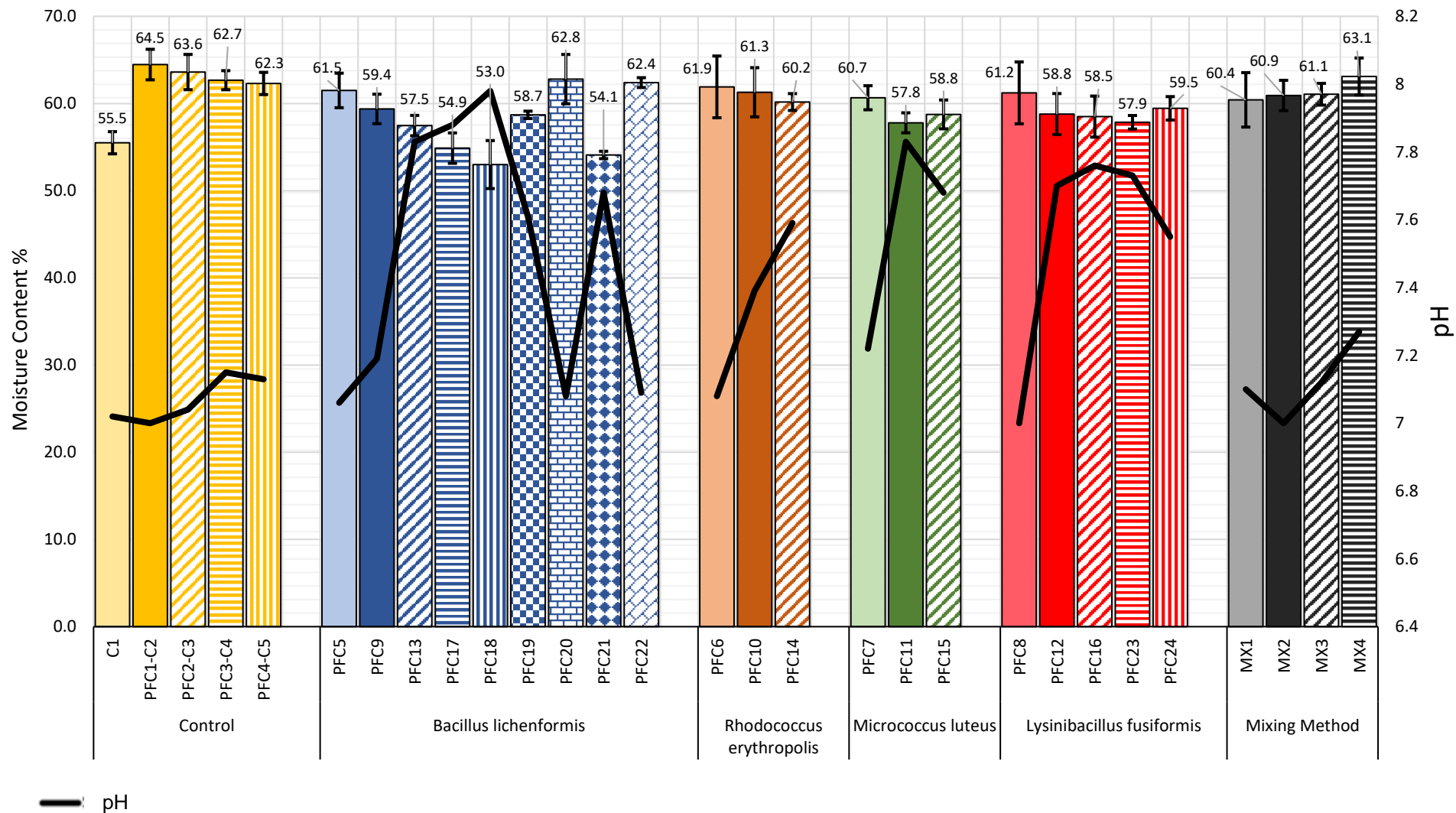


Figure 4.5 Moisture Content % along with the end test pH for Flow column (PFC5-PFC24), Control (C1-C5) and Mixing method (MX1-MX4) Experiments

4.2.1 Main Observations

The main observations in the strength change behaviour can be summarised as follows:

- A small strength increase (by 8%) was noted with the added water flowing out of the sample (PFC1-C2) compared to the natural sample, which is possibly due to some density increase/ consolidation effect.
- Strength gains for the nutrient only samples (PFC2-C3) are therefore compared to the water under pressure samples (PFC1-C2) and were found to be 67.1% higher than that of the water flushing of the samples although the moisture contents of the two specimens were very close (around 64%). This is possibly due to broth composition (salts, of which NaCl, have been used for soil stabilisation by ionic charge manipulation and as a group tend to flocculate soil particles and affect the strength, see e.g. Brandon et al 2009).
- In the Bio-stimulation control experiments (PFC3-C4) and (PFC4-C5), where Cementation reagents were also added along with the nutrient, the maximum increase in strength was recorded to be 72.1% higher than that of control (PFC1-C2). Therefore, the solution of cementation reagent and nutrient broth had some effect on the strength of the soil (and generate a small amount of calcite as well) potentially due to some small biostimulation effects due to the added nutrients and/or reactions with chemical substances in the natural soil (chemical characterisation of the sample is required to elucidate this).
- Despite of all the same treatment variables for these two experimental sets, (PFC4-C5) provided slightly better strength compared to (PFC3-C4), which could be due to the shorter curing period. Al-Qabany & Soga, (2013), mentioned the phenomenon that long curing in the anaerobic conditions (wrapped in protective film) can cause a reverse action (dissolution of precipitated crystals). A similar trend was observed in results of (PFC9 & PFC19) and (PFC12 & PFC23) where longer curing periods have caused a slight drop (by 1.5%) in UCS strength.
- On the other hand, for Batch 1 (PFC5-PFC8), the addition of bacteria in the nutrient broth (without cementing reagents) appears to cause a drop in the strength of the samples in most cases but one. In Batch 1 the lower water

content compared to control (PFC1-C2) might have caused a certain strength gain. On the other hand, it could be due to the fact that the addition of nutrients, caused an increase in organic biomass in the soil. As external added bacteria could perhaps produce a competing effect in consuming substances in the natural soil without the addition of cementing agents.

All treatment solutions with bacteria and cementing reagents (Batch 2-6) increased strength compared to the nutrient broth only;

- Samples inoculated with *Bacillus licheniformis* (PFC18, PFC 21 and PFC13), had the highest strength gain followed by samples inoculated respectively with *Lysinibacillus fusiformis* and *Micrococcus luteus* (solutions of 0.5 M) (all statistically significant at a 95% confidence level (p-value < 0.05, based on t-test results in Table 5.1).

4.2.2 Effect of Cementation Reagent Concentration on UCS strength

- For all these strains solutions of molarities lower than 1M (except 0.25 M) performed better than the 1M solutions, which is consistent with the literature (e.g. Al-Qabany and Soga, 2013 or Ng et al., 2014 -using different bacteria). The possible explanations for this are the urease activity inhibition at higher CaCl_2 concentrations (Whiffin, 2004) and the faster CaCO_3 precipitation in higher concentration solutions causing random, non-homogeneous crystal distribution, unlike lower cementation solution concentrations (Mujah et al, 2017).
- The 1M reagent solution samples inoculated with *Micrococcus luteus* (PFC11) and *Lysinibacillus fusiformis* (PFC12) had however higher strengths than the respective 1 M reagent solution samples of *Bacillus licheniformis* (PFC9). It is therefore possible that other optimised treatment composition for each monoculture could have performed better than *Bacillus licheniformis*. However, in this study because of the limited amount of in situ soil *Bacillus licheniformis* was selected for further testing (for reasons explained in section 4.1).
- For all different reagent solution concentrations, *Rhodococcus erythropolis* appeared to perform less well than the other strains, without significant strength increases (based on t-test).

4.2.3 CaCO₃ Content and UCS Strength

The recorded strength increases in the samples were also reflected in terms of CaCO₃ content, which was generally found higher for the higher strength increases as shown in figure 4.4 and figure 4.12; some small anomalies were however noted.

- The highest CaCO₃ contents of an average of 1.28% correspond to an average strength increase of 110 kPa (PCF18: *Bacillus licheniformis* and 0.75 M reagent solution). A general increase in CaCO₃ content with an increase in cementation reagent concentration has been observed, where 0.75 M showed higher % of precipitated CaCO₃ compared to the lower concentrations of 0.25 M and 0.50 M. However, 1.0 M cementation reagent was unable to produce better results compared to 0.75 M that is possibly due to the other limiting treatment variables such as population of bacterial strain used and treatment duration.
- The amount of CaCO₃ precipitation in the organic soil was comparatively less as compared to the sandy soils, for instance van Paassen et al., (2010), reported 3.5% CaCO₃ in sandy soil. This difference can be attributed to soluble organic matter and other organic ligands that are inhibitors to new CaCO₃ crystals precipitation and growth of existing CaCO₃ crystals (Lebron & Suarez, 1998). Researchers have explained this inhibition mechanism in the context of different factors. Lin & Singer (2006), proposed that, when the organic molecules are absorbed onto a mineral surface, depending on the saturation conditions they can either induce dissolution or impair crystal growth. Other researchers have given that the organic matter content prevents CaCO₃ precipitation by coating the existing CaCO₃ crystals surfaces, thus blocking their nucleation sites and preventing homogeneous crystal growth (Lebron & Suarez 1996, 1998).
- The relationship between CaCO₃ content and strength increase is soil dependent. It is therefore difficult to compare with the literature (i.e. mostly on sand biocementation), especially as organic matter can inhibit CaCO₃ precipitation and crystal growth (Lebron & Suarez, 1996 and 1998). Indicatively however it can be mentioned that Duraisamy (2016) recorded unconfined compressive strengths between 120-200 kPa for CaCO₃ contents between 0.8%-1.33% for fine sand.

- Further analysis of the CaCO₃ precipitation is presented in the shape of SEM-EDS images and spectra results (see section 4.7), where SEM pictures confirm the formation of well distributed precipitation products on the soil particles and indicative EDS spectra from targeted sites on the samples show clear Ca and C peaks concurring with CaCO₃ precipitation.

4.2.4 Bacterial Concentration

Two bacterial populations, 1×10^8 cfu/mL and 1×10^7 cfu/mL were used in this study. The increase in bacterial population is directly reflected in the shape of increase in urease activity and vice versa. When keeping the other variable fixed, it can be noted that more bacterial population produced higher UCS and CaCO₃ content for all the strains.

A short comparison of six of the best result producing combinations (based on two bacterial strains *Bacillus licheniformis* and *Lysinibacillus fusiformis*, for both populations and two cementation Reagent concentrations 0.75M and 1.0M) is presented in Figure 4.6.

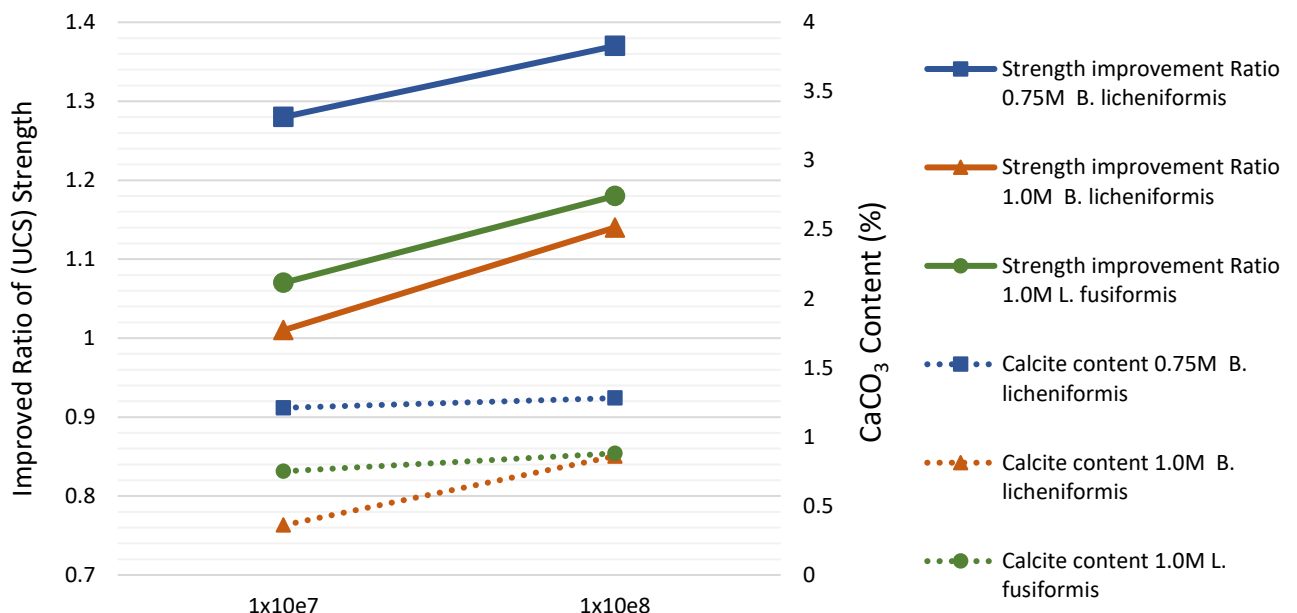


Figure 4.6 Effect of the concentration of Bacterial population of *Bacillus licheniformis* and *Lysinibacillus fusiformis* (1×10^8 cfu/mL and 1×10^7 cfu/mL) and reagent (0.75 and 1.0M) on the UCS strength q_u and CaCO₃ content % of the MICP treated soils

It can be observed that the lower bacterial concentration (of 1×10^7 cfu/mL) is the limiting factor here for the strength improvement and CaCO_3 precipitation. However, 0.75M produced better results overall.

A similar trend was also observed when *Bacillus licheniformis* in both 1×10^8 cfu/mL and 1×10^7 cfu/mL populations was inoculated in much lower (0.25M) concentration of cementation solution i.e. (PFC17) and (PFC20). Here again 1×10^7 cfu/mL population concentration produced 13.7% less strength as compared to 1×10^8 cfu/mL population.

Moreover, the overall strength for this test combination was 25.6% lower compared to the highest gained strength which indicates that the 0.25M concentration of cementation reagent was not optimised for treatment. However, higher or lower the cementing reagent concentration does not necessarily lead to better results in terms of strength and that there is some optimal concentration for the treatment.

4.2.5 Ammonia Concentration

The results of the average final readings of the ammonia measured by the method described in the (3.7.2.2) are presented in Figure 4.4 along-with the CaCO_3 contents %.

- It can be observed that the amount of precipitated CaCO_3 can be linked to the production of ammonia. The increase in urea hydrolysis is directly related to the increase in CaCO_3 % as described in reactions (2.12-2.17), which thereby result in an increase in NH_4^+ concentration.
- However, it is noted that the measured NH_4^+ concentrations exceed the allowable limits of total ammonia (NH_3 and NH_4^+) for drinking water according to UK legislation, set to 0.5 mg/L (The Water Supply (Water Quality) (Amendment) Regulations, 2018). This is also reported by several researchers such as (Keykha et al., 2018; Keykha et al., 2014). Some recommendations to mitigate this undesirable outcome are given in the discussion in Chapter 6.

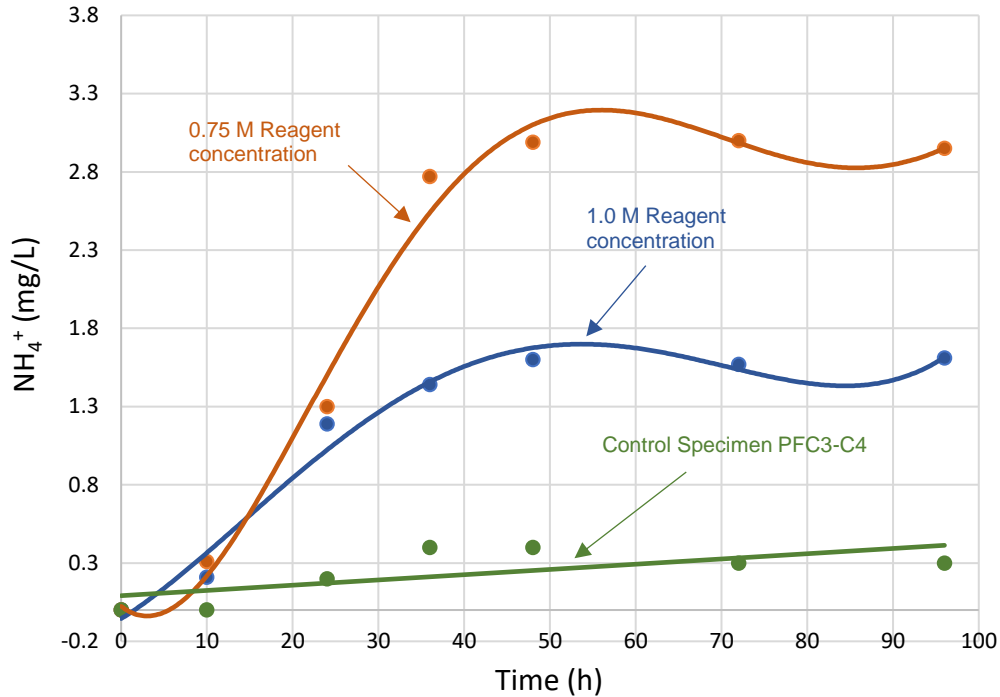


Figure 4.7 Variation of ammonia concentration in effluent overtime with *Bacillus l.*

The graph in Figure 4.7), is for the variation in ammonia generation at different reagent concentrations, calculated as per method described in (3.7.2.1) for the microorganism *Bacillus licheniformis* at concentration 1×10^8 cfu/mL. All treatment sets with different bacterial strains and population count produced the similar results. Here for general representation, plot of only one microorganism is presented.

4.2.6 Moisture Content and pH

The plot of average moisture content and the mean pH for the MICP column experiments is presented above in Figure 4.5.

- As implicated by the chemical equations (2.12-2.17) the increase in soil pH was observed following high carbonate precipitation. However, the final pH changes in soil samples were moderate to high compared to the pH natural sample.
- Samples treated with 1.0 M reagent solution had the highest pH increase and overall the less amount of reaction products compared to the respective 0.75M reagent solution samples.

A similar trend was observed in the pH measurement of the effluent over time. Below is the variation in effluent pH at different reagent concentrations, for the microorganism *Bacillus licheniformis* at concentration 1×10^8 cfu/mL.

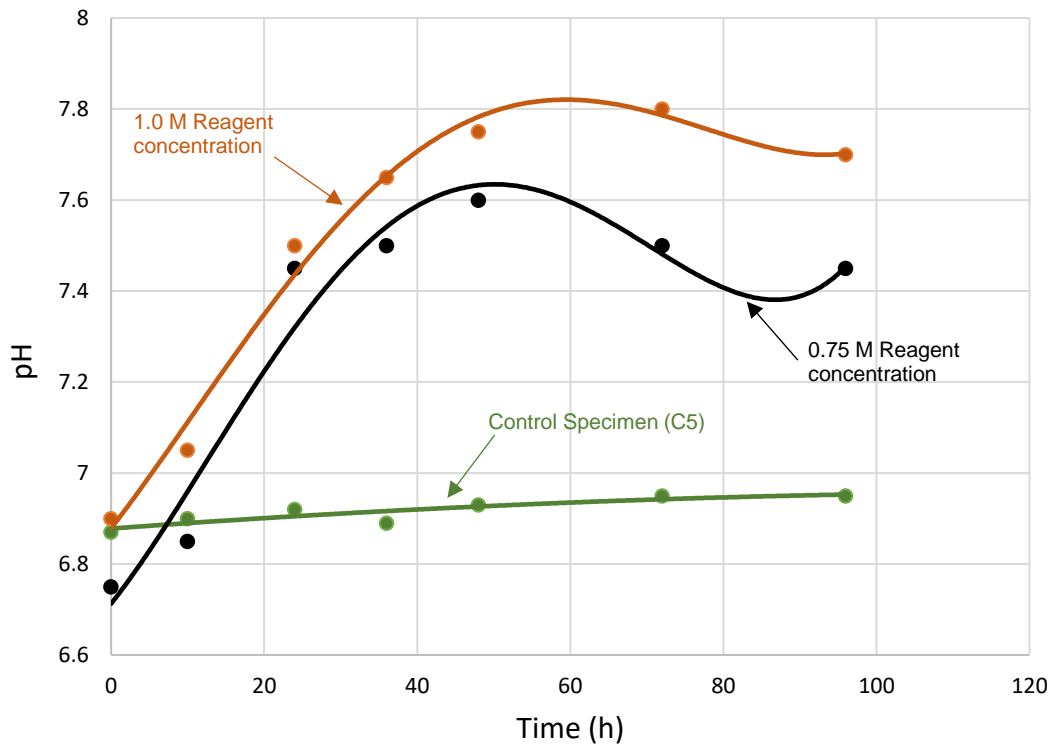


Figure 4.8 Variation of mean pH in effluent overtime with *Bacillus licheniformis*

Moreover, 0.5M reagent concentration showed a lower pH and 0.25M the lowest pH (with some inconsistencies) in both the soil samples and in the effluent but also did not produce high CaCO_3 content and UCS strength.

The effect of moisture content on strength would be small as measured water content variations were overall very small, but a general trend in decrease in moisture content was observed with an increase in CaCO_3 and UCS strength.

When keeping the other variable fixed, it is noted that 0.75M cementation reagent led to higher NH_4^+ concentrations than 1M cementitious reagent solution for *Bacillus licheniformis* (see Figure 4.7). This higher NH_4^+ concentration measurement in the effluent from the treatment shows higher urease activity, and is consistent with the higher strength increase, which is also higher for the 0.75M compared to 1M cementing solution. the lower strength gain for 1M cementitious reagent solution

treatment implies that increasing the cementing reagent concentration does not necessarily lead to better results in terms of strength and that there is some optimal concentration for the treatment. In general, higher reagent concentrations led to lower NH_4^+ concentrations, the lower NH_4^+ concentrations and strength can be attributed to urease activity inhibition at higher CaCl_2 concentrations and was also observed in the literature (e.g. Whiffin, 2004). At the same time, it is also noted that 1M cementation reagent produced higher pH levels compared to 0.75M cementation reagent (see Figure 4.8). The higher pH levels are also attributed to higher concentration of residual CaCl_2 and urea due to lower urease activity.

Though the CaCO_3 precipitation content mainly controls and determines the improvement in UCS strength but the results indicate that for the Pressure flow treatment of the soil it is the combination of all the above described factors that contributes toward the total strength change of the treated soil.

4.2.7 Bio-Stimulation Control Samples (PFC3-C4 & PFCC4-C5)

Bio-stimulation is the process that involves with the modification of soil environment by addition of various electron acceptors and rate limiting nutrients to stimulate the existing bacterial culture capable of biocementation. To check if the existing microbiological substrate is capable to produce the CaCO_3 the experimental soil was bio-stimulated with the standard aqueous solution of 3g/L nutrient broth and equimolar (1:1 M) solution of urea and calcium chloride. Both experimental series were treated for 7 days, but (PFC3-C4) was tested for UCS after 7 days curing while the (PFC4-C5) was cured for only 1 day.

- Neither of these test series showed a considerable increase in the UCS strength (only about 3% increase in strength was observed compared to the control sample, (PFC2-C3).
- This could be due to the fact that in the soil the population of calcite producing capable bacteria was not enough, moreover the concentration of the injected reagent and other variables such as treatment duration and injection frequency could also be the limiting factors which need further research. Dhami et al., (2017), have mentioned that bio-stimulation requires more treatment duration to achieve comparable strengths to that of bio-augmentation.

4.2.8 Mixing Method set (MX1-MX4)

A thorough comparative analysis of the geotechnical properties of all the experimental sets is provided above in Figures 4.3, 4.4 and 4.5. Furthermore, for a better result comparison between injection method and mixing method a plot of best performing experimental sets for each bacterial strain is provided in Figure 4.9 along with the mixing experimental set. In the mixing experimental set, the bacterial solution was mechanically mixed with the soil instead of injection as explained in section (3.5.2).

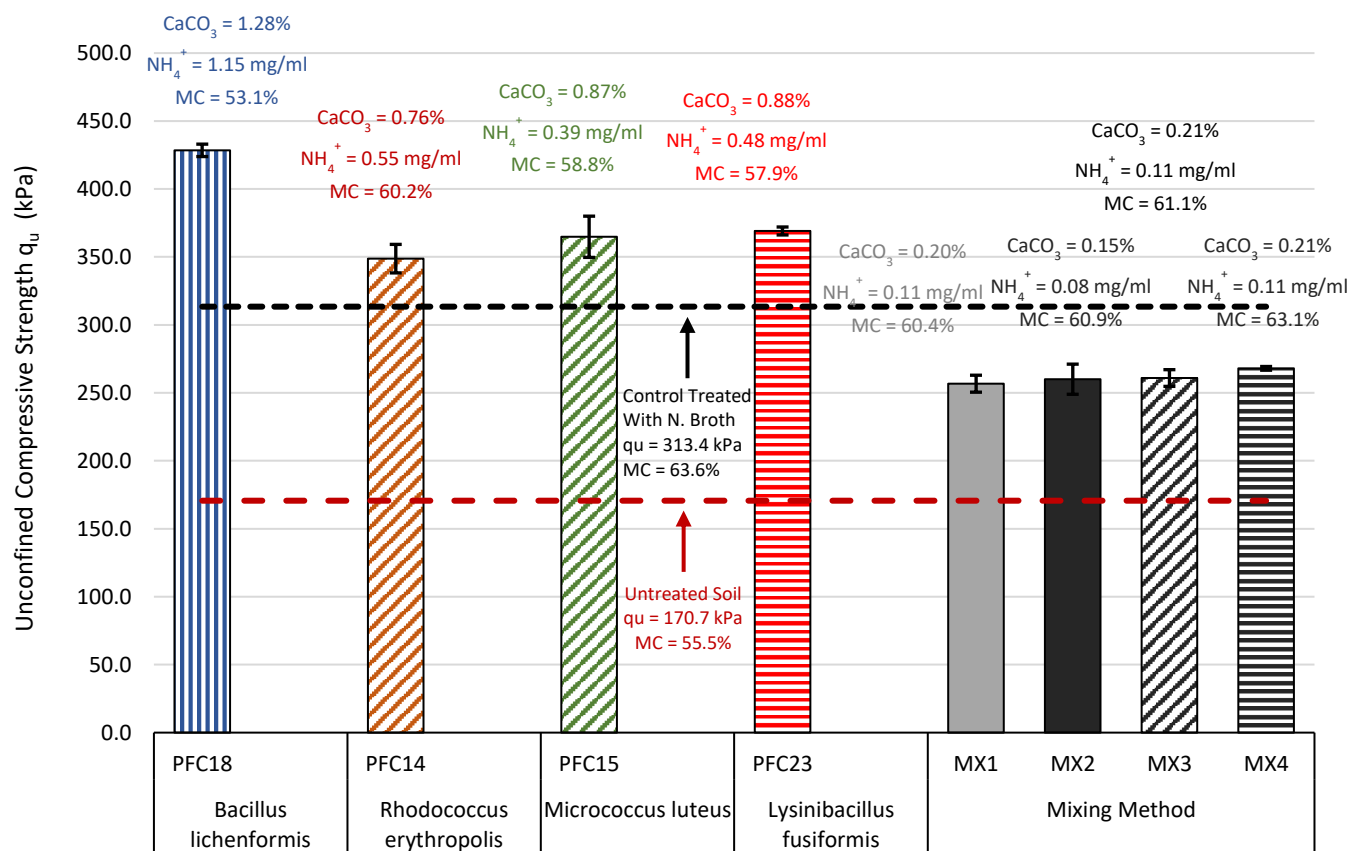


Figure 4.9 Summarised Results for the comparison of injection and mixing methods

- Despite the fact of producing the CaCO₃ precipitation approximately equal to the (PF7 and PFC8) (see Figure 4.4), the mixing method was unable to produce much better results. Although, it showed some degree of improvement approximately 40% compares to untreated soil but still it produced 16.3% and 17.20% less strength as compare to control (PFC2-C3) and (PFC8) respectively (see Figure 4.3),. This is consistent with Yasuhara et al., (2012),

who also reported about 20% less strength while using mixing method as compare to injecting cementation reagents.

- A quite possible reason for the lower strength achievement in the mixing method is breaking of the bonds (formed by the calcite to join soil particle together) during the handling of soil after the treatment. As soil was mixed with bacteria and cementation reagent and after treatment period the UCS samples were made and tested, while in the injection method the UCS ready samples were treated in the plexiglass mould. Moreover, in the tests, the samples were prepared with a very short mellowing period (mellowing is the period between inserting the treatment and the compaction time). Which may have also prevented the further growth of initially precipitated CaCO_3 crystals.
- The effect of moisture content on strength would be small as measured water content variations were small in between injection method and mixing method.

4.3 Stress-Strain Behavior

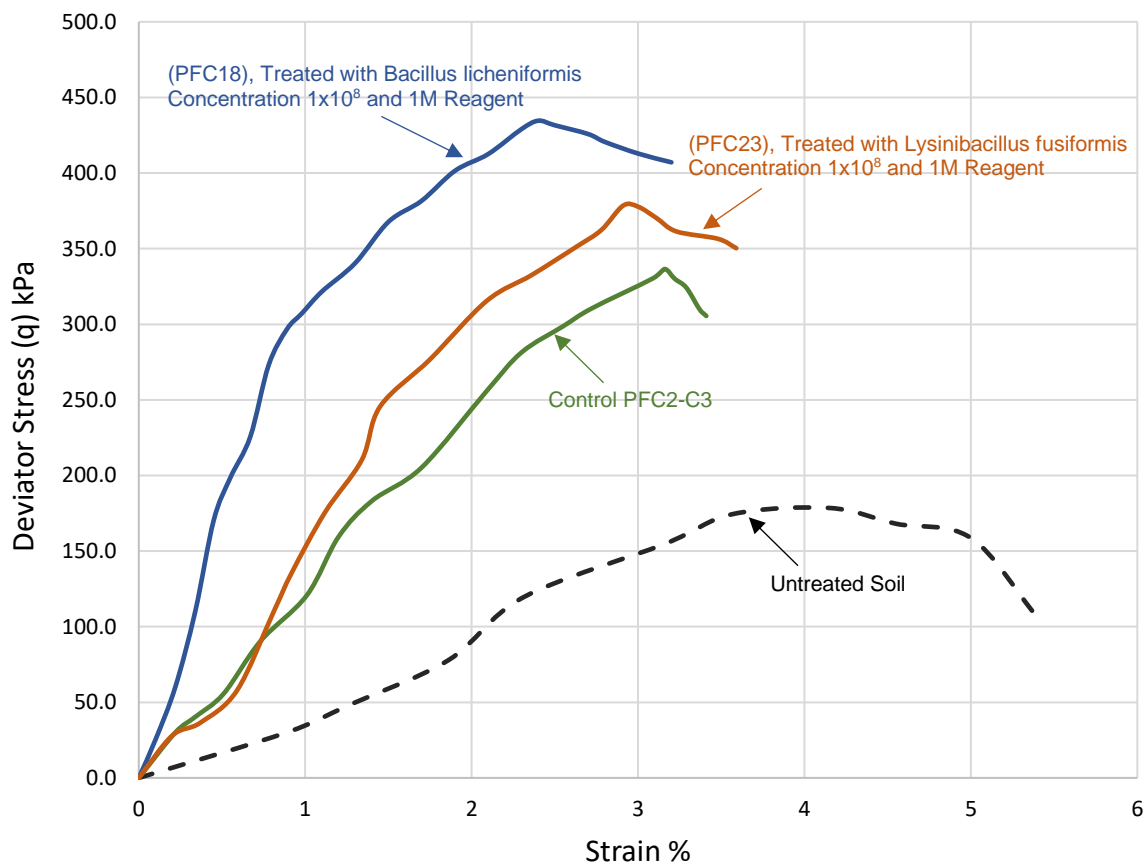


Figure 4.10 Stress-strain behaviour of indicative treated, untreated and control samples

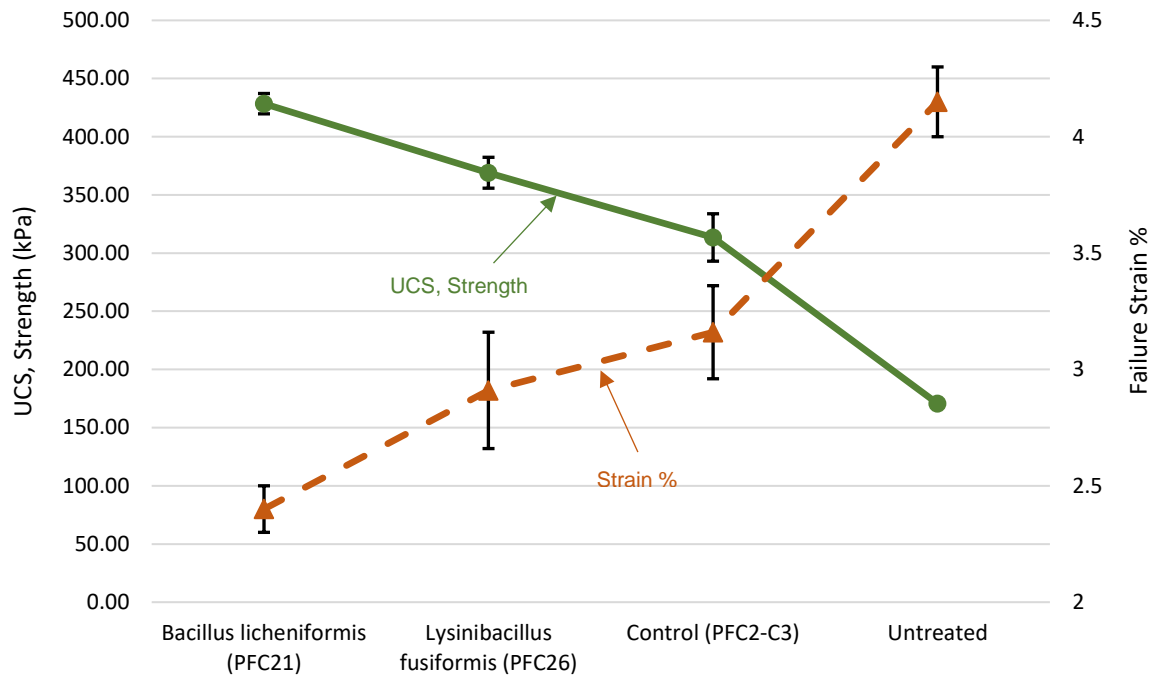


Figure 4.11 Comparison of overall, stress-strain evolution

The stress vs strain behaviour of untreated soil, control sample (PFC2-C3) and two best result producing experimental set (PFC18, for *Bacillus licheniformis*) and (PFC23, for *Lysinibacillus fusiformis*) at 1M concentration of cementation reagent is presented in figure 4.9.

- It can be observed that the untreated soil showed the maximum UCS strength (178.5 kPa) at a strain of approximately 4.15%, and exhibited a ductile behaviour.
- Results indicates that the application of Pressure column flow treatment increased the ascending slope of the stress-strain curve. The failure strain for all the treated samples decreased considerably, about (3.0 for PFC23, and 2.5 for PFC18). The area under the curve increased for the treated samples and much more brittleness was observed as compared to untreated soil.
- The overall progression of the stress-strain behaviour is shown in figure 4.10. it can be seen that an increase in the UCS strength have an opposite effect on the failure strain %, which is also an indication of brittle behaviour of the high CaCO_3 content samples. However, some samples showed some post peak strength that may be associated to the overall distribution of the CaCO_3 across the samples.

4.4 Distribution of CaCO₃ Precipitation across Samples

The homogeneous distribution of the precipitated CaCO₃ in the treated samples is considered as a function of evenly distribution of carbonate-producing bacteria in the soil. CaCO₃ inducing bacterial solutions used in the soil stabilisation have much lower viscosity and can flow like water but on the basis of the size of bacteria, they are not expected to pass through the soil pores having throat size less than 0.4µm, which can cause a major problem evenly distribution of bacteria especially in fine grained soils. Several researchers (Al Qabany, Soga & Santamarina 2012; Harkes et al., 2010; Whiffin, van Paassen & Harkes 2007) have reported that uniform distribution of microorganisms and the resulting nonhomogeneous distribution of CaCO₃ crystals and bioclogging remains a challenge.

In this research the uniform distribution of the treatment (which would imply a uniform distribution of bacteria) was checked by measuring the CaCO₃ distribution in the treated samples at three different height locations (i.e. top, middle and bottom), and results are plotted below in figure 4.11.

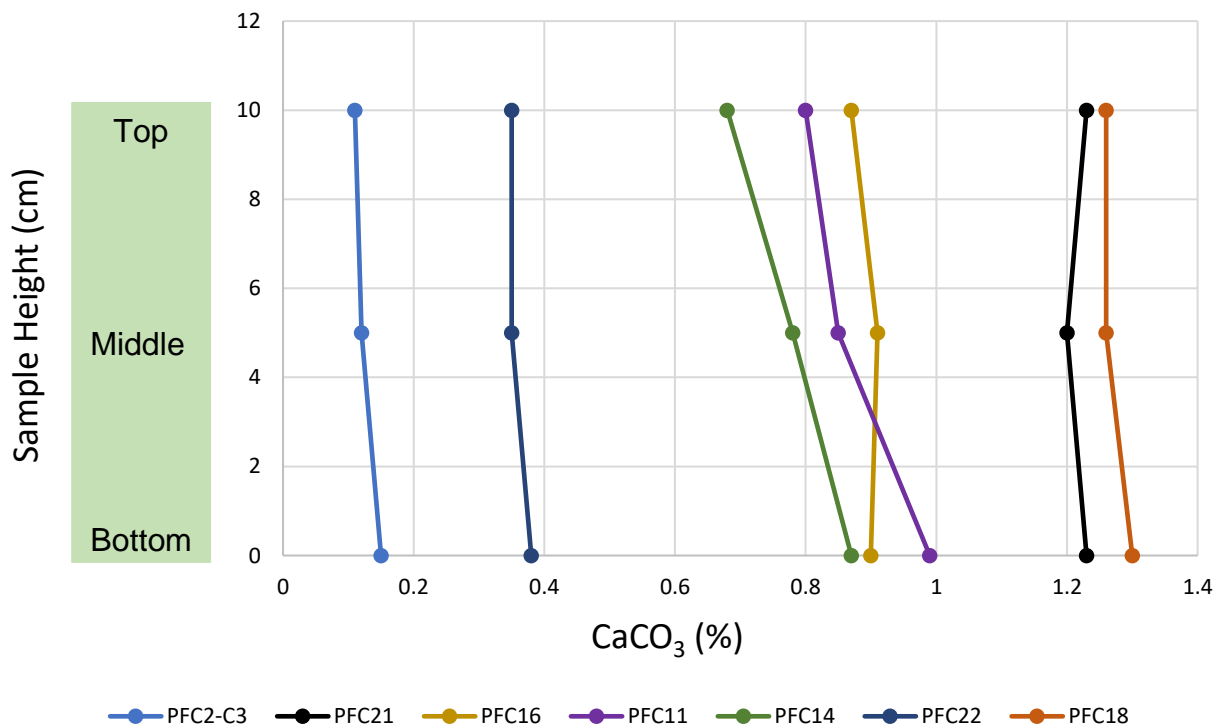


Figure 4.12 CaCO₃ % distribution along the treated samples height

- From the above plot it can be seen that almost all the experimental series produced a uniformly distributed CaCO_3 along the height of the samples. which indicates that the provision of two layers of perforated disks and filter papers performed well in uniformly distributing the bacteria solutions by avoiding turbulent inflow and clogging at the inlet and outlet.
- However, a slightly increasing trend in the CaCO_3 % has been observed in the bottom parts of the samples as compare to top, that could possibly due to the pressure of 150 kPa which may have caused the migration of more bacteria population toward the bottom layers. The variation in flow pressure can produce different quantity of the precipitated calcite and the soil strength (Ng et al., 2014), but to reduce the number of variables in this research the pressure was kept constant for all the MICP experiments. This is another aspect which requires further research.

4.5 Summary of Changes in UCS Strength of Treated Samples

A comparative summary of average UCS strength for each experimental group in terms of (%) strength change as compared to control sample treated with nutrients only (PFC2-C3) (average $q_u = 313.43$ kPa) is given below in Table 4.2, and a plot of strength changes is provided below in figure 4.12. The p-values refer to results of paired t-test for the comparison of the average q_u values of MICP pressure flow column experiments dataset with the control (PFC2-C3) dataset (all statistically significant at 95% confidence level, values are mean \pm SD at (n=3) and p-value<0.05). The evaluation of the results indicates that the Cementation Reagent molarities lower than 1M (except 0.25 M) performed better than the 1M solutions. The samples inoculated with inoculated with *Bacillus licheniformis* and with 0.75M Reagent concentration produced highest improvement in UCS strength compared to the PFC2-C3.

Table 4.2 Summary of UCS strength change

Strain	Bioaugmentation (PFC5-8)	Bioaugmentation + 0.25M reagents (PFC17 & PFC20)	Bioaugmentation + 0.50M reagents (PFC13-16)	Bioaugmentation + 0.75M reagents (PFC18 & PFC21)	Bioaugmentation + 1.0M reagents (PFC9-12), (PFC19) & (PFC22-24)
<i>Bacillus licheniformis</i>	q _u = 236.43 kPa Δ q _u = -24.59 % p-value = 0.00854	q _u = 340.92 kPa Δ q _u = 8.78 % p-value = 0.0278	q _u = 381.97 kPa Δ q _u = 21.9 % p-value = 0.0118	q _u = 428.43 kPa Δ q _u = 36.69 % p-value = 0.00415	q _u = 351.93 kPa Δ q _u = 12.28 % p-value = 0.09014
		q _u = 299.81 kPa Δ q _u = -4.34 % p-value = 0.0457		q _u = 404.20 kPa Δ q _u = 29.0 % p-value = 0.0375	q _u = 355.39 kPa Δ q _u = 13.39 % p-value = 0.0926
					q _u = 315.67 kPa Δ q _u = 0.71 % p-value = 0.0497
<i>Rhodococcus erythropolis</i>	q _u = 256.85 kPa Δ q _u = -17.9 % p-value = 0.0216	-	q _u = 348.75 kPa Δ q _u = 11.27 % p-value = 0.0547	-	q _u = 327.21 kPa Δ q _u = 4.40 % p-value = 0.0430
<i>Micrococcus luteus</i>	q _u = 275.49 kPa Δ q _u = -12.1 % p-value = 0.0593	-	q _u = 364.79 kPa Δ q _u = 16.5 % p-value = 0.0253	-	q _u = 363.12 kPa Δ q _u = 15.85 % p-value = 0.0367
<i>Lysinibacillus fusiformis</i>	q _u = 325.53 kPa Δ q _u = +3.86 % p-value = 0.0488	-	q _u = 367.37 kPa Δ q _u = 17.21 % p-value = 0.0391	-	q _u = 363.57 kPa Δ q _u = 15.99 % p-value = 0.0482
					q _u = 369.06 kPa Δ q _u = 17.78 % p-value = 0.05071
					q _u = 332.62 kPa Δ q _u = 6.12 % p-value = 0.0721

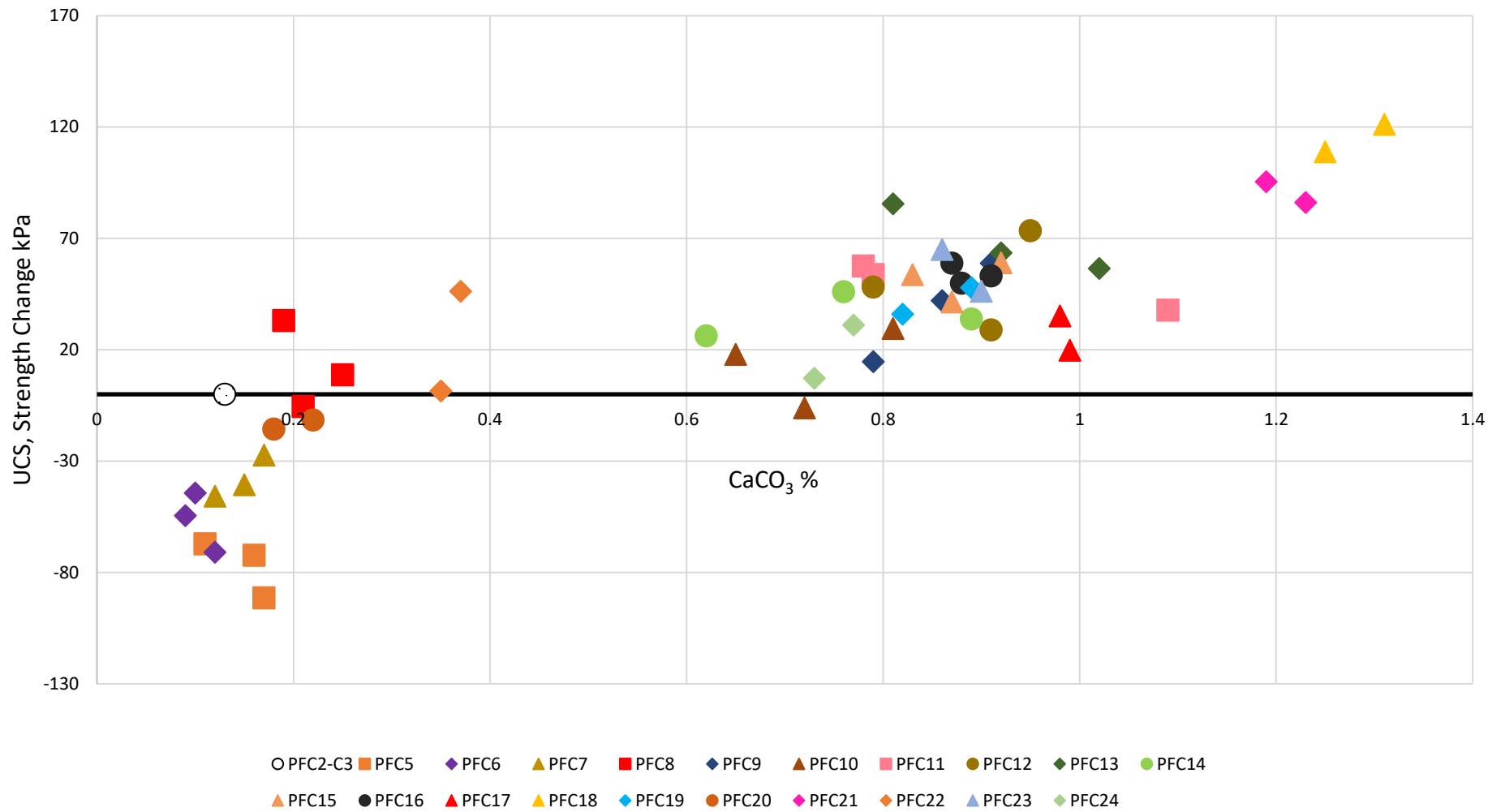


Figure 4.13 UCS, Strength change comparison compared to control (PFC2-C3)

4.6 Effect of MICP Colum Flow Pressure Treatment on Soil Compressibility and Consolidation Characteristics

The compressibility and consolidation behaviour of the treated and untreated soil was studied by undertaking conventional oedometer consolidation tests. For this purpose, two oedometer samples were cut out of the treated soil sample with (1×10^8 cfu/mL *Bacillus licheniformis* with cementing reagent solution of 1M), from the pressure flow column experiment. One sample was tested in the saturated condition, and other was in unsaturated condition. Moreover, consolidation testing of the untreated saturated soil sample was performed.

4.6.1 Sample Preparation

Because of the respective dimensions of the pressure flow column sample and the oedometer ring, it was not possible to obtain intact samples of the pressure flow column soil. For this reason, the samples from the treated soil was prepared by cutting the soil from the treated UCS size sample, and the oedometer consolidation ring was filled loosely with the chunks of the treated soil and the big visible voids were filled by hand without using any compression frame and excessive pressure to avoid further sample disturbance as much as possible.

For the untreated soil, the oedometer samples were prepared by statically compacting the soil in the oedometer ring at a rate of 1mm/min to the original field dry density of 0.919 g/cm^3 . Samples were wrapped in the cling film and were stored for 24 hours before starting the consolidation test.

The two saturated specimens (one treated and one untreated) were left to swell (free swelling) in the oedometer cell that was filled with water until no further height change was recorded; this was followed by compression at a stepwise increasing applied pressure of 25-400 kPa, which was followed by unloading; conversely the unsaturated treated specimen was subjected to compression and unloading without initial saturation/swelling stage. The consolidation pressure was applied in 5 stages (25, 50, 100, 200 and 400 kPa), and unloading in two stages (200, and 50 kPa).

The compression results of samples at these loading and unloading pressures in the shape of void ratio versus \log_{10} pressure curves is presented below in figure 4.13.

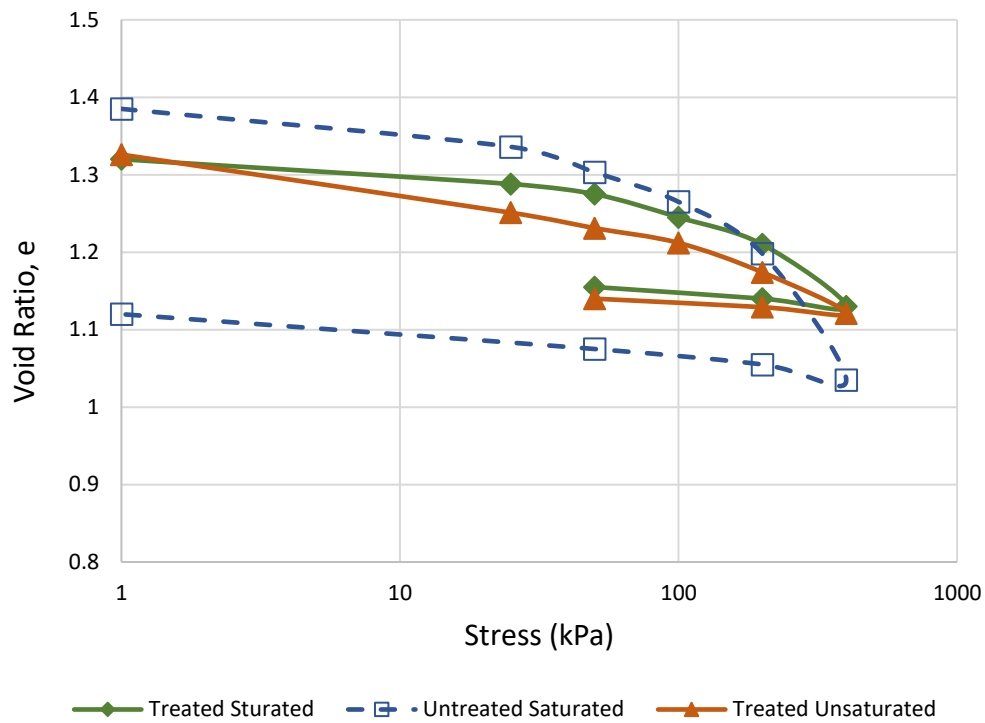


Figure 4.14 Oedometer test results (Void ratio vs Pressure)

- The curves show a clear difference in the compressibility behaviour between the untreated soil and the treated samples, which suggests that the MICP treatment used in this research changed the void ratio for the treated samples which was less as compare to untreated soil.
- Less swelling was observed in the saturated treated specimen as compare to saturated untreated specimen, which also indicates the positive effect of the treatment.
- A considerable reduction in the compressibility of the treated soil has been observed, but the MICP stabilisation treatment was not able to eliminate the compressibility of organic soil completely.
- The gradient of the treated saturated and unsaturated samples indicates that the specimens reaches their first consolidation yield point beyond the stage of applied stress of 50 kPa, which is possibly due to brakeage of bonds between the soil grains and the precipitated calcite crystals.

- However, after this stress level, the specimens still predominantly showed an elastic behaviour, the likely reason for this is the presence of solid calcite crystal particles that filled the soil voids, and which continue to take more stress with very little deformation until next loading stage of 100 kPa, that appears to be the second consolidation yield stress.
- Furthermore, the untreated soil showed an abrupt consolidation stress behaviour between the loading stage of 200 kPa to 400 kPa, which indicates the fact that another higher consolidation stress should be applied in the oedometer testing to vividly display the compressibility behaviour. Hence, this issue has been addressed in the oedometer testing of the Electrokinetic-Biocementation treated samples (see section 5.8).

4.6.2 Coefficient of Compressibility

The changes in the Soils' coefficient of compressibility (m_v) under the different applied stresses for consolidation is given as:

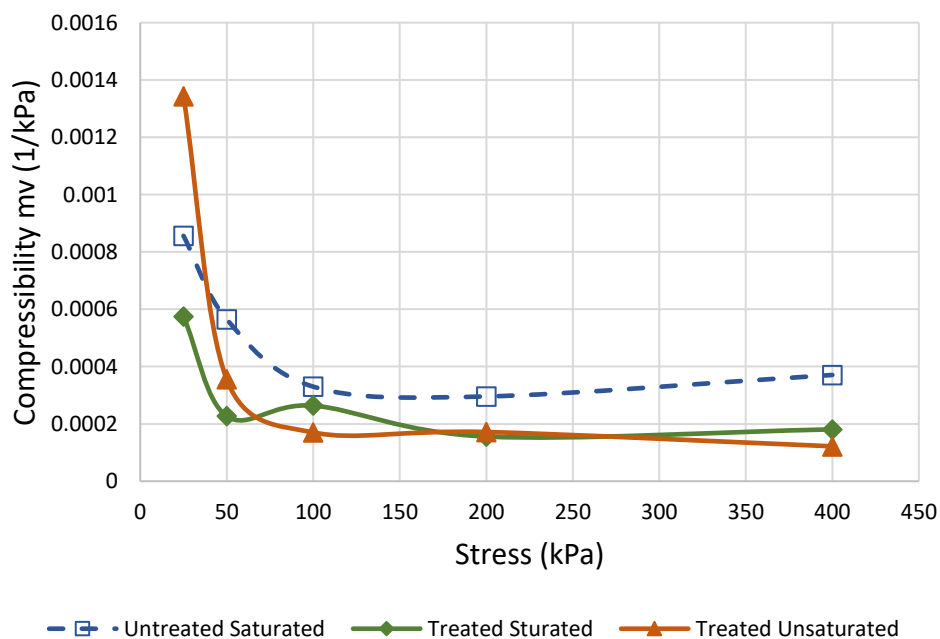


Figure 4.15 Coefficient of volume compressibility (m_v) vs Pressure

- The values of the (m_v) at the initial consolidation stages for the untreated soil were higher compare to the saturated treated specimens, which indicates the reduction in void ratio due to the cementation precipitation.

- However, at higher applied consolidation stresses, the (m_v) values for treated and untreated specimens became approximately the same. The SWRC analysis was conducted on some samples and a comparison with untreated and Electrokinetic-Biocementation treated samples was provided in the next chapter (section 5.9). Moreover, the microstructural analysis of some samples in the form of SEM-EDS images is also provided in the section 4.7 and Appendix F.

4.6.3 Coefficient of Consolidation and Secondary Compression

The coefficient of consolidation (C_v) for the Pressure flow column treated and untreated soil specimens were plotted by three graphical methods, namely Taylor Square root of time fitting method, Casagrande log t method and Parabolic isochrone method. A comparative result of the (C_v) values for the untreated and treated samples and is given below in Table 4.3 and 4.4 respectively. the values for Index of secondary compression are given in %.

Table 4.3 Coefficient of consolidation, and Coefficient of secondary compression for untreated soil under different applied pressures

Untreated Soil				
Applied Pressure Interval (kPa)	C_v ($m^2/year$)			Secondary compression Ca (%)
	Taylor sqrt	Log t	Parabolic isochrone	
0-25	10.87	3.36	1.66	0.13
25-50	0.526	0.47	0.36	0.12
50-100	10.34	4.14	0.78	0.39
100-200	4.37	0.089	0.53	0.29
200-400	2.01	3.22	0.97	0.49
400-800	2.49	2.42	1.32	0.18

Table 4.4 Coefficient of consolidation, and Coefficient of secondary compression for Pressure Flow Column treated soil (PFC-18) under different applied pressures

Pressure Flow Column (PFC-18)				
Applied Pressure Interval (kPa)	MICP C_v ($m^2/year$)			Secondary compression C_a (%)
	Taylor sqrt	Log t	Parabolic isochrone	
0-25	4.07	1.12	1.35	0.09
25-50	3.87	0.44	0.29	0.07
50-100	6.91	0.87	0.78	0.11
100-200	4.04	0.093	0.33	0.30
200-400	2.86	0.24	0.45	0.74
400-800	3.09	0.52	0.91	0.86

It can be observed that at the same stress level, the treated specimen showed lower values for (C_v) compared to untreated soil. This indicates that the MICP pressure flow column treatment caused a reduction in primary consolidation. However, some loading stages showed small anomalies, and displayed very less secondary compression. This may be subjected to some uncertainties in the consolidation data interpretation (i.e. the determination of exact time for the end of primary consolidation, or the incorrect analysis of the linear part of the square-root time curve where it is not well defined).

4.7 SEM-EDS Results

To support further the findings of the UCS and the acid digestion results, and to assess the morphology of the reaction products (in particular $CaCO_3$) scanning electron microscope (SEM) and energy dispersed spectrum (EDS) analyses were performed on selected samples. Below are some SEM images with description. While more SEM-EDS images are provided in Appendix F.

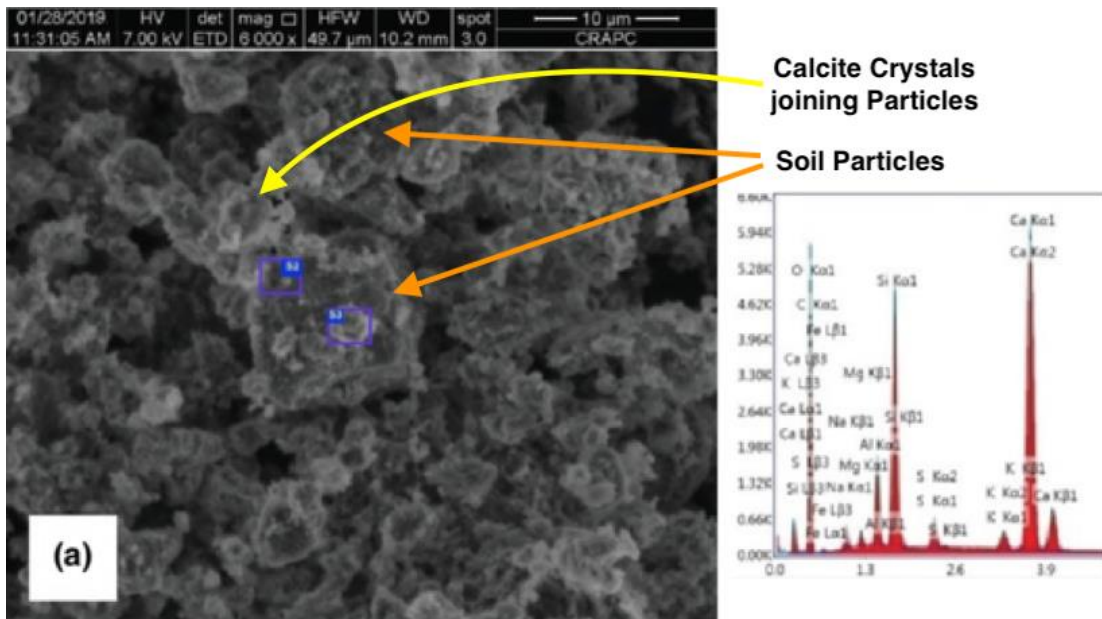


Figure 4.16 (a) from PFC18

Precipitated CaCO_3 crystals around the soil particle taken at 6000x magnification and zoom of $50\mu\text{m}$, in a 7-day treated sample using the 1×10^8 cfu/mL concentration of *Bacillus licheniformis*, and using Cementing Regent: (3 g/L Nutrient Broth supplement + 0.75 M Urea + 0.75 M Calcium chloride).

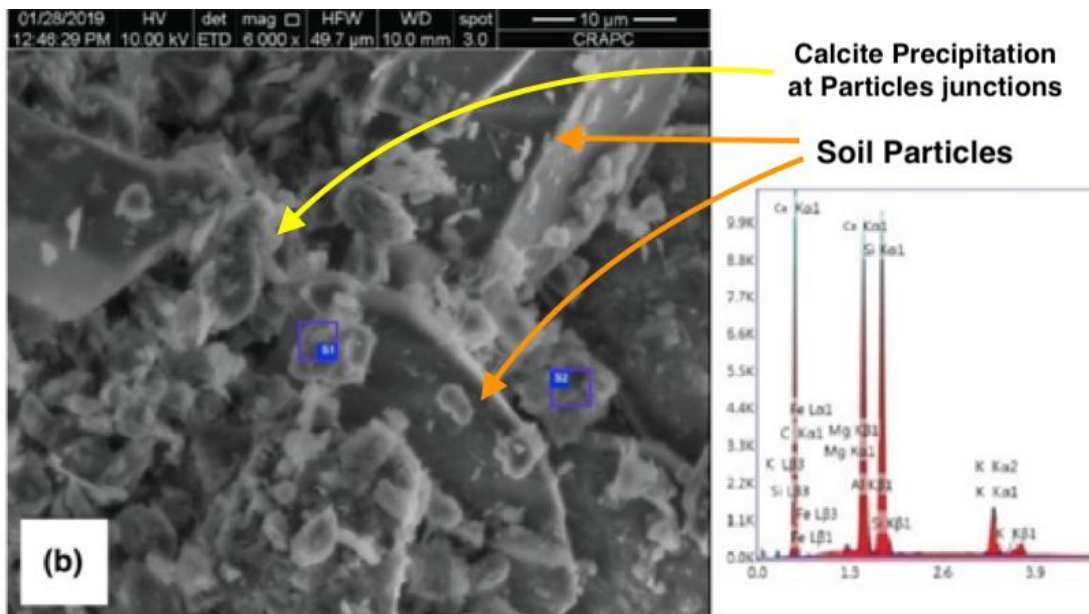


Figure 4.16 (b) from PFC18

CaCO₃ Crystals surrounding the soil particles, taken at 6000x magnification and zoom of 50µm, in a 7-day treated sample using the 1 x 10⁸ cfu/mL concentration of *Bacillus licheniformis*, and using Cementing Regent: (3 g/L Nutrient Broth supplement + 0.75 M Urea + 0.75 M Calcium chloride).

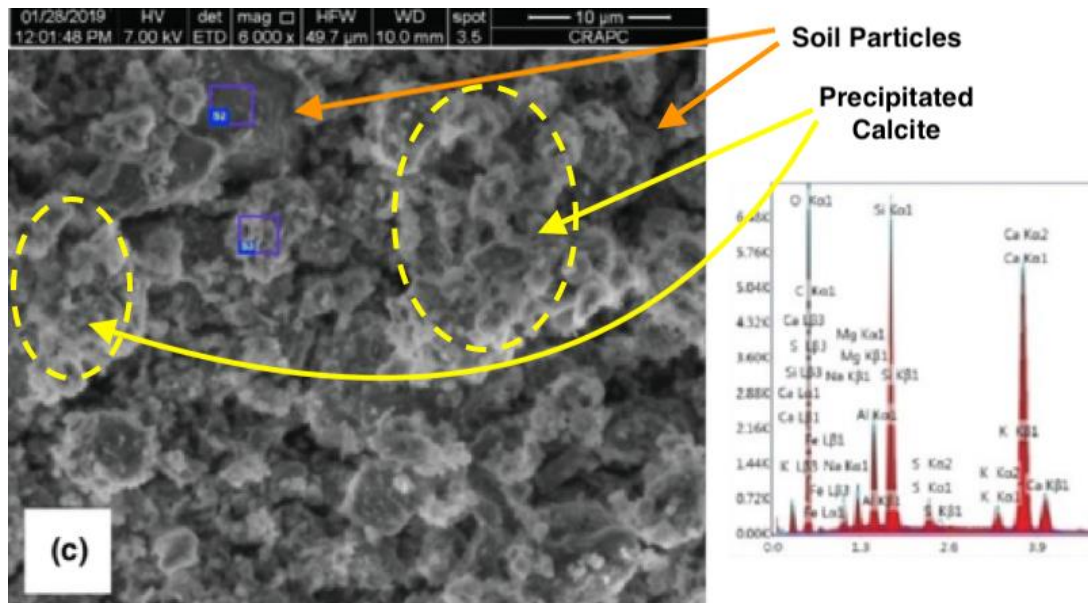


Figure 4.16 (c) from PFC23

CaCO₃ crystal sheet formation around the soil particles, picture taken 6000x magnification and zoom of 80µm for a 7-day treated sample, using *Lysinibacillus Fusiformis* and using Cementing Regent: (3 g/L Nutrient Broth supplement + 1.0 M Urea + 1.0 M Calcium chloride).

4.8 Executive Results Summary of Injection Method Treatment

This section provides a comprehensive summary of the injection methods experimental sets results. Total 24 pressure flow column experiment sets (including four control and one untreated control), and four sets of Mixing experiments were conducted, and three samples were treated for each individual experimental set. From the results it is concluded that:

- The maximum gain in strength was recorded to be 150.9% and 35.7% higher than that of untreated soil (C1) and control (PFC1-C2) respectively.
- Samples inoculated with *Bacillus licheniformis* (PFC18, PFC 21 and PFC13), had the highest strength gain followed by samples inoculated respectively with *Lysinibacillus fusiformis* and *Micrococcus luteus*. For all different reagent solution concentrations, *Rhodococcus erythropolis* appeared to perform less well than the other strains.
- The highest CaCO₃ contents of an average of 1.28% correspond to an average strength increase of 110 kPa (PCF18: *Bacillus licheniformis* and 0.75 M reagent solution). A general increase in CaCO₃ content with an increase in cementation reagent concentration has been observed, where 0.75 M showed higher % of precipitated CaCO₃ compared to the lower concentrations of 0.25 M and 0.50 M. However, 1.0 M cementation reagent was unable to produce better results compared to 0.75 M.
- A uniform distribution of precipitated CaCO₃ along the height of the samples has been observed.
- The effect of moisture content on strength would be small as measured water content variations were overall very small, but a general trend in decrease in moisture content was observed with an increase in CaCO₃ and UCS strength.
- The measured NH₄⁺ concentrations exceeded the allowable limits of total ammonia (NH₃ and NH₄⁺) for drinking water according to UK legislation, set to 0.5 mg/L (The Water Supply (Water Quality) (Amendment) Regulations, 2018).
- As implicated by the chemical equations (2.12-2.17) the increase in soil pH was observed following high carbonate precipitation. The final pH changes in soil samples were moderate to high compared to the pH natural sample. However, the pH has been found within the viability limit of the selected bacterial strains.

- It has been found that the CaCO_3 precipitation using the four selected microorganisms, especially for *Bacillus licheniformis* was optimised in the pH range of 7.2 to 7.85.
- The mixing method (MX1-MX4) experimental set was unable to produce much better results.
- The oedometer testing indicated a considerable reduction in the compressibility of the treated soil. The values of the (m_v) at the initial consolidation stages for the untreated soil were higher compare to the saturated treated specimens, which indicates the reduction in void ratio due to the cementation precipitation. Moreover, the calculated (C_v) values also indicates that the MICP pressure flow column treatment caused a reduction in primary consolidation.
- The SEM and EDS analyses further supported the CaCO_3 precipitation and acid digestion results.

Chapter 5

RESULTS AND DISCUSSION OF EK-BIOCEMENTATION EXPERIMENTS

The results of the Electrokinetic pure system (water only) and Electro-Biostimulation (Nutrients only) and Electro-Bioaugmentation (Nutrients and *Bacillus Licheniformis*) treatments are presented and discussed in this chapter. For the Electrokinetic treatment the experimental plan given in the table 3.7 was followed. First a control Electrokinetic experiment (EK1-C1) was performed at the natural moisture content of the soil, where soil was let to dry out due to electroosmosis (without adding any water at the anode compartment); this showed an average of 13.6% change (shrinkage) in the volume of the soil. In the second Electrokinetic control experiment (EK1-C2) an equal amount (13.6%) of water was added at the anode to compensate for the shrinkage and to check if the soil volume can be maintained during the Electrokinetic treatment. Subsequently the main Electrokinetic treatment was performed on samples having three different degree of saturations for each batch as described in section 3.9.5.

5.1 UCS Results and Analysis

The UCS strength results for all the main Electrokinetic experiments are compared below in the figure 5.1; the UCS measurements are also supported by CaCO_3 and NH_4^+ measurements shown in Fig 5.2. End of treatment moisture content % and plotted in figures 5.3.

The open rectangular surface and dimensions of the cell allowed the extraction of duplicate UCS specimens (50mm diameter and 100 mm height cylinders) from three different locations in the soil sample, namely from the areas next to the two electrolyte chambers (right and left) and from the middle of the sample (i.e. total 6 UCS specimens for each treatment). In below figure 5.1, 5.2 the average UCS and CaCO_3 values of the two specimens from each location are plotted with error bars showing maximum and minimum values.

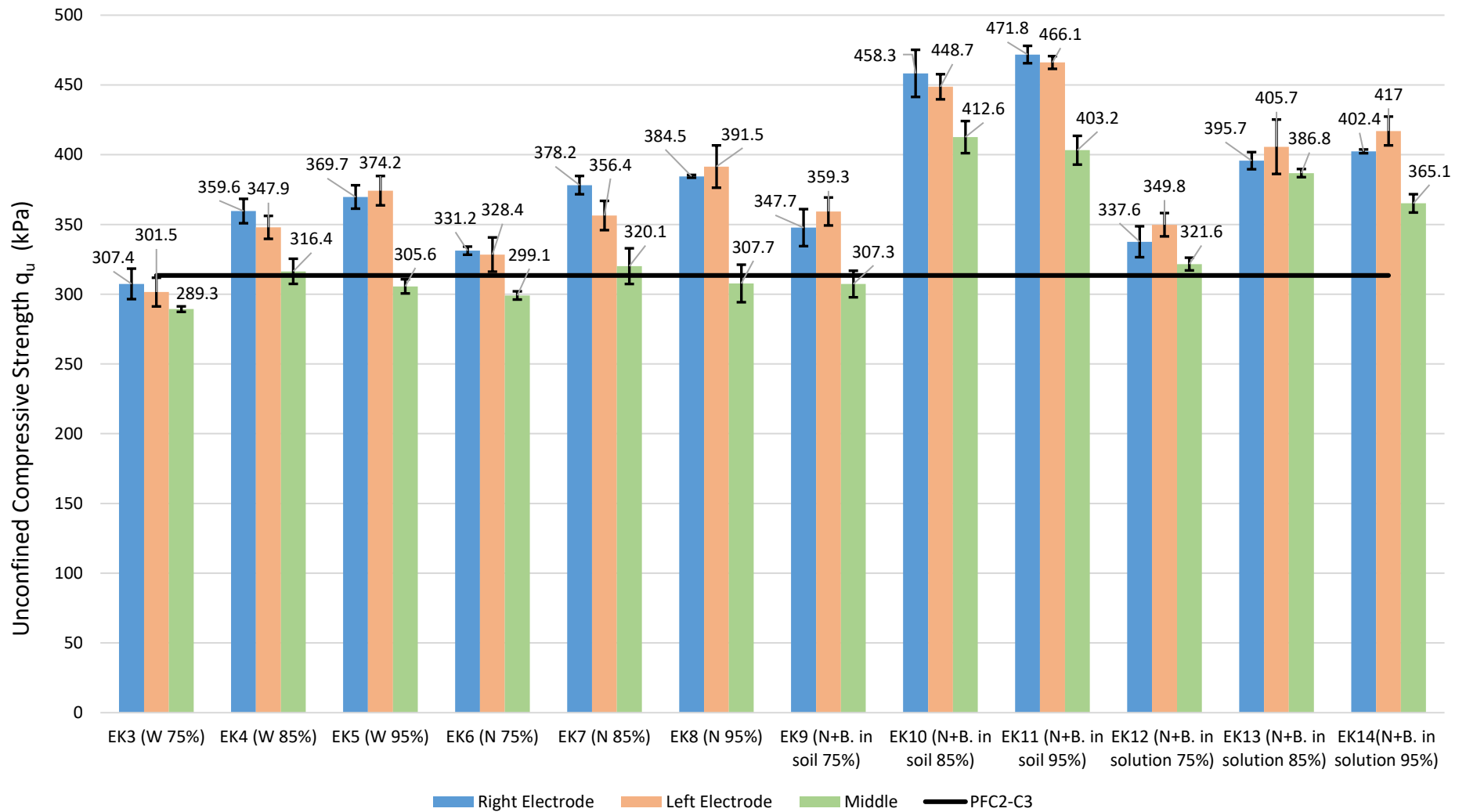


Figure 5.1 UCS strength comparison for EK-Biocementation (EK3-EK14) experiments

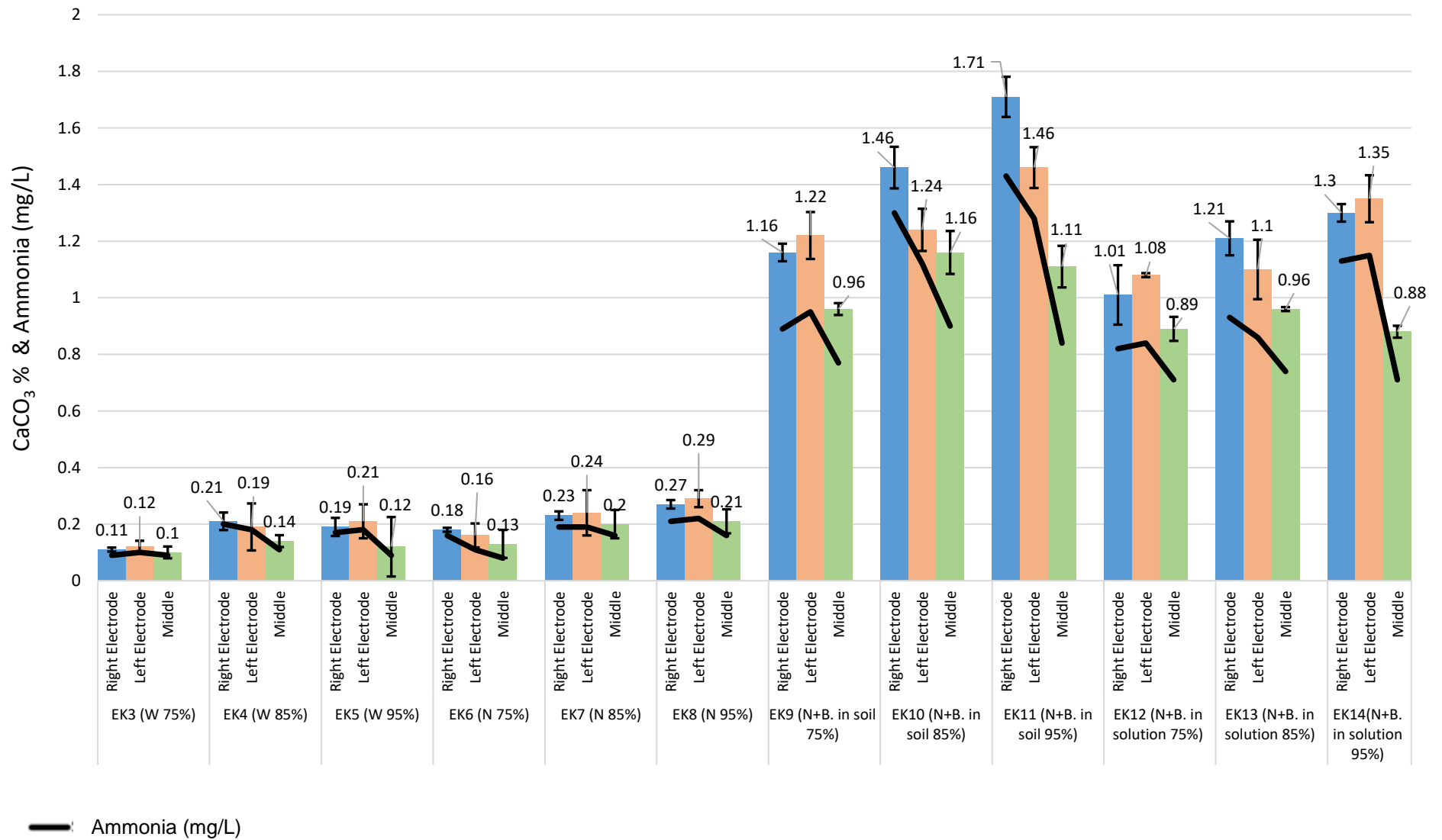


Figure 5.2 CaCO₃ % along with the resultant Ammonia concentration for EK-Biocementation (EK3-EK14) experiments

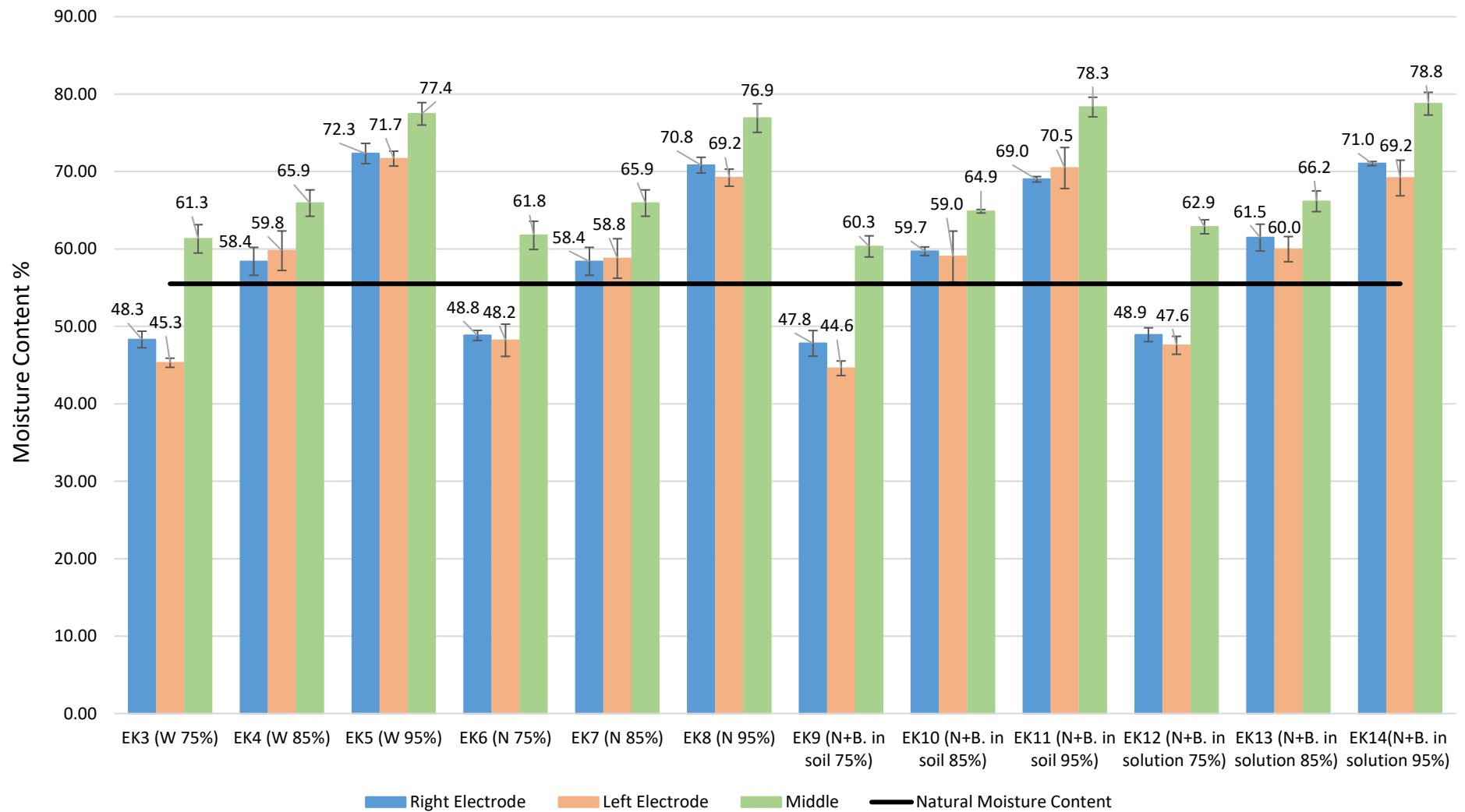


Figure 5.3 Moisture Content % change at the end of EK-Biocementation (EK3-EK14) experiments

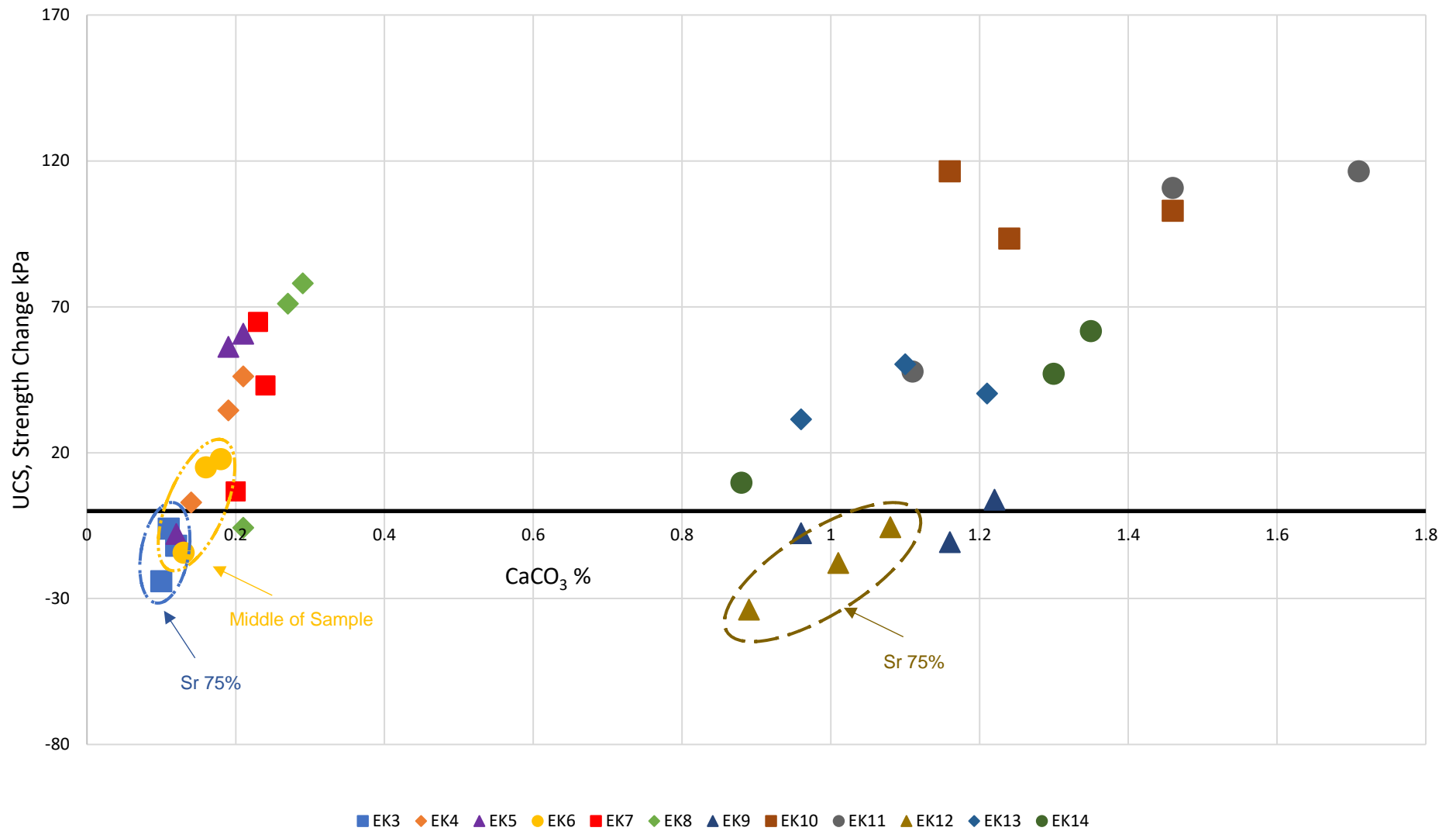


Figure 5.4 UCS, strength Change of EK samples compared to respective MICP (PFC2-C3) and (PFC22) experiments

5.1.1 Main Observations

Based on these figures, the main observations are as follows:

- The EK treatment considerably enhanced the soil strength compared to the pressure flow treatment even for the water and nutrients only experimental sets. This shows that the Electrokinetic stabilisation treatment (without MICP) is also effective for the organic soil.
- In the pure EK stabilisation (Batch 1), the average increase in the soil strength near the electrode area has almost doubled compared to the corresponding pressure flow column experiment (PFC1-C2). Only a very small % of the precipitated calcite was measured which indicates that the strength improvement in these experimental sets is mainly due to the Electrokinetic phenomena effects, as expected and sets the baseline for comparison with the EK-bioaugmentation tests.
- The EK-samples treated with nutrients only (Batch 2, no added bacteria), had approximately 24.6 % higher strengths compared to that of the respective MICP experiment control set (PFC2-C3). The further improvement in the soil strength compared to the PFC tests (which was attributed to the action of salts) can be due to changes in the physicochemical properties of the soil first induced by electrochemical reactions during EK (see Chapter 2).
- The maximum increase in strength (for full treatment set, i.e. nutrients + cementation reagent + bacteria) due to EK was recorded to be 10.1 % higher (EK-11) compared to the maximum strength achieved in the MICP treatment method (PFC-18), and 32.8 % higher as compare to the respective pressure flow column experiment (PFC-19) where same bacterial strain i.e. (*Bacillus licheniformis*) and same population concentration of 1×10^8 cfu/mL and same (1M) reagent concentration has been used. This higher strength is possibly due to the combined result of the EK stabilisation and the cementation effect produced by the microorganism action.

- The EK-experiments (Batch 3, premixed microorganisms), provided overall better results compared to all other treatment arrangements. (Batch 4 EK-injected microorganisms) did not perform as impressively as (Batch 3) compared to control and showed a relatively less strength gains of about 20% in parts of the sample compared to 32.8 % achieved in (Batch 3). But in general, the electrokinetic injection led to better results than pressure flow column even at same degree of saturation (i.e. 85%) and this was the case whether bacteria were premixed in the soil (as in the flow column tests) or injected electrokinetically into the soil. Whilst the non-uniformity of the treatment needs to be addressed and further investigated, the observed increase in strength and calcite content in parts of the sample shows promise that electrokinetics could be a viable technique for treating the organic soil. This also indicates that the treatment variables used in the EK stabilisation technique were effective. However, further optimisation of the treatment variables given in the table 3.4 can be made such as using different concentration of microorganism and cementation reagent which possibly could further enhance the efficiency of the treatment.
- A comparative plot of the UCS strength change (compared to the respective controls) against the precipitated % of CaCO_3 is given in figure 5.4. And a plot of mean CaCO_3 precipitation % along with average final readings of the ammonia measured by the method described in the (3.7.2.2) the at the end of EK treatment, of each EK experiment from three different locations i.e. (near both electrodes and at the center of the sample) is given above in figure 5.2. Consistently with the increase in strength, the calcite precipitation increased significantly compared to column flow experiments with a maximum increase of (98.8%, 34.88% and 69.8%) at the right electrode, middle of sample and left electrode respectively. Note that despite the polarity reversal, strength and CaCO_3 contents were the highest at the right electrode (from where the injection started), which is difficult to explain. one possible explanation for this is that, at the start of the treatment, the natural pH of the soil (pH) was favourable for the production of the calcite, but due to lack of drainage in the EK system the full migration of chemical species under the influence of electro-

chemical reaction did not take place, which ultimately resulted in accumulation of moisture in the middle and also caused the soil acidity next to the electrodes.

- Comparing (Batch 3), where the bacteria were mixed into the soil to (Batch 4), where bacterial strain in the aqueous solution of nutrients was injected into soil electrokinetically, it can be seen that the mixing method (Batch 3) produced better results compared to EK bacterial injection into soil (Batch 4). However, strength increase and CaCO_3 contents indicated that the latter method did transport microorganisms across the soil; lower strengths compared to mixing could be due to several factors in addition to bacteria transport e.g. non-efficient stirring of nutrient-bacteria solution in the electrolyte chambers during the EK treatment. The lower pH near the electrodes could have affected bacterial metabolic activity. This aspect requires further research, as it is vital for the in-situ implementation of the treatments.
- Looking at the NH_4^+ concentration measurements, it can be seen that whereas the average strength increase for (EK10) was around 26%, the maximum average of the produced NH_4^+ concentration was found to be 177% higher as compared to the respective Pressure flow column experimental set of (PFC19). An efficient provision for mitigating or managing this by-product will be of essence for in situ applications. The lower NH_4^+ concentration as well as the lower CaCO_3 content at the end of the pressure flow column experiments could be due to some washing away of the bacteria under the applied pressure.

5.1.2 Effect of Moisture Content on UCS Strength

The final moisture content at three different locations in the soil sample i.e. (near both electrodes and at the center of the sample) at the end of EK treatment were monitored to determine any effects of uneven moisture content distribution to the measured strengths and are plotted in figure 5.3. The variation in moisture content showed a particular behaviour in regulating the soil strength. It was observed that:

- In the experiments with nutrients only (Batch 2), considerable strength gains of 20.7% and 24.9% were recorded for (EK7) and (EK8) respectively, close to the electrodes compared to the respective pressure column flow sample (PFC2-

C3, average $q_u = 313.43$ kPa). However, the strength in the middle of the sample only increased by 2% compared to the pressure flow column (the higher water content at the middle points of EK sample may have had an effect on this 65.9% vs 63.6% for EK7 and PFC2-C3 respectively).

- In the treatments with bacteria and cementation reagent (i.e. Batch 3 & Batch4), the variation in moisture content in all EK experiments, near the electrodes and at middle points respectively are consistent for all degrees of saturation, thus the increase in strength is due to the combined EK-bacteria treatment rather than moisture content effects. The strengths next to the two electrodes were also very consistent (less than 3% difference). This could be possibly attributed to the better distribution of the treatments in the soil when EK is used. Specimens showed considerably higher strength gains compared to the respective pressure flow column test (PFC19) (significant at a 95% confidence level, see table 5.1), even at the middle point which had a higher moisture content compared to (PFC19). On the other hand, the water contents of the areas close to the two electrodes were consistent to that of (PFC19) therefore the increase in strength cannot be partly attributed to water content effects.
- The consistently lower strengths at the middle points of the EK samples (compared to the electrode area) for all tests could be attributed to their higher moisture content, as water accumulated in the middle due to polarity reversal. In future work it will therefore be necessary to provide an effective drainage arrangement at this point.

5.2 Effect of Degree of Saturation (S_r) on the effectiveness of the EK treatment

Three different degree of saturations (S_r) i.e., 75%, 85% and 95 % of the soil samples were used for the EK treatment. The 85% was the base (S_r) for the samples after moisture content adjustment to counteract volume change as explained in Chapter 2, whereas the other two (S_r) are of +/-10% compared to this value. A comparative plot for the changes in the UCS strength is given above in the figure 5.4, where results of the (EK3-EK8) experimental sets are compared to respective average UCS strength

of pressure flow column test (PFC2-C3) and (EK9-EK14) compared with the relevant test set of (PFC19).

- The influence of degree of saturation on the EK results can be observed in all the EK treatments i.e. without bacteria and those with bacteria, with the success of the treatment generally increasing with increasing degrees of saturation (strengths are higher). The increase in the strength with the increase in (S_r), is consistent with the literature (e.g. Wahab et al., 2018; Asadi et al., 2013). The possible reason for this is the increase in the moisture into the interparticle spaces instead of intercellular spaces of the organic soil, which can boost the advancement of acidic and alkaline fronts.
- The increase in degree of saturation affected favourably the effectiveness of the treatment as an increase in strength is observed in all experimental sets; an exception to this is the measured strength in the middle of the sample, where the intermediate degree of saturation ($S_r = 85\%$) showed better results than the higher degree of saturation. This is possibly due to large accumulation of moisture in high ($S_r = 95\%$) in the middle of the samples due to polarity reversal.
- Hence, for all experimental sets, the ($S_r = 85\%$), showed least variation in moisture content and effective strength gain throughout the soil specimen. The higher ($S_r = 95\%$) displayed slightly better strengths (3%) compared to ($S_r = 85\%$) but mainly in areas near to the electrodes. On the other hand, lower ($S_r = 75\%$) was not able to produce considerable increase in soil strength despite the fact of having lower moisture content.

Similar to the PFC treatment, the CaCO_3 precipitation content mainly controls and determines the improvement in UCS strength of the EK treated soil. However, the results indicate that for the EK treatment of the soil it is the combination of all the above described factors that contributes toward the total strength change of the treated soil.

5.3 Stress Strain Behaviour

A relative comparison of the EK highest strength result with the highest pressure flow column experimental result, control sample and untreated soil is presented in figure 5.5, which shows that:

- The EK-treated samples tested for UCS showed more brittle behaviour, even for the samples having similar moisture and calcite content compared to relevant pressure flow column experiments presumably due to the higher biocement content. The maximum UCS strength of (471.8 kPa) was observed for the EK-treatment, at a lower strain (approximately 2.15%). Moreover, despite of having higher moisture content, the samples from the middle EK portion also showed a more ductile behaviours compared to the PFC experiments. Which indicated that though the moisture content has some effect here on soil strength but the stress-strain behaviour seems independent of it.

A comparison of different failure behaviours (ductile and brittle) in the sample pictures is given below in figure 5.6.

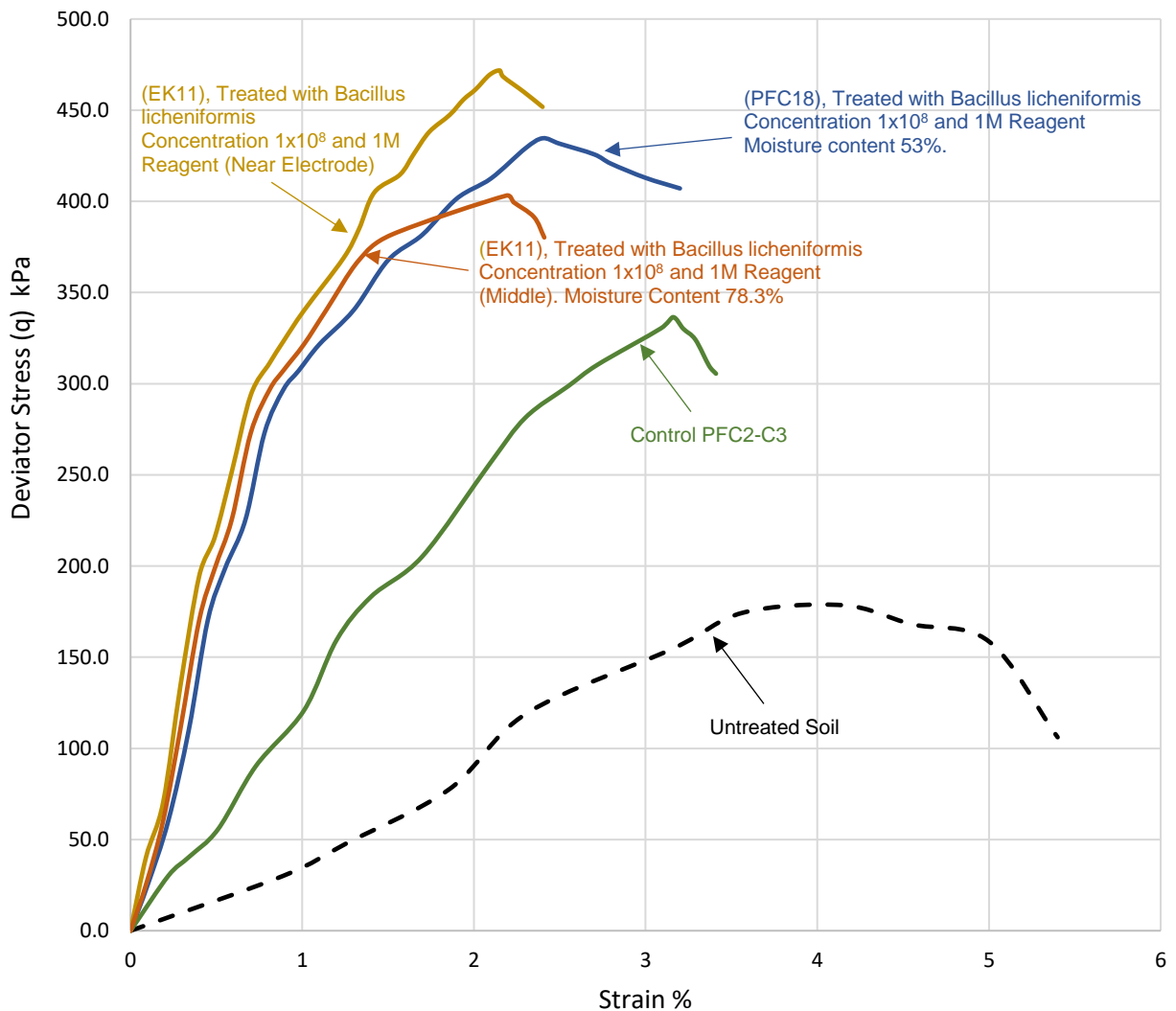


Figure 5.5 Stress-Strain relationship of EK, PFC treated, and control samples

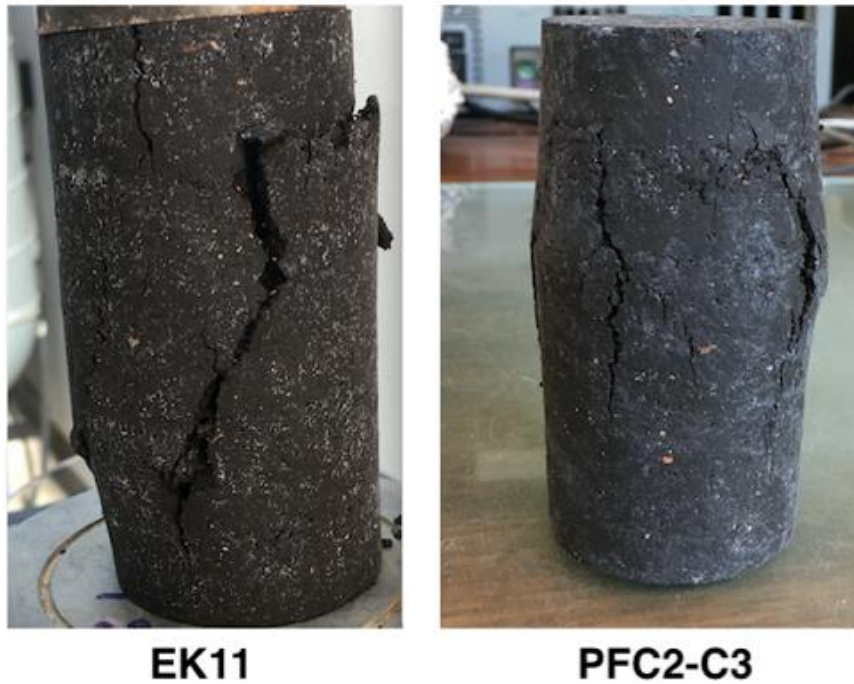


Figure 5.6 Different failure behaviours

5.4 Summary of UCS Strength Change in Treated Samples

A comparative summary of average UCS strength for experimental groups (EK3-EK8) in terms of (%) strength compared to respective pressure flow column control sample treated with nutrients only (PFC2-C3) (average $q_u = 313.43$ kPa), and for experimental groups (EK9-EK14) compared with relevant pressure flow column experimental dataset (PFC19) (average $q_u = 355.39$ kPa) is presented below in table 5.1. The p-values here refer to results of paired t-test for the comparison of the average q_u values of EK-Biocementation dataset with the corresponding pressure flow column experiments. Here (all statistically significant at 95% confidence level, values are mean \pm SD at (n=2) and p-value<0.05).

Table 5.1 UCS strength change summary for EK experiments

	Right Electrode	Middle	Left Electrode	Pressure Flow Column
EK3 (Water only, $S_r = 75\%$)	$q_u = 307.42$ kPa $\Delta q_u = -2.0 \%$ p-value = 0.0130	$q_u = 289.32$ kPa $\Delta q_u = -7.81 \%$ p-value = 0.0976	$q_u = 301.51$ kPa $\Delta q_u = -3.94 \%$ p-value = 0.414	$q_u = 313.43$ kPa $\Delta q_u = \text{N/A}$ p-value = N/A
EK4 (Water only, $S_r = 85\%$)	$q_u = 359.61$ kPa $\Delta q_u = 14.73 \%$ p-value = 0.0338	$q_u = 316.42$ kPa $\Delta q_u = 0.95 \%$ p-value = 0.0438	$q_u = 347.93$ kPa $\Delta q_u = 11.01 \%$ p-value = 0.0563	
EK5 (Water only, $S_r = 95\%$)	$q_u = 369.72$ kPa $\Delta q_u = 17.96 \%$ p-value = 0.0137	$q_u = 305.22$ kPa $\Delta q_u = -2.62 \%$ p-value = 0.0201	$q_u = 374.25$ kPa $\Delta q_u = 19.40 \%$ p-value = 0.003	
EK6 (Nutrients only, $S_r = 75\%$)	$q_u = 331.24$ kPa $\Delta q_u = 5.68 \%$ p-value = 0.0615	$q_u = 299.14$ kPa $\Delta q_u = -4.56 \%$ p-value = 0.0913	$q_u = 328.37$ kPa $\Delta q_u = 4.77 \%$ p-value = 0.048	
EK7 (Nutrients only, $S_r = 85\%$)	$q_u = 378.29$ kPa $\Delta q_u = 20.7 \%$ p-value = 0.0260	$q_u = 319.89$ kPa $\Delta q_u = 2.06 \%$ p-value = 0.683	$q_u = 355.45$ kPa $\Delta q_u = 13.41 \%$ p-value = 0.081	
EK8 (Nutrients only, $S_r = 95\%$)	$q_u = 384.47$ kPa $\Delta q_u = 22.67 \%$ p-value = 0.0380	$q_u = 307.68$ kPa $\Delta q_u = -1.83 \%$ p-value = 0.0544	$q_u = 391.54$ kPa $\Delta q_u = 24.92 \%$ p-value = 0.0402	
EK9 (Nutrients + <i>Bacillus l.</i> in soil, $S_r = 75\%$)	$q_u = 347.73$ kPa $\Delta q_u = -2.16 \%$ p-value = 0.322	$q_u = 307.21$ kPa $\Delta q_u = -13.55 \%$ p-value = 0.0355	$q_u = 359.3$ kPa $\Delta q_u = 1.10 \%$ p-value = 0.2835	$q_u = 355.39$ kPa $\Delta q_u = \text{N/A}$ p-value = N/A
EK10 (Nutrients + <i>Bacillus l.</i> in soil, $S_r = 85\%$)	$q_u = 457.98$ kPa $\Delta q_u = 28.87 \%$ p-value = 0.0166	$q_u = 411.51$ kPa $\Delta q_u = 15.80 \%$ p-value = 0.0038	$q_u = 448.46$ kPa $\Delta q_u = 26.19 \%$ p-value = 0.0149	
EK11 (Nutrients + <i>Bacillus l.</i> in soil, $S_r = 95\%$)	$q_u = 471.80$ kPa $\Delta q_u = 32.75 \%$ p-value = 0.0202	$q_u = 403.17$ kPa $\Delta q_u = 13.44 \%$ p-value = 0.0429	$q_u = 466.13$ kPa $\Delta q_u = 31.16 \%$ p-value = 0.0328	
EK12 (Nutrients + <i>Bacillus l.</i> in solution, $S_r = 75\%$)	$q_u = 337.59$ kPa $\Delta q_u = -4.97 \%$ p-value = 0.0705	$q_u = 349.82$ kPa $\Delta q_u = -1.57 \%$ p-value = 0.0401	$q_u = 321.56$ kPa $\Delta q_u = -9.52 \%$ p-value = 0.0410	
EK12 (Nutrients + <i>Bacillus l.</i> in solution, $S_r = 85\%$)	$q_u = 395.68$ kPa $\Delta q_u = 11.34 \%$ p-value = 0.0138	$q_u = 386.84$ kPa $\Delta q_u = 8.85 \%$ p-value = 0.0319	$q_u = 405.65$ kPa $\Delta q_u = 14.14 \%$ p-value = 0.0104	
EK12 (Nutrients + <i>Bacillus l.</i> in solution, $S_r = 95\%$)	$q_u = 402.39$ kPa $\Delta q_u = 13.22 \%$ p-value = 0.0603	$q_u = 417.03$ kPa $\Delta q_u = 17.24 \%$ p-value = 0.0113	$q_u = 365.14$ kPa $\Delta q_u = 2.74 \%$ p-value = 0.2833	

5.5 pH Change in the EK treatment

Due to the applied electric potential a pH gradient forms which can cause a considerable decrease in the pH near the anode. As bacterial metabolic activity and the CaCO_3 production require an alkaline environment (Achal et al., 2009), the pH in the EK experiments was adjusted by:

- Reversing the polarity every 24-hours, to avoid the buildup of H^+ ions near any particular electrode, and to distribute these uniformly across the soil.
- Adding the solution of cementation reagent in three equal proportions (at day1, day 3 and day 7) to lower pH by diluting the solutions in the electrolytes chamber.

To assess the effectiveness of these measures in controlling the pH during the EK process, the change in the pH of the electrolyte chambers was monitored. As all EK treatments presented similar results; those of set EK11 are indicatively presented (see Figure 5.7). Moreover a 3-D representation of pH variation across soil specimen under EK treatment (at 27 different locations, along the length and depth) is shown in Figure 5.8.

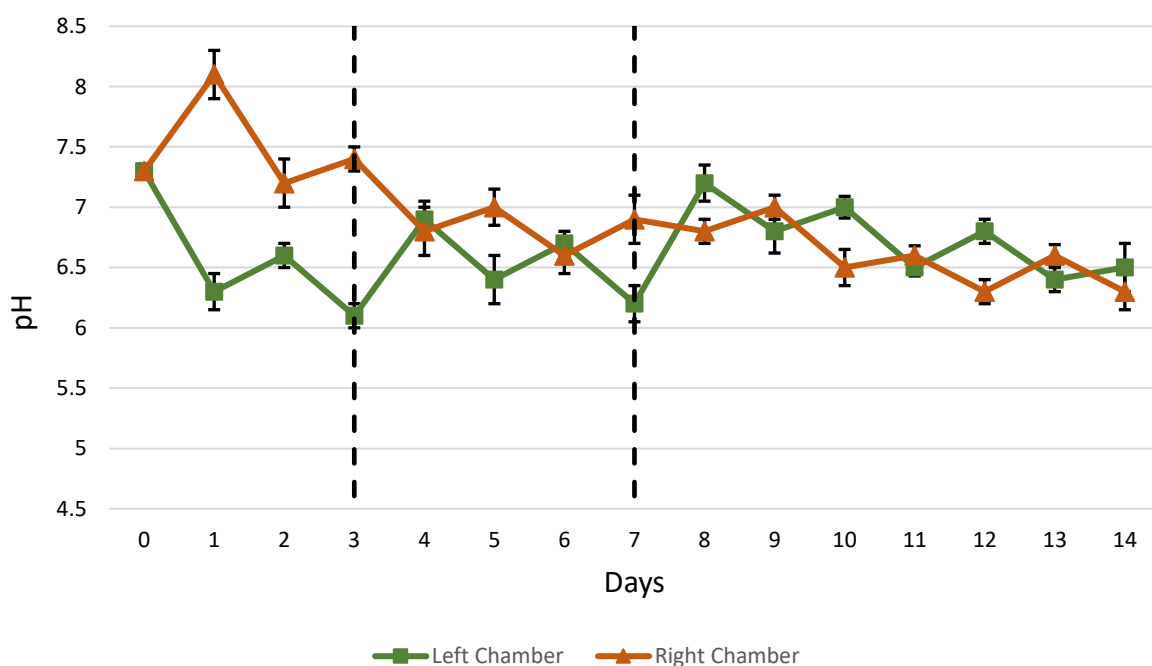
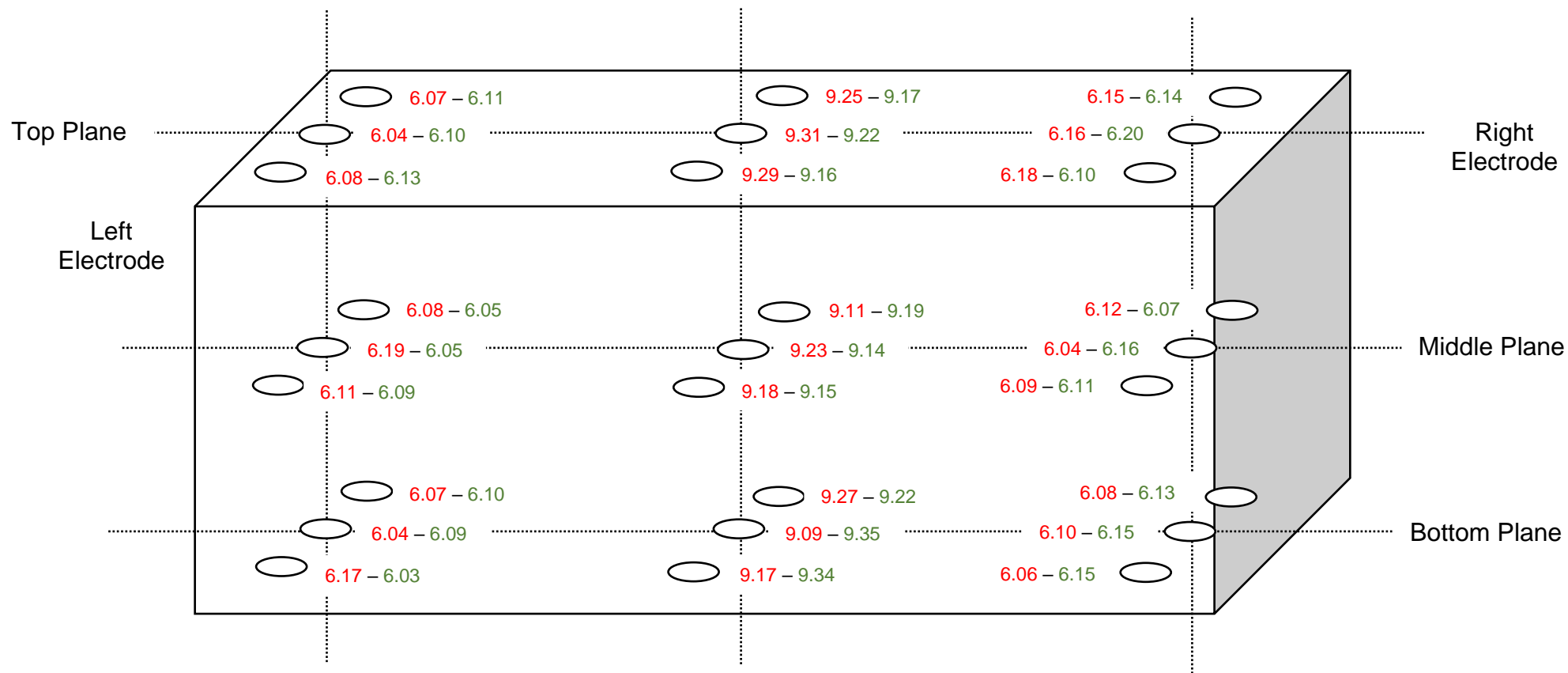


Figure 5.7 pH variation in right and left electrolyte chambers over 14 day



Red (EK10), Green (EK11)

Figure 5.8 pH change variation across the soil specimen at the end of EK treatment

- From figure 5.7 it is clear that reversing polarity every 24-hours, and supplying the nutrients in three portions were effective in maintaining the pH of both compartments close to the pH of the natural soil (as in the beginning of the experiment). However, these techniques were unable to further increase the pH to the favourable level (8.0-8.5 pH) as described in Keykha et al., (2014). Hence, for this purpose, the pH electronic controllers would have been a better choice.
- The higher pH at the right electrode in the first few days is the possible reason for the high CaCO₃ content and UCS strength at this location.
This also indicates that a higher CaCO₃ precipitation could have been achieved under more alkaline conditions. This requires further study and optimisation.
- A relatively higher pH in the middle was measured for all the EK experiments, due to accumulation of OH⁻ ions in the middle of the sample due to polarity reversal. Yet, as mentioned earlier, strengths in the middle were lower, so this also supports the interpretation that strengths decreased as a result of the higher moisture contents at the middle points.

5.6 Temperature Variation

A plot of average temperature variations of both right and left chambers for the EK-Bioaugmentation experiments (EK6-EK11) is given in figure 5.9, with the error bars representing the mean difference of all experimental set values.

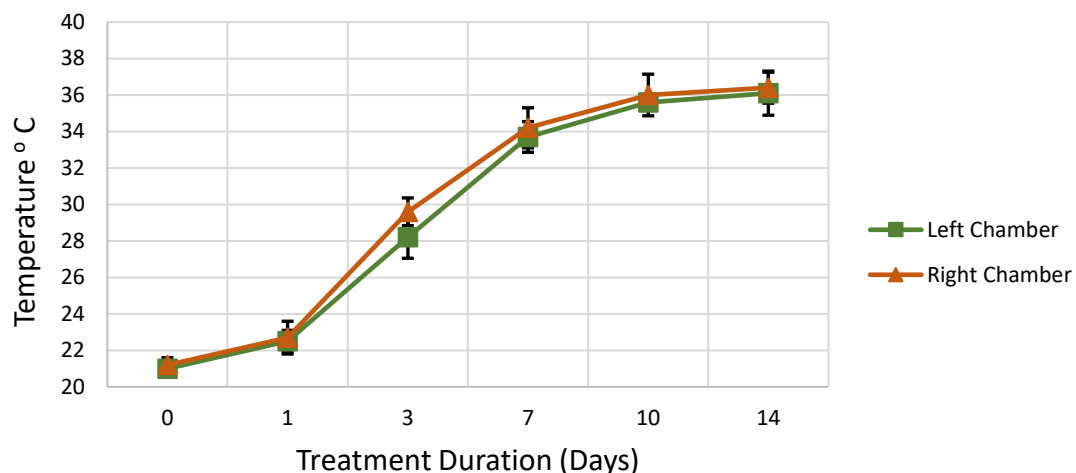


Figure 5.9 Temperature variation for both right and left chambers over time

- A rapid increase in temperature was observed in all EK experiments in the first 168-hours of the treatment. The increase is mainly due to the rise in the electric resistance of the soil surrounding the electrodes, which is caused by an increase in the CaCO₃ content. The high increase in temperature can also cause the excessive water evaporation, and can produce shrinkage cracks in the sample (Keykha and Asadi, 2017).
- The maximum temperature observed during the 14-days EK treatment was about 37.25° C, which indicates that the selected graphite made of 99% pure graphite sheet (Processed Graphite Laminate SLS), very effectively controlled the rise in temperature, and successfully eliminated the effect of heat on the soil treatment, which could potentially have a detrimental effect on bacteria. For instance, as observed by (Keykha et al., 2014) where a maximum temperature at the end of 175-hours was reported to be close to 55°C with an increase of 120% from the starting temperature of 25°C.

5.7 Voltage and Electric Current Variation

In order to monitor the voltage variation across the soil specimen during the EK treatment, the 210 mm long sample was divided into five equal portions and voltages were measured at these locations i.e. at 42, 84, 126, 168 and 210 mm. The voltage gradient helps to monitor the efficiency of the EK treatment at any time, as it is directly related to the soil conductivity (Keykha et al., 2014). Due to the polarity reversal every 24-hours the voltage variation across the soil specimen was abrupt. To demonstrate the variation, the plot of the right electrode at every subsequent polarity reversal (when it acts as anode) against the distance from the cathode is given in Figure 5.10 from which the following observations can be made:

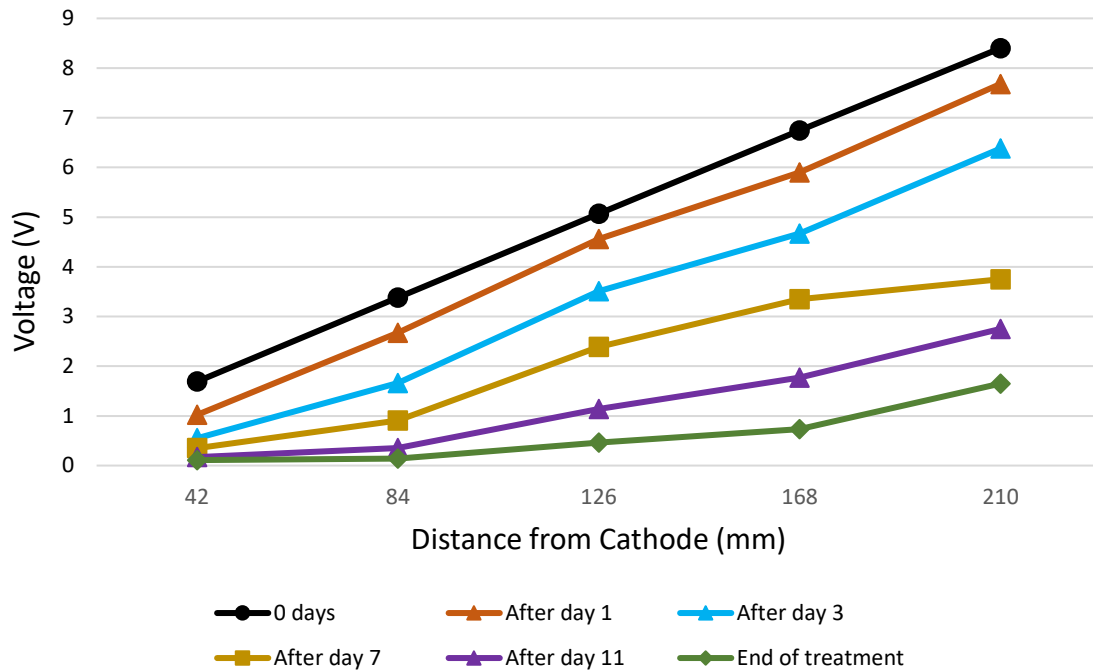


Figure 5.10 Voltage change across soil specimen during 14 days treatment for (EK11)

- Due to the uniform electric conductivity of the soil at the start of the experiment, a linear distribution of the voltage was observed between two electrodes. Due to the presence of CaCl_2 and urea the voltage in the area near the anode remained higher in the first 72-hours of the treatment.
- This persisted surge in voltage in the area near electrode developed a maximum electric gradient, which governed the electro-chemical phenomena such as electroosmotic flow of water towards the center of the sample, electrolysis of the pore fluid, and electromigration of chemical species and electrophoresis of bacteria.
- However, after the initial 72-h, a continuous decline in the passing voltage across the soil specimen was observed, that is attributed to the development of high electric resistance in the soil possibly due to precipitation of CaCO_3 in the soil and the migration of excessive water from the anode area.
- Moreover, after the polarity reversal, the soil near the cathode (originally anode) still showed high resistance to the electric current especially after the initial 72-h, which also indicates the uniform CaCO_3 precipitation at both regions next to electrodes.

A similar trend was observed in the electric current variation during all the EK-treatment experiments. At the start of the treatment, a relatively higher current passing through the samples was observed, which tends to gradually decrease. Soil resistivity increased during the first 10 days of treatment, and ultimately reached an almost constant value at the end of the treatment. A plot of the Electric current (I) and electric resistivity (R) evolution during the treatment duration is given in Figure 5.11.

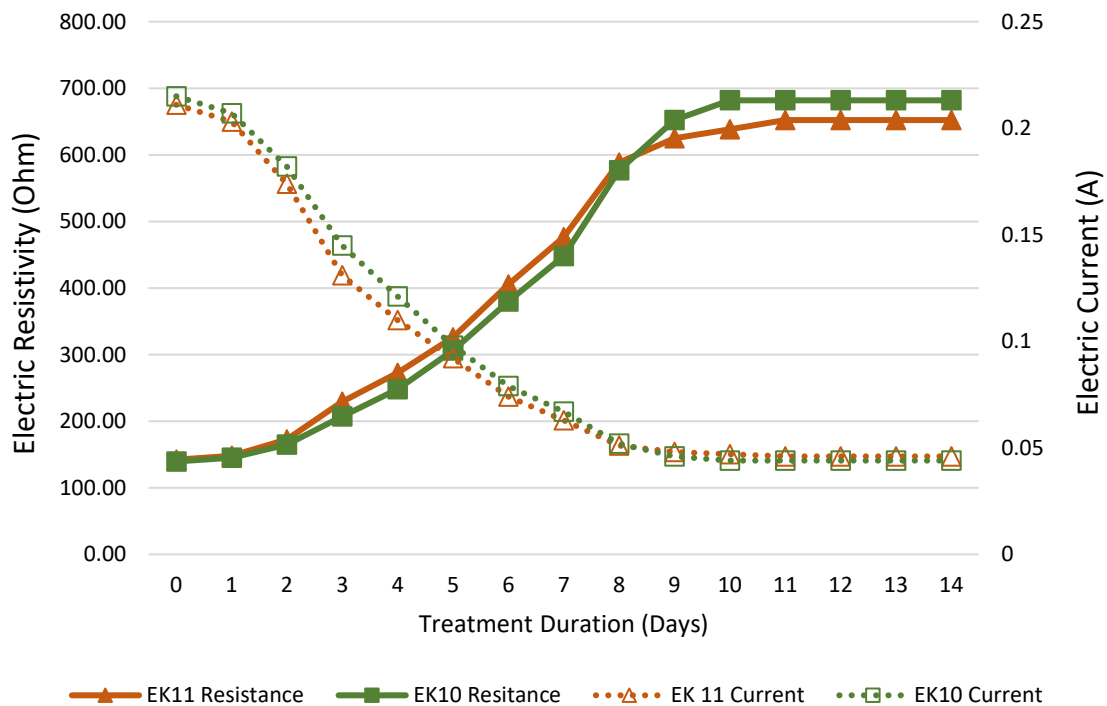


Figure 5.11 Electric current (I) and Electric Resistivity (R) variation during EK treatment

The Electric resistivity of the soil (R) used here is obtained by dividing the electric current (I) passing at any moment through the soil specimen by the total voltage (V) applied across the specimen. In the early stages of the EK treatment, the higher rate of electrochemical reactions and resultant higher ionic concentration also boosts the electric conductivity. While, with the increasing treatment duration, due to advection and diffusion processes the ionic concentration decreases, which lowers the rate of adsorption of cations to the soil particles and also the rate of electromigration lead to lower ionic distribution, lower electric current flow and higher electric resistivity across the soil specimen (Jeyakanthan et al., 2011).

5.8 Effect of EK-Biocementation Treatment on the Soil Compressibility and Consolidation Characteristics

The effectiveness of the EK treatment was also assessed by comparing the compressibility and consolidation behaviour of the treated and untreated soil. For this purpose, two oedometer samples were cut and prepared of the EK-treated soil (EK11- with 1×10^8 cfu/mL *Bacillus licheniformis* and cementing reagent solution of 1M). One treated sample was tested in saturated condition, and other was in unsaturated condition. The untreated soil was only tested in saturated conditions.

5.8.1 Sample Preparation

The sample for the treated soil was prepared by cutting an oedometer specimen directly from the EK treatment box sample. However, the top 2 cm of the soil in the EK cell were not used, to avoid any inconsistencies due small surface cracks formed from the escaping gases. The rest of the sample preparation protocol remained the same as given earlier in section 4.6.1. The oedometer results in terms of void ratio versus \log_{10} pressure curves are given in figure 5.12.

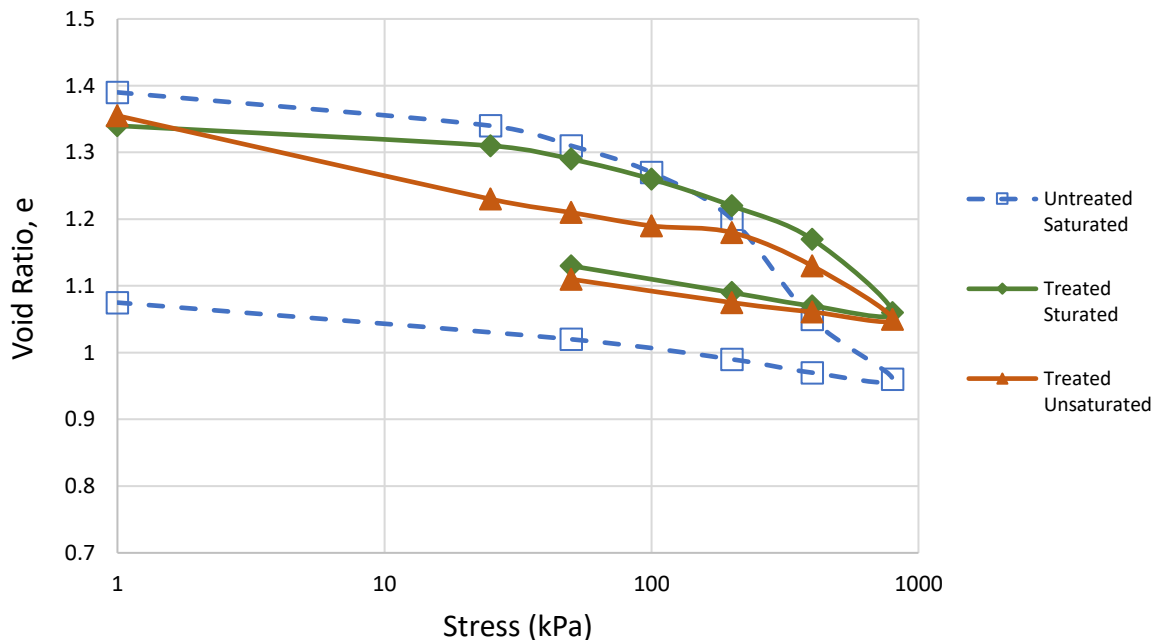


Figure 5.12 Oedometer test results (Void ratio vs Pressure)

As in the case of consolidation tests of the pressure flow column experiments, the two saturated specimens (one treated and one untreated) were left to swell (free swelling)

in the oedometer cell that was filled with water prior to compression at an applied pressure of 25-800 kPa in 6 stages (25, 50,100,200, 400 and 800 kPa) followed by unloading, in three stages (400, 200 and 50-0 kPa); the unsaturated treated specimen was subjected to compression and unloading without initial saturation/swelling stage.

- Similarly, less swelling and considerable reduction in compressibility has also been observed here, however, the treated samples predominantly showed the elastic behaviour well after the 100 kPa loading stage, which indicates that the EK-treatment has effectively increased the primary consolidation yield stress.
- It should be noted that, the differences in the void ratios of the unsaturated treated and saturated treated specimens are due to the initial conditions prior to compression (i.e. free swelling vs compression starting at unsaturated state, hence no increase in the initial void ratio) but the gradients of both compression and swelling curves are practically the same.
- Moreover, both saturated and unsaturated specimen cross the untreated (zero suction) normal consolidation line but there is practically no difference between the unsaturated and saturated treated specimens indicating that the biocement bonding is the main factor controlling this behaviour rather than suction which is a known behaviour of cemented soils (Zhang et al, 2015) In fact a similar observation can be made in the PFC results in Chapter 4).

5.8.2 Coefficient of Compressibility

The variation in the Soils' coefficient of compressibility (m_v) under the different applied stresses for consolidation is plotted below in figure 5.13.

- It can be observed that the (m_v) values for the untreated soil remained higher compared to the treated saturated specimen. This indicates the decrease in the compressibility of the treated organic soil, when the voids are potentially filled with the solid CaCO_3 crystals that also develop cementation bonds between the particles of the treated soil. The initial high value for the treated specimen tested in unsaturated condition is due to the high void ratio at the start of the experiment (i.e. without free swelling).

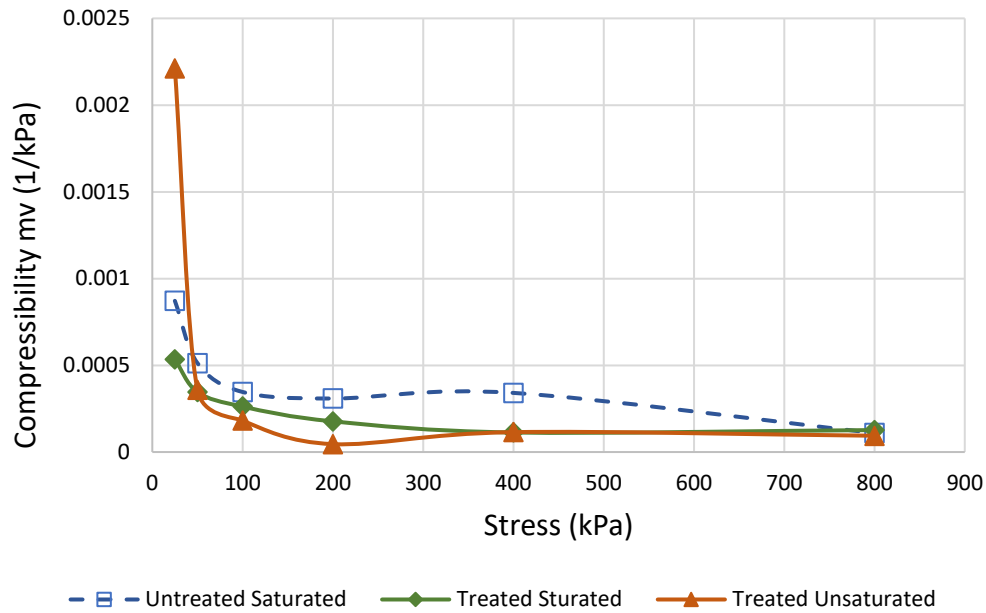


Figure 5.13 Coefficient of compressibility (m_v) vs Pressure

5.8.3 Coefficient of Consolidation and Secondary Compression

The coefficient of consolidation (C_v) for the EK-treated soil sample was plotted determined by using the same three methods given in section 4.6.3. The values of (c_v) from the plotted consolidation data are given below in Table 5.2.

Table 5.2 Coefficient of consolidation, and Coefficient of secondary compression for EK-treated soil (EK11) under different applied pressures.

EK-treated (EK11)				
Applied Pressure Interval (kPa)	c_v ($m^2/year$)			Secondary compression C_a (%)
	Taylor sqrt	Log t	Parabolic isochrone	
0-25	3.58	0.81	1.14	0.04
25-50	3.53	0.2	0.57	0.02
50-100	6.8	0.098	0.72	0.015
100-200	2.58	0.16	0.13	0.77
200-400	2.59	0.059	0.16	0.68
400-800	2.90	0.119	0.288	1.13

The effect of the CaCO₃ precipitation can be observed from the consolidation behaviour of the soil, for any applied pressure the (C_v) values for the EK-treated specimen is lower than the untreated soil (Table 4.2) and at same stress stages even better than the pressure flow column treated sample (Table 4.3).

Moreover, the oedometer data set has shown that the consolidation of treated specimens at any specific stress level has taken more much time as compare to untreated soil. This can be attributed to filling of pore due to precipitation of calcite which also thereby decrease the dissipation of water from the soil. This assumption can be further verified by comparing the hydraulic conductivity or the water retention characteristics of the treated and untreated soil.

5.9 Soil Water Retention SWRC Analysis

Soil Water Retention Curve (SWRC) measurements of the untreated soil and indicative treated soils from both pressure flow column and EK-biocementation were performed using WP4C chilled-mirror dew point potentiometer. The measurements are plotted according to McKeen, (1992) analysis, in terms of gravimetric water contents of the soils against the suction in units of pF.

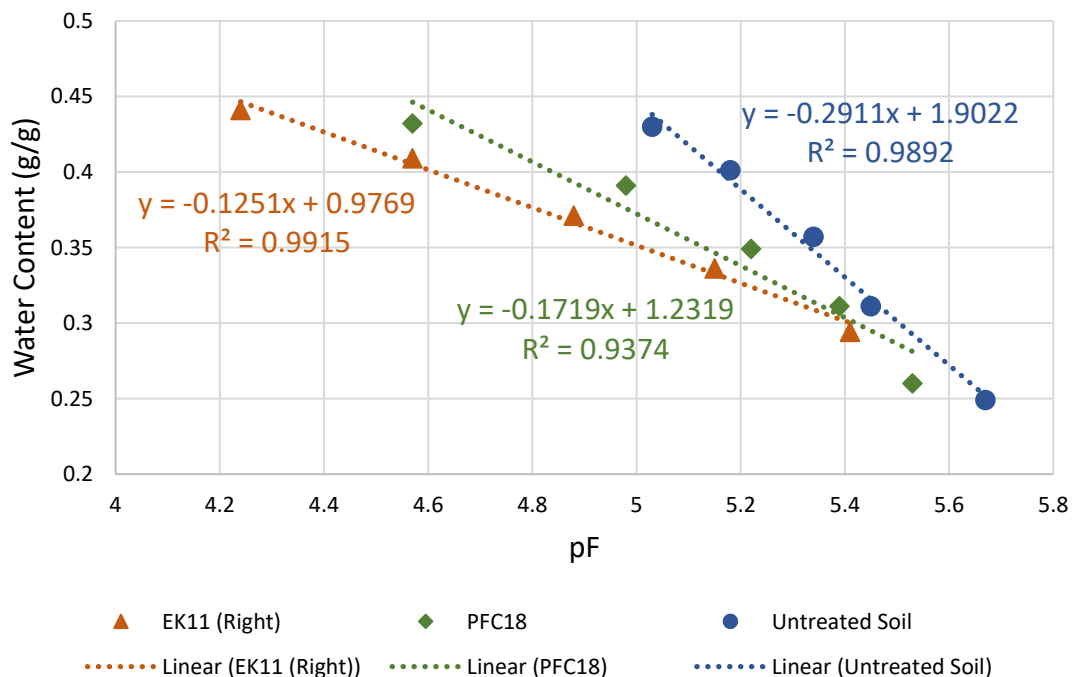


Figure 5.14 SWRC results for untreated and treated soils based on chilled-mirror dew point potentiometer

- From the plotted results it can be seen that, the bio-cementation treatment has effectively reduced the slope of the fitted straight lines; Where the untreated soil suction slope (0.29) is clearly above the maximum limit of 0.17 given in the McKeen classification scheme, and the untreated organic soil can be classified as the exceptionally high expansive soil. The McKeen classification scheme is given in Appendix C.
- The pressure flow column treatment has caused a slight decreased in the fitted straight line slope and have changed the soil behaviour from exceptionally high expansive soil to high expansive soil. The EK-biocementation further improved the soil, as indicated by the gentler slope of 0.12, changing the behaviour to that of a moderately expansive soil according to McKeen classification scheme.
- In general, the treated soil curves plot below the untreated soil SWRC i.e. for the same water content lower suctions are required for the treated soils. On the other hand, at higher suctions, there is a small effect only on the rate of desaturation (as shown by the slope formed by the points of the curve at the higher suctions) especially between PCF18 and the untreated soil. It would have been expected that if calcite precipitation led to a decrease in the pore and pore throat size and also potentially some increase in the particle surface roughness (hence specific surface), both these factors would have led to higher water retention at the same suction. However as argued in Saffari et al. (2019) there can be a competing effect of the changes in the double-layer thickness which could be the cause of the observed behaviour (a decrease in the double layer, which leads to lower matric suctions at the same water saturation).

5.10 Executive Results Summary of EK-Biocementation Treatment

A comprehensive summary of findings of the EK-Biocementation treatment experiments is provided in this section. Total 12 EK-Biocementation experiment sets in 4 batches were conducted and each individual experiment was duplicated. The Electrokinetic treatment was performed on samples having three different degree of saturations for each batch.

- The maximum increase in strength (for full treatment set, i.e. nutrients + cementation reagent + bacteria) due to EK was recorded to be 10.1 % higher (EK-11) compared to the maximum strength achieved in the MICP treatment method (PFC-18), and 32.8 % higher as compare to the respective pressure flow column experiment (PFC-19) where same bacterial strain i.e. (*Bacillus licheniformis*) and same population concentration of 1×10^8 cfu/mL and same (1M) reagent concentration has been used.
- Consistently with the increase in strength, the calcite precipitation increased significantly compared to column flow experiments with a maximum increase of (98.8%, 34.88% and 69.8%) at the right electrode, middle of sample and left electrode respectively.
- The consistently lower strengths at the middle points of the EK samples (compared to the electrode area) for all tests could be attributed to their higher moisture content, as water accumulated in the middle due to polarity reversal.
- For all experimental sets, the ($S_r = 85\%$), showed least variation in moisture content and effective strength gain throughout the soil specimen. The higher ($S_r = 95\%$) displayed slightly better strengths (3%) compared to ($S_r = 85\%$) but mainly in areas near to the electrodes. On the other hand, lower ($S_r = 75\%$) was not able to produce considerable increase in soil strength despite the fact of having lower moisture content.
- The maximum average of the produced NH_4^+ concentration was found to be 177% higher as compared to the respective Pressure flow column experimental set of (PFC19), whereas the average strength increase for (EK10) was around 26%.
- The increase in soil pH was observed following high carbonate precipitation. The final pH changes in soil samples were moderate to high compared to the

pH natural sample. However, a relatively higher pH in the middle was measured for all the EK experiments, due to accumulation of OH^- ions in the middle of the sample due to polarity reversal.

- The oedometer data set has shown less swelling and considerable reduction in compressibility in the EK treated samples. The treated samples also predominantly showed the elastic behaviour well after the 100 kPa loading stage, which indicates that the EK-treatment has effectively increased the primary consolidation yield stress. The (m_v) values for the treated soil was measured considerably less compared to the untreated specimen. This indicates the decrease in the compressibility of the treated organic soil, when the voids are potentially filled with the solid CaCO_3 crystals that also develop cementation bonds between the particles of the treated soil.
- The effect of the CaCO_3 precipitation can be observed from the consolidation behaviour of the soil, for any applied pressure the coefficient of consolidation (C_v) values for the EK-treated specimen is lower than the untreated soil and at same stress stages even better than the pressure flow column treated sample.
- The Soil Water Retention Curve (SWRC) analysis shows that the pressure flow column treatment has caused a slight decreased in the fitted straight line slope from 0.29 to 0.17 and have changed the soil behaviour from exceptionally high expansive soil to high expansive soil. The EK-biocementation further improved the soil, as indicated by the gentler slope of 0.12, changing the behaviour to that of a moderately expansive soil according to McKee classification scheme.

Chapter 6

DISCUSSION, CONCLUSIONS AND RECOMMENDATIONS

In this study two innovative methods, Pressure Flow Column treatment and EK-Biocementation have been used to improve the engineering properties of organic soil from the East Anglian peat. The assessment of the degree of improvement is based on the gain in strength, quantity of CaCO_3 precipitated, modifications to the consolidation behaviour and changes in the water retention ability of the organic soil. Due to certain limitations such as quantity of the experimental material (explained in section 3.2.1) soil from only one layer was used here for experimental work. However, the analysis of the complete borehole materials indicated other layers of peat (having higher organic matter and moisture content) at the depth of 6m and 8m in borehole 1 and borehole 2 respectively, which will require further independent study. The results presented and explained in this thesis are based on laboratory scale experiments. It follows that (to prove that the technique is effective in the field) a further stage of field study is required. The present study has not included characteristics of organic soil such as decay, accumulation, wastage and oxidation which may be important for field behaviour.

The key assumption in this work is that the whole quantity of the organic soil used for Pressure Flow Column and even for EK-Bioremediation treatment is considered to be homogeneous in its physio-chemical and engineering characteristics. No standard apparatuses exist for both Pressure flow column and EK-Biocementation treatment. Researchers (Lear et al., 2004; Keykha & Asadi, 2017; Hassan et al., 2016; Ng et al., 2014; and many more) have developed their own apparatuses in accordance to their research aims and objectives. In the current study equipment for both treatments has been designed and manufactured, and lot of improvements were made during the course of research as explained in chapter 3.

This chapter will start with a summarised comparison between Pressure Flow Column and EK-Biocementation treatment methods for CaCO_3 Content, pH, Ammonia content, UCS strength, and Moisture content presented in Table 6.1. The advantages

and disadvantages of the both treatment methods based on the experiments are added in the Table 6.2. Subsequently, the practical applicability of both treatment methods based on the results of these lab-scale experiments is rationalised. Eventually, through discussion on results, limitations and relevant recommendations of both treatment methods and conclusions are provided.

6.1 Results Comparison of Pressure Flow Column and EK-Biocementation Treatment Methods

Table 6.1 Results Comparison between PFC and EK Treatments

Measured Parameter	Pressure Flow Column	EK-Biocementation
<i>Bacillus lichenformis</i> , Bacterial Population, 1×10^8 cfu/mL		
Experiment ID	PFC9	EK10
UCS q_u (kPa)	351.9	458.3
CaCO ₃ (%)	0.85	1.46
Ammonia (mg/L)	0.60	1.30
Moisture Content (%)	59.4	59.7
pH	7.19	8.77
<i>Bacillus lichenformis</i>		
Experiment ID	PFC21	EK14
Bacterial Population	1×10^7 cfu/mL	1×10^8 cfu/mL
UCS q_u (kPa)	404.2	417.0
CaCO ₃ (%)	1.21	1.35
Ammonia (mg/L)	0.95	1.15
Moisture Content (%)	54.1	78.8
pH	7.68	9.09
<i>Bacillus lichenformis</i> (Best Results)		
Experiment ID	PFC18	EK11
Bacterial Population	1×10^8 cfu/mL	1×10^8 cfu/mL
UCS q_u (kPa)	428.4	471.8
CaCO ₃ (%)	1.28	1.71
Ammonia (mg/L)	1.15	1.43
Moisture Content (%)	53.0	78.3
pH	7.98	9.17

The results comparison of different parameters for Pressure Flow Column treatment and EK-Biocementation methods is given in Table 6.1. For a comparative analysis the comparison for both treatment methods is provided between the tests conducted under same conditions i.e. (same bacterial strain and population concentration used).

The results indicate that:

- The EK-experiments provided overall better results and considerably enhanced the soil strength compared to the pressure flow treatment. The maximum increase in strength due to EK treatment was recorded to be 10.1 % higher (EK-11) compared to the maximum strength achieved in the MICP treatment method (PFC-18), and 32.8 % higher as compare to the respective pressure flow column experiment (PFC-19) where same bacterial strain i.e. (*Bacillus licheniformis*) and same population concentration of 1×10^8 cfu/mL and same (1M) reagent concentration has been used. This higher strength is possibly due to the combined result of the EK stabilisation and the cementation effect produced by the microorganism action.
- Consistently with the increase in strength, the calcite precipitation increased significantly compared to column flow experiments with a maximum increase of (98.8%, 34.88% and 69.8%) at the right electrode, middle of sample and left electrode respectively.
- For the EK treatment the maximum average of the produced NH_4^+ concentration for (EK10) was found to be 177% higher as compared to the respective Pressure flow column experimental sets of (PFC9 & PFC19). The lower NH_4^+ concentration as well as the lower CaCO_3 content at the end of the pressure flow column experiments could be due to some washing away of the bacteria under the applied pressure.

6.2 Advantages and Disadvantages of Pressure Flow Column and EK-Biocementation treatment methods

A brief summary of advantages and the shortcoming of the both treatments based on the experiments is provided in Table 6.2.

Table 6.2 Advantages and Disadvantages of PFC and EK-Biocementation treatments

	Advantages	Disadvantages
Pressure Flow Column	<ul style="list-style-type: none"> • The samples treated for the PFC are pre-made to the sizes of the standard UCS, which were directly tested for strength determination after treatment without any further preparation. • Relatively less electric energy required for the PFC experiments compared to the EK. In the PFC experiments the electric potential only required while pumping the Cementation Reagent, while in the EK treatment the continuous supply of DC current required. • The use of indigenous bacterial strains for the PFC treatment enables these to survive and perform effectively under same environmental and chemical conditions. 	<ul style="list-style-type: none"> • The Pressure flow stabilisation mould, the Cementation Reagent containers and the pressure flow pipes needs to be sterilised after each treatment experiment to avoid cross contamination. • The Aseptic technique makes it relatively costly and time-compelling method. • The high bacterial cell concentration supplied to the soil sample have certainly increased the amount of calcite precipitated, however it has been found difficult to achieve bacterial concentrations higher than 1×10^8 cfu/mL at 37°C within a practical growth time (7-10 days).
EK-Biocementation	<ul style="list-style-type: none"> • The sufficiently large size of the EK stabilisation box enables to stabilise specimen volume of up to 5376 cm³, and provides extraction of 6 UCS samples from each experiment. • The provision of open rectangular surface enables the easy extraction of gases generated at the electrodes during the EK process and eliminates the soil heaving in the top layer. • The Polarity reversal have successfully controlled the changes in pH caused by the Electrolysis reaction. • The use of 99% pure graphite sheet (Processed Graphite Laminate SLS) electrodes have successfully eliminated the effect of heat on the soil treatment, which could potentially have a detrimental effect on bacteria. 	<ul style="list-style-type: none"> • The UCS size samples needed to be prepared from the treated soil mass for the strength determination. • The NH₄⁺ concentration for the EK treatment experiments was found to be higher compared to the PFC experiments. • The treatment duration is longer compared to the PFC treatment. • The consistently lower strengths at the middle points of the EK samples (compared to the electrode area) for all tests could be attributed to their higher moisture content, as water accumulated in the middle due to polarity reversal. In future work it will therefore be necessary to provide an effective drainage arrangement at this point.

6.3 Practical Applicability of Pressure Flow Column and EK-Biocementation Treatment Methods

In the geotechnical context the peat or organic soils are considered as “problematic” due to their low undrained shear strength, low bulk density, very high-water holding capacity, creep behaviour and generally high compressibility. These properties are interrelated to each other and effects the overall peat behaviour, for instance, creep behaviour and high compressibility associate with large settlements under existing and new structures like foundations and road or railway embankments. Hydro-geological changes in the peat have caused significant settlements and landslides at several location in the UK (Farrell, E. R. 2012). According to Hobbs (1986), 6.3% land in UK, 10.4% in Scotland and 12.4% in Northern Ireland, and historically many structures like canals and dykes has been constructed with or on peat. Hence, from geotechnical engineering aspect it is essential to understand the engineering behaviour of peat and to implement the innovative methods to stabilise it both for the new and existing structures on these soils.

This research focuses on the improvement of the engineering characteristics of organic soil from the East Anglian peat. The results of the experimental research indicate that PFC and EK-Biocementation treatments have effectively enhanced the engineering and hydromechanical characteristics of the East Anglian Peat Fens, and have the potential of successful upscale and *in-situ* applications. The use of biocementation through Pressure flow or through EK on organic soil/peat is very little explored. Several field trials and up-scaled experiments were performed to validate the effectiveness of MICP *in-situ* conditions. A brief summary of the Up-scaled MICP treatment experiments is provided in the section 2.9 and Table 2.11 where different uerolytic bacterial strains (*S. pasteurii* by Lee at al., 2019 & Gomez et al., 2019) has been used to achieve MICP mainly on sands (Van Paassen, 2011) and residual soils (Martinez, 2012). Based on the treatment variable such as applied pressure of the Cementation reagent and the applied voltage used in this research and their comparison with the variables employed by other researchers in up-scale trials it can be concluded that these treatment methods can be implemented for the MICP treatment of the organic soil/peat at the *in-situ* scale. However, the determination of the optimum treatment variables for the field application can only be determined by the upscale laboratory experiments.

6.4 Discussion on Pressure Flow Column (cementation) Treatment Results

In this study first the indigenous, non-pathogenic and ureolytic bacterial strains which are capable of producing CaCO_3 were isolated from the experimental soil. (Ureolytic bacteria are abundantly present in the soil and being indigenous the isolated bacteria would survive and perform effectively under different environmental and chemical conditions.) Besides, the urea hydrolysis reaction is considered to be a straight forward and easily controlled mechanism for CaCO_3 precipitation in MICP treatment (Duraishamy, 2016).

- The gain in shear strength of the organic soil after Pressure Flow Column treatment was recorded in the range of 8-72% compared to the relevant control samples, which is comparable to the strength improvement reported by the Lu et al., (2010) of about 25-120% and for fine sands. However, the absolute values of UCS are relatively higher compared to MICP treated loose sand (Van Paasen et al., 2009; Keykha et al., 2014, 2018, Asadi & Keykha, 2017). This could be because the untreated soil here has some shear strength due to overburden or confining pressure whereas the researchers just referred to conduct MICP cementation loose sand.
- In the present study it has been found that the amount of CaCO_3 in terms of percentage of soil mass which can effectively contribute to the soil strength is 0.85-1.28%, where 1.28% is the maximum amount of CaCO_3 precipitated. Although this validates the hypothesis that the CaCO_3 can be effectively precipitated in organic soil through urea hydrolysis, the amount of the CaCO_3 precipitation measured in this study is comparatively lower compared to that of fine sands i.e. 3.5% reported by Whiffin et al., (2007). This disparity in the % of CaCO_3 precipitation is fundamentally due to the obstructive internal structure of organic matter and its soluble ligands toward the CaCO_3 crystallisation and their growth (Lebron & Suarez, 1998). The inhibition mechanism for the developed of CaCO_3 crystals by the organic matter is explained by Lin & Singer (2006), as “the organic matter blocks the nucleation sites by developing a protective coating, thus prevents the formation of new CaCO_3 crystals and also

prevents the homogeneous growth of existing CaCO_3 crystals. However, the overall saturation conditions of the organic soil will determine the dissolution of growth of the CaCO_3 crystals”.

- The failure mechanism in the MICP treated organic soil is different from that of MICP treated sand. Van Paasen et al., (2009), explained that in bio-cemented sands the failure under applied stress occurs on breaking the bond between the sand particles and equally strong precipitated CaCO_3 . However, in the organic soils the characteristics of the organic matter (particles) controls the overall failure mechanism as the failure would occur either through the weak organic matter or through failure of bond between weak organic soil particles and strong precipitated CaCO_3 crystals.
- Due to the urea hydrolysis reaction, the unwanted end-products such as NH_4^+ ions, ammonia (NH_3) and ammonium salt are produced during MICP treatment. The production of NH_4^+ ions is vital for the pH increase and to accelerate the rate of urea hydrolysis, but the higher concentration of these would have a hostile impact on the environment such as degradation of air quality due to high ammonia concentration and ground and surface water acidification due to discharged NH_4^+ ions and therefore can adversely impact human health, animal and plant life and even a potential threat for the aquatic organisms (Keyka et al 2018). In this study it has been observed that the amount of the produced NH_4^+ ions is a direct function of the rate of urea degradation, which ultimately governs the CaCO_3 precipitation and improvement in strength. The lower reagent concentration especially (0.75 M) has produced higher NH_4^+ concentrations compared to the (1.0 M) reagent.
- As expected, the produced NH_4^+ ions due to degradation of urea increased the pH, which produced favourable conditions for further urea hydrolysis, however in the experiments it has been found that the CaCO_3 precipitation using the four selected microorganisms, especially for *Bacillus licheniformis* was optimised in the pH range of 7.2 to 7.85. This pH range is lower as compared to other CaCO_3 producing bacteria such as (pH 8.7-9.5) for *S. pasteurii* reported by (DeJong et al., 2010; Matrinez et al., 2013 etc.). This relatively low pH eliminates the

possibility of the conversion of the NH_4^+ ions into ammonium salt which usually occurs in high alkaline conditions of (pH 9.5). Similarly, the conversion of ammonium into nitrate (NO_3^-) through nitrification process by bacteria is also a process that occurs in a relatively higher alkaline environment, that is another possible method to decrease the NH_4^+ concentration while using bacterial strains such as *Pseudomonas nitrifiers*, through denitrification of ammonium produced during the urea hydrolysis.

6.4.1 Limitations and Relevant Recommendations for the Pressure Flow Column Treatment

- Since the bacteria produce the enzyme through urease activity which is required for the urea hydrolysis and they also act as nucleation sites for the CaCO_3 precipitation. Hence the concentration of the bacterial species added for the bio-cementation and the concentration of the cementation reagent are two interdependent factors that control the treatment. As anticipated, the amount of the CaCO_3 precipitation increased with increasing the bacterial concentration provided that a sufficient concentration of cementation reagent is supplied. In this research based on the rate of bacterial growth (section 4.1.1) and upon their ability to produce urease (section 4.1.2) only two concentrations i.e. 1×10^8 cfu/mL and 1×10^7 cfu/mL have been used, therefore it would be interesting to access the effect of higher bacterial concentration on the efficiency of the treatment in-terms of CaCO_3 precipitation % and further gain in strength. Moreover, in the cementation reagent the equimolar concentrations of the urea and calcium chloride have been mixed and supplied for all the treatment sets. The effect of non-equimolar solution on the metabolic activity of the bacteria should be examined in future work.
- The concentration of the produced NH_4^+ ions in most of the experimental sets has been found in excess of the allowable limits of total ammonia (NH_3 and NH_4^+) for drinking water according to UK legislation, set to 0.5 mg/L (The Water Supply (Water Quality) (Amendment) Regulations, 2018). For the successful field application of this technique there is a need to eliminate the excessive ammonium concentration. Traditionally, the excessive ammonia in the

treatment effluent is removed by flushing with a large quantity of the water. However, an alternative approach which emphasizes the mitigation of ammonium entering in the soil is gaining popularity. Keykha & Asadi, (2017), have designed and used an EK cell which facilitated the removal of NH_4^+ ions from the purpose-built reaction chamber provided in the cell. Similarly, in another laboratory study Keykha et al., (2018), have reported a successful treatment of the bacteria and urea solution with Zeolite to eliminate the NH_4^+ ions before these injected into the sand sample for MICP treatment.

- Despite the fact that microorganisms showed consistent extracellular enzyme activity throughout the duration of 96-hours (section 4.1.2), but a decline in the effluent pH from the optimum value has been observed after 48 hours (figure 5.8), which indicates that the rate of soil treatment was higher in the first 48 hours. DeJong et al., (2010), have mentioned this initial period as very crucial for the soil strength improvement as preliminary bonding between soil particles takes shape in this period. Hence based on this factor and based on the assumption that further increase in the treatment duration would proportionally increase the pH, and would generate excessive alkaline environment which is not suitable for the *Bacillus licheniformis*, the treatment duration of 3 days was adopted for all the experimental sets. On the other hand, it is expected that the amount of CaCO_3 precipitation will increase with an increase in the treatment duration, which is also clear for the figure (4.7) that indicates that even after 96-hours the concentration of the NH_4^+ ions in the effluent was almost constant, which is an indirect indication of continuous urea hydrolysis and CaCO_3 precipitation. Therefore, it is essential to determine the peak of the effective CaCO_3 precipitation (that would contribute toward the soil strength) and the optimum treatment duration (also important from an economic point of view) in order to effectively bio-cement the soil. Therefore, other treatment durations should be considered in the future work. A possible problem with a longer treatment period is the non-homogeneous precipitation of CaCO_3 due to local superposition on the nucleation sites (bacterial cell wall) (Hammes and Verstraete, 2002). This will ultimately cause cell death and a decline in the treatment efficiency. In addition to this, another recommendation is to cultivate the urease externally by mixing the bacteria with urea, and then utilise the pure

urease instead of urea + bacterial solution to precipitate the CaCO_3 . However, this would require a different protocol of microbial activity and further specialised microorganism handling training.

- In this study, the bacteria are premixed in the soil during the sample preparation (section 4.6.1) to prove that bio-cementation would work for this organic soil and to avoid the impediments regarding the uniform bacteria delivery in the soil specimen. However, this is not a feasible approach for large scale in-site application of the method. The delivery of the bacteria and cementation reagent under existing infrastructure still remains a major challenge and can lead to increase costs. Duraisamy (2016), has presented some effective results while employing the deep mixing approach to supply the gram-positive bacteria (similar to this study) into the soil. The possible reason for pre-mixing working in this case could be the ability of the gram-positive bacteria to withstand the external forces that were applied during mixing due to their thick and rigid cell walls which potentially protect bacterium from lysis or puncture. However, the deep mixing method is avoided by other researchers due to the same concern of bacterial viability under industrial mixing stresses.
- The flow pressure of the injected cementation reagent can be another factor that affects Pressure Flow Column treatment. Ng et al., (2014), have showed that the variation in flow pressure can produce different quantities of precipitated CaCO_3 and soil strength. Excessive pressure led to development of excessive pore pressures. Very low flow pressure led to localised CaCO_3 precipitation due to an insufficient injection distance. However, to reduce the number of variables in this research the pressure is kept constant to (150 kPa) for all the Pressure Flow Column experiments. Therefore, it is another aspect which requires further research.

6.5 Discussion on EK-Biocementation Treatment Results

The electrochemical phenomena generated due to application of electric potential are mainly responsible for the transportation of the bacteria and chemical species across the soil. The calcium ions (Ca^{2+}) have a positive charge hence can be transported via electromigration (Chen, 2003) and when are added in the dissolved form as reagent then can also be transported via electro-osmosis. Similarly, Urea ($\text{CO}(\text{NH}_2)_2$) is a non-ionic organic compound and can be transported via electro-osmosis when dissolved in the reagent. *Bacillus licheniformis* is a gram-positive bacterium, and showed a higher enzyme urease activity (section 4.1.2), and since having negative surface charge so can migrate under the application of electric potential.

- EK-Biocementation provided better results compared to the pressure flow treatment. The maximum gain in strength was recorded as 10.1 % higher (EK-11) compared to the maximum strength achieved in the Pressure Flow Column treatment method (PFC-18), and 32.8 % higher compared to the respective pressure flow column experiment (PFC-19) where same bacterial strain i.e. (*Bacillus licheniformis*) and same population concentration of 1×10^8 cfu/mL was used.
- EK treatment has been conducted on three different degrees of saturations. The increase in the soil strength with degree of saturation is observed in all experimental sets, but with an exception to the middle of the sample (with respect to the electrodes). An intermediate degree of saturation ($S_r = 85\%$) showed better results than both higher and lower degrees of saturation. This was especially the case for the middle of specimen. However, for a specific degree of saturation (S_r) the variation in moisture content at different locations of the soil specimen i.e. (near electrodes and in middle) has been found consistent, which indicates that the gain in strength is independent of the moisture content and is due to the combined effect of EK-bacteria treatment.
- Associated with increased soil strength an increase in the CaCO_3 content % has also been observed for the EK-biocemented soil samples. The maximum CaCO_3 precipitation has been found to be approximately twice (98.8%) higher

compared to the relevant column flow experiment. The lowest CaCO₃ precipitation % has been observed in the middle of the samples (1.24%), which is till 34.88% higher compared to the Pressure Flow Column treatment. This indicates that despite having higher water content in the middle, the EK-treatment still managed to bio-cement the organic soil effectively.

- The NH₄⁺ ion concentration for the EK treatment has been found to be significantly higher up to (177%) compared to the respective pressure flow column experimental set.

6.5.1 EK-Biocementation Treatment (Limitations and Recommendations)

- Based on the results obtained from the Pressure Flow Column treatment, only one bacterial strain of *Bacillus licheniformis*. at the concentration of 1 x 10⁸ cfu/mL has been used for the EK-Biocementation treatment, while the other 4 bacterial strains and the diluted concentration of 1 x 10⁷ cfu/mL have been ignored. Though, the selected bacterial strain and the population concentration has showed an effective treatment result, further research it is strongly recommended to employ other ureolytic bacterial strains which are capable of producing CaCO₃ for the EK-biocementation.
- The accumulation of higher moisture contents near the middle of the samples is possibly due to polarity reversal, the build-up of more NH₄⁺ ions concentration and the relatively higher pH in the middle portion of the samples are the main factors behind the less effective soil treatment in this portion, which resulted in lower CaCO₃ precipitation and strength improvement. All these factors highlight the need for an improved design of the EK treatment cell by having an effective drainage arrangement.
- A constant voltage gradient of 0.4 V/cm was maintained throughout the EK treatment tests. The selection of this low intensity electric potential was made on the basis of recommendations presented in the literature and to avoid any potential harm to the bacteria. However, Mena et al., (2016), have shown that higher voltage gradient of 1.5 V/cm has provided the more effective results

compared to the lower voltage gradient, and did not affect the indigenous bacterial species. Therefore, it would be worth analysing the effect of higher electric potential on the soil treatment, as the voltage gradient can be utilised to accelerate the rate of negatively charged bacterial migration via electro-osmosis. In addition to this the application of higher electric gradient could potentially reduce the treatment duration (14 days in this research), which can effectively reduce the energy consumption and cost related to the EK treatment.

- A 24-hours periodic polarity reversal has been employed in all the EK treatment experiments. The main purpose of the polarity reversal was to enhance the treatment process by inducing the EK phenomena from both ends at the same time, and to regulate the pH gradient that would form due to the hydrolysis reaction. The polarity reversal has managed to regulate the pH of both compartments so they are close to the natural and starting pH. This has effectively produced a homogeneous treatment at both ends (near electrodes), but the polarity reversal also has caused the incomplete migration of bacteria and chemical species from one end to other. This is due to the short period (24-hours) of polarity reversal. Researchers have different recommendations regarding the polarity reversal duration, Mena et al., (2016), have reported that 24-hour polarity reversal is more effective than a long duration reversal. On the other hand, Keykha et al., (2014), have mentioned that polarity reversal after 150-hours produced better results as it allows the complete migration of species from one end to other before polarity reversal.
- Thus, another recommendation is to examine the effect of reversing polarity at different rates. Moreover, the above explained phenomena of insufficient applied voltage gradient and incomplete migration of bacteria and chemical species due to short periodic polarity reversal could be the potential factors for the lower treatment results achieved in EK (Batch 4) experiments, where the bacterial strain was prepared in aqueous solution of Nutrients and were introduced at the electrolyte chamber to be injected into soil via electrochemical reactions.

- The concentration of the cementation reagent is another factor that requires further investigation in the case of EK-biocementation treatment. Here in this research, the experiments were started with the (1.0 M) concentration cementation reagents and delivered promising results thus the concentration was kept constant to 1.0 M to decrease the number of variables and experiments. However, the (0.75 M) reagent concentration which provided best results for Pressure Flow Column treatment should be used for further treatment.

6.6 Conclusions

From this experimental research it can be concluded that Pressure Flow biocementation and Electrokinetic-Biocementation treatment have effectively and considerably contributed to enhancing the engineering and hydromechanical characteristics of the East Anglian Peat Fens. Generally, MICP was mostly used for sands, hence this successful application of MICP treatment for the organic soil will broaden its application to other soil types. After this series of experimental tests, the following conclusions can be drawn from the research:

- The main aim of proving the feasibility of bio-cementation, as a potential method of improving Peat Fens soil was achieved, as the maximum increase in soil strength compared to untreated soil (C1) has been found to be 128.48% and 151.63% higher for Pressure Flow Column treatment and EK-biocementation respectively.
- The maximum increase in strength obtained from EK treatment was recorded to be 10.1 % higher (EK-11) as compared to the maximum strength achieved in the Pressure Flow Column treatment method (PFC-18), and 32.8 % higher as compared to the respective pressure flow column experiment (PFC-19) where same bacterial strain i.e. (*Bacillus licheniformis*.) and same population concentration of 1×10^8 cfu/mL has been used. This confirmed that the soil pH and the application of low intensity direct current in the EK treatment can boost the microbial metabolic activity.
- The primary objective of assessing the optimised treatment conditions was achieved. The most effective treatment parameters for the MICP treatment are (*Bacillus licheniformis*.) with the population concentration of 1×10^8 cfu/mL, Cementation Reagent concentration of (0.75 M), treatment duration of (3 days) at the reagent flow pressure of 150 kPa.
- The objective of isolating and screening suitable bacterial strains for biocementation has been achieved. The study has identified four new indigenous, non-pathogenic, ureolytic bacterial strains i.e. (*Bacillus*

licheniformis, *Rhodococcus erythropolis*, *Micrococcus luteus*, and *Lysinibacillus fusiformis*) which have the potential to precipitate the CaCO_3 through urea hydrolysis.

- The maximum CaCO_3 content was found to be 1.28% and 1.71% for the Pressure Flow Column treatment and EK-biocementation respectively. Whereas, it has been noted that a minimum of 0.85% CaCO_3 precipitation is required to attain the determinate strength gain. On the other hand, it was noticed that 0.85% CaCO_3 was sufficient for strength gains of 71-87% compared to that of untreated soil.
- An efficient treatment of the soil and the avoidance of an extreme pH front formation was achieved by polarity reversal. However, the period of polarity reversal requires further research. Moreover, the maximum temperature observed during the 14-days EK treatment was about 37.25°C , which indicates that the electrodes made of 99% pure graphite sheet (Processed Graphite Laminate SLS), very effectively controlled the rise in temperature, and successfully eliminated the effect of heat on the soil treatment.
- For all EK experimental sets, a saturation ratio of 85% showed least variation in moisture content and effective strength gain throughout the soil specimen. Higher values ($S_r = 95\%$) displayed slightly better strengths but mainly in areas near to the electrodes. On the other hand, lower saturations ($S_r = 75\%$) was not able to produce significant increase in soil strength.
- The key objective of measure unwanted end-products has been achieved. The resulting NH_4^+ concentrations for both treatment methods has been found to be considerably above the allowable limit of 0.5 mg/L. This indicates that NH_4^+ mitigation techniques explained in the beginning of this chapter should be utilised.
- Both treatments have effectively improved the stress-strain and consolidation behaviour of the organic soil.

- The scanning electron microscopy (SEM) and energy dispersed spectrum (EDS) analysis confirmed the precipitation of CaCO_3 crystals in the treated organic soil.

References

- Abdallah, I., Malkawi, H., Ahmed, S.A., and Osama, T.A., (1999). Effects of Organic Matter on the Physical and the Physicochemical Properties of an Illitic Soil, *Applied Clay Science*, Vol. 14, pp.257-278.
- Achal, V., Mukherjee, A., Basu, P.C., Reddy, M.S., (2009). Strain improvement of *Sporosarcina pasteurii* for enhanced urease and calcite production. *Journal of Industrial Microbiology* 36(7):981-8. DOI: 10.1007/s10295-009-0578-z
- Achal, V., Mukherjee, A., Kumari, D., Zhang, Q., (2015). Biomineralization for sustainable construction—a review of processes and applications. *Earth Sci Rev* 148:1–17.
- Ahmad, K., Kassim, K. N., & Taha, M. R., (2006). Electroosmotic flows and electromigrations during electrokinetic processing of tropical residual soil *Malaysian Journal of Civil Engineering*, 18(2), 74-88.
- Al-Khafaji, A. W. N., & Andersland, O. B., (1981). Compressibility and strength of decomposing fibre. *Geotechnique*, 31, 497-508.
- Al Qabany, A., Soga, K., and Santamarina, C., (2012), Factors Affecting Efficiency of Microbially Induced Calcite Precipitation, *J. Geotech. Geoenviron. Eng.*, Vol. 138, No. 8, pp. 992–1001, [https://doi.org/10.1061/\(ASCE\)GT.1943-5606.0000666](https://doi.org/10.1061/(ASCE)GT.1943-5606.0000666)
- Al Qabany, A., Soga, K., (2013). Effect of chemical treatment used in micp on engineering properties of cemented soils. *Geotechnique* 63(4):331-339.
- Al-Thawadi, S.M., (2008). High strength in-situ biocementation of soil by calcite precipitating locally isolated ureolytic bacteria. PhD Thesis, Murdoch University, Perth, WA.
- Al-Thawadi, S.M., (2011). Ureolytic bacteria and calciumcarbonate formation as a mechanism of strength enhancement of sand. *J Adv Sci Eng Res* 1:98-114.
- Al-Thawadi, SM., (2013). Consolidation of sand particles by aggregates of calcite nanoparticles synthesized by ureolytic bacteria under non-sterile conditions. *J Chem Sci Technol* 2(3):141-146.
- Alshawabkeh, A. N. (2001). Basics and application of electrokinetic remediation. Handouts prepared for a short course. Handouts Prepared for a Short Course. Federal University of Rio de Janeiro, Rio de Janeiro.

- American Society for Testing and Materials (ASTM) (2014). ASTM D2974-14: Standard Test Methods for Moisture, Ash and Organic Matter of Peat and Other Organic Soils, West Conshohocken, PA: ASTM International.
- American Public Health Association/American Water Works Association/Water Environmental Federation (APHA/AWWA/WEF). (2005). Standard methods for the examination of water and wastewater, Washington, DC.
- Acar, Y. B., & Alshawabkeh, A. N. (1993). Principles of electrokinetic remediation. *Environmental Science & Technology*, 27(13), 2638-2647.
- Arias, D., Cisternas, L. A., Rivas, M. (2017). Biomineralization Mediated by Ureolytic Bacteria Applied to Water Treatment: A Review, *Crystals*, 7 (11): 345 <https://doi:10.3390/cryst7110345>
- Arman, A. 1971. Discussion in *Geotechnique*, 21, 418-421 on a paper by Skempton & Petley (1970).
- ARUP (2010) Risk-based framework for geotechnical asset management: Phase 2 Report. (online) Available from: <https://highwaysengland.co.uk/knowledge-compendium/knowledge/publications/a-risk-based-framework-for-geotechnical-asset-management/index.html>. Assessed 23/01/2020
- Asadi, A., Huat, B.B.K., Hanafi, M.M., (2010). Physicochemical sensitivities of tropical peat to electrokinetic environment. *Geosci J* 14, 67-75
- Asadi, A., Huat, B. K. B., Nahazanan, H., & Keykhah, H. A. (2013). Theory of Electroosmosis in Soil. *International Journal of Electrochemical science*, 8(1016-1025).
- ASTM. (2006). "Standard test method for unconfined compressive strength of cohesive soil." D2166-06, West Conshohocken, PA.
- ASTM D2974-20e1 (2018). Standard test method for determining the water (Moisture) content, ash content, and organic material of peat and other organic soils.
- ASTM D5715-00 (2006). Standard test method for estimating the degree of humification of peat and other organic soils (visual/manual method).
- Avery, B.W. (1980). *Soil Classification for England and Wales (Higher Categories)*. Soil Survey Technical Monograph No.14.
- Bachmeier, K. L., Williams, A. E., Warmington, J. R., and Bang, S. S. (2002). "Urease activity in microbiologically-induced calcite precipitation. *J. Biotechnol.*, 93(2), 171-181.

- Barba, S, Villaseñor, J, Cañizares, P, Rodrigo, M. (2018). Strategies for the electrobioremediation of oxyfluorfen polluted soils. *Electrochimica Acta*.
- Barber, K. E., (1981). *Peat Stratigraphy and Climatic Change*. Balkema, Rotterdam.
- Barden, L., (1983). Application of consolidation theory for peat to the design of a reclamation scheme by preloading. *Quarterly Journal of Engineering Geology*, 16, 103-112.
- Barden, L., and Poskitt, T. J., (1972). The consolidation of peat. *Geotechnique*, 22, 27-52.
- Barden, L., and Vickers, B. (1975). Consolidation of fibrous peat. *Journal of the Geotechnical Engineering Division of the American Society of Civil Engineers*. Vol. 101, GT8, pp 741-753.
- Barker, J. E., Rogers, C. D. F., Boardman, D. I., and Peterson, J., (2004). Electrokinetic stabilisation: an overview and case Study, *Ground Improvement* 8(2): 47-58.
- Béguin, R., et al. (2019). Experimental Tests of Soil Reinforcement Against Erosion and Liquefaction by Microbially Induced Carbonate Precipitation. In: Bonelli S., Jommi C., Sterpi D. (eds) *Internal Erosion in Earthdams, Dikes and Levees. EWG-IE 2018. Lecture Notes in Civil Engineering*, vol 17. Springer, Cham
- Bisset, K.A., and Street, J., (1973). Morphological Phases in the Swarm of *Bacillus licheniformis*. *Journal of General Microbiology*. 76: 369-373
- Boelter, D.H., (1974). The hydrologic characteristics of undrained organic soils in the Lake States. In: *Histosols, their characteristics, classification and use* (Ed. M. Stelly), Soil Science Society of America Special Publication No.6: 33-46.
- Botusharova, S., Gardner, D., and Harbottle, M., (2020). Augmenting microbially induced carbonate precipitation of soil with the capability to self-heal. *Journal of Geotechnical and Geoenvironmental Engineering* 146(4), article number: 4020010
- Boylan, N., Jennings, P., and Long, M., (2008). Peat slope failure in Ireland. *Quarterly Journal of Engineering Geology and Hydrogeology*, 41, 93–108.
- Brandon, T.L., Brown, J.J., Daniels, W. L., De Fazio, T.L., Filz, G.M., Mitchell, J.K., Musselman, J., and Forsha, C., (2009). Rapid stabilisation/polymerisation of wet clay soils; literature review. Report AFRL

- British Standards Institution (1999). Code of Practice for Site Investigations. London: BSI, BS 5930.
- BSI (1990). BS 1377: 1990: Methods of test for soils for civil engineering purposes. Classification tests. BSI, London, UK.
- BSI (2005). BS ISO 10390:2005 Soil quality. Determination of pH, BSI, London, UK.
- BSI (2017) BS EN ISO 11508:2017 Soil quality. Determination of particle Density, BSI, London, UK.
- BSI (2018). BS EN ISO 14688-1:2018 Geotechnical investigation and testing- Identification and classification of soil. Part 1: Identification and description, BSI, London, UK.
- Burbank, M.B., Weaver, T.J., Williams, B.C., and Crawford, R.L., (2012). Urease activity of ureolytic bacteria isolated from six soils in which calcite was precipitated by indigenous bacteria. *Geomicrobiol J* 29(4):389-395.
- Cabalar, A.F., Karabash, Z., Erkmen, O., (2018). Stiffness of a biocemented sand at small strains, *European Journal of Environmental and Civil Engineering*, 22(10): 1238-1256
- Cacchio, P., Ercole, C., Cappuccio, G., and Lepidi, A. (2003). "Calcium carbonate precipitation by bacterial strains isolated from a limestone cave and from a loamy soil." *Geomicrobiol. J.*, 20(2), 85-98.
- Canakci, H., Sidik, W., Kilic, I.H., (2015). Effect of bacterial calcium carbonate precipitation on compressibility and shear strength of organic soil. *Soils and Foundations* 2015;55(5):1211-1221.
- Casagrande, A., (1936). The determination of the preconsolidation load and its practical significance. In *Proceedings of the 1st International Conference on Soil Mechanics and Foundation Engineering*, 22-26 June, 1936, Cambridge, MA, vol. 3, pp. 60-64.
- Casagrande, L., (1966). Construction of embankments across peaty soils. *Proceedings of Boston Society of Civil Engineers*, 73, No 3, July.
- Chen, M., Xu, P., Zeng, G., Yang, C., Huang, D. and Zhang, J. (2015). Bioremediation of Soils Contaminated with Polycyclic Aromatic Hydrocarbons, Petroleum, Pesticides, Chlorophenols and Heavy Metals by Composting: Applications, Microbes and Future Research Needs. *Biotech. Advances*, 33, 745-755.
- Cheng, L., (2012). Innovative ground enhancement by improved microbially induced CaCO₃ precipitation technology. PhD Thesis, Murdoch University, Perth, WA.

- Cheng, L., Cord-Ruwisch, R., and Shahin, M.A., (2013). Cementation of sand soil by microbially induced calcite precipitation at various degrees of saturation. *Can Geotech J* 50(1):81–90.
- Cheng, L., Cord-Ruwisch, R., (2014). Upscaling effects of soil improvement by microbially induced calcite precipitation by surface percolation. *Geomicrobiol J* 31(5):396–406.
- Cheng, L., Shahin, M.A., Addis, M., Hartanto, T., Elms, C., (2014). Soil stabilisation by Microbial-Induced Calcite Precipitation (MICP): investigation into some physical and environmental aspects. In: 7th International Congress on Environmental Geotechnics. Melbourne, Australia.
- Choi, S.G., Wu, S., and Chu, J., (2016). Biocementation for sand using an eggshell as calcium source. *J. Geotech. Geoenviron. Eng.*, 142, 06016010.
- Choi, S.G., Hoang, T., and Park, S.S., (2019). Undrained Behavior of Microbially Induced Calcite Precipitated Sand with Polyvinyl Alcohol Fiber, *Applied Sciences*, 9, 1214; doi:10.3390/app9061214
- Chu, J., Ivanov, V., Naeimi, M., Stabnikov, V., and Liu, H.L., (2014). Optimization of calcium-based bioclogging and biocementation of sand, *Acta Geotechnica* (2014) 9:277-285.
- Clements, L.D., Miller, B.S., Streipsa, U.N., (2002). Comparative Growth Analysis of the Facultative Anaerobes *Bacillus subtilis*, *Bacillus licheniformis*, and *Escherichia coli*. *Systematic and Applied Microbiology*, 25(2): 284-286
- Clymo, R. S. (1983). Peat: Ecosystems of the world. In Gore, A., ed., *Mires: Swamp, Bog, Fen and Moor. Ecosystems of the World* 4: 159-224.
- Coulter, J.K., (1957). Development of the peat soils in Malaya. *Malaysian Agricultural Journal* 40: 188-199.
- Dadda, A., (2017), Relation between microstructural properties and strength parameters of biocemented sands; Proceedings of the 6th International Young Geotechnical Engineers' Conference (iYGEC6) 16-17 Sept. 2017, Seoul National University, Seoul, Korea
- Danjo, J., and Kawasaki, S., (2016). Microbially Induced Sand Cementation Method Using *Pararhodobacter* sp. Strain SO1, Inspired by Beachrock Formation Mechanism, *Materials Transactions*, <https://doi:10.2320/matertrans.M-M2015842>
- Dawson, Q.L., (2006). Low-lying agricultural peatland sustainability under managed water regimes. PhD thesis, Cranfield University at Silsoe.
- Degago, S. A., Grimstad, G., Jostad, H. P., Nordal, S., and Olsson, M., (2011). Use and misuse of the isotache concept with respect to creep hypotheses A and B. *Geotechnique*, 61, No. 10, 897–908.

- DeJong, J. T., Mortensen, B., & Martinez, B., (2007). Bio-soils interdisciplinary science and engineering initiative, Final Report on Workshop, 84 pp. Arlington, VA, USA: National Science Foundation.
- DeJong, J.T., Mortensen, B.M., Martinez, B.C., and Nelson, D.C., (2010). Bio-mediated soil improvement. *Ecological Engineering* 36(2): 197-210.
- DeJong, J.T., Soga, K., Kavazanjian, E., (2013). Biogeochemical processes and geotechnical applications: opportunities and challenges, *Geotechnique* 63, No. 4, 287-301. [<http://dx.doi.org/10.1680/geot.SIP13.P.017>]
- Den Haan, E. J., (1996). A compression model for non-brittle soft clays and peat. *Geotechnique*, 46, 1–16.
- Department of Transport (2017) Connecting people a strategic vision for rail; moving Britain ahead. (online) Available from: <https://www.gov.uk/government/publications/a-strategic-vision-for-rail>. Accessed 26/03/2020
- Dhami, N.K., Reddy, M.S., and Mukherjee, A., (2013). Biomineralization of calcium carbonates and their engineered applications: a review. *Frontiers Microb* 4:1-13.
- Dhami, N. K., Alsubhi, W. R., Watkin, E., and Mukherjee, A. (2017). “Bacterial community dynamics and biocement formation during stimulation and augmentation: implications for soil consolidation.” *Front. Microbiol.* DOI: 10.3389/fmicb.2017.01267.
- Driessen, P.M., and Rochimah, L., (1976). The physical properties of lowland peats from Kalimantan. Soil Resources Institute, Bogor, Indonesia. *Bulletin* 3: 567-573.
- Dupraz, C., Reid, R.P., Braissant, O., Decho, A., Norman R.S., and Visscher, P.T., (2009). Processes of carbonate precipitation in modern microbial mats. *Earth-Science Reviews* 96(3): 141-162. <https://doi.org/10.1016/j.earscirev.2008.10.005>
- Duraisamy, Y., (2016). Strength and stiffness improvement of bio-cemented Sydney sand. PhD thesis, University of Sydney, Australia.
- Edil, T. B., and Wang, X., (2000). Shear strength and K_0 of peats and organic soils. In *Geotechnics of High Water Content Materials*, ASTM STP 1374 (eds Edil, T. B. and Fox, P. J.). Pennsylvania: ASTM, pp. 209-225.
- EN ISO 14688-1:2002. Geotechnical Investigation and Testing-Identification and Classification of Soil. Part 1: Identification and Description (ISO14688-1:2002).

- EN ISO 14688-2:2004. Geotechnical Investigation and Testing-Identification and Classification of Soil. Part 2: Principles of Classification (ISO14688-2:2004).
- Esring, M.I., and Henkel, D.J., (1968), The use of electrokinetics in the raising of submerged partially buried metallic objects, Soil Engineering Series Research Report, No. 7, Cornell University, Ithaca, N.Y.
- European commission (EC) (2010) Opinion of the Committee of the Regions and Action Plan on Urban Mobility OJ C 232, 27.8.2010, p 29-35 (online) Available from:
<https://eur-lex.europa.eu/LexUriServ/LexUriServ.do?uri=OJ:C:2010:232:0029:0035:EN:PDF>. Accessed 25/04/2020.
- Everley, R.A., Mott, T. M., Wyatt, S. A., Toney D. M., and Croley, T. R., (2008). Liquid chromatography/mass spectrometry characterization of *Escherichia coli* and *Shigella* species. J. Am. Soc. Mass Spectrom. 19 1621-1628. 10.1016/j.jasms.2008.07.003.
- Farrell, E. R. (2012). Organics/peat soils. Manual of Geotechnical Engineering, institution of Civil Engineers. Chapter 35, 463-479.
- Farrell, E. R., and Hebib, S., (1998). The determination of the geotechnical properties of organic soils. In Proceedings of the International Symposium on Problematic Soils. Sendai, Japan.
- Farrell, E. R., Jonker, S. K., Knibbelerb, A. G. M., and Brinkgreve, R. B. J., (1999). The use of direct simple shear test for the design of a motorway on peat. In Proceedings of the 12th European Conference on Soil Mechanics and Geotechnical Engineering, vol. 2 (eds Barends, F. B. J. et al.). Brookfield, VT: Balkema, pp. 1027-1033.
- Ferris, F.G., Phoenix, V., Fujita, Y., and Smith, R.W., (2004). Kinetics of calcite precipitation induced by ureolytic bacteria at 10 to 20°C in artificial groundwater. Geochim Cosmochim Acta 68(8):1701-1710.
- Fourie, A.B., Jones, C.J.F.P., (2010). Improved estimates of power consumption during dewatering of mine tailings using electrokinetic geosynthetics (EKGs), Geotextiles and Geomembranes, 28: 181–190.
- Fu, H., Yuan, L., Wang, J., Cai, Y., Hu, X., and Geng, X., (2019). Influence of High voltage gradients on Electrokinetic Dewatering for wenzhou Clay Slurry improvement, Soil Mechanics and Foundation Engineering, 55 (6): 400-407.

- Gao, Y., Hang, L., He, J., and Chu, J., (2018). Mechanical behaviour of biocemented sands at various treatment levels and relative densities *Acta Geotechnica*
- Gao, Y., Xinyi, Tang, X., Chu, J., & He, J., (2019). Microbially Induced Calcite Precipitation for Seepage Control in Sandy Soil, *Geomicrobiology Journal*, 36:4, 366-375.
- Gill, R.T., et al., (2016). Sustainability assessment of electrokinetic bioremediation compared with alternative remediation options for a petroleum release site. *Journal of Environmental Management*, 2016. 184(1): p. 120-131.
- Gill, R.T., Harbottle, M.J., Smith, J.W.N., and Thornton, S.F., (2014). Electrokinetic-enhanced bioremediation of organic contaminants: A review of processes and environmental applications. *Chemosphere* 107, pp. 31-42.
- Glendinning, S., Lamont-Black, J., Jones, C. J. F. P., and Hall, J., (2008). Treatment of lagooned sewage sludge in situ using electrokinetic geosynthetics, *Geosynthetics International*, 15(3): 192-204
- Gomez, M.G., Anderson, C.M., Graddy, C.M.R., DeJong, J.T., Nelson, D.C., and Ginn, T.R., (2017). Large-Scale Comparison of Bioaugmentation and Biostimulation Approaches for Biocementation of Sands *J. Geotech. Geoenviron. Eng.*, 143(5): 04016124
- Gomez, M.G., Graddy, C.M.R., DeJong, J.T., & Nelson, D.C., (2019). Biogeochemical changes During Bio-cementation Mediated by Stimulated and Augmented Ureolytic Microorganisms *Scientific Reports* 9:11517.
- Gowthaman, S., Mitsuyama, S., Nakashima, K., Komatsu, M., Kawasaki, S., (2019). Biogeotechnical approach for slope soil stabilization using locally isolated bacteria and inexpensive low-grade chemicals: A feasibility study on Hokkaido expressway soil, Japan, *Soils and Foundations* 59: 484-499
- Guy, L., Gilles, G., and Fabien, B., (2004). A case record of electroosmotic consolidation of soft clay with improved soil-electrode contact. *Canadian Geotechnical Journal*, 41(6), 1038-1038.
- Hamdan, N., Kavazanjian, E. Jr., Rittmann, B.E., and Karatas, I., (2016). Carbonate Mineral Precipitation for Soil Improvement Through Microbial Denitrification, *Geomicrobiology Journal*, DOI: 10.1080/01490451.2016.1154117
- Hammes, F., Verstraete, W., (2002). Key roles of ph and calcium metabolism in microbial carbonate precipitation. *Rev Environ Sci Bio/Technol* 1:3-7.

- Hanrahan, E. T., (1954). An investigation into some physical properties of peat. *Geotechnique*, 4, 108–123.
- Hanrahan, E. T., (1964). A road failure on peat. *Geotechnique*, 14, 185–202.
- Hanrahan, E. T., Dunne, J. M., and Sodha, V. G., (1967). Shear strength of peat. In *Proceedings of the Geotechnical Conference, Oslo*, vol. 1, 193-198.
- Harbottle, M.J., Lear, G., Sills, G. C., and Thompson, I. P., (2009), Enhanced biodegradation of pentachlorophenol in unsaturated soil using reversed field electrokinetics. *Journal of Environmental Management* 90 (5), pp. 1893-1900.
- Harkes, M.P., van Paassen, L.A., Booster, J.L., Whiffin, V.S., and van Loosdrecht, M.C.M., (2010). Fixation and distribution of bacterial activity in sand to induce carbonate precipitation for ground reinforcement. *Ecol Eng* 36 (2):112–117.
- Hassan, I., Mohamedel Hassan, E., Yanful, E.K., and Yuan, Z.C., (2016). A review article: Electrokinetic Bioremediation Current Knowledge and New Prospects. *Advances in Microbiology*, 6, 57-72. <https://dx.doi.org/10.4236/aim.2016.61006>
- Hataf, N., and Baharifard, B., (2020). Reducing Soil Permeability Using Microbial Induced Carbonate Precipitation (MICP) Method: A Case Study of Shiraz Landfill Soil, *Geomicrobiology Journal*, 37:2, 147-158
- Hausmann, M. R. (1990). *Engineering principles of ground modification*: McGraw-Hill
- Hobbs, N. B. (1986). Mire morphology and the properties and behavior of some British and foreign peats. *Quarterly Journal of Engineering Geology*, 19, 7-80.
- Hobbs, N. B. (1987). A note on the classification of peat. *Geotechnique*, 37(3), 405-407.
- Hogan, J. M., van der Kamp, G., Barbour, S. L., and Schmidt, R., (2006). Field methods for measuring hydraulic properties of peat deposits. *Hydrological Processes*, 20, 3635–3649.
- Inagaki, Y., Tsukamoto, M., Mori, H., Sasaki, T., Soga, K., Al Qabany, A., and Hata, T., (2011). The influence of injection conditions and soil types on Soil improvement by microbial functions, *Geo-Frontiers 2011*, ASCE, pp. 4021-4030
- Ingram, H. A. P., (1983). Hydrology. In *Ecosystems of the World. Vol. 4A: Mires: Swamp, Bog, Fen and Moor* (ed. Gore, A. J. P.). Oxford: Elsevier, pp. 67–158.

- Ivanov, V., Stabnikov, V., and Chu, J., (2016), Sealing of sand using spraying and percolating biogROUTS for the construction of model aquaculture pond in arid desert, *International Aquatic Research* (2016) 8:207–216
- Ivanov, V., Stabnikov, V., (2017). *Construction Biotechnology: Biochemistry. Microbiology and Biotechnology of construction materials and processes*, Springer, Singapore.
- Iyer, R. (2001). *Electrokinetic Remediation. Particulate Science and Technology*, 19, 219-228. DOI: 10.1080/02726350290057813.
- Jayasekera, S., "Stabilising volume change characteristics of expansive soils using electrokinetics: a laboratory based investigation." 2007.
- Jayasekera, S. (2008). *An investigation into modification of the engineering properties of salt affected soils using electrokinetics. Dissertation/Thesis, University of Ballarat.*
- Jayasekera, S. and Hall, S., "Modification of the properties of salt affected soils using electrochemical treatments." *Geotechnical and Geological Engineering*. 25(1), 2007, pp. 1-10.
- Jones, C.J.F.P., Lamont-Black, J., Glendinning, S., White, C., and Alder, D., (2014). The environmental sustainability of electrokinetic geosynthetic strengthened slopes. *Engineering Sustainability ICE* 167 (ES3), 95e107.
- Kellner, E., Waddington, J. M., and Price, J. S., (2005). Dynamics of biogenic gas bubbles in peat: potential effects on water storage and peat deformation. *Water Resource Research*, 41, W08417. DOI:10.1029/2004WR003732.
- Keykha, H.A., Huat, B.B.K., and Asadi, A., (2014a). Electro-biogROUTING stabilisation of soft soil. *Environ Geotech* 2(5):292–300. doi: 10.1680/envgeo.13.00068.
- Keykha, H., A., Huat, B.B.K., and Asadi, A., (2014b). Electrokinetic stabilisation of soft soil using carbonate-producing bacteria, *Geotechnical & Geological Engineering*, 32: 739-747.
- Keykha, H.A., Asadi, A., & Zareian, M., (2017). Environmental Factors Affecting the Compressive Strength of Microbiologically Induced Calcite Precipitation-Treated Soil, *Geomicrobiology Journal*, 34:10, 889-894.
- Keykha, H.A., Asadi, A., (2017). Solar powered electro-bio-stabilization of soil with ammonium pollution prevention system. *Advances in Civil Engineering Materials*, Vol. 6, No. 1, 2017, pp. 360–371, <https://doi.org/10.1520/ACEM20170001>. ISSN 2379-1357.

- Keykha, H.A., Mohamadzadeh, H., Asadi, A., and Kawasaki, S., (2018). Ammonium-free carbonate producing bacteria as an eco-friendly soil biostabilisation. *Geotechnical Testing Journal* 42, no. 1 (2018): 19-29. doi.org/10.1520/GTJ20170353
- Lageman, R., Godschalk, M.S., (2007), Electro-bioreclamation. A combination of in situ remediation techniques proves successful at a site in Zeist, the Netherlands. *Electrochimica Acta*; 52(10 SPEC. ISS.):3449-3453.
- Lamont-Black, J., Jones, C.J.F.P., and White, C., (2015). Electrokinetic geosynthetic dewatering of nuclear contaminated waste, *Geotextiles and Geomembranes*, 43: 359-362.
- Lamont-Black, J., Jones, C.J.F.P., and Alder, D., (2016). Electrokinetic strengthening of slopes - Case history, *Geotextiles and Geomembranes*, 44(3), 319-331
- Lamont-Black, J. Hall, J.A., Glendinning, S. Jones, C.J.F.P., and White, C. (2012). Stabilisation of a railway embankment using electrokinetic geosynthetics. In *Earthworks in Europe (Radford TA (ed.))*. Geological Society, London, UK, Special Publication no. 26, pp. 125–139.
- Landva, A. O., (1980a). Vane testing in peat. *Canadian Geotechnical Journal* 17, 1-19.
- Landva, A. O., and Pheaney, P. E., (1980). Peat fabric and structure. *Canadian Geotechnical Journal*, 17, 416–435.
- Landva, A. O., and La Rochelle, P., (1983). Compressibility and shear characteristics of Radforth peats. In *Testing of Peat and Organic Soils*, STP 820 (ed. Jarrett, P. M.), West Conshohocken, PA: ASTM, pp. 157-191.
- Landva, A. O., Korpijaakko, E. O. and Pheaney, P. E. (1983). Geotechnical classification of peats and organic soils. In *Testing of Peat and Organic Soils*, STP 820 (ed. Jarrett, P. M.), West Conshohocken, PA: ASTM, 37-51.
- Lea, N. D., and Brawner, C. O., (1963). Highway design and construction over peat deposits in Lower British Columbia. *Highway Research Record*, 7, 1-32.
- Lear, G., Harbottle, M.J., van der Gast, C.J., Jackman, S.A., Knowles, C.J., Sills, G., and Thompson, I.P., (2004). The effect of electrokinetics on soil microbial communities. *Soil Biology & Biochemistry* 36(2004) 1751-1760.
- Lear G., Harbottle M.J., Sills G., Knowles C.J., Semple K.T., Thompson I.P., (2007). Impact of electrokinetic remediation on microbial communities within PCP contaminated soil, *Environmental Pollution* 146: 139-146.
- Lebron, I., and Surez, D.L., (1996). Calcite nucleation and precipitation, kinetics as effected by dissolved organic matter at 25°C and pH 4-7.5. *Geom. Cosmochim. Acta* 60(15), 2765-2776.

- Lebron, I., and Surez, D.L., (1998). Kinetics and mechanisms of precipitation of calcite as affected by PCO_2 and organic ligands at 25°C . *Geom. Cosmochim. Acta* 62(3), 405-416.
- Lee, M., Gomez, M.G., San, Pablo., A.C.M., Kolbus, C.M., Graddy, C.M.R., DeJong, J.T., Nelson, D.C., (2019). Investigating Ammonium By-product Removal for Ureolytic Bio-cementation Using Meter-scale experiments, *Scientific Reports*, 9:18313.
- Lefebvre, G., Langlois, P., Lupien, C., and Lavallee, J., (1984). Laboratory testing on in situ behaviour of peat as embankment foundation. *Canadian Geotechnical Journal*, 21, 322-337.
- Li, P., Qu, W., (2012). Microbial carbonate mineralization as an improvement method for durability of concrete structures. *Adv Mat Res* 365:280–286
- Liaki, C. (2006) Physicochemical study of electrokinetically treated clay soils using carbon and steel electrodes. PhD thesis, University of Birmingham, UK.
- Liaki, C., Rogers, C.D.F., & Boardman, D.I., (2010). Physico-chemical effects on clay due to electromigration using stainless steel electrodes. *Journal of Applied Electrochemistry*, 40(6), 1225-1237.
- Lian, B., Hu, Q., Chen, J., Ji, J., and Teng, H. (2006). "Carbonate biomineralization induced by soil bacterium *Bacillus megaterium*." *Geochim. Cosmochim. Acta*, 70(22), 5522-5535.
- Lieszkowski, I. P., & Ozden, Z. S., (1977). Effects of volume change and alkalinity of water on the permeability of peat. Proceedings 17th Muskeg Research Conference, National Research Council, Canada.
- Lin, Singer, (2006). Inhibition of calcite precipitation by orthophosphate: speciation and thermodynamic considerations. *Geochim. Cosmochim. Acta* 70(10). 2530-2539.
- Lucas, R.E., (1982). *Organic Soils (Histosols). Formation, distribution, physical and chemical properties and management for crop production*. Michigan State University Research Report No. 435 (Farm Science).
- MacFarlane, I. C., (1969). *Muskeg Engineering Handbook*. University of Toronto Press.
- MacFarlane, I. C., and Allen, C. M., (1964). An examination of some index test procedures for peat. In *Proceedings of the 9th Muskeg Research Conference NRC, ACSSM Technical Memo*, 81, 171–183.

- Mahawish, A., Bouazza, A., and Gates, W.P., (2018). Improvement of Coarse Sand Engineering Properties by Microbially Induced Calcite Precipitation. *Geomicrobiology* 35:10 pp. 887-897. DOI: 10.1080/01490451.2018.1488019
- Mahawish, A., Bouazza, A., Gates, W.P., (2018). Effect of particle size distribution on the bio-cementation of coarse aggregates, *Acta Geotechnica* (2018) 13:1019-1025.
- Martinez, B.C., (2012). Up-scaling of microbial induced calcite precipitation in sands for geotechnical ground improvement. PhD Thesis, University of California, Davis, CA.
- Martinez, B.C., DeJong, J.T., Ginn, T.R., Mortensen, B.M., Barkouki, T.H., Hunt, C. Tanyu, B., Major, D., Experimental optimization of microbial induced carbonate precipitation for soil improvement. *ASCE J. Geotech. Geoenviron. Eng.*, 139 (4) (2013), pp. 587-598
- Marvasi, M., Gallagher, K.L., Martinez, L. C., Pagan, W.C.M., Santiago, R.R., Vega, G.C., and Visscher, P.T., (2012). Importance of B4 Medium in Determining Organomineralization Potential of Bacterial Environmental Isolates, *Geomicrobiology Journal*, 29:10, 916-924. DOI: 10.1080/01490451.2011.636145
- Mavroulidou, M., Morgan, N.L., Sibanda, T., Serumaga, M., and Bhamidimarri, R., (2011). Innovative environmentally responsible techniques of ground improvement stimulating natural processes In *Proceedings of the 12th International Conference on Environmental Science and Technology, CEST 2011, Rhodes, Greece* (Lekkas TD (ed.)) University of the Aegean, pp. A1210-A1217
- Masi, M., Ceccarini, A., and Iannelli, R., (2017). Model-based optimization of field-scale electrokinetic treatment of dredged sediments *The Chemical Engineering Journal*; 328:87-97.
- Masi, M., Iannelli, R., and Losito, G. (2016). Ligand-enhanced electrokinetic remediation of metal-contaminated marine sediments with high acid buffering capacity *Environmental Science and Pollution Research*, 23:10566 – 10576.
- McKeen, R. Gordon. "A model for predicting expansive soil behavior." In *Proc., 7th Int. Conf. on Expansive Soils*, vol. 1, pp. 1-6. Reston, VA: ASCE, 1992.
- Mena, E., Villasenor, J., Canizares, P., Rodrigo, M.A., (2016). Effect of electric field on the performance of soil electro-bioremediation with a periodic polarity reversal strategy. *Chemosphere*, 146, 2016. 300-307. <https://doi.org/10.1016/j.chemosphere.2015.12.053>

- Mesri, G., (2007). Engineering properties of fibrous peats. *Journal of Geotechnical and Geoenvironmental Engineering*, 133, 850–866.
- Michel, J.C., Riviere, L.M., and Bellon-Fontaine, M.N., (2001). Measuring of the wettability of organic materials in relation to water content by the capillary rise method. *European Journal of Soil Science* 52(3): 459 -467.
- Mitchell, J. K. (1993). *Fundamentals of Soil Behaviour* (2nd ed.). New York: John Wiley & Sons Inc.
- Mitchell, J. K., and Soga, K., (2005). *Fundamentals of Soil Behavior* (3rd Edition). New York: Wiley.
- Micic, S. Shang, J. Q., and Lo, K. Y., (2001). Electrokinetic Strengthening of Marine Clay Adjacent to Offshore Foundations Proceedings of the Eleventh (2001) international Offshore and Polar Engineering Conference Stavanger, Norway, June 17-22, 2001
- Miyakawa, I., (1960). Some aspects of road construction in peaty or marshy areas in Hokkaido. Civil Engineering Research Institute, Hokkaido Development Bureau, Sapporo, Japan.
- Mizuno, A., and Hori, Y., (1988). Destruction of Living Cells by Pulsed High-Voltage Application. *IEEE Transactions on Industry Applications*, 24, 387-394. <http://dx.doi.org/10.1109/28.2886>
- Montoya, B., DeJong, J., (2015). Stress-strain behavior of sands cemented by microbially induced calcite precipitation. *J Geotech Geoenviron Eng* 141(6):04015019
- Montoya, B.M., DeJong, J.T., Boulanger, R.W., (2013). Dynamic response of liquefiable sand improved microbial induced calcite precipitation, *Geotechnique*, 63(4): 302-312
- Mortensen, B. M., Haber, M. J., DeJong, J. T., Caslake, L. F., and Nelson, D. C., 2011, "Effects of Environmental Factors on Microbial Induced Calcium Carbonate Precipitation," *J. Appl. Microbiol.*, Vol. 111, No. 2, pp. 338–349.
- Mosavat, N., Oh, E., and Chai, G, (2012). A Review of Electrokinetic Treatment Technique for Improving the Engineering Characteristics of Low Permeable Problematic Soils. *International Journal of GEOMATE*, June, 2012, Vol. 2, No. 2 (Sl. No. 4), pp. 266-272

- Mosavat, N., (2014). Electrokinetic treatment of fine-grained soils with chemical enhancement solutions. PhD thesis, Griffith University.
- Mujah, D., Shahin, M., and Cheng, L., (2017). State-of-the-art review of biocementation by Microbially Induced Calcite Precipitation (MICP) for soil stabilisation. *Geomicrobiology journal*, 34(6):524-537
- Nafisi, A., Montoya, B.M., and T. Evans. M., (2020). Shear Strength Envelopes of Biocemented Sands with Varying Particle Size and Cementation Level, *Journal of Geotechnical and Geoenvironmental Engineering*, 146(3): 04020002
- Nemati, M., Voordouw, G., (2003). Modification of porous media permeability, using calcium carbonate produced enzymatically in situ. *Enzyme Microbial Technol* 33(5):635–642.
- Ng, W. S., Lee, M. L., Tan, C. K., and Hii, S. L. (2014). Factors affecting improvement in engineering properties of residual soil through microbial-induced calcite precipitation. *J. Geotech. Geoenviron. Eng. ASCE*, ISSN 1090-0241/04014006(11). DOI: 10.1061/(ASCE)GT.1943-5606.0001089.
- Nicholson, W.L., Munakata, N., Horneck, G., Melosh, H.J., Setlow, P., (2000). Resistance of *Bacillus* Endospores to extreme terrestrial and extraterrestrial environments. *Microbiol. Mol. Biol. Rev.* 2000 Sep; 64(3): 548-572. DOI: 10.1128/membr.64.3.548-572.2000
- Nunan, N., Wu, K., Young, I.M., Crawford, J.W., and Ritz, K., (2003). Spatial distribution of bacterial communities and their relationships with the microarchitecture of soil. *Microbiology Ecology* 44: 203-215.
- Omeregic, A.I., Palombo, E.A., Ong, D.E.L., and Nissom, P.M., A feasible scale-up production of *Sporosarcina pasteurii* using custom-built stirred tank reactor for in-situ soil biocementation, *Biocatalysis and Agricultural Biotechnology*, 24, March 2020,101544
- O'Kelly, B. (2005). Method to compare water content values determined on the basis of different over drying temperatures. *Géotechnique*, 55(4), 329–332.
- O'Leary A. M., Whyte P., Madden R. H., Cormican M., Moore J. E., and Mc Namara E., (2011). Pulsed field gel electrophoresis typing of human and retail foodstuff *Campylobacters*: an irish perspective. *Food Microbiol.* 28 426-433. 10.1016/j.fm.2010.10.003
- O'Loughlin, C. D. (2007). Simple and sophisticated methods for predicting settlement of embankments constructed on peat. *Soft Ground Engineering*, Engineers Ireland. Portlaoise, Ireland.

- O'Loughlin, C. D., and Lehane, B. M., (2001). Modelling the onedimensional compression of fibrous peat. In Proceedings of the 15th ICSMGE Conference, Istanbul, pp. 223–226.
- Pace, N.L. (1997). A molecular view of microbial diversity and the biosphere. *Science* 276 734-740. 10.1126/science.276.5313.734
- Pamukcu, S., Weeks, A., & Wittle, J. K. (1997). Electrochemical extraction and stabilization of selected inorganic species in porous media. *Journal of Hazardous Materials*, 55(1-3), 305-318.
- Patel, R., (2014). MALDI-TOF MS for the diagnosis of infectious diseases. *Clinical Chemistry*, 61:1, 100-111. DOI: 10.1373/clinchem.2014.221770
- Peppicelli, C., Cleall, P., Sapsford, D., Harbottle M.J., (2018). Changes in metal speciation and mobility during electrokinetic treatment of industrial wastes: Implications for remediation and resource recovery. *Science of the Total Environment*, 624: 1488-1503.
- Petersen, O., Deboz, K., Schjonning, Christensen, B.T., and Elmholt, S., (1997). Phospholipid fatty acid profiles and C availability in wet-stable macro-aggregates from conventionally and organically farmed soils. *Geoderma* 78: 181-196.
- Petrova-Botusharova S., (2017). Self-healing geotechnical structures via microbial action, PhD Thesis, Cardiff University
- Pheaney, P. E., (1980). Peat fabric and structure. *Canadian Geotechnical Journal*, 17, 416-435.
- Prescott, L.M., Harley, J.P., and Klein, D.A., (1996). *Microbiology* (3rd Edition): 40-72. W.C. Brown, Publishers, Dubuque, IA.
- Puustjarvi, V., and Robertson, R. A., (1975) In *Peat in Horticulture*. Edited by Robinson and Lamb Academic Press London pp. 23–38.
- Qian, C., Pan, Q., Wang, R., (2010). Cementation of sand grains based on carbonate precipitation induced by microorganism. *Sci China Technol Sci* 53(8):2198–2206.
- Radforth, N. W., (1969). Classification of muskeg. In: MacFarlane, I. C., (ed.) *Muskeg Engineering Handbook*. University of Toronto Press.

- Radforth N.M., and Brawner C. O., (1996). *Muskeg and the Northern Environment in Canada*, University of Toronto Press, Toronto, Ontario, Canada.
- Rebata-Landa, V., (2007). *Microbial activity in sediments: effects on soil behavior*. PhD Thesis, Georgia Institute of Technology, Atlanta, GA, 173.
- Rezanezhad, F., Price, J.S., Quinton, W.L., Lennartz, B., Milojevic, T., and Cappellen, P.V., (2016). Structure of peat soils and implications for water storage, flow and solute transport: A review update for geochemists. *Chemical Geology Journal*. 429:1, 2016, pp 75-84.
- Rozas, F., and Castellote, M., (2012). Electrokinetic remediation of dredged sediments polluted with heavy metals with different enhancing electrolytes, *Electrochimica Acta*, 86: 102-109.
- Saffari, R., Nikooee, E., Habibagahi, G., van Genuchten, M.Th., (2019). Effects of Biological Stabilization on the Water Retention Properties of Unsaturated Soils, *Journal of Geotechnical and Geoenvironmental Engineering*, 145(7): 04019028
- Sato, A., Kawasaki, S., Hata, T., and Hayashi, T., (2016). Possibility for solidification of peaty soil by using microbes, *International Journal of GEOMATE*, June, 2016, 10 (22):2071-2076.
- Shang, J., Mohamedelhassan, E., and Ismail, M., "Electrochemical cementation of offshore calcareous soil." *Canadian Geotechnical Journal*. 41(5), 2004, pp. 877-893.
- Sharma, M., Satyam, N., Reddy, K.R., (2019). Investigation of various gram-positive bacteria for MICP in Narmada Sand, India, *International Journal of Geotechnical engineering*, DOI: 10.1080/19386362.2019.1691322
- Shenbagavalli, S., & Mahimairaja, S. (2011). Electro kinetic remediation of contaminated habitats. *African Journal of Environmental Science and Technology*, 4(13), 930-935.
- Singhal, N., Kumar, M., Kanaujia, P.K., and Viridi, J.S., (2015). MALDI-TOF mass spectrometry: an emerging technology for microbial identification and diagnosis. *Front Microbiol*. 2015; 6: 791. DOI: 10.3389/fmicb.2015.00791
- Skempton, A. W., & Petley, D. J., (1970). Ignition loss and other properties of peats and clays from Avonmouth, King's Lynn and Cranberry Moss. *Geotechnique*, 20, 343-356.

- Stabnikov, V., Ivanov, V., Chu, J., (2015). Construction Biotechnology: a new area of biotechnological research and applications. *World J Microbiol Biotechnol* (2015) 31:1303-1314.
- Stevenson, F.J. (1994). *Humus Chemistry: Genesis, Composition, Reactions* 2nd Ed., John Wiley & Sons, Inc., New York, NY.
- Stevenson, L.G., Drake, S.K., Shea, Y.R., Zelazny, A.M., and Murray P.R., (2010b). Evaluation of matrix-assisted laser desorption ionization-time of flight mass spectrometry for identification of clinically important yeast species. *J. Clin. Microbiol.* 48 3482-3486. 10.1128/JCM.00687-09.
- Tagliaferri, F., Waller, J., Ando, E., Hall, S.A., Viggiani, G., Besuelle, P., DeJong, J.T., (2011). Observing strain localisation processes in bio-cemented sand using x-ray imaging. *Granular Matter* 13(3):247–250.
- Tajudin, S. (2012). *Electrokinetic Stabilisation of Soft Clay*. PhD thesis, University of Birmingham, UK.
- Tan, K.H., (2005). *Soil Sampling, Preparation, and Analysis*, Boca Raton, FL: Taylor & Francis/CRC Press, 2005.
- Tang, J. He., Xin. X., Hu, H., and Liu, T., (2018). Biosurfactants enhanced heavy metals removal from sludge in the electrokinetic treatment, *Chemical Engineering Journal*, 334: 2579-2592
- Terzaghi, K., & Peck, R. B., (1948). *Soil Mechanics in Engineering Practice*. Wiley, New York (1st Edition).
- Terzaghi, K. and Peck, R. (1967). *Soil Mechanics in Engineering Practice*. 2nd Edition, John Wiley, New York.
- Terzis, D., and Laloui, L., (2019). Cell-free soil bio-cementation with strength, dilatancy and fabric characterization, *Acta Geotechnica*, 14:639–656
- Turer, D., and Genc, A., (2007). Strengthening of soft clay with electrokinetic stabilization method. Paper presented at the 6th symposium on electrokinetic remediation (EREM 2007), Spain.
- Theel, E.S., Schmitt B. H., Hall. L., Cunningham, S. A., Walchak, R. C., and Patel, R., (2012). Formic acid-based direct, on-plate testing of yeast and *Corynebacterium* species by Bruker Biotyper matrix-assisted laser-desorption ionization-time of flight mass spectrometry. *J. Clin. Microbiol.* 50 3093-3095. 10.1128/JCM.01045-12.

- Valat, B., Jouany, C., and Riviere, L.M., (1991). Characterisation of the wetting properties of air-dried peats and composts. *Soil Science* 152 (2): 100 – 107.
- van Paassen, L., (2009). Biogrout: ground improvement by microbially induced carbonate precipitation. PhD Thesis, Delft University of Technology, Delft, Netherlands, p203.
- van Paassen, L.A., Ghose, R., van der Linden. T.J.M., van der Star. W.R.L., and van Loosdrecht. M.C.M., (2010a). Quantifying biomediated ground improvement by ureolysis: large-scale biogrout experiment. *J Geotech Geoenviron Eng* 136(12):1721-1728.
- van Paassen, L.A., (2011). Bio-mediated ground improvement: From laboratory experiment to pilot applications. *Geo-Frontiers: Advances in Geotechnical Engineering*, 4099-4108. Dallas: ASCE.
- Vary, P.S. (1994). Prime time for *Bacillus megaterium*. *Microbiology*, 140(5), 1001-1013.
- Venda Oliveira, P.J., Costa, M.S., Costa, J.N.P., and Nobre, M.F., (2015). Comparison of the ability of two bacteria to improve the behaviour of a sandy soil. *Journal of Materials in Civil Engineering*, 27(1): 06014025
- von Post, L. (1922). Sveriges Geologiska Undersoknings torvinventering och nogra av dess hittils vunna resultat (SGU peat inventory and some preliminary results). *Svenska Mosskulturforeningens Tidskrift*, Jonkoping, Sweden, 36, 1-37.
- Wahab, A., Embong, Z., Naseem, A.A., Madun, A., Zainorabidin, A., and Kumar, V., (2018). The Effect of Electrokinetic Stabilization (EKS) on Peat Soil Properties at Parit Botak area, Batu Pahat, Johor, Malaysia. *Indian Journal of Sci. Tech.* 11(44). 2018.
- West, L. J., & Stewart, D. I. (1995). Effect of zeta potential on soil electrokinesis. *Geoenvironment 2000: Characterization, Containment, Remediation, and Performance in Environmental Geotechnics, Vols 1 and 2*(46), 1535-1549.
- Wheeler, B.D and M.C.F Proctor, (2000) Ecological gradients, subdivisions and terminology of north-west European mires. *Journal of Ecology* 88: 187-203.
- Whiffin, V. S. (2004). "Microbial CaCO₃ precipitation for the production of biocement." Ph.D. dissertation, Murdoch Univ., Perth, Western Australia, Australia.
- Whiffin, V. S., van Paassen, L. A., and Harkes, M. P., (2007). Microbial Carbonate Precipitation as a Soil Improvement Technique, *Geomicrobiology Journal*, 24 (5): 417-423

- Wei, S., Cui, H., Jiang, Z., Liu, H., He, H., and Fang, N., (2015). Biomineralization processes of calcite induced by bacteria isolated from marine sediments. *Braz J Microbiol* 46(2):455–464.
- Yamaguchi, H., Ohira, Y., Kogue, K., and Mori, S., (1985a). Deformation and strength properties of peat. In *Proceedings of the 11th International Conference on Soil Mechanics and Foundation*, San Francisco, vol. 2, pp. 2461-2464.
- Yamaguchi, H., Ohira, Y., Kogue, K., and Mori, S., (1985b). Undrained shear characteristics of normally consolidated peat under triaxial compression and extension tests. *Japanese Society of Soil Mechanics and Foundations Engineering*, 25(3), 1-18.
- Yasuhara, H., Neupane, D., Hayashi, K., and Okamura, M., (2012). Experiments and predictions of physical properties of sand cemented by enzymatically-induced carbonate precipitation. *Soil Found.* 52, 539-549. doi: 10.1016/j.sandf.2012.05.011
- Yeung, A.T., Scott, T.B., Gopinath, S., Menon, R. M., and Hsu, C., (1997). Design, Fabrication, and Assembly of an apparatus for electrokinetic emediation studies. *Geotechnical testing journal*, GTJODJ, 20(2), 199-210.
- Young, I.M., and Crawford, J.W., (2004), Interactions and self-organisation in the soil-microbe complex. *Science* 304: 1634-1637.
- Zhao, Q., Li, L., Li, C., Li, M., Amini, F., and Zhang, H., (2014a). Factors affecting improvement of engineering properties of micp-treated soil catalyzed by bacteria and urease. *J Mater Civ Eng* 26(12):04014094. doi: 10.1061/(ASCE)MT.1943-5533.0001013.
- Zhang, X., Mavroulidou, M., and Gunn, M., (2015). Mechanical properties and behaviour of a partially saturated lime-treated, high plasticity clay. *Engineering Geology*. 193. <https://doi.org/10.1016/j.enggeo.2015.05.007>
- Zomorodian, S.M.A., Ghaffari, H., and O'Kelly, B.C., (2019). Stabilisation of crustal sand layer using biocementation technique for winderosion control *Aeolian Research*, 40: 34-41

APPENDIX (A).

Batch Testing Results for Borehole (WS01) 8m Long Sample.

Location	pH	Moisture Contents %	Ignition Loss %	Organic Content %
0.4m	7.2	18.717	32.3038	29.5960
1m	7.4	11.343	19.3718	16.1466
1-2, 1m	7.1	33.364	27.5318	24.6330
1-2, 2m	7.1	39.226	30.4975	27.7174
2-3, 2m	7.0	28.325	33.4110	30.7475
2-3, 3m	7.1	29.040	26.2590	23.3093
3-4, 3m	7.2	35.645	29.3893	26.5648
3-4, 4m	7.4	38.801	27.8320	24.9452
4-5, 4m	7.2	27.733	26.9855	24.0649
4-5, 5m	7.2	30.325	27.9667	25.0854
5-6, 5m	7.1	37.076	30.3304	27.5436
5-6, 6m	6.6	307.976	97.3999	97.2959
6-7, 6m	6.9	50.537	37.5515	35.0536
6-7, 7m	6.9	145.556	66.5717	65.2345
7-8, 7m	6.8	245.367	92.1451	91.8309
7-8, 8m	7.3	36.931	26.0805	23.1237

Table 1

Batch Testing Results for Borehole (WS02) 8m Long Sample.

Location	pH	Moisture Contents %	Ignition Loss %	Organic Content %
0-2m	7.15	55.463	52.7246	50.8336
1-2, 1m	7.3	27.920	49.1969	47.1648
1-2, 2m	7.25	39.256	34.5211	31.9019
2-3, 2m	7.3	35.248	31.3476	28.6015
2-3, 3m	7.2	39.878	33.0668	30.3895
3-4, 3m	7.2	33.694	29.3067	26.4789
3-4, 4m	7.15	25.753	44.9603	42.7587
4-5, 4m	7.2	25.620	25.3215	22.3344
4-5, 5m	7.2	36.798	36.6631	34.1296
5-6, 5m	7.15	21.655	19.6445	16.4302
5-6, 6m	7.05	33.376	34.3457	31.7195
6-7, 6m	7.05	21.380	20.1069	16.9112
6-7, 7m	7.2	21.699	24.2647	21.2353
7-8, 7m	7.1	29.896	25.1124	22.1169
7-8, 8m	6.8	78.805	61.3935	59.8492

Table 2

APPENDIX (B).

The Isolation of bacteria is done by using 1 g of soil from each soil sample to the bottle of 99 ml of distilled water. After thoroughly mixing, 1 ml of the 10^{-2} (1:100) dilution was transferred to a second bottle of 99 ml of distilled water with a new pipette and mix (result in 10^{-4} dilution). Then transferring 1 ml of the 10^{-4} dilution to the final bottle of distilled water and mix (result in 10^{-6}) dilution).

Using a new pipette to transfer 1 ml of solution from each dilution tube into an individual Petri plate. Then Added about 15 ml of Tryptic soya agar (TSA) to the plate; then put the lid on the plate and swirled gently so that the agar covers the bottom of the plate.

Repeated this process for each soil sample, using the 1000 μ l or 200 μ l pipette and aseptic technique, transfer the proper amount of soil dilution to each of the petri dishes as indicated in table below.

Final Dilution	Microbial solution at		
	10^{-2}	10^{-4}	10^{-6}
10^{-2}	1000	-	-
10^{-3}	100	-	-
10^{-4}	-	1000	-
10^{-5}	-	100	-
10^{-6}	-	-	1000
10^{-7}	-	-	100

“-“ not applicable

Dilution Scheme

APPENDIX (C).

The McKean Classification Scheme Table.

Category	Slope ^a	C _n ^b	H ^c %	Expansion
i	> 0.17	-0.027	10	Special Case
ii	0.10 to 0.17	-0.227 to -0.12	5.3	High
iii	0.08 to 0.10	-0.12 to 0.04	1.8	Moderate
iv	0.05 to 0.08	-0.04 to 0	-	Low
v	< 0.05	0	-	Non-expensive

APPENDIX (D).

To calibrate the output of the tested samples by using an ultraviolet-visible spectrophotometer the Ammonium chloride Standards were prepared.

- 1 mM Ammonium Chloride standard was prepared by diluting 5 μL of the 100 mM Ammonium Chloride standard with 495 μL of double distilled H_2O .
- Then Using 100 mM Ammonium Chloride standard, six standard curve dilutions were prepared in microplate or microcentrifuge tubes as described in table below.

Ammonium Chloride Standard Dilution Scheme,

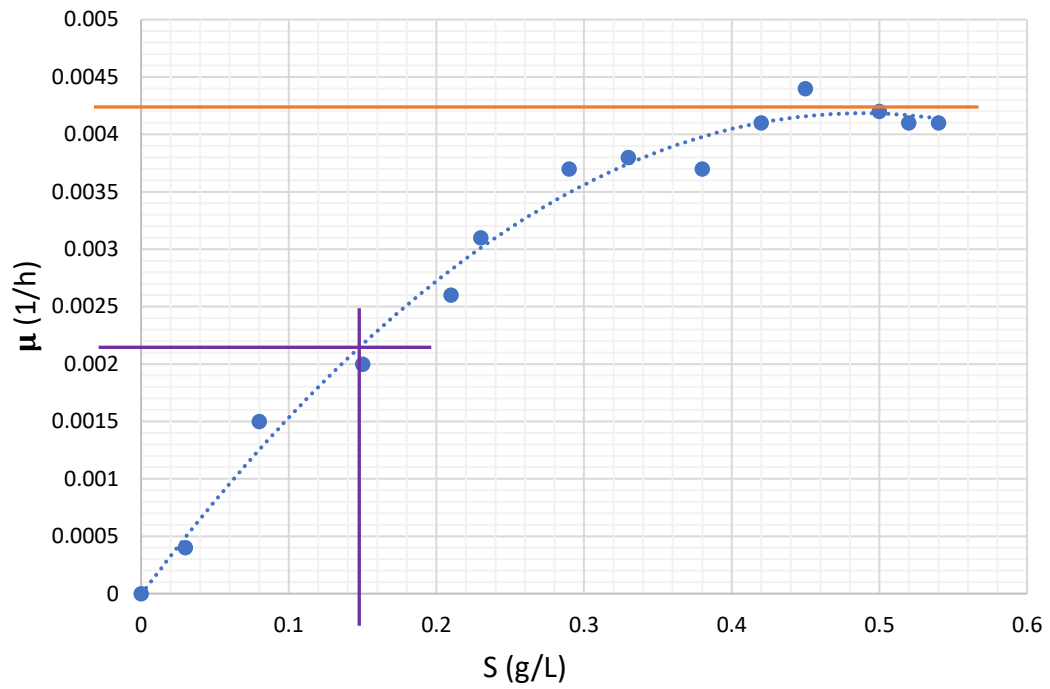
Standard No	Volume of Standard (μL)	ddH ₂ O (μL)	Final volume standard in micro vials (μL)	End Concentration Ammonium Chloride in micro vials (nmol/vial)
1	0	300	100	0
2	12	288	100	4
3	24	276	100	8
4	36	264	100	12
5	48	252	100	16
6	60	240	100	20

The diluted standard solutions are unstable and cannot be stored for later use, so a fresh set of standards was prepared for every use. Moreover, each standard dilution was set up to produce duplicate readings (i.e., 2 x 100 μL).

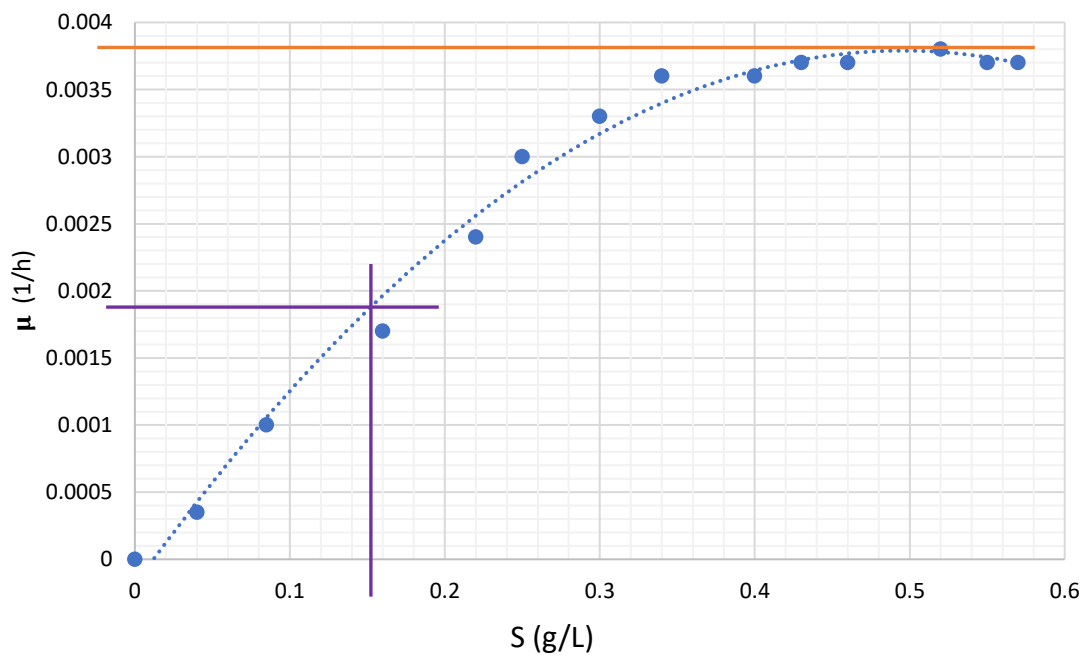
APPENDIX (E).

The arithmetic plots of (μ) vs (S) according to Monod microbial kinetic model.

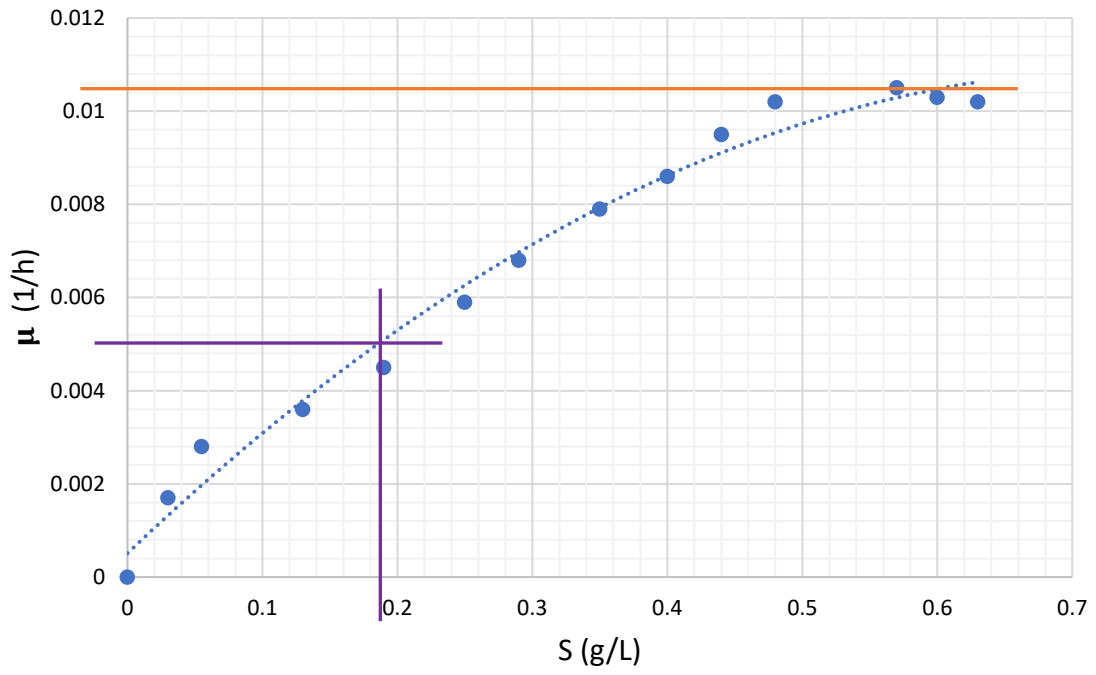
Bacillus licheniformis



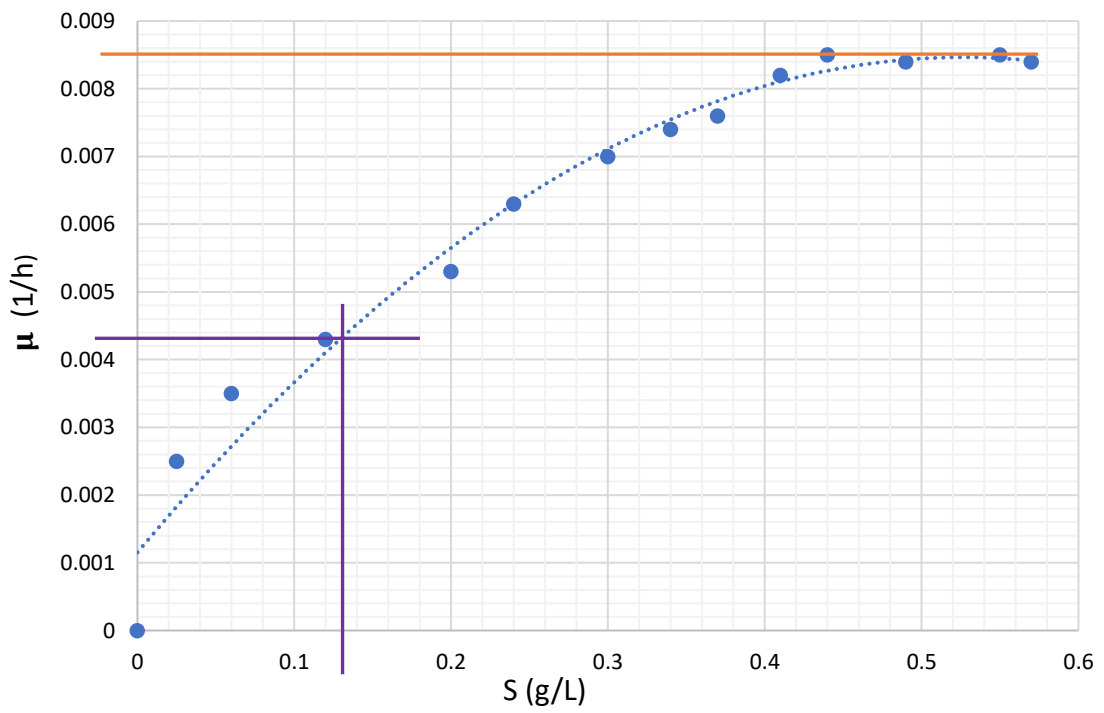
Micrococcus luteus



Lysinibacillus fusiformis

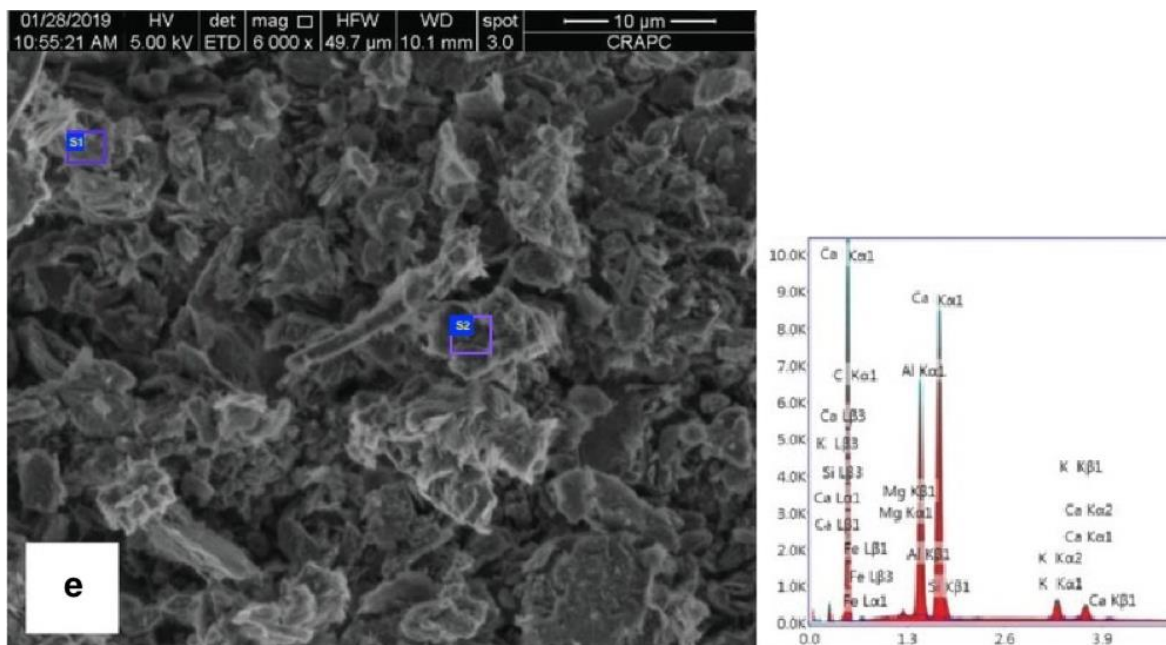
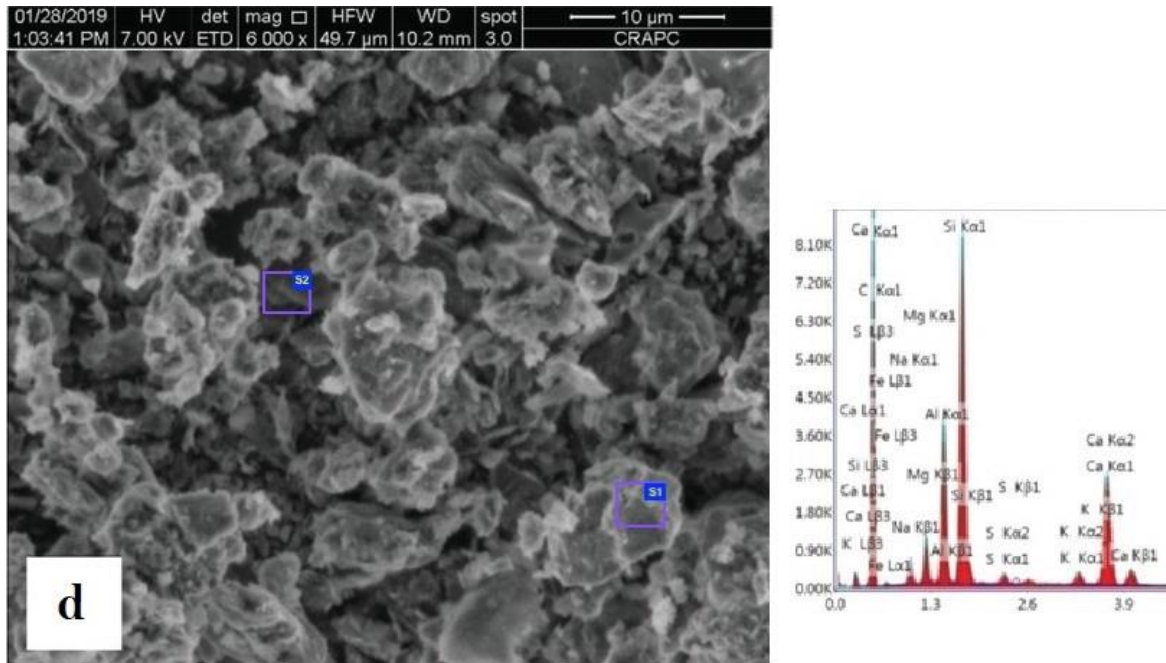


Rhodoccus erythropolis



APPENDIX (F).

Additional SEM-EDS Images.



Crystalline CaCO_3 cloud formation Formation around the soil particles, picture taken 6000x magnification and zoom of 80µm for a 7-day treated sample, using *Lysinibacillus Fusiformis* and using Cementing Regent: (3 g/L Nutrient Broth supplement + 0.75 M Urea + 0.75 M Calcium chloride).

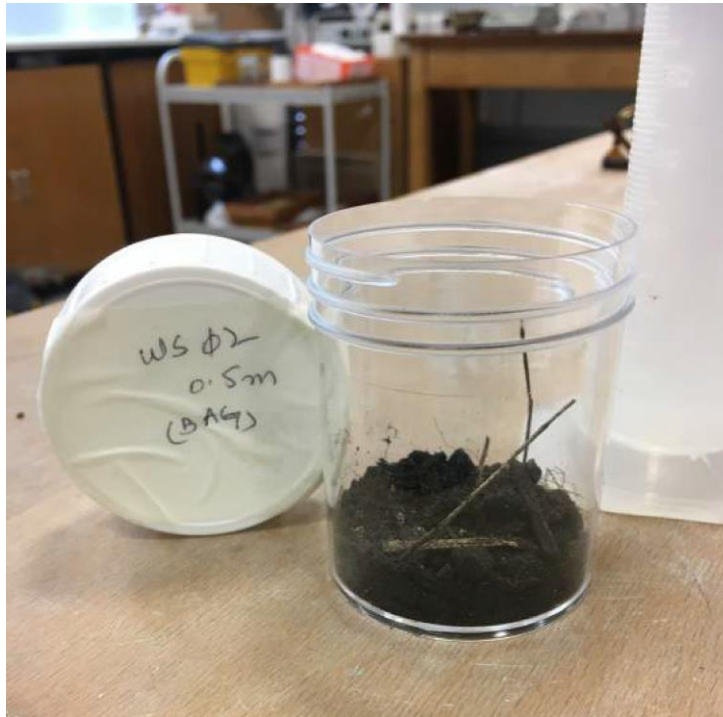
Archive Pictures:



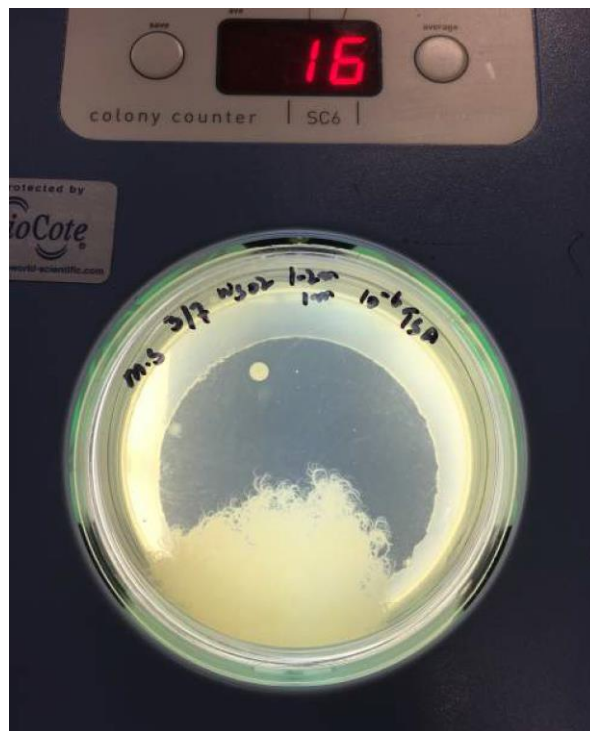
Clay sample from WS02 (5 m depth) with organic content 16.4302 %



Purified Strain (*Micrococcus luteus*)



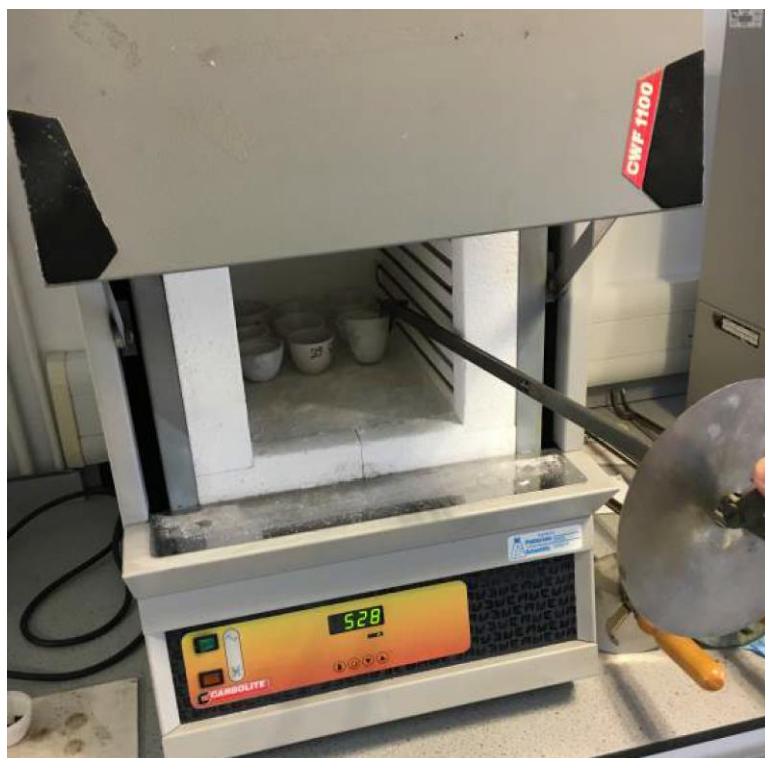
Soil sample ready for pH testing with 50.8336 % organic content



Un-purified *Bacillus licheniformis* colony



Soil Samples placed on Electrothermal Isomental for preheating, prior to determination of organic contents,



Samples placed in muffle furnace for combustion at 550°C



Peat sample with 97.2959 % organic contents



20g Peat sample with 91.8309 % organic contents before combustion in muffle furnace



20g Peat sample with 91.8309 % organic contents after combustion in muffle furnace



Soil Samples with different % of induced calcite precipitation



Urease Activity Assay kit

APPENDIX (G).

MELDI Classification Results

(from next page)

Bruker Daltonik MALDI Biotyper Classification Results



Project Info:

Project Name: **28072017MUHAMMAD SOIL1**
 Project Description:
 Project Owner: admin@FLEX-PC
 Project Creation Date/Time: 2017-07-28T13:09:45.981
 Project Analyte Count: 24
 Project Type: Development
 Validation: not present
 Validation Position:

Result Overview

Analyte Name	Analyte ID	Organism (best match)	Score Value	Organism (second best match)	Score Value
B2 (++)(A)	1a	Bacillus licheniformis	2.138	Bacillus licheniformis	2.008
B3 (-)(C)	2a	not reliable identification	1.544	not reliable identification	1.456
B4 (-)(C)	3a	not reliable identification	1.418	not reliable identification	1.305
B5 (-)(C)	4a	not reliable identification	1.289	not reliable identification	1.268
B6 (-)(C)	5a	not reliable identification	1.248	not reliable identification	1.231
B7 (-)(C)	6a	not reliable identification	1.43	not reliable identification	1.367
B8 (-)(C)	7a	not reliable identification	1.409	not reliable identification	1.375
B9 (-)(C)	8a	not reliable identification	1.491	not reliable identification	1.287
B10 (-)(C)	9a	not reliable identification	1.382	not reliable identification	1.368

B11 (-)(C)	10a	not reliable identification	1.307	not reliable identification	1.265
B12 (-)(C)	11a	not reliable identification	1.541	not reliable identification	1.536
C2 (+)(B)	1b	Bacillus licheniformis	1.827	not reliable identification	1.549
C3 (-)(C)	2b	not reliable identification	1.367	not reliable identification	1.319
C4 (-)(C)	3b	not reliable identification	1.421	not reliable identification	1.37
C5 (-)(C)	4b	not reliable identification	1.348	not reliable identification	1.292
C6 (-)(C)	5b	not reliable identification	1.275	not reliable identification	1.252
C7 (-)(C)	6b	not reliable identification	1.651	not reliable identification	1.45
C8 (-)(C)	7b	not reliable identification	1.302	not reliable identification	1.292
C9 (-)(C)	8b	not reliable identification	1.442	not reliable identification	1.355
C10 (-)(C)	9b	not reliable identification	1.437	not reliable identification	1.365
C11 (-)(C)	10b	not reliable identification	1.638	not reliable identification	1.379
C12 (-)(C)	11b	not reliable identification	1.594	not reliable identification	1.584
D2 (+++)(A)	BTS1	Escherichia coli	2.467	Escherichia coli	2.392
E2 (+++)(B)	BTS2	Escherichia coli	2.537	Escherichia coli	2.402

Matching Hints

Matched Pattern	Comment
Acinetobacter baumannii B389 UFL	Member of the Acinetobacter baumannii /calcoaceticus complex. Extraction must be performed to permit reliable species identification.
Acinetobacter calcoaceticus B388 UFL	Member of the Acinetobacter baumannii /calcoaceticus complex. Extraction must be performed to permit reliable species identification.
Aeromonas caviae CECT 838T DSM	Species of this genus have very similar patterns: Therefore distinguishing their species is difficult.
Aeromonas jandaei CECT 4228T DSM	Species of this genus have very similar patterns: Therefore distinguishing their species is difficult.
Aeromonas veronii CECT 4257T DSM	Species of this genus have very similar patterns: Therefore distinguishing their species is difficult.
Aeromonas veronii CECT 5761T DSM	Species of this genus have very similar patterns: Therefore distinguishing their species is difficult.
Bacillus atrophaeus DSM 675 DSM	is a member of Bacillus subtilis group. The quality of spectra (score) depends on the degree of sporulation: Use fresh material.
Bacillus funiculus DSM 15141T DSM	The quality of spectra (score) depends on the degree of sporulation: Use fresh material.
Bacillus indicus DSM 15820T DSM	The quality of spectra (score) depends on the degree of sporulation: Use fresh material.
Bacillus licheniformis 992000432 LBK	is a member of Bacillus subtilis group. The quality of spectra (score) depends on the degree of sporulation: Use fresh material.
Bacillus licheniformis CS 54_1 BRB	is a member of Bacillus subtilis group. The quality of spectra (score) depends on the degree of sporulation: Use fresh material.
Bacillus licheniformis DSM 13T DSM	is a member of Bacillus subtilis group. The quality of spectra (score) depends on the degree of sporulation: Use fresh material.
Bacillus mojaviensis DSM 9205T DSM	is a member of Bacillus subtilis group. The quality of spectra (score) depends on the degree of sporulation: Use fresh material.
Bacillus muralis DSM 16288T DSM	The quality of spectra (score) depends on the degree of sporulation: Use fresh material.
Bacillus psychrosaccharolyticus DSM 6T DSM	The quality of spectra (score) depends on the degree of sporulation: Use fresh material.
Bacillus simplex CS 206_1aI BRB	The quality of spectra (score) depends on the degree of sporulation: Use fresh material.
Bacillus simplex DSM 1321T DSM	The quality of spectra (score) depends on the degree of sporulation: Use fresh material.

Bacillus soli DSM 15604T DSM	The quality of spectra (score) depends on the degree of sporulation: Use fresh material.
Bacillus sp LB_101250b_09 ERL	The quality of spectra (score) depends on the degree of sporulation: Use fresh material.
Bacillus subtilis DSM 5611 DSM	is a member of Bacillus subtilis group. The quality of spectra (score) depends on the degree of sporulation: Use fresh material.
Bacillus subtilis ssp spizizenii DSM 15029T DSM	is a member of Bacillus subtilis group. The quality of spectra (score) depends on the degree of sporulation: Use fresh material.
Bacillus subtilis ssp subtilis DSM 10T DSM	is a member of Bacillus subtilis group. The quality of spectra (score) depends on the degree of sporulation: Use fresh material.
Bacillus subtilis ssp subtilis DSM 5660 DSM	is a member of Bacillus subtilis group. The quality of spectra (score) depends on the degree of sporulation: Use fresh material.
Burkholderia thailandensis DSM 13276T HAM	Burkholderia thailandensis is closely related and shows very similar spectra to the highly pathogenic Burkholderia pseudomallei / mallei which are not included in the MALDI Biotyper database. For differentiation an adequate identification method has to be selected by an experienced professional.
Campylobacter upsaliensis 412_01 NVU	closely related to Campylobacter helveticus
Citrobacter freundii 13158_2 CHB	Species of this genus have very similar patterns: Therefore distinguishing their species is difficult.
Clostridium beijerinckii 1072_ATCC 25752T BOG	Species beijerinckii / diolis of the genus Clostridium have very similar patterns: Therefore distinguishing their species is difficult.
Clostridium clostridioforme 1021_NCTC 11224T BOG	Species bolteae / clostridioforme of the genus Clostridium have very similar patterns: Therefore distinguishing their species is difficult.
Enterobacter cloacae 13159_1 CHB	is a member of Enterobacter cloacae complex
Escherichia coli ATCC 25922 CHB	closely related to Shigella and not definitely distinguishable at the moment
Escherichia coli ATCC 25922 THL	closely related to Shigella and not definitely distinguishable at the moment
Escherichia coli DH5alpha BRL	closely related to Shigella and not definitely distinguishable at the moment
Escherichia coli DSM 1103_QC DSM	closely related to Shigella and not definitely distinguishable at the moment
Escherichia coli DSM	closely related to Shigella and not definitely distinguishable at the moment

1576 DSM	
Escherichia coli DSM 30083T HAM	closely related to Shigella and not definitely distinguishable at the moment
Escherichia coli DSM 682 DSM	closely related to Shigella and not definitely distinguishable at the moment
Escherichia coli MB11464_1 CHB	closely related to Shigella and not definitely distinguishable at the moment
Escherichia coli Nissl VML	closely related to Shigella and not definitely distinguishable at the moment
Escherichia coli RV412_A1_2010_06a LBK	closely related to Shigella and not definitely distinguishable at the moment
Pseudomonas gessardii CIP 105469T HAM	is a member of Pseudomonas fluorescens group
Pseudomonas migulae CIP 105470T HAM	is a member of Pseudomonas fluorescens group
Pseudomonas mucidolens LMG 2223T HAM	is a member of Pseudomonas fluorescens group
Pseudomonas putida B400 UFL	is a member of Pseudomonas putida group
Rhodococcus equi 559 LAL	synonym of Corynebacterium hoagii

Meaning of Score Values

Range	Description	Symbols	Color
2.300 ... 3.000	highly probable species identification	(+++)	green
2.000 ... 2.299	secure genus identification, probable species identification	(++)	green
1.700 ... 1.999	probable genus identification	(+)	yellow
0.000 ... 1.699	not reliable identification	(-)	red

Meaning of Consistency Categories (A - C)

Category	Description
A	Species Consistency: The best match was classified as 'green' (see above). Further 'green' matches are of the same species as the first one. Further 'yellow' matches are at least of the same genus as the first one.
B	Genus Consistency: The best match was classified as 'green' or 'yellow' (see above). Further 'green' or 'yellow' matches have at least the same genus as the first one. The conditions of species consistency are not fulfilled.
C	No Consistency: Neither species nor genus consistency (Please check for synonyms of names or microbial mixture).

Analyte1



Analyte Name: B2
 Analyte Description:
 Analyte ID: 1a
 Analyte Creation Date/Time: 2017-07-28T13:11:54.213
 Applied MSP Library(ies):
 Applied Taxonomy Tree: Bruker Taxonomy

Rank (Quality)	Matched Pattern	Score Value	NCBI Identifier
1 (++)	Bacillus licheniformis DSM 13T DSM	2.138	1402

2 (++)	Bacillus licheniformis 992000432 LBK	2.008	1402
3 (-)	Bacillus licheniformis CS 54_1 BRB	1.574	1402
4 (-)	Sphingomonas aquatilis DSM 15581T HAM	1.348	93063
5 (-)	Clostridium bifermentans 2274_CCUG 35556 A BOG	1.329	1490
6 (-)	Clostridium tertium 1048_NCTC 541 BOG	1.324	1559
7 (-)	Streptomyces avidinii B190 UFL	1.323	1895
8 (-)	Pseudomonas putida B400 UFL	1.295	303
9 (-)	Clostridium beijerinckii 1072_ATCC 25752T BOG	1.269	1520
10 (-)	Pseudomonas proteolytica DSM 15321T HAM	1.248	219574

Analyte2

Analyte Name: B3
 Analyte Description:
 Analyte ID: 2a
 Analyte Creation Date/Time: 2017-07-28T13:11:54.432
 Applied MSP Library(ies):
 Applied Taxonomy Tree: Bruker Taxonomy

Rank (Quality)	Matched Pattern	Score Value	NCBI Identifier
1 (-)	Bacillus sp LB_101250b_09 ERL	1.544	185979
2 (-)	Bacillus simplex CS 206_1aI BRB	1.456	1478
3 (-)	Aspergillus flavus 1081 PFM	1.298	5059
4 (-)	Lactobacillus agilis DSM 20509T DSM	1.267	1601
5 (-)	Lactobacillus plantarum DSM 20205 DSM	1.253	1590
6 (-)	Agromyces rhizosphaerae HKI 302_DSM 14597T HKJ	1.241	88374
7 (-)	Lactobacillus suebicus DSM 5008 DSM	1.234	152335
8 (-)	Rhodococcus equi 559 LAL	1.233	43767
9 (-)	Bacillus soli DSM 15604T DSM	1.232	220688
10 (-)	Lactobacillus casei DSM 20011T DSM	1.23	1582

Analyte3

Analyte Name: B4
 Analyte Description:
 Analyte ID: 3a
 Analyte Creation Date/Time: 2017-07-28T13:11:54.229
 Applied MSP Library(ies):
 Applied Taxonomy Tree: Bruker Taxonomy

Rank (Quality)	Matched Pattern	Score Value	NCBI Identifier
1 (-)	Candida lambica CBS 603 CBS	1.418	53655
2 (-)	Staphylococcus sciuri ssp rodentium DSM 16827T DSM	1.305	147469
3 (-)	Streptomyces badius B192 UFL	1.28	1941
4 (-)	Bacillus simplex DSM 1321T DSM	1.261	1478
5 (-)	Clostridium cadaveris 1074_ATCC 25783T BOG	1.251	1529
6 (-)	Leptotrichia trevisanii ENR_0561 ENR	1.247	109328
7 (-)	Aeromonas caviae CECT 838T DSM	1.237	648
8 (-)	Citrobacter freundii 13158_2 CHB	1.209	546
9 (-)	Staphylococcus warneri DSM 20036 DSM	1.202	1292
10 (-)	Clostridium paraputrificum 1083_ATCC 17796 BOG	1.198	29363

Analyte4

Analyte Name: B5
 Analyte Description:
 Analyte ID: 4a
 Analyte Creation Date/Time: 2017-07-28T13:11:54.588
 Applied MSP Library(ies):
 Applied Taxonomy Tree: Bruker Taxonomy

Rank (Quality)	Matched Pattern	Score Value	NCBI Identifier
1 (-)	Pseudomonas vancouverensis CIP 106707T HAM	1.289	95300
2 (-)	Clostridium novyi A 1025_NCTC 538 BOG	1.268	1542
3 (-)	Clostridium baratii 1084_ATCC 25782 BOG	1.265	1561
4 (-)	Lactobacillus curvatus DSM 20010 DSM	1.251	28038
5 (-)	Lactobacillus oligofermentans DSM 15708 DSM	1.245	293371
6 (-)	Campylobacter jejuni MB_6111_05 THL	1.24	197
7 (-)	Lactobacillus plantarum DSM 20205 DSM	1.24	1590
8 (-)	Rhodococcus globerulus B312 UFL	1.216	33008
9 (-)	Alicyclobacillus acidoterrestris DSM 3924 DSM	1.215	1450
10 (-)	Clostridium tetani 1089_ATCC 10779 BOG	1.213	1513

Analyte5

Analyte Name: B6
 Analyte Description:
 Analyte ID: 5a
 Analyte Creation Date/Time: 2017-07-28T13:11:54.510
 Applied MSP Library(ies):
 Applied Taxonomy Tree: Bruker Taxonomy

Rank (Quality)	Matched Pattern	Score Value	NCBI Identifier
1 (-)	Lactobacillus fermentum DSM 20391 DSM	1.248	1613
2 (-)	Starkeya novella B516 UFL	1.231	921
3 (-)	Novosphingobium subterraneum DSM 12447T HAM	1.212	48936
4 (-)	Burkholderia thailandensis DSM 13276T HAM	1.199	57975
5 (-)	Lactobacillus zeae DSM 20178T DSM	1.195	57037
6 (-)	Actinomyces viscosus DSM 43327T DSM	1.176	1656
7 (-)	Mycobacterium tuberculosis W206 R_445 PGM	1.165	1773
8 (-)	Kandleria vitulina DSM 20405T DSM	1.144	1630
9 (-)	Staphylococcus vitulinus DSM 15615T DSM	1.14	71237
10 (-)	Clostridium cadaveris 1074_ATCC 25783T BOG	1.132	1529

Analyte6

Analyte Name: B7
 Analyte Description:
 Analyte ID: 6a
 Analyte Creation Date/Time: 2017-07-28T13:11:54.245
 Applied MSP Library(ies):
 Applied Taxonomy Tree: Bruker Taxonomy

Rank (Quality)	Matched Pattern	Score Value	NCBI Identifier
1 (-)	Bacillus simplex DSM 1321T DSM	1.43	1478
2 (-)	Enterococcus faecium 11037 CHB	1.367	1352
3 (-)	Bacillus simplex CS 206_1aI BRB	1.339	1478
4 (-)	Campylobacter lari 165_98 NVU	1.336	201
5 (-)	Bacillus muralis DSM 16288T DSM	1.286	264697
6 (-)	Enterobacter cloacae 13159_1 CHB	1.282	550
7 (-)	Citrobacter freundii 13158_2 CHB	1.265	546
8 (-)	Chryseobacterium scophthalmum LMG 13028T HAM	1.234	59733
9 (-)	Enterococcus faecium VRE_PX_16086218 MLD	1.231	1352
10 (-)	Staphylococcus sciuri ssp carnaticus DSM 15613T DSM	1.23	147468

Analyte7

Analyte Name: B8
 Analyte Description:
 Analyte ID: 7a
 Analyte Creation Date/Time: 2017-07-28T13:11:54.557
 Applied MSP Library(ies):
 Applied Taxonomy Tree: Bruker Taxonomy

Rank (Quality)	Matched Pattern	Score Value	NCBI Identifier
1 (-)	Cryptococcus neoformans_var_grubii ICB175_SDA_NaCl CBS	1.409	178876
2 (-)	Pseudomonas umsongensis LMG 21317T HAM	1.375	198618
3 (-)	Lactobacillus salivarius DSM 20492 DSM	1.331	1624
4 (-)	Lactobacillus salivarius DSM 20554 DSM	1.318	1624
5 (-)	Bacillus sp LB_101250b_09 ERL	1.285	185979
6 (-)	Streptomyces phaeochromogenes B265 UFL	1.247	1923
7 (-)	Aeromonas jandaei CECT 4228T DSM	1.234	650
8 (-)	Lactobacillus sakei ssp carnosus DSM 15740 DSM	1.225	214325
9 (-)	Arthrobacter tecti DSM 16407T DSM	1.213	271433
10 (-)	Chryseobacterium scophthalmum LMG 13028T HAM	1.211	59733

Analyte8

Analyte Name: B9
 Analyte Description:
 Analyte ID: 8a
 Analyte Creation Date/Time: 2017-07-28T13:11:54.416
 Applied MSP Library(ies):
 Applied Taxonomy Tree: Bruker Taxonomy

Rank (Quality)	Matched Pattern	Score Value	NCBI Identifier
1 (-)	Enterococcus faecium VRE_PX_16086218 MLD	1.491	1352
2 (-)	Pseudomonas caricapapayae LMG 2152T HAM	1.287	46678
3 (-)	Staphylococcus intermedius P_45A JUT	1.248	1285
4 (-)	Arthrobacter pascens DSM 20545T DSM	1.228	1677
5 (-)	Pseudomonas umsongensis LMG 21317T HAM	1.22	198618
6 (-)	Staphylococcus delphini P_22A JUT	1.214	53344
7 (-)	Pseudomonas jessenii CIP 105274T HAM	1.207	77298
8 (-)	Acinetobacter calcoaceticus B388 UFL	1.204	471
9 (-)	Staphylococcus delphini h_7c JUT	1.197	53344
10 (-)	Staphylococcus sciuri ssp rodentium DSM 16827T DSM	1.19	147469

Analyte9

Analyte Name: B10
 Analyte Description:
 Analyte ID: 9a
 Analyte Creation Date/Time: 2017-07-28T13:11:54.650
 Applied MSP Library(ies):
 Applied Taxonomy Tree: Bruker Taxonomy

Rank (Quality)	Matched Pattern	Score Value	NCBI Identifier
1 (-)	Lactobacillus versmoldensis DSM 14857T DSM	1.382	194326
2 (-)	Arthrobacter koreensis DSM 16760T DSM	1.368	199136
3 (-)	Bacillus sp LB_101250b_09 ERL	1.362	185979
4 (-)	Streptomyces phaeochromogenes B265 UFL	1.309	1923
5 (-)	Arthrobacter gandavensis DSM 15046T DSM	1.306	169960
6 (-)	Pseudomonas aeruginosa 19955_1 CHB	1.271	287
7 (-)	Bacillus simplex DSM 1321T DSM	1.219	1478
8 (-)	Bacillus funiculus DSM 15141T DSM	1.206	137993
9 (-)	Filobasidium uniguttulatum CBS 1727 CBS	1.205	5212
10 (-)	Clostridium novyi A 1025_NCTC 538 BOG	1.173	1542

Analyte10

Analyte Name: B11
 Analyte Description:
 Analyte ID: 10a
 Analyte Creation Date/Time: 2017-07-28T13:11:54.323
 Applied MSP Library(ies):
 Applied Taxonomy Tree: Bruker Taxonomy

Rank (Quality)	Matched Pattern	Score Value	NCBI Identifier
1 (-)	Pseudomonas aeruginosa 19955_1 CHB	1.307	287
2 (-)	Lactobacillus sakei ssp carnosus DSM 15740 DSM	1.265	214325
3 (-)	Streptomyces lavendulae B264 UFL	1.264	1914
4 (-)	Starkeya novella B516 UFL	1.252	921
5 (-)	Acidovorax avenae ssp avenae DSM 7227T HAM	1.242	80870
6 (-)	Enterococcus faecium 11037 CHB	1.215	1352
7 (-)	Staphylococcus sciuri ssp rodentium DSM 16827T DSM	1.212	147469
8 (-)	Candida lusitaniae 45 PSB	1.198	36911
9 (-)	Pseudomonas savastanoi ssp savastanoi LMG 5011 HAM	1.186	29438
10 (-)	Pseudomonas mucidolens LMG 2223T HAM	1.182	46679

Analyte11

Analyte Name: B12
 Analyte Description:
 Analyte ID: 11a
 Analyte Creation Date/Time: 2017-07-28T13:11:54.260
 Applied MSP Library(ies):
 Applied Taxonomy Tree: Bruker Taxonomy

Rank (Quality)	Matched Pattern	Score Value	NCBI Identifier
1 (-)	Bacillus muralis DSM 16288T DSM	1.541	264697
2 (-)	Bacillus simplex DSM 1321T DSM	1.536	1478
3 (-)	Bacillus simplex CS 206_1aI BRB	1.471	1478
4 (-)	Bacillus mojavensis DSM 9205T DSM	1.382	72360
5 (-)	Nocardia sp MB_9090_05 THL	1.369	1817
6 (-)	Bacillus sp LB_101250b_09 ERL	1.336	185979
7 (-)	Bacillus subtilis ssp spizizenii DSM 15029T DSM	1.286	96241
8 (-)	Bacillus subtilis ssp subtilis DSM 5660 DSM	1.245	135461
9 (-)	Bacillus indicus DSM 15820T DSM	1.206	246786
10 (-)	Lactobacillus fuchuensis DSM 14341 DSM	1.181	164393

Analyte12

Analyte Name: C2
 Analyte Description:
 Analyte ID: 1b
 Analyte Creation Date/Time: 2017-07-28T13:11:54.447
 Applied MSP Library(ies):
 Applied Taxonomy Tree: Bruker Taxonomy

Rank (Quality)	Matched Pattern	Score Value	NCBI Identifier
1 (+)	Bacillus licheniformis 992000432 LBK	1.827	1402
2 (-)	Bacillus licheniformis DSM 13T DSM	1.549	1402
3 (-)	Bacillus licheniformis CS 54_1 BRB	1.548	1402
4 (-)	Clostridium bifermentans 2274_CCUG 35556 A BOG	1.47	1490
5 (-)	Nocardia sp MB_9090_05 THL	1.412	1817
6 (-)	Lactobacillus paracasei ssp paracasei DSM 5622T DSM	1.371	47714
7 (-)	Clostridium novyi 1082_ATCC 17861T BOG	1.284	1542
8 (-)	Campylobacter upsaliensis 412_01 NVU	1.282	28080
9 (-)	Lactobacillus paracasei ssp paracasei DSM 20207 DSM	1.279	47714
10 (-)	Arthrobacter globiformis DSM 20124T DSM	1.278	1665

Analyte13

Analyte Name: C3
 Analyte Description:
 Analyte ID: 2b
 Analyte Creation Date/Time: 2017-07-28T13:11:54.494
 Applied MSP Library(ies):
 Applied Taxonomy Tree: Bruker Taxonomy

Rank (Quality)	Matched Pattern	Score Value	NCBI Identifier
1 (-)	Lactobacillus versmoldensis DSM 14857T DSM	1.367	194326
2 (-)	Lactobacillus plantarum DSM 20205 DSM	1.319	1590
3 (-)	Clostridium novyi A 1025_NCTC 538 BOG	1.289	1542
4 (-)	Clostridium difficile MB_7869_05 THL	1.242	1496
5 (-)	Pseudomonas migulae CIP 105470T HAM	1.237	78543
6 (-)	Enterococcus faecium VRE_PX_16086218 MLD	1.231	1352
7 (-)	Lactobacillus curvatus DSM 20019T DSM	1.212	28038
8 (-)	Bacillus simplex CS 206_1aI BRB	1.211	1478
9 (-)	Arthrobacter ramosus IMET 10685T HKJ	1.163	1672
10 (-)	Enterococcus faecium 20218_1 CHB	1.155	1352

Analyte14

Analyte Name: C4
 Analyte Description:
 Analyte ID: 3b
 Analyte Creation Date/Time: 2017-07-28T13:11:54.385
 Applied MSP Library(ies):
 Applied Taxonomy Tree: Bruker Taxonomy

Rank (Quality)	Matched Pattern	Score Value	NCBI Identifier
1 (-)	Aeromonas veronii CECT 5761T DSM	1.421	654
2 (-)	Staphylococcus condimentii DSM 11675 DSM	1.37	70255
3 (-)	Bacillus simplex DSM 1321T DSM	1.361	1478
4 (-)	Staphylococcus aureus ssp aureus DSM 346 DSM	1.345	46170
5 (-)	Aeromonas caviae CECT 838T DSM	1.337	648
6 (-)	Staphylococcus warneri DSM 20316T DSM	1.324	1292
7 (-)	Aeromonas veronii CECT 4257T DSM	1.31	654
8 (-)	Staphylococcus aureus ATCC 25923 THL	1.297	1280
9 (-)	Bacillus sp LB_101250b_09 ERL	1.278	185979
10 (-)	Lactobacillus kimchii DSM 13961T DSM	1.268	103818

Analyte15

Analyte Name: C5
 Analyte Description:
 Analyte ID: 4b
 Analyte Creation Date/Time: 2017-07-28T13:11:54.635
 Applied MSP Library(ies):
 Applied Taxonomy Tree: Bruker Taxonomy

Rank (Quality)	Matched Pattern	Score Value	NCBI Identifier
1 (-)	Bacillus sp LB_101250b_09 ERL	1.348	185979
2 (-)	Streptomyces phaeochromogenes B265 UFL	1.292	1923
3 (-)	Staphylococcus intermedius P_52B JUT	1.279	1285
4 (-)	Saprochaete clavata CBS 425_71 CBS	1.276	44064
5 (-)	Staphylococcus intermedius P_54A JUT	1.267	1285
6 (-)	Arthrobacter crystallopoietes DSM 20117T DSM	1.252	37928
7 (-)	Staphylococcus lugdunensis DSM 4804T DSM	1.244	28035
8 (-)	Aeromonas caviae CECT 838T DSM	1.242	648
9 (-)	Staphylococcus lugdunensis DSM 4806 DSM	1.235	28035
10 (-)	Saprochaete clavata CBS 969_87 CBS	1.224	44064

Analyte16

Analyte Name: C6
 Analyte Description:
 Analyte ID: 5b
 Analyte Creation Date/Time: 2017-07-28T13:11:54.603
 Applied MSP Library(ies):
 Applied Taxonomy Tree: Bruker Taxonomy

Rank (Quality)	Matched Pattern	Score Value	NCBI Identifier
1 (-)	Clostridium cochlearium 1077_ATCC 17787T BOG	1.275	1494
2 (-)	Starkeya novella B516 UFL	1.252	921
3 (-)	Peptoniphilus ivorii DSM 10022T DSM	1.232	54006
4 (-)	Staphylococcus lugdunensis DSM 4804T DSM	1.227	28035
5 (-)	Clostridium novyi A 1025_NCTC 538 BOG	1.222	1542
6 (-)	Lactobacillus aviarius ssp aviarius DSM 20654 DSM	1.221	147810
7 (-)	Staphylococcus vitulinus DSM 9931 DSM	1.22	71237
8 (-)	Candida valida MYRV4_10 ERL	1.217	4926
9 (-)	Staphylococcus lugdunensis DSM 4806 DSM	1.193	28035
10 (-)	Bacillus funiculus DSM 15141T DSM	1.191	137993

Analyte17

Analyte Name: C7
 Analyte Description:
 Analyte ID: 6b
 Analyte Creation Date/Time: 2017-07-28T13:11:54.198
 Applied MSP Library(ies):
 Applied Taxonomy Tree: Bruker Taxonomy

Rank (Quality)	Matched Pattern	Score Value	NCBI Identifier
1 (-)	Bacillus simplex DSM 1321T DSM	1.651	1478
2 (-)	Bacillus simplex CS 206_1aI BRB	1.45	1478
3 (-)	Bacillus muralis DSM 16288T DSM	1.415	264697
4 (-)	Bacillus subtilis ssp subtilis DSM 5660 DSM	1.415	135461
5 (-)	Enterococcus faecium 11037 CHB	1.308	1352
6 (-)	Bacillus psychrosaccharolyticus DSM 6T DSM	1.299	1407
7 (-)	Staphylococcus aureus ATCC 33591 THL	1.28	1280
8 (-)	Candida krusei 36 PSB	1.277	4909
9 (-)	Bacillus subtilis DSM 5611 DSM	1.277	1423
10 (-)	Bacillus subtilis ssp subtilis DSM 10T DSM	1.256	135461

Analyte18

Analyte Name: C8
 Analyte Description:
 Analyte ID: 7b
 Analyte Creation Date/Time: 2017-07-28T13:11:54.728
 Applied MSP Library(ies):
 Applied Taxonomy Tree: Bruker Taxonomy

Rank (Quality)	Matched Pattern	Score Value	NCBI Identifier
1 (-)	Lactobacillus aviarius ssp aviarius DSM 20654 DSM	1.302	147810
2 (-)	Staphylococcus lugdunensis DSM 6670 DSM	1.292	28035
3 (-)	Pseudomonas umsongensis LMG 21317T HAM	1.283	198618
4 (-)	Clostridium sordellii 1070_ATCC 9714T BOG	1.25	1505
5 (-)	Staphylococcus delphini h_5d JUT	1.241	53344
6 (-)	Lactobacillus agilis DSM 20509T DSM	1.24	1601
7 (-)	Clostridium tetani type 1 1049_NCTC 279T BOG	1.218	1513
8 (-)	Streptomyces lavendulae B264 UFL	1.213	1914
9 (-)	Staphylococcus vitulinus DSM 9931 DSM	1.21	71237
10 (-)	Rhizobium radiobacter B166 UFL	1.186	358

Analyte19

Analyte Name: C9
 Analyte Description:
 Analyte ID: 8b
 Analyte Creation Date/Time: 2017-07-28T13:11:54.291
 Applied MSP Library(ies):
 Applied Taxonomy Tree: Bruker Taxonomy

Rank (Quality)	Matched Pattern	Score Value	NCBI Identifier
1 (-)	Acinetobacter baumannii B389 UFL	1.442	470
2 (-)	Clostridium novyi A 1025_NCTC 538 BOG	1.355	1542
3 (-)	Enterococcus faecium 11037 CHB	1.355	1352
4 (-)	Enterococcus faecium VRE_PX_16086218 MLD	1.354	1352
5 (-)	Acinetobacter calcoaceticus B388 UFL	1.333	471
6 (-)	Bacillus simplex DSM 1321T DSM	1.307	1478
7 (-)	Bacillus simplex CS 206_1aI BRB	1.275	1478
8 (-)	Comamonas testosteroni DSM 50244T HAM	1.26	285
9 (-)	Acidovorax facilis DSM 649T HAM	1.25	12917
10 (-)	Clostridium baratii 1018_NCTC 10986 BOG	1.248	1561

Analyte20

Analyte Name: C10
 Analyte Description:
 Analyte ID: 9b
 Analyte Creation Date/Time: 2017-07-28T13:11:54.681
 Applied MSP Library(ies):
 Applied Taxonomy Tree: Bruker Taxonomy

Rank (Quality)	Matched Pattern	Score Value	NCBI Identifier
1 (-)	Staphylococcus sciuri ssp rodentium DSM 16827T DSM	1.437	147469
2 (-)	Lactobacillus versmoldensis DSM 14857T DSM	1.365	194326
3 (-)	Candida valida MYRV4_10 ERL	1.239	4926
4 (-)	Pseudomonas gessardii CIP 105469T HAM	1.236	78544
5 (-)	Streptomyces lavendulae B264 UFL	1.209	1914
6 (-)	Arthrobacter pyridinolis B384 UFL	1.205	1663
7 (-)	Staphylococcus xylosus DSM 20266T DSM	1.201	1288
8 (-)	Lactobacillus plantarum ssp argentoratensis DSM 16365T DSM	1.2	271881
9 (-)	Clostridium novyi A 1025_NCTC 538 BOG	1.197	1542
10 (-)	Sphingomonas adhaesiva DSM 7418T HAM	1.185	28212

Analyte21

Analyte Name: C11
 Analyte Description:
 Analyte ID: 10b
 Analyte Creation Date/Time: 2017-07-28T13:11:54.151
 Applied MSP Library(ies):
 Applied Taxonomy Tree: Bruker Taxonomy

Rank (Quality)	Matched Pattern	Score Value	NCBI Identifier
1 (-)	Bacillus sp LB_101250b_09 ERL	1.638	185979
2 (-)	Aspergillus flavus 1081 PFM	1.379	5059
3 (-)	Starkeya novella B516 UFL	1.366	921
4 (-)	Sphingobacterium faecium DSM 11690T HAM	1.326	34087
5 (-)	Staphylococcus lugdunensis 20659_1 CHB	1.325	28035
6 (-)	Streptomyces lavendulae B264 UFL	1.307	1914
7 (-)	Staphylococcus lugdunensis DSM 4805 DSM	1.286	28035
8 (-)	Lactobacillus suebicus DSM 5007T DSM	1.274	152335
9 (-)	Staphylococcus cohnii ssp cohnii DSM 20261 DSM	1.258	74704
10 (-)	Streptomyces griseus B261 UFL	1.257	1911

Analyte22

Analyte Name: C12
 Analyte Description:
 Analyte ID: 11b
 Analyte Creation Date/Time: 2017-07-28T13:11:54.151
 Applied MSP Library(ies):
 Applied Taxonomy Tree: Bruker Taxonomy

Rank (Quality)	Matched Pattern	Score Value	NCBI Identifier
1 (-)	Bacillus simplex CS 206_1aI BRB	1.594	1478
2 (-)	Bacillus simplex DSM 1321T DSM	1.584	1478
3 (-)	Bacillus muralis DSM 16288T DSM	1.564	264697
4 (-)	Bacillus sp LB_101250b_09 ERL	1.418	185979
5 (-)	Gordonia aichiensis DSM 43978T DSM	1.372	36820
6 (-)	Acinetobacter baumannii B389 UFL	1.343	470
7 (-)	Clostridium clostridioforme 1021_NCTC 11224T BOG	1.296	1531
8 (-)	Bacillus atrophaeus DSM 675 DSM	1.282	1452
9 (-)	Bacillus subtilis ssp subtilis DSM 5660 DSM	1.272	135461
10 (-)	Lactobacillus paracasei ssp paracasei DSM 8742 DSM	1.232	47714

Analyte23

Analyte Name: D2
 Analyte Description:
 Analyte ID: BTS1
 Analyte Creation Date/Time: 2017-07-28T13:11:54.354
 Applied MSP Library(ies):
 Applied Taxonomy Tree: Bruker Taxonomy

Rank (Quality)	Matched Pattern	Score Value	NCBI Identifier
1 (+++)	Escherichia coli ATCC 25922 THL	2.467	562
2 (+++)	Escherichia coli DSM 682 DSM	2.392	562
3 (+++)	Escherichia coli DSM 1576 DSM	2.376	562
4 (+++)	Escherichia coli DSM 1103_QC DSM	2.371	562
5 (+++)	Escherichia coli DH5alpha BRL	2.337	562
6 (+++)	Escherichia coli MB11464_1 CHB	2.303	562
7 (++)	Escherichia coli ATCC 25922 CHB	2.298	562
8 (++)	Escherichia coli DSM 30083T HAM	2.259	562
9 (++)	Escherichia coli Nissl VML	2.219	562
10 (++)	Escherichia coli RV412_A1_2010_06a LBK	2.206	562

Analyte24

Analyte Name: E2
 Analyte Description:
 Analyte ID: BTS2
 Analyte Creation Date/Time: 2017-07-28T13:11:54.713
 Applied MSP Library(ies):
 Applied Taxonomy Tree: Bruker Taxonomy

Rank (Quality)	Matched Pattern	Score Value	NCBI Identifier
1 (+++)	Escherichia coli ATCC 25922 THL	2.537	562
2 (+++)	Escherichia coli MB11464_1 CHB	2.402	562
3 (+++)	Escherichia coli DSM 682 DSM	2.352	562
4 (+++)	Escherichia coli DH5alpha BRL	2.341	562
5 (++)	Escherichia coli DSM 1103_OC DSM	2.291	562
6 (++)	Escherichia coli DSM 1576 DSM	2.276	562
7 (++)	Escherichia coli ATCC 25922 CHB	2.27	562
8 (++)	Escherichia coli Nissl VML	2.248	562
9 (++)	Escherichia coli DSM 30083T HAM	2.215	562
10 (++)	Escherichia fergusonii DSM 13698T HAM	2.207	564